Elicitation and evasion of plant innate immunity by beneficial and pathogenic bacteria

Jonas Sebastian Pfeilmeier

September 2017

Thesis submitted to the University of East Anglia for the degree of Doctor of Philosophy

The Sainsbury Laboratory

John Innes Centre

Norwich, United Kingdom

The dissertation has been jointly supervised by Cyril Zipfel (The Sainsbury Laboratory, Norwich, UK) and Jacob Malone (John Innes Centre, Norwich, UK). This work has been supported by a Norwich Research Park Fellowship.

Abstract

Plasma membrane-localized pattern recognition receptors (PRRs) are central components of the plant innate immune system. PRRs perceive characteristic microbial features, termed pathogen-associated molecular patterns (PAMPs), leading to pattern-triggered immunity (PTI). As PAMPs from both pathogenic and beneficial bacteria are potentially recognized, both must employ strategies to evade and/or suppress PTI. Here, I show that exopolysaccharides (EPS) and flagella-driven motility, both of which are regulated by the secondary messenger cyclic-di-GMP, are important virulence factors at different stages during *Pseudomonas syringae* pv. *tomato* (*Pto*) DC3000 infection of *Arabidopsis thaliana*. High levels of cyclic-di-GMP impaired flagellin accumulation in different *Pseudomonas* species, and helped bacteria to evade recognition by the PRR FLAGELLIN SENSING 2. In this case, immune evasion was fully explained by the effect of cyclic-di-GMP on flagellin synthesis rather than on EPS production. Nevertheless, an EPS-deficient *Pto* DC3000 mutant, Δ*alg/psl/wss*, showed compromised virulence, and a combination of two types of EPS appeared to be required for optimal *in planta* proliferation. In a complementary project, I tested whether PAMP recognition affects the interaction between the legume *Medicago truncatula* and its symbiotic partner *Sinorhizobium meliloti*. I transferred the PRR EF-TU RECEPTOR (EFR) from *A. thaliana* to *M. truncatula*, conferring recognition of the bacterial EF-Tu protein. Expression of *EFR* protected *M. truncatula* against the root pathogen *Ralstonia solanacearum* without compromising the overall symbiotic interaction with nitrogen-fixing *S. meliloti*. My results indicate that rhizobium either avoids PAMP recognition, or actively suppresses immune signalling during the infection process. Finally, I engineered a PAMP in *S. meliloti* by replacing the eliciting inactive flg22 epitope (derived from flagellin) with an eliciting epitope. My results suggest that legumes can be engineered with novel PRRs, as a biotechnological approach for broad-spectrum disease resistance, without perturbing the nitrogen-fixing symbiosis. Overall, my work contributes to our understanding of the molecular interaction between plants and bacteria.

Acknowledgments

"You have to keep busy. After all, no dog's ever pissed on a moving car."

Tom Waits

I would like to thank my two supervisors Cyril Zipfel and Jake Malone for the opportunity to join their labs, their ideas on the project and guidance throughout the years. It has been an incredibly instructive time for me and formed my thinking and attitude towards science. Thanks to all the past and present members of the Zipfel group and the Malone group for their support and the shared life experiences. It has been a great time for me and the group dynamics within the lab and outside of it made me feel to be part of something very special. I am grateful to Allan Downie, Sonali Roy and Jeoffrey George, as well as Feng Feng and Myriam Charpentier, for the help and input on the Medicago work. Thanks to Lucia Grenga and Freddy Boutrot for proof-reading my thesis. Overall, working at The Sainsbury Laboratory and the John Innes Centre was intense, stimulating, and very enjoyable.

Special thanks to Jeoffrey George, Lukas Harnisch, Daniel Couto, Sara Ben Khaled, Jan Bettgenhaeuser, Lucia Grenga, Eleftheria Trampari, Richard Little, Tom Scott, Andy Dawson, Sonali Roy, Rea Kourounioti, John Fozard, and Giuseppe Facchetti for being good friends and enriching my social life in Norwich and beyond.

I am very proud of the achievements with the TSL/JIC/UEA football group – we were playing such good football. Futhermore, I was very fortunate to become part of the NBI Book Tree reading group – I enjoyed every meeting and to getting exposed to so many books.

Thanks to all my friends for their visits in Norwich and their encouragement, and especially thanks to Christa, Karle, and Felix for their unconditional support in whatever I am doing in life. And thanks to Alicia who made my last weeks in Norwich very special!

Contents

List of Figures

List of Tables

Abbreviations

BAK1	BRASSINOSTEROID INSENSITIVE 1-ASSOCIATED KINASE 1
BLAST	Basic local alignment search tool
cdG	Cyclic di-GMP
cfu	Colony forming units
CDPK	Calcium-dependent protein kinase
ddH_2O	double distilled H_2O
dpi	Days post infection
DNA	Deoxyribonucleic acid
EFR	ELONGATION FACTOR-TU RECEPTOR
elf18	18 amino acid peptide derived from *Escherichia coli*
EPS	Exopolysaccharides
flg22	See $flg22^{Pa}$
$flg22^{Pa}$	22 amino acid peptide derived from *Pseudmonas aeruginosa*
$flg22^{mod}$	modified 22 amino acid peptide based on *Sinorhizobium meloloti*
FLS2	FLAGELLIN SENSING 2
GC	Gas chromatography
GUS	β-Glucuronidase
h	hour(s)
IT	Infection thread
KB	King's medium B
LB	Lysogeny broth
LC-MS/MS	Liquid chromatography-tandem mass spectrometry
LRR	Leucine rich repeat
MC	Micro-colony
MPK	Mitogen activated protein kinase
OD	Optical density
PAMP	Pathogen-associated molecular pattern
PRR	Pattern recognition receptor
PTI	Pattern (or PRR, or PAMP)-triggered immunity
Pto	*Pseudomonas syringae* pv *tomato*
RLK	Receptor-like kinase
RLP	Receptor-like protein
RLCK	Receptor-like cytoplasmic kinase
RLU	Relative light units
RNA	Ribonucleic acid
ROS	Reactive oxygen species
Sm	*Sinorhizobium meliloti*
SM	Swimming medium
TY	Tryptone yeast
TRV	tobacco rattle virus
T3SS	Type-3 secretion system
VIGS	Virus-induced gene silencing
v/v	Volume of solute/volume of solution
WT	Wild-type
w/v	Mass of solute/volume of solution
X-gal	5-bromo-4-chloro-3-indolyl-β-D-galactoside

Chapter 1

Introduction

1.1 Human-plant associations

Plants are autotrophic organisms, which use energy from light to conduct photosynthesis and produce complex organic compounds out of simple substances present in their surroundings, such as water and oxygen. Humans and other animals depend on plants as a basic source for their energy supply. Beside food, plants also provide essential products such as fibers, fuels, and drugs for humans. Moreover, the cultural development of mankind is closely connected to the development and evolution of plants (Thompson, 2010). Today's major crop plants have been domesticated over a continuous breeding process for millennia. Our ancestors learned to cultivate plants, harvest the seeds and practice agriculture. Depending on the geographical region, evolutionary adaption to survive in different climatic conditions and under other pressures such as drought, frost, pests and pathogens secured the persistence of agricultural plants. Seeds initially collected from wild plants, were selected and systematically bred over the years. With growing knowledge of genetics during the 20th century, new breeding methods promoted the development of high-yield varieties. In addition, people learned to create or foster conditions that optimize plant growth. Field irrigation supplies sufficient water, fertilizer ensures nutrient availability and greenhouses allow plant growth in otherwise unfavorable climates. Nonetheless, complete control of environmental conditions is difficult to achieve, especially for biotic factors such as diseases caused by plant pathogens. Modern agricultural practices, including crop monocultures that are selected for maximum yield and consumer-desired traits, provide a fertile ground for pathogens. A major goal of plant pathology is to gain expertise in epidemic plant diseases and convey it to farming strategies to meet agricultural demands. Additionally, the discovery of parallels between the immune system of plants and animals promoted this research field to the forefront of plant molecular biology. Remarkable advances in the understanding of disease resistance focusing on molecular and cellular mechanisms have created a comprehensive concept of plant immunity (Dangl et al., 2013, Dodds and Rathjen, 2010).

In this introductory chapter, I will describe how microbial elicitors are recognized by plant immune receptors activating several immune responses. Successful pathogens must evolve virulence strategies to evade recognition and/or suppress plant immunity. Similarly, beneficial bacteria are also exposed to potential immune recognition. I will briefly discuss three different mechanisms employed by bacteria that determine the outcome of plant-bacteria interactions and are involved in evasion of plant immunity: this includes the use of secreted effector proteins, the role of extracellular polysaccharides (exopolysaccharides; EPS) and natural allele variation observed in bacterial immune elicitors.

1.2 Plant-microbe interactions

Plants live in constant contact with a vast number and huge variety of microorganisms, including bacteria, fungi and oomycetes. The microbiomes of the phyllosphere and rhizosphere play critical roles in the adaption of the plant to its environment (Berendsen et al., 2012, Müller et al., 2016). Specialized microbes can be beneficial or detrimental to their host. Plants solely rely on an innate immune system consisting of passive and active defences to resist potential attack by most microbial pathogens (Cui et al., 2015, Boutrot and Zipfel, 2017, Lee et al., 2017). Associations with beneficial microbes could be either in an intimate mutualistic symbiosis that requires elaborate communication processes of both partners, or in a commensal relationship, in which the microbe stimulates plant growth or protects the host from potential harm (Pieterse et al., 2014, Vorholt, 2012, Lugtenberg and Kamilova, 2009). Living in close relation with their host, it is vital for both pathogenic and beneficial microbes to avoid immune responses.

1.2.1 Plant pathogenic bacteria

Plants have to cope with unfavourable environmental conditions like biotic stress due to pathogen attack. They rely on an innate immune system, which enables them to resist most microbial pathogens. Pathogens need a high degree of specialization to overcome the plant immune system and cause disease. Although pathogens are relatively rare among all microbes, they are a major threat to plant survival and an effective immune system is needed to fend them off (Jones and Dangl, 2006, Dangl et al., 2013). Pathogenic microbes can be bacteria, fungi or oomycetes following either a necrotrophic, biotrophic, or hemibiotrophic lifestyle (Glazebrook, 2005). Nutrients are limited on the plant surface, so the first critical step for a pathogen is to get inside the host tissue and overcome initial barriers such as the waxy leaf cuticle, apoplastic antimicrobial compounds and the cell wall. Pathogenic bacteria move into the plant through stomata, hydathodes, or wounds, and mostly proliferate in the apoplast, the intercellular space of plant tissue (Beattie and Lindow, 1995). Some pathogenic bacteria, such as *Xylella fastidiosa* and phytoplasma use sap-feeding insects as vectors for the penetration of host tissue and multiply intracellularly (Rapicavoli et al., Sugio and Hogenhout, 2012). While there are many bacterial pathogens with high scientific and economic impact (Mansfield et al., 2012), I will focus here mostly on the lifestyle and virulence determinants of *Pseudomonas syringae*. Collectively, the *P. syringae* species complex has a broad host range, but pathogen variants (pathovars) are restricted to one or a few plant species, which reflects a strong adaption to specific hosts and is largely

determined by the type-3 secreted effector repertoire (Lin and Martin, 2007, Lindeberg et al., 2009). *Pseudomonas syringae* pathovar *tomato* (*Pto*) DC3000 is the causal agent of the bacterial speck disease on tomato (*Solanum lycopersicum*) and thale cress (*Arabidopsis thaliana*). *Pto* DC3000 has a hemibiotrophic lifestyle and colonizes the intercellular spaces of leaves and other aerial parts of plants (Xin and He, 2013). Over the past 30 years, *Pto* DC3000 has emerged as a model organism to study the molecular mechanisms underlying bacterial virulence and host immunity (Xin and He, 2013). This led to the development of various genetic resources in both *Pto* DC3000 and *A. thaliana* and has facilitated the exploration of the molecular details of plant-pathogen interactions.

The disease cycle of *P. syringae* strains follows two sequential phases. In the initial epiphytic stage, the bacteria must cope with abiotic stresses, such as desiccation, ultraviolet irradiation, and rapid temperature changes on the leaf surface. In the subsequent endophytic phase, *P. syringae* can multiply aggressively in the apoplastic space of a susceptible host plant under suitable environmental conditions. At later stages during the infection, host cells die and the leaf shows extensive necrotic tissue. During these stages of pathogenesis, the bacterium is exposed to changing environmental conditions. Thus, the bacteria have to respond to a variety of external cues, integrating the outputs of various signalling networks into an appropriate response regulating the complex infection process. *P. syringae* relies on regulatory pathways controlled by small signalling molecules, such as quorum sensing acyl-homoserine lactones, or the intracellular secondary messenger cyclic-di-GMP (cdG). These pathways guide epiphytic survival, invasion of the plant tissue, virulence and proliferation (Quiñones et al., 2005, Vakulskas et al., 2015, Records and Gross, 2010). Metabolic adaptation to cold and osmotic shock, and desiccation stress contribute to the epiphytic survival of *P. syringae* (Lindow et al., 1993, Freeman et al., 2013). In addition, bacterial EPS molecules have been shown to play an important role to plant surface colonization and infection (Laue et al., 2006, Yu et al., 1999, Yu et al., 2013). Another class of compounds that contribute to bacterial virulence are secondary metabolites, often referred to as phytotoxins (Bender et al., 1999). One of the best studied phytotoxic molecules is the polyketide coronatine, which mimics the phytohormone jasmonic acid (JA) and stimulates JA signalling to reopen closed stomata, hence promoting bacterial entry (Melotto et al., 2006). A major virulence determinant of hemibiotrophic pathogens is the secretion of effector proteins that manipulate the structure or function of host components and to promote pathogenesis (Lindeberg et al., 2012, Win et al., 2012). The contribution of bacterial effectors

and EPS to evasion and suppression of plant immunity will be discussed in more detail below (Chapter 1.4).

1.2.2 Beneficial plant-associated bacteria

1.2.2.1 Plant growth-promoting rhizobacteria

Plants have beneficial associations with a variety of microbes that colonize the rhizosphere, a soil layer influenced by the plant root. The microbial community in the rhizosphere is very different from that in the surrounding soil and depends on the host genotype, suggesting that plants are able to shape their microbiome (Müller et al., 2016, Hacquard et al., 2017). An example of microbes forming beneficial interactions with plants are soil-borne bacteria that enhance plant growth after root colonization and are called plant growth-promoting rhizobacteria (PGPR) (Lugtenberg and Kamilova, 2009, van Loon, 2007, Pieterse et al., 2014). PGPR have been identified in over two dozen genera of rhizobacteria and plant growth-promoting or biocontrol actions can be realized through multiple mechanisms (Kim et al., 2011). Plant growth promotion could be accomplished by providing nutrients or other important elements to the plant or by stimulation of plant growth via production of plant hormones (Pieterse et al., 2014, Zamioudis and Pieterse, 2012). Other PGPR are described as biological disease control agents. They occupy ecological niches in the plant rhizosphere, suppressing deleterious soil-borne pathogens through the production of antimicrobial compounds, through nutrient scavenging, or niche occupation. In addition, PGPR act through a phenomenon known as induced systemic resistance (ISR) in the host, which primes above ground plant tissues for enhanced resistance against foliar pathogens or even insect herbivores (Haas and Defago, 2005, Lugtenberg and Kamilova, 2009, Pieterse et al., 2014). For example, *Pseudomonas protegens* Pf-5 is a soil bacterium that colonizes the rhizosphere and contributes to plant health by suppression of a wide variety of plant diseases over a broad host range (Loper et al., 2007). *P. protegens* Pf-5 produces multiple secondary metabolites, including antibiotic polyketide compounds pyoluteorin and 2,4-diacetylphloroglucinol (2,4-DAPG), that underpin its biocontrol capacities (Loper et al., 2007). Besides its antimicrobial activity, 2,4-DAPG is involved in conferring ISR against foliar pathogen infections (Iavicoli et al., 2003, Weller et al., 2012). In addition to the production of antibiotics, siderophore secretion and metabolic features, such as broad catabolic pathways, an expanded array of efflux systems and numerous genes conferring tolerance to oxidative stress enable *P. protegens* Pf-5 to cope with environmental stress and microbial competition in the rhizosphere (Loper et al., 2007, Loper et al., 2012).

1.2.2.2 Nitrogen-fixing rhizobia

A well-studied example of beneficial microbes that directly promote plant growth are *Rhizobium* bacteria that can form intimate symbiotic relationships with legumes. These bacteria initiate the formation of root nodules, in which they fix atmospheric nitrogen in exchange for plant-produced carbohydrates. Rhizobia produce and release Nod factors (lipochitin oligosaccharides), which are recognized by host receptors and trigger an intracellular signalling process leading to cell re-differentiation, organogenesis and infection of root nodules (Figure 1) (Oldroyd et al., 2011). While rhizobial infection can happen in cracks between epidermal cells, the typical entry route is via root hair infections. Rhizobia attach to root hairs, which curl and entrap the growing microcolony. This is followed by initiation and elongation of infection threads (ITs), which are plant-derived tubular structures inside the root hair that guide the proliferating bacteria through the epidermal and cortical cell layers towards the nodule primordia. Ultimately, rhizobia get released into the nodule by an endocytosis-like process and form membrane-encased symbiosomes, which develop into bacteroids fixing atmospheric nitrogen (Oldroyd et al., 2011). *M. truncatula* produces nodule-specific cysteine-rich peptides to control irreversible terminal differentiation of rhizobia to elongated and polyploid endosymbionts (Van de Velde et al., 2010). The characterization of plant mutants impaired at different stages of the symbiotic process has identified components required to establish and control microbial infection (Oldroyd, 2013). Perception of Nod factors by the *M. truncatula* LYSM DOMAIN RECEPTOR KINASE 3 (LYK3) and NOD FACTOR PERCEPTION (NFP) trigger the symbiotic signalling pathway and initiate nuclear calcium oscillations. The calcium-calmodulin dependent kinase DOES NOT MAKE INFECTIONS 3 (DMI3; or CCAMK in *L. japonicus*) decodes the calcium signal and interacts with the transcription factor INTERACTING PROTEIN OF DMI3 (IPD3; or CYCLOPS in *L. japonicus*) to coordinate infection with organogenesis (Madsen et al., 2010, Miller et al., 2013, Singh et al., 2014). To establish and maintain the symbiotic process, continuous communication between the legume and rhizobium is required. Beside Nod factors, rhizobia produce other factors that are critical for infection and accommodation in the host cell, such as lipopolysaccharides, exopolysaccharides and cyclic beta-glucans (Downie, 2010). Despite the intimate interaction and signal exchange between both partners, it is an open question whether the infecting bacterium is recognized as a foreign invader by the plant innate immune system (Cao et al., 2017).

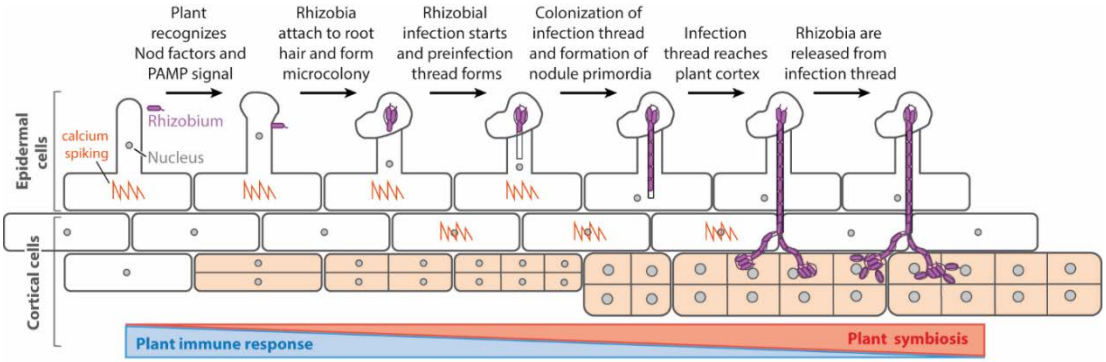

Figure 1.1. Rhizobial infection process of legume roots. Nod factor perception activates the symbiosis signalling pathway (red), leading to calcium oscillations, initially in epidermal cells but later also in cortical cells. The balance between immune response and symbiosis during nodule development. Rhizobial PAMPs activate a transient immune response (blue), which is downregulated during continuation of symbiosis process. Rhizobia form microcolony at curled root hair cells. Infection threads are formed by the plant cell at the site of root hair curls and allow invasion of the rhizobia into the root tissue. Nodule primordia develop below the site of bacterial infection and form by de novo initiation of a nodule meristem in the cortical cells. The infection threads grow towards the emergent nodules and ramify within the nodule tissue. Ultimately, the bacteria are released into membrane-bound compartments inside the cells of the nodule, where the bacteria can differentiate into a nitrogen-fixing state. Figure taken from (Cao et al., 2017) and modified.

1.3 Activation of plant immunity

Unlike mammalian immune systems, the plant immune system lacks both specialized and mobile defender cells as well as antibody-mediated immunity. Instead, plant cells rely on cell-autonomous innate immunity. This is characterized by a two-layered surveillance system consisting of plasma membrane-localized and intracellular immune receptors that specifically sense the presence of microbes and pathogens, respectively, and trigger local and systemic immune responses to restrict pathogen growth (Figure 1.2) (Dodds and Rathjen, 2010). The first layer of plant immunity employs cell surface-localized pattern recognition receptors (PRRs) that perceive pathogen (or microbe)-associated molecular patterns (PAMPs or MAMPs) and trigger local and systemic immune responses (Boutrot and Zipfel, 2017). Typical examples of PAMPs are fungal chitin, bacterial peptidoglycan or flagellin that are released during infection and elicit a defence response (Boller and Felix, 2009). Similarly to these exogenous microbial elicitors, endogenous plant molecules released during infection or wounding, called damage-associated molecular patterns (DAMPs) can also be detected by PRRs. Activation of PRRs by binding PAMPs or DAMPs results in PRR-triggered immunity (PTI) (Couto and Zipfel, 2016). Characteristic PTI responses involve immune reactions including the production of reactive oxygen species (ROS), transcription of defence-related genes and cell wall fortification (Boller and Felix, 2009). Since PTI is activated by conserved features of entire groups of microbes, it has the potential to ward off a broad

range of microbes and stop their proliferation in the apoplastic space (Boller and Felix, 2009, Boutrot and Zipfel, 2017).

Successful pathogens have adapted to their preferred host and evolved ways to overcome this first layer of plant immunity in order to cause disease (Macho and Zipfel, 2015). A well studied strategy to suppress PTI employed by pathogenic bacteria, fungi and oomycetes is the delivery of virulence effector proteins into the host cell or in the apoplast. Secreted effectors actively interfere with host immune signalling, thereby facilitating infection. In turn, intracellular immune receptors, mainly represented by nucleotide binding site (NBS) leucine-rich repeat (LRR) proteins, can recognize effectors directly or indirectly through their action on host proteins and activate the second layer of plant immunity called effector-triggered immunity (ETI) (Cui et al., 2015, Li et al., 2015).

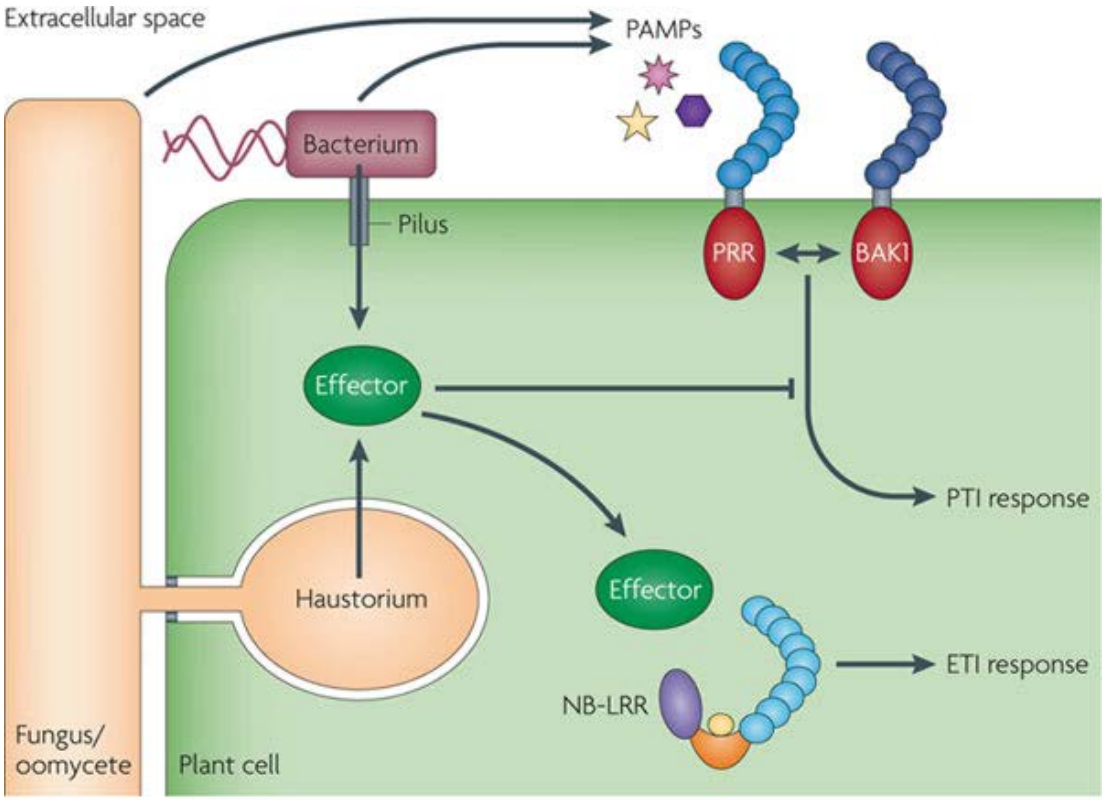

Figure 1.2. Schematic of plant innate immunity. Invading pathogens release molecules into the extracellular space, termed pathogen-associated molecular patterns (PAMPs) such as chitin or flagellin, that are perceived by cell surface pattern recognition receptors (PRRs) and elicit pattern-triggered immunity (PTI). Pathogenic bacteria, fungi and oomycetes secrete effector proteins into the host cell that often function to suppress PTI. However, many effectors are recognized by intracellular nucleotide-binding (NB)-leucine rich repeat (LRR) receptors, which initiate effector-triggered immunity (ETI). Figure taken from (Dodds and Rathjen, 2010).

Historically, effectors are also known as avirulence proteins (Avr), because the pathogen carrying an effector that is recognized by the corresponding NBS-LRR is not virulent on this host plant, as the effector recognition leads to immunity. This interaction has been characterized as race-specific gene-for-gene resistance (Hammond-Kosack and Jones, 1997, Flor, 1971). The concept of the two-layered plant immune system, comprising PTI and ETI, has been described in an evolutionary context in the "zig-zag model" (Jones and Dangl, 2006). According to the zig-zag model, disease susceptibility is a consequence of suppression of host immunity. It describes the molecular interaction of pathogens and their hosts as a continuous evolutionary arms race, in which the original virulence activity of effectors is turned into avirulence activity, since effector action is steadily monitored by NBS-LRR proteins. Finally, natural selection favors those pathogen isolates that can avoid ETI by either loss or modification of the recognized effector, or by evolving new effectors helping to suppress ETI again (Jones and Dangl, 2006, Win et al., 2012). Although the zig-zag model provides a helpful framework to explain the molecular basis of compatible and incompatible plant-microbe interactions, plant responses towards a variety of microbes, especially towards symbionts and necrotrophs, cannot always be fully explained in terms of PTI and ETI (Thomma et al., 2011, Cook et al., 2015).

Recently, an alternative view describing plant innate immunity as a system to detect invasion has been suggested (Cook et al., 2015). As such, the plant surveys microbial activity in the intercellular space and inside the host cell. Microbial features correspond to invasion patterns that get recognized by plant immune receptors. In contrast to the strict definition of PAMPs and effectors, invasion patterns are described as a continuous spectrum of molecules representing a varying scope of microbial diversity and with different functional roles for the microbe (Cook et al., 2015). As such, understanding plant immunity as a surveillance system to detect invasion can have advantages to describe the simultaneous perception of multiple ligands during an infection and the co-evolution between receptor and ligands. Nevertheless, in this thesis, I will mostly focus on the specific perception of individual PAMPs by well-characterized PRRs, and I will use the established terminology as it is outlined below (Chapter 1.4 and 1.5).

The signalling events initiated as part of ETI overlap with those associated with PTI, including ROS production, activation of mitogen-activated protein kinases (MAPKs) and transcriptional reprogramming (Dodds and Rathjen, 2010, Tsuda and Katagiri, 2010, Thomma et al., 2011). Despite these similar characteristics, ETI is an accelerated and amplified response compared to PTI, and often results in a hypersensitive response (HR), which is a plant-specific form of

programmed cell death (Jones and Dangl, 2006). While it is not clear what actually stops pathogen growth, HR has been interpreted as an effective mechanism to restrict biotrophic pathogen growth simply by withdrawing the nutrient source (Greenberg and Yao, 2004). Besides triggering a rapid immune response in single cells, pathogen signals activate a systemic signalling network integrating various phytohormones and other signalling molecules that allows an extended immune response over time and space (Spoel and Dong, 2012, Pieterse et al., 2012). This systemic acquired resistance (SAR) primes uninfected tissue against subsequent pathogen attack (Fu and Dong, 2013).

PTI effectively contributes to basal disease resistance against adapted pathogens as well as non-host resistance against non-adapted pathogens by inducing local and systemic immune responses (Boutrot and Zipfel, 2017, Lee et al., 2017).

1.4 PAMP perception

1.4.1 Activation of pattern recognition receptors

Cell surface-localized pattern recognition receptors (PRRs) are the first line of active defence and enable the plant to recognize 'non-self' molecules (Couto and Zipfel, 2016). PTI is triggered by the perception of PAMPs, which are molecular signatures of microorganisms and constitute 'non-self'. PAMPs are often highly conserved and can represent whole classes of microbes (*e.g*. chitin for fungi) or are at least universally present in various species (*e.g*. flagellin in proteobacteria), which allows the plant to detect a variety of microbes with a limited set of receptors (Boutrot and Zipfel, 2017). Major advances have been made in the past 15 years to elucidate the molecular mechanisms underlying microbial perception at the plasma membrane and the activation of intracellular immune signalling leading to defence response (Figure 1.3) (Couto and Zipfel, 2016). Typically, plant PRRs are plasma membrane-localized proteins that exhibit a modular structure and invariantly contain an extracellular ligand binding (ecto)domain. Receptor-like kinases (RLKs) also contain a single-pass transmembrane domain and an intracellular kinase, while receptor-like proteins (RLPs) harbor alternatively a single-pass transmembrane domain and a cytoplasmic C-terminal extension, or a glycosylphosphatidylinositol (GPI) anchor. The PRR ectodomains display a variety of structural and functional domains including leucine-rich repeats (LRRs), lysine motifs (LysMs), lectin motifs, or epidermal growth factor (EGF)-like domains (Boutrot and Zipfel, 2017).

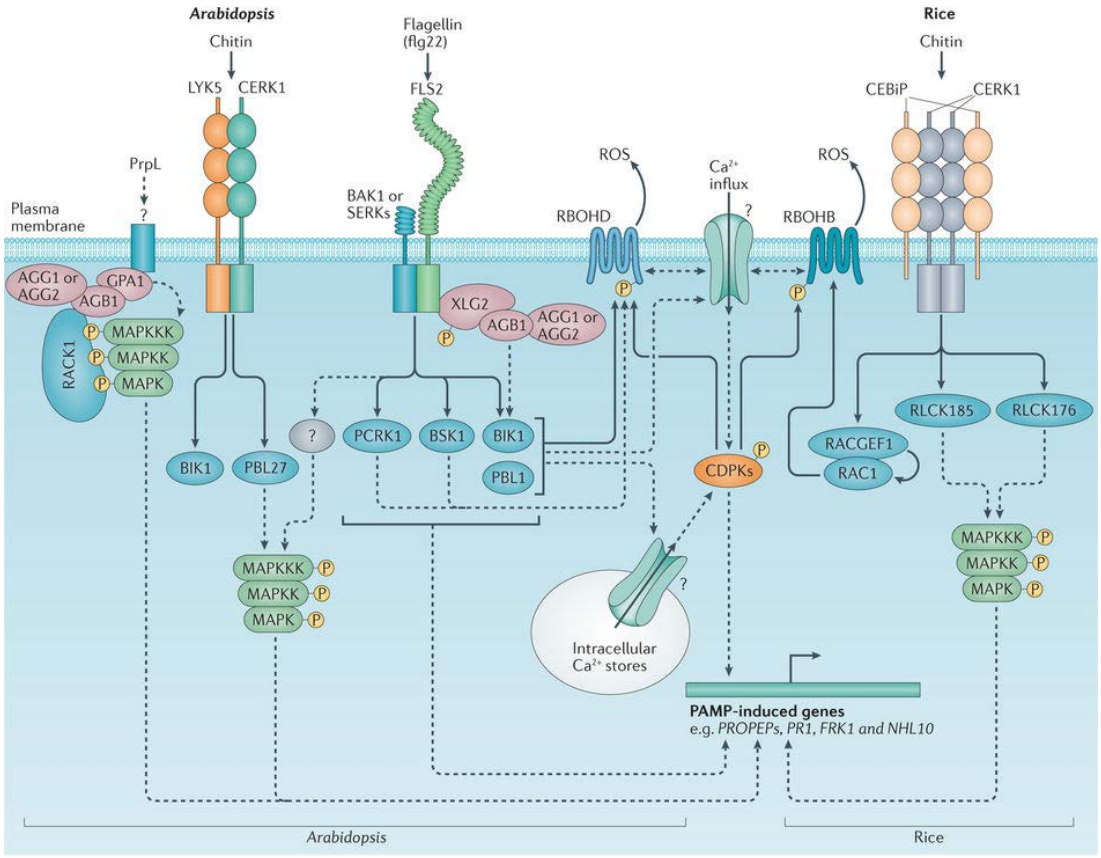

Figure 1.3. Pattern-triggered immunity signalling. Perception of pathogen-associated molecular patterns (PAMPs) by pattern recognition receptors (PRRs) induces pattern-triggered immunity (PTI) signalling. Although different PRR complexes can signal through distinct components, they rely on similar mechanisms. For example, PRR activation leads to complex formation with co-receptor(s), phosphorylation of downstream targets, such as receptor-like cytoplasmic kinases (RLCK), phosphorylation of the NADPH oxidase RBOHD leading to production of reactive oxygen species (ROS), initiation of a transient Ca^{2+} influx and activation of mitogen-activated protein kinase (MAPK) cascades. Figure originally published in (Couto and Zipfel, 2016).

Several PAMP-PRR pairs have been identified for pathogens of mono- and dicotyledonous plants and described in varying detail regarding the molecular mechanisms of ligand binding and signal activation. Two of the best studied PRRs in plants are FLAGELLIN SENSING 2 (FLS2) and ELONGATION FACTOR TU RECEPTOR (EFR) recognizing bacterial flagellin (or the eliciting epitope flg22) and EF-Tu (or the eliciting epitope elf18), respectively (Kunze et al., 2004, Zipfel et al., 2006, Felix et al., 1999, Gomez-Gomez and Boller, 2000). Both PRRs belong to the LRR-RLK family XII in *A. thaliana*, and are characterized by an ectodomain of LRRs for PAMP perception, and an intracellular kinase domain involved in signal transduction. Multiple *A. thaliana* RLKs have been identified that recognize PAMPs or DAMPs (Boutrot and Zipfel, 2017). Fungal chitin is perceived by LysM-CONTAINING RECEPTOR-LIKE KINASE 5 (LYK5), which acts together with its co-receptor CHITIN ELICITOR RECEPTOR KINASE 1 (CERK1) to activate intracellular immune signalling in *A. thaliana* (Miya et al., 2007, Petutschnig et al., 2010, Cao et al., 2014). Bacterial cell wall component peptidoglycan (PGN)

triggers plant immune responses (Gust et al., 2007, Erbs et al., 2008). PGN is directly bound by the LysM-containing RLPs LYM1 and LYM3 and mediates defence signalling together with CERK1 (Willmann et al., 2011, Erbs and Newman, 2012). Lipopolysaccharides (LPS) are abundant structures on the surface of bacterial cells and induce plant immune responses (Silipo et al., 2005). Recently, the lectin S-domain RLK LORE from *A. thaliana* has been shown to be required for perception of LPS from various bacterial species (Ranf et al., 2015).

Pathogens actively degrade the structural barriers of the plant during the infection process. After the breakdown of plant tissue, certain components can function as danger signals, generally considered as DAMPs, to induce innate immunity (Boller and Felix, 2009). For example, the plant cell wall component oligogalacturonide is perceived by the EGF-repeat containing WAK1 to initiate an immune response (Brutus et al., 2010). Similarly, perception of the endogenous wound-inducible peptide AtPep1 by the LRR-RLKs PEP RECEPTOR 1 (PEPR1) and PEPR2 stimulates plant immune responses (Yamaguchi et al., 2006, Yamaguchi et al., 2010). The lectin-RLK DORN1 has been identified as a receptor for extracellular ATP, and is required for typical PAMP-induced immune responses (Choi et al., 2014). Recently, LecRK-I.8 has been identified in *A. thaliana* to bind extracellular NAD^+ contributing to basal resistance against bacterial pathogens (Wang et al., 2017).

1.4.2 Recognition of bacterial flagellin

The bacterial flagellum is a long, thin filament extending from the cell surface, is composed of up to 20,000 molecules of flagellin proteins (FliC) and is a major driver of bacterial motility (Ramos et al., 2004). Flagellin has a conserved internal part that builds the architecture of the filamentous flagellum, and a surface exposed variable domain that differs in length between species with a molecular mass range from 28 to 80 kDa in the case of FliC (Ramos et al., 2004). Given its abundance and importance to bacterial life, flagellin is a potent elicitor of the innate immune systems of animals and plants (Fliegmann and Felix, 2016). In pathogenic species, flagellar motility is an important factor for colonization and virulence (Finlay and Falkow, 1997). Interestingly, the innate immune systems of both animals and plants independently evolved PRRs to detect bacterial flagellin (Figure 1.4) (Fliegmann and Felix, 2016). Plant FLS2 receptor and mammalian TOLL-LIKE RECEPTOR 5 (TLR5) bind specific epitopes of flagellin and trigger an immune response (Smith et al., 2003, Gomez-Gomez and Boller, 2000). The C- and N-terminus of FliC are embedded in the inner core forming the architectural structure of the flagellum and are therefore highly conserved in many species (Ramos et al., 2004). FLS2 specifically recognizes flg22, a highly conserved region in the N-terminus of the protein comprising a sequence of 22-amino acid residues (Felix et al., 1999,

Gomez-Gomez et al., 1999), whereas mammalian TLR5 detects the conserved D1 domain on flagellin monomers (Smith et al., 2003).

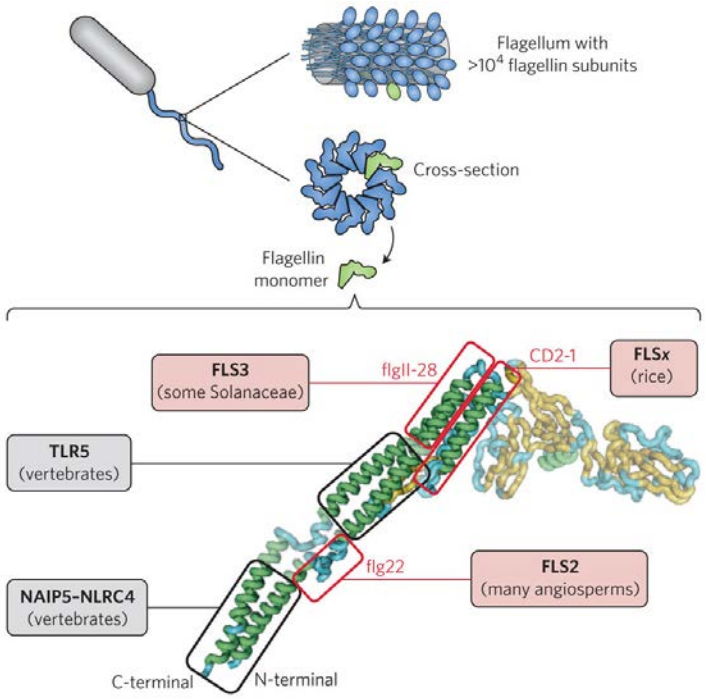

Figure 1.4. Distinct epitopes of flagellin are recognized by different PRRs from plants and animals. Bacterial flagellum is composed of multiple flagellin subunits. PAMP epitopes are recognized by plant PRRs (outlined in red), such as FLS2 in many angiosperms, FLS3 in tomato and other *Solanaceae* and the yet unknown FLSx in rice. Vertebrate PRRs TLR5 and NAIP5-NLRC4 perceive two distinct epitopes in the conserved domains (outlined in black). Figure originally from (Fliegmann and Felix, 2016).

The 22-amino acids of the flg22 peptide represent an elicitor-active epitope of flagellin. Hence, many studies about plant immunity and immune signalling use the synthetic peptide flg22 based on the sequence of *Pseudomonas aeruginosa*, instead of the complete bacterial flagellin to elicit the plant immune system. Flagellin proteins may be cleaved or degraded during the infection process to reveal the immunogenic epitope (Felix et al., 1999, Gomez-Gomez et al., 1999, Gomez-Gomez and Boller, 2000). Flg22 recognition seems to be conserved in most plant species and functional FLS2 orthologues have been characterized in rice (*Oryza sativa*) (Takai et al., 2008), *Nicotiana benthamiana* (Hann and Rathjen, 2007), tomato (*Solanum lycopersicum*) (Robatzek et al., 2007) and grapevine (*Vitis vinifera*) (Trda et al., 2014). However, differences in the specificity of flg22 recognition have been discovered. Shortened or modified flg22 peptides have revealed a differing elicitation potential. While the truncated flg15 peptide acts as an agonist in tomato, it has an antagonistic effect in *A. thaliana* (Felix et al., 1999, Bauer et al., 2001). Mutagenesis studies on FLS2 ectodomains

defined the species-specific LRRs involed in flg22 recognition (Dunning et al., 2007, Mueller et al., 2012). Together, functional and structural studies revealed that the flg22-FLS2 recognition system follows the address-message concept, in which the N-terminus of flg22 is required for binding and the C-terminus for receptor activation (Meindl, 2000, Sun et al., 2013).

Several studies have shown that perception of the same PAMP epitope varies quantitatively in different plant species and ecotypes (Albert et al., 2010, Veluchamy et al., 2014). For example, extensive variation in flg22 perception has been observed across a large set of *A. thaliana* accessions and *Brassicaceae* relatives. Both variability of FLS2 and of the signalling components downstream of receptor activation seem to contribute to quantitative variation in plant populations (Vetter et al., 2016, Vetter et al., 2012).

Interestingly, plants seem to be able to recognize multiple epitopes within flagellin. Genome analysis of multiple field-isolated *P. syringae* strains revealed a domain of flagellin consisting of 28-amino acids, called flgII-28, that is under high positive selection pressure (Cai et al., 2011). The flgII-28 peptide triggers ROS in tomato leaves as well as stomatal closure, and confers induced resistance to *Pto* DC3000 when infiltrated into plant leaves before spray infection with the pathogen (Cai et al., 2011). The *Solanaceae*-specific FLS3 has been identified as the receptor for flgII-28 peptide in tomato (Figure 1.4) (Hind et al., 2016). Furthermore, rice plants are able to detect an additional epitope of approximately 35 amino acid residues, termed CD2-1, in the C-terminal half of flagellin from the pathogen *Acidovorax avenae* (Figure 1.4) (Katsuragi et al., 2015). This indicates that at least three flagellin perception systems exist in plants. However, the corresponding receptor detecting the CD2-1 epitope in the flagellin protein has not yet been identified. Together, these findings indicate that at least two flagellin perception systems seem to co-exist in tomato and in rice, where they would maximise plant defence and reduce the chance of PAMP evasion.

1.4.3 Role of flagellin recognition in plant immunity

The role of flagellin for recognition in resistance of *A. thaliana* towards pathogenic bacteria has been examined in several studies. Growth of the virulent pathogen *Pto* DC3000 after spray infection was restricted on *A. thaliana* ecotype L*er*-0 plants carrying flagellin receptor FLS2 compared to *fls2* mutants (Zipfel et al., 2004). Similarly, the ecotype Ws-0, which is a natural *fls2* mutant and is more susceptible to *Pto* DC3000, but can be complemented by expression of a functional FLS2, thereby restricting pathogenic growth (Zipfel et al., 2004). This study presented the first evidence that PAMP detection affects bacterial virulence by

demonstrating that the lack of receptor benefits bacterial growth. Flagellin recognition by FLS2 has also been shown to contribute to resistance to non-host pathogens in *A. thaliana*. The tobacco pathogen *P. syringae* pv. *tabaci* (*Ptab*) Δ*fliC* mutant lacking the flagellin gene *fliC* could elicit disease symptoms and multiply in non-host *A. thaliana* plants compared to the avirulent wild-type strain (Li et al., 2005). Furthermore, the bean pathogen *P. syringae* pv. *phaseolicola* RW60 and a *Pto hrpA*$^{-}$ mutant lacking the type-3 secretion system (T3SS), which are both considered as non-host pathogens, showed enhanced growth and elicited stronger disease symptoms on L*er*-0 wild-type compared to the *fls2* mutant (de Torres et al., 2006). FLS2 has been identified as a genetic determinant for basal resistance against compatible, non-host and non-pathogenic *P. syringae* in *A. thaliana* and *N. benthamiana* (Hann and Rathjen, 2007, Forsyth et al., 2010). Furthermore, suppression of FLS2-mediated immunity by type-3 secreted effectors and by coronatine are important for successful *Pto* DC3000 infection of *A. thaliana* (Hann and Rathjen, 2007, Zeng and He, 2010). Together, these studies strongly indicated the biological function of flagellin detection in plant defence, and the importance of flagellin perception to confer resistance against non-adapted and adapted *Pseudomonas* pathogens.

Remarkably, *Pto* DC3000 Δ*fliC* showed similar growth as the wild-type strain after inoculation of *A. thaliana* by infiltration (Clarke et al., 2013). In contrast, two *Ptab* Δ*fliC* and Δ*motABCD* mutants; defective in flagella and flagellar motor proteins respectively, are both impaired in motility and show reduced virulence in tobacco leaves (Ichinose et al., 2003, Kanda et al., 2011, Ichinose et al., 2013). The contribution of flagellar motility to bacterial virulence seems to differ between the *Pseudomonas* species *Pto* DC3000 and *Ptab*. Likewise, the importance of flagellin recognition to basal resistance might be species-dependent. A study focussing on flagellin from *Xanthomonas campestris* pv. *campestris* (*Xcc*) revealed that a single amino acid residue in the flg22 sequence of a *Xcc* strain determined the elicitation capacity of FLS2-dependent immune response in *A. thaliana*. Isogenic *Xcc* strains expressing eliciting-active or -inactive flagellin variants grew similarly on *A. thaliana,* independent of the infection method (Sun et al., 2006). The authors stated that possession of eliciting flagellin is not sufficient to restrict the growth of virulent *Xcc* in *A. thaliana,* and concluded that plant-microbe interactions involve multiple layers of defence and counterdefence that shape the specific outcome of a natural infection, and might vary between respective host and pathogen species (Sun et al., 2006). Furthermore, particular experimental conditions might be necessary to visualize the contribution of flagellin to basal resistance. Reduced growth of the pathogen *Pto* DC3000 due to flg22 recognition was only observed when the plants were

infected by spraying the pathogen on the leaf surface but not by infiltration into the apoplast (Zipfel et al., 2004, Zeng and He, 2010). Defence against the adapted pathogen *Pto* DC3000 might only be effective when the flg22-triggered immune response is activated in an early stage of the colonisation process. By infiltrating the bacteria into the plant tissue, the initial hurdles, such as stomatal immunity, are bypassed and further defensive action is not efficient enough to prevent infection. Additionally, other elicitors beside flagellin are present during the infection and may affect the outcome of the interaction.

1.5 PTI signalling

After extracellular ligand perception, intracellular signal transduction activates defence responses. Numerous elements have been identified that initiate signalling cascades and control proper functioning of the immune receptor complexes at the plasma membrane, including co-receptors, regulatory proteins and downstream substrates of signal transduction (Couto and Zipfel, 2016). The immune receptor FLS2 represents a paradigmatic example of research on PTI signalling in *A. thaliana*. The ectodomain of FLS2 can directly bind flg22 peptide, mediating intracellular immune signalling through auto- and transphosphorylation events with other components of the receptor complex, such as the co-receptor BRASSINOSTEROID INSENSTITIVE 1-ASSOCIATED RECEPTOR KINASE 1 (BAK1) (Chinchilla et al., 2007, Heese et al., 2007, Schulze et al., 2010, Schwessinger et al., 2011). BAK1 (also called SERK3) belongs to the SOMATIC-EMBRYOGENESIS RECEPTOR-LIKE KINASE (SERK) family and is also involved in plant development through its association with the brassinosteroid (BR) receptor BR INSENSITIVE 1 (BRI1) (Li et al., 2002, Nam and Li, 2002). After ligand perception, FLS2 immediately oligomerizes with BAK1 and SERKs (Schulze et al., 2010, Roux et al., 2011). Co-crystallization of flg22 peptide together with FLS2 (which has 28 LRRs) and BAK1 (which has 5 LRRs) ectodomains gave further insight into the PAMP perception mechanisms (Sun et al., 2013). The crystal structure revealed that flg22 interacts with FLS2 in a binding groove formed by 14 LRRs and that the flg22 C-terminus is sandwiched between FLS2 and BAK1, suggesting that the ligand facilitates complex formation and acts as a molecular ‘glue’ between both receptors (Sun et al., 2013). Although BAK1 is not required for flg22 binding to FLS2, it is an essential co-receptor that is required for full signalling activation. BAK1 complex formation with FLS2 after flg22 treatment results in transphosphorylation events and activation of downstream responses (Chinchilla et al., 2007, Schulze et al., 2010, Schwessinger et al., 2011, Roux et al., 2011, Sun et al., 2013, Heese et al., 2007). BAK1 also forms heteromers with EFR in a ligand-dependent manner and

positively regulates FLS2-, EFR- and PEPR1/2-mediated responses (Roux et al., 2011, Schwessinger et al., 2011). Furthermore, enhanced pathogen growth in BAK1-defective *A. thaliana* and *Nicotiana benthamiana* plants underline the major role of BAK1 in plant immunity (Heese et al., 2007, Roux et al., 2011, Chaparro-Garcia et al., 2011).

Beside its role in BR signalling and PTI, BAK1 is involved in programmed cell death (PCD) regulation, together with its closest paralogue BAK1-LIKE1 (BKK1)/SERK4 (Kemmerling et al., 2007, He et al., 2007). BKK1 seems to act partially redundantly with BAK1 in PTI signalling since BKK1 also interacts with FLS2 and EFR after PAMP treatment (Roux et al., 2011). However, the *bak1-4 bkk1-1* double mutant exhibits pleiotropic defects in development and spontaneous cell death resulting in seedling lethality (He et al., 2007). The discovery of the BAK1 allele *bak1-5*, which is specifically impaired in PTI, but not in BR signalling or PCD control, allowed scientists to uncouple the function of BAK1 in PTI from the other pathways (Schwessinger et al., 2011). Subsequently, the non-lethal *bak1-5 bkk1-1* double mutant was shown to be less sensitive to flg22, elf18, AtPep1 than the *bak1-5* single mutants (Roux et al., 2011).

Activated PRR complexes transduce the signal to initiate diverse cellular PTI responses. A family of receptor-like cytoplasmic kinases (RLCKs) containing *BOTRYTIS* INDUCED KINASE 1 (BIK1), AVRPPHB SUSCEPTIBLE 1 (PBS1), PBS1-LIKE 1 (PBL1), and PBS1-LIKE 2 (PBL2) interact with FLS2 and possibly with BAK1 (Lu et al., 2010, Zhang et al., 2010). After flg22 perception, BIK1 is activated through transphosphorylation with the FLS2-BAK1 receptor complex and subsequently released from the complex, propagating signalling by phosphorylation of downstream components. The importance of the BIK1 subfamily members in PAMP signalling was confirmed genetically, as *bik1*, *pbs1* and *pbl1* mutants showed defective PTI responses to flg22, elf18, AtPep1 and chitin (Lu et al., 2010, Liu et al., 2013, Zhang et al., 2010). Furthermore, *bik1* plants are impaired in flg22-induced resistance and are more susceptible to non-virulent *Pseudomonas syringae* pv. *tomato* (*Pto*) DC3000 *hrcC*$^{-}$, a mutant lacking the T3SS (Zhang et al., 2010). In addition, BIK1 is also involved in ethylene (ET) signalling and resistance to the necrotrophic pathogen *Botrytis cinerea* (Laluk et al., 2011, Liu et al., 2013). Several other RLCKs (e.g. PCRK1, BSK1) are also involved in PTI signalling (Figure 1.3) (Couto and Zipfel, 2016).

Some kinases of the immune receptor complex are also part of other signalling pathways. Beside the particular composition of the receptor complex, a distinctive phosphorylation pattern of receptor kinases and associated elements might determine the specificity of the signalling pathway (Schwessinger et al., 2011, Couto and Zipfel, 2016). Conclusions made

from studying FLS2 signalling complexes may also be applicable to other RLK signalling pathways, as common components are involved in different signalling complexes. Interestingly, heterologuous expression of *AtEFR* in *N. benthamiana* or in tomato plants, which lack an endogenous EF-Tu perception system, conferred responsiveness to elf18/26 and resistance to multiple plant pathogens (Zipfel et al., 2006, Lacombe et al., 2010). This demonstrates that the elements downstream of EFR activation are conserved in different plant families. However, other PRR-PAMP systems, such as chitin perception in *A. thaliana* and rice, show differences between individual plant species regarding signal perception and signal transduction mechanisms (Couto and Zipfel, 2016).

1.5.1 Immune responses after signal activation

Immune signalling is initiated through activation of PRRs at the plasma membrane, which associate with cytoplasmic partners such as RLCKs, NADPH oxidases, MAPKs or calcium-dependent protein kinases (CDPKs) and activate an array of PTI signalling outputs (Figure 1.3) (Couto and Zipfel, 2016). Plants with mutations in central components of the immune signalling pathways are compromised in specific immune responses triggered by PAMP perception and are usually more susceptible to infection with pathogens.

Early signalling events after PAMP perception have been studied extensively and used as hallmarks for PTI responses (Boller and Felix, 2009, Yu et al., 2017). Within minutes of perception, plant cells respond with changes of ion fluxes, which lead to membrane depolarization and a transient influx of cytosolic Ca^{2+} from the apoplast that probably serves as second messenger to activate CDPKs and further downstream responses (Seybold et al., 2014). Although the actual channel(s) mediating PAMP-induced Ca^{2+} influx remain to be discovered, pharmacological inhibition of Ca^{2+} channels before PAMP treatment resulted in a strong reduction of other immune responses such as ROS production, MAPK activation and defence gene induction in *N. benthamiana* (Segonzac et al., 2011, Ranf et al., 2011) and similarly in *A. thaliana* (Kwaaitaal et al., 2011). The PRR complex associated RLCKs BIK1 and PBL1 are required for the cytosolic Ca^{2+} burst (Ranf et al., 2014, Monaghan et al., 2015, Li et al., 2014).

The PAMP-triggered oxidative burst is characterized by a rapid and transient production of ROS by the NADPH oxidase RBOHD in *A. thaliana* and the homologous RBOHB in *N. benthamiana* (Zhang et al., 2007, Segonzac et al., 2011, Nühse et al., 2007). The ROS burst may have various functions: directly harming microbes as a local toxin, contributing to cell wall cross-linking as a defence mechanism, and/or inducing defence responses as secondary

stress signals (Torres, 2010). RBOHD enzymes localize at the plasma membrane and have a C-terminal cytoplasmic extension with two Ca^{2+} binding EF-hand domains. Regulation of AtRBOHD in response to external stimuli has been linked to phosphorylation and calcium binding of the enzyme (Ogasawara et al., 2008, Torres, 2010). Interestingly, upon PAMP treatment BIK1 phosphorylates RBOHD at specific sites in a calcium-independent manner enhancing PAMP-induced ROS burst and contributing to antibacterial immunity (Li et al., 2014, Kadota et al., 2014), again highlighting the central role of BIK1 during PTI signalling in *A. thaliana*.

Another early response after PAMP treatment is the initiation of MAPK cascades, which leads to activation of transcription factors and massive changes in gene expression (Lee et al., 2015). MAPK cascades consist of hierarchically ordered protein kinases that are activated by sequential phosphorylation events. The four enzymes MPK3, MPK4, MPK6 and MPK11 have been identified to play a role in PTI signalling in *Arabidopsis* (Meng and Zhang, 2013). The closely related MPK3 and MPK6 directly activate various WRKY transcription factors upon flg22 treatment (Asai et al., 2002). WRKY transcription factors are key players in the regulation of defence-related gene expression and act as positive or negative regulators on W-box sequences in the promoters of various pathogen-related genes (Pandey and Somssich, 2009). Almost 1,000 genes are induced and approximately 200 genes are down-regulated within 30 minutes following flg22 or elf26 treatment (Boller and Felix, 2009).

An example of the outcome of transcriptional reprogramming is the deposition of callose, a β-1,3-glucan polymer, at the infection site. Callose deposition is thought to reinforce the cell wall, however its specific mechanism conferring resistance against bacteria is not really understood (Boller and Felix, 2009). Mutant plants lacking the callose synthase PMR4 are more susceptible to *Pto* DC3000 *hrcC*$^-$ indicating that PMR4-dependent callose deposition contributes to antibacterial immunity (Kim et al., 2005).

One of the main entrance points for bacteria to the inside of plant tissue are natural openings such as stomata (Melotto et al., 2008). Closure of stomata upon PAMP perception is a typical response of PTI and loss of PAMP-induced stomatal closure increases susceptibility to bacterial pathogens (Melotto et al., 2008, Zeng and He, 2010). Interestingly, the plant pathogen *Pto* DC3000 produces the phytotoxin coronatine, which counteracts stomatal closure and promotes bacterial virulence (Melotto et al., 2008, Zeng and He, 2010).

Although these cellular responses are widely used in research as characteristics of plant defence, the underlying mechanisms and biological functions are not clear in every case. The

goal of future research is to understand how activation of PRR complexes is linked to the execution of immune responses and the establishment of immunity.

1.5.2 Activation of PTI by beneficial bacteria

PAMP perception and PTI signalling are well established for plant-pathogen interactions. Given that PAMPs are universal microbial signatures, they are also a feature of beneficial microbes. Increasing evidence suggests that symbiotic rhizobia and endophytic PGPR are initially recognized as potential invaders by the plant (Zamioudis and Pieterse, 2012, Cao et al., 2017). Association of plants with beneficial bacteria usually takes place in the rhizosphere and PTI signalling in roots seems to function similarly to foliar tissues. In roots, the PAMPs/DAMPs flg22, chitin, PGN and Pep1 trigger a similar response as in the shoot, including ROS production, MAPK phosphorylation, callose deposition and defense gene transcription (Millet et al., 2010, Poncini et al., 2017, Wyrsch et al., 2015). Interestingly, *A. thaliana* roots do not respond to the PAMP elf18 (Wyrsch et al., 2015, Millet et al., 2010). This demonstrates that there can be differences in PAMP perception and immune signalling between plant organs. Expression studies showed that *A. thaliana* roots express *FLS2,* but not *EFR* (Robatzek et al., 2006, Wyrsch et al., 2015, Beck et al., 2014). Transcription of a PAMP-inducible marker gene and typical immune responses were observed in *A. thaliana* roots after flg22, peptidoglycan and chitin application (Millet et al., 2010). Furthermore, heat-killed bacteria of a non-pathogenic *P. fluorescens* strain activated PTI responsive genes and callose deposition in roots (Millet et al., 2010). Other elicitors such as cell wall preparations, flagellin, siderophores and LPS originating from selected ISR-eliciting rhizobacteria had the potential to induce early immune responses in tobacco suspension cells (van Loon et al., 2008). Symbiotic rhizobia also trigger PTI, as *Mesorhizobium loti* triggers defence-associated responses in the legume *Lotus japonicus*, such as ethylene production, MAPK activation and defence gene transcription in a similar way to flg22 peptide (Lopez-Gomez et al., 2012). Transcriptomic studies in different legume species reported initial upregulation of defence-related genes upon first encounter with its rhizobial symbiont and downregulation during the onset of symbiosis (Lohar et al., 2006, Libault et al., 2010, Breakspear et al., 2014). Overall, this indicates that rhizobia trigger an immune response at the beginning of the symbiotic process (Cao et al., 2017). Hence, similar to pathogenic bacteria, beneficials seem to employ elaborate strategies to evade recognition or suppress the immune response of the host.

1.6 Evasion and suppression of plant immunity

Pathogens need strategies to overcome resistance and to cause disease in plants. Successful infection of many plant pathogens depends on the secretion of diverse virulence factors such as enzymes, toxins and other host manipulating molecules to the extracellular environment or directly into the host cytosol. The secretion of effector proteins to suppress host plant immunity has been extensively studied (Macho and Zipfel, 2015, Win et al., 2012). Besides the secretion of effector proteins, *Pto* DC3000 employs phytotoxins, plant hormones, EPS and detoxification enzymes to suppress plant immunity and to increase virulence (Ichinose et al., 2013, Xin and He, 2013). Beneficial bacteria might possess comparable abilities to overcome plant immunity including the deployment of effectors, EPS and modulation of the plant hormone system (Zamioudis and Pieterse, 2012, Loper et al., 2012). Besides active interference with PTI signalling, bacteria have evolved ways to circumvent PAMP detection by diversifying or modifying PAMP structures or sequences (Pel and Pieterse, 2013, Trdá et al., 2015). Post-translational modifications of PAMPs, such as glycosylation of flagellin, seems to be ubiquitous among different bacteria and contributes to their virulence, possibly due to evasion of PAMP recognition (Taguchi et al., 2003, Takeuchi et al., 2003, Hirai et al., 2011). Modulation of PAMP expression or accumulation was reported in several studies. A flagellin deletion mutant of the non-adapted *P. syringae* pv. *tabaci* shows increased virulence on the nonhost *A. thaliana* compared to wild-type (Li et al., 2005). Similarly, deletion of the flagellar gene cluster was observed in field populations of *X. fuscans* pv. *fuscans*, which were non-motile but remained pathogenic on bean, suggesting an fitness advantage (Darrasse et al., 2013). Furthermore, various bacteria secrete the alkaline protease AprA to degrade excess flagellin monomers released during plant infection (Pel et al., 2014, Bardoel et al., 2012).

In the following section, I will summarize how allelic variation of PAMPs, secretion of effector proteins and EPS production help bacteria evade plant immunity.

1.6.1 Allelic variation of PAMPs

The innate immune system often targets for recognition microbial epitopes that are indispensable, evolutionarily conserved, and widely distributed. PAMPs are often highly conserved microbial structures. This allows the plant to detect a wide range of microbes with a limited set of PRRs. It is easy to imagine that selective pressure imposed by host-defence responses on the bacteria would lead to structural alterations resulting in avoidance of recognition. However, such alterations could result in a fitness cost, as PAMPs fulfil essential or vital cellular functions in the microbe. Hence, there are two opposing selective forces that

shape the evolution of PAMPs, with the outcome differing for each PAMP and species (McCann et al., 2012, Pel and Pieterse, 2013).

Although many bacteria have identical N-terminal sequences of EF-Tu proteins, some plant-associated species show diversity in the 18 amino acids of the immunogenic epitope elf18 compared to the reference sequence of *E. coli* (Kunze et al., 2004, Lacombe et al., 2010). The elf18 epitope of the plant pathogens *X. fastidiosa, Pto* DC3000 and selected *Xcc* strains are polymorphic with four to five amino acid changes, and exhibit strongly reduced eliciting activity on *A. thaliana* (Kunze et al., 2004). The allelic diversity of elf18 epitopes represent a hint that even highly conserved structures like the EF-Tu protein can be adapted to evade immune recognition.

Flagellin is widespread among many bacterial species and it seems to be the major elicitor of PTI in plant infections with *Pto* DC3000 (Smith and Heese, 2014). Interestingly, several bacterial species, such as *Agrobacterium tumefaciens*, *Sinorhizobium meliloti* (Felix et al., 1999), *Xanthomonas campestris pv. campestris* (*Xcc*) (Wozniak et al., 2003, Sun et al., 2006), *Mesorhizobium loti* (Lopez-Gomez et al., 2012) and *Pseudomonas cannabina* pv. *alisalensis* (formerly *P. syringae* pv. *maculicola*) ES4326 (Clarke et al., 2013) show non-synonymous mutations in the immunogenic epitope flg22 of the flagellin encoding gene *fliC* and are not recognized by AtFLS2. Furthermore, it has been suggested that alteration in the flg22 sequence of the PGPR *Burkholderia phytofirmans* represents an adaptation to avoid recognition by FLS2 in the grapevine host (Trda et al., 2014). Thus, the natural variation of flg22 sequence may be due to evolutionary pressure to avoid recognition and shape the outcome of plant-bacteria interactions.

Variation of flg22 sequence could not only be observed between different species, but also within different strains of a single species. As described above, flg22 alleles of *Xcc* strains show differences in their defence activation potential (Sun et al., 2006). A single amino acid change in the flg22 sequence is sufficient to attenuate or eliminate perception of flg22 by FLS2 in *A. thaliana* (Sun et al., 2006). However, the mutation had no effect on pathogen growth during infection.

A comparative genome analysis of multiple isolates from the 1960s and today, collected in different locations around the world, gave new insights into the microevolution of the plant pathogen *P. syringae* (Cai et al., 2011). The two immunogenic flagellin domains flg22 and flgII-28 are under strong selective pressure, since diverse alleles of both domains have been found with differing immunogenic potential (Cai et al., 2011). It appears that an ancestral flgII-28 allele was completely replaced by a newly derived, less immunogenic variation in

most contemporary *Pto* DC3000 populations worldwide, suggesting that the pathogen continuously adapts to the host by minimizing its recognition by the tomato immune system (Cai et al., 2011). Furthermore, allelic variations of flg22 were found in different populations of *Pto* DC3000 exhibiting lower elicitation potential compared to the known epitope of *Pto* DC3000, which is similar to the reference flg22 epitope of *P.* aeruginosa, flg22^{Pa}, and is a strong elicitor (Cai et al., 2011). This study indicates that growth of successful pathogens might be limited by PTI and pathogens are under selection pressure to further minimize PAMP recognition (Cai et al., 2011). The importance of allelic diversity in flg22 and flgII-28 in evading plant immunity was addressed in a study by the same group using purified peptides and a *Pto* Δ*fliC* mutant complemented with different *fliC* alleles (Clarke et al., 2013). The allelic diversity in *fliC* did not affect growth of *Pto* DC3000 in tomato; however, differences in disease development were observed. Yet, bacterial growth was significantly compromised in *A. thaliana* when *Pto* DC3000 carried a flgII-28 allele with a single amino acid mutation. *fliC* alleles differing in immunogenic potential were all expressed under control of their native promoters and in the same genetic background of *Pto* Δ*fliC,* ruling out further effects due to genetic variability. Furthermore, *in vitro* assays confirmed that the strains showed similar motility (Clarke et al., 2013).

Accumulating evidence suggests that *Rhizobium* bacteria evade plant immunity during the symbiotic infection process (Cao et al., 2017, Gourion et al., 2015). The flg22 epitope of the legume symbiont *Sinorhizobium meliloti*, flg22^{Sm}, is divergent in the otherwise conserved domain and does not elicit typical defence responses in plants (Felix et al., 1999). Neither crude flagellin extract nor synthetic flg22^{Sm} peptide are able to trigger a ROS burst in *A. thaliana* (Felix et al., 1999). Additionally, it has been shown that *Lotus japonicus* is able to detect flg22^{Pa}, but not the purified flagellin from its symbiont *Mesorhizobium loti*, which suggests that LjFLS2 is unable to perceive flagellin from the symbiotic partner (Lopez-Gomez et al., 2012). Activation of flg22-triggered immunity through external application of immunogenic flg22^{Pa} during symbiosis negatively affects nodulation at an early stage (Lopez-Gomez et al., 2012). Plant defence responses led to reduced rhizobial infections and delayed nodule organogenesis. However, flg22^{Pa} had no effect on the formation of nodules once the symbiosis was established (Lopez-Gomez et al., 2012). These findings strongly suggest that *Rhizobia* have evolved to escape detection by FLS2. Reduced stimulation of plant defence might have provided an evolutionary advantage to establish the mutualistic interaction.

A systematic approach to discover proteinaceous PTI elicitors took advantage of the contrasting selection forces imposed on PAMPs (McCann et al., 2012, Mott et al., 2016).

Screening of six bacterial plant pathogen genomes (three *P. syringae* and three *X. campestris* pathovars) for positively selected residues in a domain of strong negative selection led to the identification of several candidate elicitors that were subsequently validated in functional and cellular immune assays (McCann et al., 2012). In a similar and more extensive approach, the authors compared the genomes of 54 *P. syringae* strains and identified six new proteinaceous elicitors of plant immunity. A xanthine/uracil permease with its immunogenic epitope xup25 was successfully characterized as the ligand for the *A. thaliana* LRR-RLK XPS1 (Mott et al., 2016).

Together, the studies described above highlight PAMP diversity, such as flagellin, in natural bacterial isolates. Furthermore, they indicate that allelic diversity in immunogenic *fliC* domains is an efficient way in overcoming PTI. This underlines the importance of PAMP recognition defining the outcome of plant-microbe interactions.

1.6.2 Bacterial type-3 secreted effectors

A common strategy for all groups of pathogenic microbes to suppress PTI is the secretion of effector proteins. There are at least six secretion systems employed by Gram-negative bacteria to deliver proteins into the extracellular environment or directly into a recipient cell. These secretion pathways, type I to type VI, differ significantly in their composition, recognition of cargo and function (Chang et al., 2014). The T3SS, in particular, plays an essential role in pathogenicity and specific attention has been dedicated to identify T3SS effector (T3E) repertoires and their biological function. Bacteria secrete effectors during infection into the apoplast, or directly into the cytoplasm using a specialized T3SS (Lindeberg et al., 2012). These T3Es have the ability to alter host cell structures and to promote virulence. Suppressing plant immunity or modifying plant physiology to support pathogen growth are key functions of effectors. Interestingly, particular sets of host processes are frequently targeted by effectors. These effector-targeted pathways (ETP) include the immune system, nutrient distribution and development (Win et al., 2012, Block and Alfano, 2011, Lindeberg et al., 2012). Each *P. syringae* strain can deliver approximately 15-20 effectors into the cell during infection (Block and Alfano, 2011). Notably, mutants defective in the T3SS machinery are not pathogenic in host plants (Collmer et al., 2000). There are many examples of T3Es that specifically interfere with PAMP-induced signal transduction (Macho and Zipfel, 2015). Representative effectors targeting PTI are briefly mentioned: The two *Pto* DC3000 effectors AvrPtoB and AvrPto target several PRRs including FLS2, EFR and BAK1 to suppress PTI by inhibiting kinase activity and by degrading the receptor via ubiquitination in the case of AvrPtoB (Xiang et al., 2008, Shan et al., 2008, Gohre et al., 2008).

Furthermore, HopAI1 functions as a protein phosphothreonine lyase that inactivates MAPK signal transduction (Zhang et al., 2007) and HopAO1, a tyrosine phosphatase, reduces EFR phosphorylation thereby interfering with plant immune signalling (Macho et al., 2014). Notably, two T3SS effector proteins from different pathogens, AvrPphB a cysteine protease from *P. syringae* and AvrAC from *Xcc,* target BIK1 thereby interfering with PTI signalling (Zhang et al., 2010, Feng et al., 2012).

The T3SS is also present in various non-pathogenic and symbiotic rhizobacteria (Preston et al., 2001, Tampakaki, 2014). T3E proteins RopAA, RopM and RopB have been discovered in *P. fluorescens* Q8r1-96 and shown to be capable of suppressing flg22-induced ROS burst in *N. benthamiana* and HR in *N. tabacum* leaves (Mavrodi et al., 2011). Rhizobia also secrete T3Es known as nodulation outer proteins (Nops). These show homology to effectors from pathogenic species and are thought to interfere with biological functions of the host (Deakin and Broughton, 2009). While there is evidence suggesting that rhizobia also use effectors to suppress plant immunity, only few rhizobial effectors (Nop proteins) have been characterized (Staehelin and Krishnan, 2015). *Sinorhizobium* sp. NGR234 translocates multiple T3Es, including NopM, NopL, NopP and NopT to interfere with immune signalling (Skorpil et al., 2005, Dai et al., 2008, Xin et al., 2012b, Ge et al., 2016b). Translocation of Nop proteins into the cytoplasm of plant cells has been confirmed for NopP of *S. fredii* and NopE1 and NopE2 of *Bradyrhizobium japonicum* (Schechter et al., 2010, Wenzel et al., 2010). In contrast to bacterial pathogens, where virulence is largely dependent on a functional T3SS, rhizobial effectors are not essential to establish effective symbiosis between *Rhizobia* and legume plants (Deakin and Broughton, 2009, Viprey et al., 1998, Marie et al., 2003).

1.6.3 Production of bacterial exopolysaccharides

EPS production is a common factor of bacteria colonizing the phyllo- and rhizosphere (Davey and O'Toole G, 2000) and has been associated with evasion or modulation of plant immunity (D'Haeze and Holsters, 2004, Silipo et al., 2010). An important process during plant infection by pathogenic bacteria is colonization of apoplastic spaces, while overcoming plant immune responses. Many plant pathogenic bacteria produce EPS during plant infection (Fett and Dunn, 1989, Brown et al., 1993, McGarvey et al., 1999). The virulence of numerous bacteria species including *P. syringae* and *X. campestris* has been correlated with their ability to produce EPS *in planta* (Fett and Dunn, 1989, Yu et al., 1999, Kemp et al., 2004, Yun et al., 2006).

A mechanistic explanation for the role of EPS in virulence has been suggested by a study showing that EPS interferes with PTI signalling by chelating calcium ions (Ca^{2+}) in the apoplast (Aslam et al., 2008). Infiltration of purified EPS from different species in *A. thaliana* leaves inhibits the PAMP-induced Ca^{2+} influx, ROS burst and defence-related gene expression (Aslam et al., 2008). EPS-defective mutants, for example a *X. campestris* pv. *campestris* (*Xcc*) mutant lacking xanthan or a *Pto* DC3000 mutant lacking alginate, are less virulent compared to wild-type bacterial strains on *A. thaliana*. Importantly, EPS did not impair binding of flg22 to FLS2 (Aslam et al., 2008). Beside its role in suppression of PTI, bacterial EPS production has been associated with protection against H_2O_2 damage (Lehman and Long, 2013) and epiphytic fitness (Poplawsky and Chun, 1998, Yu et al., 1999, Kemp et al., 2004, Dunger et al., 2007).

1.7 Conclusion

Plants have beneficial and pathogenic associations with microbes. Perception of PAMPs leads to PTI that efficiently protects the plant against a broad range of pathogens. Successful pathogens must evolve virulence strategies to overcome PTI and to cause disease. This is often achieved through evasion of PAMP recognition and/or secretion of virulence effectors to suppress PTI. The microbial community in the rhizosphere and phyllosphere critically affect plant physiology and performance. Nitrogen-fixing rhizobia form an intimate symbiosis with the leguminous host. Many other plant-growth promoting rhizobacteria with commensal lifestyles modulate both plant growth and disease suppression. Nonetheless, beneficial bacteria are also exposed to potential immune recognition and must have strategies to evade and/or suppress PTI. The secretion of EPS may be a common strategy applied by pathogenic and commensal bacteria to evade plant immunity. Furthermore, allelic variation in immunogenic epitopes, such as flg22 and elf18, help the bacteria to evade PAMP recognition. It is currently unclear whether the variability in PAMP epitopes observed in various bacteria species reflects an adaptive response underlying the interaction outcome and contributes to the success of the bacteria as pathogens or symbionts.

1.8 Aim of the thesis

It is becoming increasingly evident that the microbiota of rhizosphere or phyllosphere play important roles in the adaptation of the plant to its environment. Both beneficial and pathogenic bacteria potentially elicit plant immunity and must have strategies to evade and/or suppress PTI. Besides the secretion of effector proteins, other factors including EPS

production contribute to a successful bacterial infection. Furthermore, it is currently unclear whether PAMP recognition has an impact on the interaction of plants with beneficial bacteria.

In this thesis, I focus on two complementary projects exploring the molecular interaction between plants with pathogenic, commensal and symbiotic bacteria:

1) I aim to study the role of bacterial exopolysaccharides from *Pseudomonas* during plant infection. The underlying hypothesis is that EPS produced by beneficial and pathogenic bacteria help them to evade and/or suppress plant immune responses. Additionally, I examine the contribution of the bacterial signalling molecule cdG, which controls the transition between sessile and motile lifestyles, including EPS and flagella production, to evasion of plant immunity.

2) The transfer of plant immune receptors detecting pathogen-associated molecular patterns (PAMPs) to crops can increase resistance against pathogens. However, it is currently unclear whether this gain of recognition specificity affects the interaction with beneficial bacteria. To this end, I aim to study the relevance of PAMP recognition, such as of the immunogenic flg22 and elf18 epitopes, during symbiotic plant-rhizobia interactions.

Chapter 2

Materials and methods

2.1 Plants and growth conditions

All plants were grown in soil in single pots in controlled environment rooms with 120-180 µmol m^{-2} s^{-2} light intensity and 75-80% rel. humidity. *A. thaliana* and *N. benthamiana* were grown at 22°C with a 10-hour or 16-hour light period, respectively. *M. truncatula* was grown at 20°C with 16-hour light period.

A. thaliana seeds were sown on Levington F2 compost and vernalized at 4°C for 7 days before germination. Two-week-old seedlings were individually transferred to single pots filled with compost mix containing Levington F2 supplemented with grit and systemic insecticide Exemptor (Bayer CropScience Ltd, Cambridge, UK). The *A. thaliana* mutants and transgenic lines used in this study were produced in the background of the ecotype Columbia (Col-0), and have been described previously as follows: *efr-1* (Zipfel et al., 2006), *fls2c* (Zipfel et al., 2004), *efr fls2* (Zipfel et al., 2006), *bak1-5 bkk1-1* (Schwessinger et al., 2011, Roux et al., 2011), *lym3-1* (Willmann et al., 2011), *cerk1-2* (Miya et al., 2007), *bak1-5 bkk1-1 cerk1-2* (Xin et al., 2016) and *fls2 efr-1 cerk1-2* (Gimenez-Ibanez et al., 2009b).

M. truncatula seeds were scarified with 98% sulfuric acid treatment for 8 min, extensively washed with water and then surface-sterilized with 10% NaOCl for 2 min. After washing with sterile water, the seeds were left for 3 h to imbibe water before being placed on inverted agar plates in the dark for 3 days at 4°C and subsequently germinated over-night at 20°C. For sterile growth, seedlings were transferred to squared 1% water agar plates and sandwiched between two Whatman filter papers (GE Healthcare, UK). Plates were incubated vertically in a growth chamber at 21°C, with a 16h light period and 80% rel. humidity.

For growth in soil, germinated seedlings were transferred to sterile 1:1 mixture of terragreen (Oil-dry UK ltd, UK) and sharp sand (BB Minerals, UK) for rhizobial infections, in loam based compost (John Innes Cereal Mix) for seed bulking, or in Jiffy Peat Pellets for inoculation with *Ralstonia solanacearum*.

2.2 Bacterial strains and growth conditions

Pto DC3000 was grown in King's medium B (KB, protease peptone 20 g/L, glycerol 10%, K_2HPO_4 1.6 g/L)) or L-medium (tryptone 10 g/L, yeast extract 5 g/L, NaCl 5 g/L, D-glucose 1 g/L) at 28°C, Pf-5 in lysogenic broth (LB, tryptone 10 g/L, yeast extract 5 g/L, NaCl 10 g/L) at 28°C and PA01 in LB at 37°C. *S. meliloti* strain 1021 (also known as *Rm*1021) *pXLGD4* p*hemA::lacZ* (*Sm*1021-*lacZ*) (Leong et al., 1985) was grown at 30°C in TY medium (tryptone 5 g/L, yeast extract 3 g/L, $CaCl_2$ 6 H_2O 1.325 g/L) containing appropriate antibiotics,

streptomycin 50 µg/mL and tetracycline 12.5 µg/mL. *R. solanacearum* strain GMI1000 was grown at 28°C in complete BG medium (bacto peptone 10 g/L, casamino acid 1 g/L, yeast extract 1 g/L). *E. coli* was grown in LB medium at 37°C.

Table 2.1. Bacterial species and strains used in this thesis.

Species/strain	Relevant characteristics	Additional information	Antibiotic resistance	Reference or source
Escherichia coli DH5α	Strain used for cloning and plasmid storage			Invitrogen
E. coli S17-1	Conjugation donor strain	*recA pro hsdR* RP4-2-Tc::Mu-Km::Tn7 integrated into the chromosome	Strep, Spec, Trim	(Simon et al., 1983), ATCC 47055
Sinorhizobium meliloti 1021	Wild-type		Strep	(Meade et al., 1982)
S. meliloti 1021 Δ*flaA*	*flaA* deletion strain	Δ*flaA*	Strep	This study
S. meliloti 1021 *flaA-flg22*^{Pa} c1 (Δ*flaA*)	*flaA* deletion strain	*flaA-flg22*^{Pa} allele was introduced into Δ*flaA* background, but was excised during second homologous recombination	Strep	This study
S. meliloti 1021 *flaA-flg22*^{Pa} c5	flg22 allele replacement strain	*flaA-flg22*^{Pa} allele was introduced into Δ*flaA* background	Strep	This study
S. meliloti 1021 *flg22*^{Pa} c2	flg22 allele replacement strain	*flg22*^{Pa} allele was introduced into wild-type background	Strep	This study
S. meliloti 1021 *flg22*^{mod} c5	flg22 allele replacement strain	*flg22*^{mod} allele was introduced into wild-type background	Strep	This study
S. meliloti 1021-lacZ	Constitutive lacZ expression	*pXLGD4* p*hemA::lacZ*	Strep, Tet	(Leong et al., 1985)
Ralstonia solanacearum GMI1000	Wild-type			(Salanoubat et al., 2002)
Pseudomonas syringae pv. *tomato* (*Pto*) DC3000	Wild-type		Rif	(Cuppels, 1986)
Pto DC3000 Δ*alg*	Alginate deficient strain	Δ*algG* Δ*algX*	Rif	This study
Pto DC3000 Δ*psl*	Psl deficient strain	Δ*pslD* Δ*pslE*	Rif	This study
Pto DC3000 Δ*wss*	Wss (acetylated cellulose) deficient strain	Δ*wssB* Δ*wssC*	Rif	This study

Pto DC3000 Δ*alg*/*psl*	See above	Δ*algG* Δ*algX* Δ*pslD* Δ*pslE*	Rif	This study
Pto DC3000 Δ*alg*/*wss*	See above	Δ*algG* Δ*algX* Δ*wssB* Δ*wssC*	Rif	This study
Pto DC3000 Δ*psl*/*wss*	See above	Δ*pslD* Δ*pslE* Δ*wssB* Δ*wssC*	Rif	This study
Pto DC3000 Δalg/*wss*/*psl*	See above	Δ*algG* Δ*algX* Δ*wssB* Δ*wssC* Δ*pslD* Δ*pslE*	Rif	This study
Pseudomonas protegens Pf-5	Wild-type		Carb, Nitr, Nal	(Paulsen et al., 2005, Howell and Stipanovic, 1979)
P. protegens Pf-5 Δ*alg*	Alginate deficient strain	Δ*algG* Δ*algX*	Carb, Nitr, Nal	This study
P. protegens Pf-5 Δ*pel*	Pel deficient strain	Δ*pelB* Δ*pelC*	Carb, Nitr, Nal	This study
P. protegens Pf-5 Δ*psl*	Psl deficient strain	Δ*pslD* Δ*pslE*	Carb, Nitr, Nal	This study
P. protegens Pf-5 Δ*alg/pel*	See above	Δ*algG* Δ*algX* Δ*pelB* Δ*pelC*	Carb, Nitr, Nal	This study
P. protegens Pf-5 Δ*alg/psl*	See above	Δ*algG* Δ*algX* Δ*pslD* Δ*pslE*	Carb, Nitr, Nal	This study
P. protegens Pf-5 Δ*pel/psl*	See above	Δ*pelB* Δ*pelC* Δ*pslD* Δ*pslE*	Carb, Nitr, Nal	This study
P. protegens Pf-5 Δ*alg/pel/psl*	See above	Δ*algG* Δ*algX* Δ*pelB* Δ*pelC* Δ*pslD* Δ*pslE*	Carb, Nitr, Nal	This study
Pseudomonas aeruginosa PA14	Wild-type		Amp, Kan	Robert Ryan, University of Dundee, Dundee, UK
P. aeruginosa PA01	Wild-type		Amp, Kan	(Stover et al., 2000), ATCC 15692
P. aeruginosa PA01 *pelG::Tn5*/Δ*pslAB*	Pel and Psl deficient strain	*pelG::Tn5* Δ*pslAB*	Amp, Kan, Tet, Gent	(Malone et al., 2010)
Agrobacterium tumefaciens GV3101:: *pMP90*	Virus-induced gene silencing	pBINTRA6 - *TRV-RNA1*	Kan, Gent, Rif	(Peart et al., 2002)
A. tumefaciens GV3101:: *pMP90*	Virus-induced gene silencing	pTV00 - *TRV*:*SU*	Kan, Gent, Rif	(Peart et al., 2002)
A. tumefaciens GV3101:: *pMP90*	Virus-induced gene silencing	pTV00 - *TRV*:*GFP*	Kan, Gent, Rif	(Peart et al., 2002)
A. tumefaciens GV3101:: *pMP90*	Virus-induced gene silencing	pYY13 - *NbFls2*	Kan, Gent, Rif	(Saur et al., 2016)
A. tumefaciens AGL1	Plant transformation	*pBIN19-CaMV35S*::*EFR-HA*	Kan	(Lacombe et al., 2010)

Antibiotics abbreviations: Strep, streptomycin; Spec, spectinomycin; Trim, trimethoprim; Rif, rifampicin; Carb, carbenicillin; Nitr, nitrofurantoin; Nal, nalidixic acid; Amp, ampicillin; Kan, kanamycin; Tet, tetracycline; Gent, gentamycin.

2.3 Bacterial transformation and genetic modification

Pseudomonas spp. were transformed by electroporation or conjugation. The *wspR19* allele was obtained from *P. fluorescens* SBW25 *wspR* carrying a R129C mutation resulting in constitutive DGC activity (Goymer et al., 2006). *wspR19* was cloned into a broad-host-range pBBR-MCS2/5 (pBBR2/5) plasmids (Kovach et al., 1995) between the *Bam*HI and *Eco*RI sites. *Pto* DC3000 and *P. protegens* Pf-5 were transformed with pBBR2-*wspR19* or pBBR2 empty vector and grown in medium supplemented with 25 µg/mL kanamycin. *P. aeruginosa* PA01 containing pBBR5-*wspR19* or the pBBR5 empty vector were grown in medium supplemented with 30 µg/mL gentamycin.

Chromosomal gene deletions and allele replacements were made *via* an adaptation of the protocol described elsewhere (Hmelo et al., 2015). Briefly, 500-600 bp homologous flanking regions to the target genes were PCR-amplified and ligated into the suicide vectors pTS1 (NCBI GeneBank: KX931445) (Scott et al., 2017) or pME3087 (NCBI GenBank: KX931444) (Voisard et al., 2007) for *Pseudomonas* transformation. The pTS1 vector is based on pME3087 and additionally contains a *sacB* gene allowing counter-selection on sucrose plates. Constructs for allele replacement in *S. meliloti* were synthesised to exchange the sequence encoding the flg22 epitope of the chromosomal *flaA* gene for $flg22^{Pa}$ (Figure A8.7) and $flg22^{mod}$ (Figure A8.8) into *Sm*1021 wild-type background or to complement *Sm* Δ*flaA* with the full length *flaA*-$flg22^{Pa}$ gene (Figure A8.9). Synthesised constructs were ligated into the pJQ200SK vector (Quandt and Hynes, 1993) and transformed by conjugation using *E. coli* S17-1.

Gene deletion was done by allelic exchange in a two-step homologous recombination process. *Pto* DC3000 was grown over-night in 50 mL L-medium and repeatedly washed in 300 mM sucrose. Cells were transformed with 50-100 ng of the gene deletion constructs in pTS1 vector by electroporation (2 mm electroporation cuvettes; Geneflow Ltd, Lichfield, UK) with 2500 Volt. Subsequently, cells were recovered in 3 mL L-medium incubated at 28°C for 3 h shaking. Colonies with successful homologous recombination leading to chromosomal integration of the plasmid were selected on plates containing 12.5 µg/mL tetracycline. Isolated colonies were grown in 50 mL L-medium overnight and a dilution series was plated on L-medium agar plates containing 5% sucrose to select for cells with a second homologous

recombination event, resulting in excision of the plasmid and in-frame deletion of the respective genes leaving 6-15 bp between the intact start and stop codons.

P. protegens Pf-5 was transformed by conjugation with *E. coli* S17-1 carrying the gene deletion constructs in pME3087 vector. Donor strain *E. coli* S17-1 and recipient *P. protegens* Pf-5 were grown overnight in 5 mL LB medium. Donor and recipient strains were washed, mixed in 1:2 ratio, spotted on sterile filter paper (0.22 µm; Milipore, Watford, UK) placed on LB agar plates and incubated overnight at 30°C. Cell mixture was scrapped off the filter paper, re-suspended, and a dilution series was plated on LB plates containing tetracycline 25 µg/mL and nitrofurantoin 100 µg/mL. Individual colonies were grown overnight in 50 mL LB medium and diluted 1:50 in fresh 5 mL LB medium to counter-select against cells with an integrated plasmid conferring tetracycline resistance. Multiple antibiotics were added to the 5 mL-culture in subsequent steps. Tetracycline was added in bacteriostatic concentration of 5 µg/mL during early exponential growth phase to arrest growth of cells that have lost the integrated plasmid. Tetracycline 5 µg/mL, piperacillin 2 mg/mL and phosphomycin 2 mg/mL were added in the mid exponential growth phase to maintain growth stasis in the tetracycline sensitive population, and to kill actively dividing cells. Next, a dilution series of the culture was plated on LB agar plates and incubated for two days at 30°C. Isolated colonies were re-streaked and tested for tetracycline sensitivity.

S. meliloti 1021 was transformed by conjugation with *E. coli* S17-1 carrying the gene replacement/deletion constructs in the pJQ200SK vector. *Sm*1021 was grown overnight in 10 mL TY medium until saturation and *E. coli* S17-1 in 5 mL LB medium until OD_{600} = 0.6. Donor and recipient strains were washed, mixed in 1:2 ratio, spotted on sterile filter paper (0.22 µm; Merck Millipore, Watford, UK) placed on LB agar plates and incubated overnight at 30°C. Cell mixture was scraped off from the filter paper, re-suspended and dilution series plated on TY plates containing gentamycin 25 µg/mL and nitrofurantoin 100 µg/mL or nalidixic acid 25 µg/mL. Isolated colonies were grown in 50 mL TY culture without antibiotics and counter-selection was done on TY plates containing 5% sucrose. In all cases, deletion strains were confirmed by PCR and sequencing.

Table 2.2. Plasmids used in this thesis.

Plasmid	Relevant characteristics	Additional information	Antibiotic resistance	Reference or source
pBBR-MCS2	Broad host-range vector		Kan	(Kovach et al., 1995)
pBBR-MCS5	Broad host-range vector		Gent	(Kovach et al., 1995)

pME3087	Suicide plasmid	ColE1 origin of replication	Tet	(Voisard et al., 2007)
pTS1	Suicide plasmid	pME3087 derivative, *sacB*	Tet	(Scott et al., 2017)
pJQ200SK	Suicide plasmid	pACYC derivative, P15a origin of replication, *lacZ sacB traJ*	Gent	(Quandt and Hynes, 1993)

Antibiotics abbreviations: Kan, kanamycin; Tet, tetracycline; Gent, gentamycin.

Table 2.3. Oligonucleotide primers used in this thesis.

ID	Name	Sequence (3‘-5‘)	Purpose
532	PFL_1019/8 UPF	CGGGATCCCCGAGTACGAACAGAACG	Pf-5 deletion of PFL_1019 (*algG*) – PFL_1018 (*algX*); (encodes BamHI)
533	PFL_1019/8 UPR	CGTCTAGAAGTAGGCATGTCGGGCAC	Pf-5 deletion of PFL_1019 (*algG*) – PFL_1018 (*algX*); (encodes XbaI)
534	PFL_1019/8 DNF	CGTCTAGAGCGCAGATCGGGCAATGAG	Pf-5 deletion of PFL_1019 (*algG*) – PFL_1018 (*algX*); (encodes XbaI)
535	PFL_1019/8 DNR	CGGAATTCCCATTTGCGCATGGACTTG	Pf-5 deletion of PFL_1019 (*algG*) – PFL_1018 (*algX*); (encodes EcoRI)
536	PFL_2973/4 UPF	CGGGATCCAAGCAGGCGTCGATCAAG	Pf-5 deletion of PFL _ 2973 (*pelB*) – PFL_ 2974 (*pelC*); (encodes BamHI)
537	PFL_2973/4 UPR	CGTCTAGACGCCTTGGCCTTAGTTGC	Pf-5 deletion of PFL _ 2973 (*pelB*) – PFL_ 2974 (*pelC*); (encodes XbaI)
538	PFL_2973/4 DNF	CGTCTAGAGAGTGACTGCCATGAAC	Pf-5 deletion of PFL _ 2973 (*pelB*) – PFL_ 2974 (*pelC*); (encodes XbaI)
539	PFL_2973/4 DNR	CGGAATTCAAGCTCTGGTCGCTGC	Pf-5 deletion of PFL _ 2973 (*pelB*) – PFL_ 2974 (*pelC*); (encodes EcoRI)
540	PFL_4210/1 UPF	CGGGATCCATCATCGACACTCCGGAC	Pf-5 deletion of PFL_4210 (*pslD*) – PFL_4211 (*pslE*); (encodes BamHI)
541	PFL_4210/1 UPR	CGTCTAGATTTCATCGAGCGGTCTTCC	Pf-5 deletion of PFL_4210 (*pslD*) – PFL_4211 (*pslE*); (encodes XbaI)
542	PFL_4210/1 DNF	CGTCTAGATGATGCACATTGCCCTG	Pf-5 deletion of PFL_4210 (*pslD*) – PFL_4211 (*pslE*); (encodes XbaI)
543	PFL_4210/1 DNR	CGGAATTCATCACCACCATCTGCTC	Pf-5 deletion of PFL_4210 (*pslD*) – PFL_4211 (*pslE*); (encodes EcoRI)
598	Pf-5 alg ctrl fwd	GACCCGAACTGGCAAGTG	Confirm gene deletion with outside-outside primers
599	Pf-5 alg ctrl rev	GCAGGTTGTCCCAGTCGC	Confirm gene deletion with outside-outside primers
600	Pf-5 wapR ctrl fwd	GAGGCCTTGCAGCATTCC	Confirm gene deletion with outside-outside primers

601	Pf-5 wapR ctrl rev	CACCAGGCACTCTGCAAG	Confirm gene deletion with outside-outside primers
602	Pf-5 pel ctrl fwd	CACCTGTACTACCACTTC	Confirm gene deletion with outside-outside primers
603	Pf-5 pel ctrl rev	CCAAGAGGCTCAGCTGTG	Confirm gene deletion with outside-outside primers
604	Pf-5 psl ctrl fwd	GTGATGGAGCGCTCGAAG	Confirm gene deletion with outside-outside primers
605	Pf-5 psl ctrl rev	CCCTTGCCGCGGTAGATG	Confirm gene deletion with outside-outside primers
763	Pto alg UPF	CGGGATCCAAGGACTACATCC AGAAC	Deletion of *alg* operon (*algG-algX*) in *Pto* DC3000
764	Pto alg UPR	CGTCTAGAGCTGTTCATCTCTG GCAC	Deletion of *alg* operon (*algG-algX*) in *Pto* DC3000
765	Pto alg DNF	CGTCTAGAGCTGGACTATGAG GTGAC	Deletion of *alg* operon (*algG-algX*) in *Pto* DC3000
766	Pto alg DNR	CGCATATGAAGCAGAGGACAT GCTGC	Deletion of *alg* operon (*algG-algX*) in *Pto* DC3000
767	Pto psl UPF	CGGGATCCATTGCCCAGGAAC TCAAGC	Deletion of *psl* (*pslD-pslE*) operon in *Pto* DC3000
768	Pto psl UPR	CGTCTAGACATCGTTCCTGAGC TCCTG	Deletion of *psl* (*pslD-pslE*) operon in *Pto* DC3000
769	Pto psl DNF	CGTCTAGAATAGGGAGCCGTG GCTGATG	Deletion of *psl* (*pslD-pslE*) operon in *Pto* DC3000
770	Pto psl DNR	CGCATATGGATCACCACCATCT GCGTGG	Deletion of *psl* (*pslD-pslE*) operon in *Pto* DC3000
771	Pto wss UPF	CGGGATCCTTGATGAGCGTCG TTCTC	Deletion of *wss* operon (*wssB-wssC*) in *Pto* DC3000
772	Pto wss UPR	CGTCTAGACGACAGGTTAGTC ATGAC	Deletion of *wss* operon (*wssB-wssC*) in *Pto* DC3000
773	Pto wss DNF	CGTCTAGAGAATAAGTCATGC CGACC	Deletion of *wss* operon (*wssB-wssC*) in *Pto* DC3000
774	Pto wss DNR	CGCATATGAACGGTCTTGAGC AGTGC	Deletion of *wss* operon (*wssB-wssC*) in *Pto* DC3000
789	Pto alg ctrl R	CAGCGGCAGATTGCTCCAGTC	Control deletion of *algG-algX* in *Pto* DC3000; use with Pf-5 alg ctrl F
790	Pto psl ctrl F	GTCGCAGCCAGGACGTCAAG	Control deletion of *pslD-pslE* in *Pto* DC3000
791	Pto psl ctrl R	CAGGCTCGATGGCCACGTTG	Control deletion of *pslD-pslE* in *Pto* DC3000
792	Pto wss ctrl F	GTTGGCCTATGGCTCGCTGC	Control deletion of *wssB-wssC* in *Pto* DC3000

793	Pto wss ctrl R	CAGGCTCGATGGCCACGTTG	Control deletion of *wssB-wssC* in *Pto* DC3000
1001	Sm flaA UPF L	CGGGATCCATGGCGATGTCGGGAATTGC	Deletion of *flaA* in *Sinorhizobium meliloti* 1021
1002	Sm flaA UPF	CGGGATCCTGCAGCTCTTCATCGACATC	Deletion of *flaA* in *Sinorhizobium meliloti* 1021
1003	Sm flaA UPR	GCTCTAGAGCTCGTCATATTCGTTGTCC	Deletion of *flaA* in *Sinorhizobium meliloti* 1021
1004	Sm flaA DNF	GCTCTAGACGCTAAGAAGACATGCAATGG	Deletion of *flaA* in *Sinorhizobium meliloti* 1021
1005	Sm flaA DNF	CGGGATCCGGAAAGGGCCATATTGTCGG	Deletion of *flaA* in *Sinorhizobium meliloti* 1021
1006	Sm flaA DNF L	CGGGATCCGCCGACCGTGTACTCAGA	Deletion of *flaA* in *Sinorhizobium meliloti* 1021
1007	Sm flaA ctrl fwd	CCAATGATTCGCTGATGCTCC	Control of deletion of *flaA* in *Sinorhizobium meliloti* 1021
1008	Sm flaA ctrl rev	GACCTTGACATAATCGCCAGC	Control of deletion of *flaA* in *Sinorhizobium meliloti* 1021
1346	Sm flaA ctrl 2 f	ATCCATCACGAGTTGAGCGG	Test site directed mutagenesis
1347	Sm flaA ctrl 2 r	GTCCGCCATTGCATGTCTTC	Test site directed mutagenesis
1348	Sm flaA ctrl 3 f	CCATCGAAAGGACGGGCTAA	Test site directed mutagenesis
1349	Sm flaA ctrl 3 r	CGGCCGGCAATTTCGAATAT	Test site directed mutagenesis
1073	pJQ200SK -16 fwd	TCACTATAGGGCGAATTG	pJQ200SK plasmid outside MCS
1074	pJQ200SK +27 rev	CACTAAAGGGAACAAAAGC	pJQ200SK plasmid outside MCS
1075	MtFLS2 fwd	CATTGCTGCACTTGGATCTC	Genotyping Medicago Tnt1 transposon line
1076	MtFLS2 rev	AAGGATGTTGGAAGGCTTTAG	Genotyping Medicago Tnt1 transposon line
1077	Tnt1-R fwd	AGTGAACGAGCAGAACCTGTG	Genotyping Medicago Tnt1 transposon line
1078	Tnt1-F rev	AGTGCTACCTCCTCTGGATG	Genotyping Medicago Tnt1 transposon line
Mt1	FLS2 5'end Fwd	AAACCAGGCTCTTTGTGGAG	qPCR Medicago *FLS2*
Mt2	FLS2 5'end Rev	ACAGCAAGAGATCCAAGTGC	qPCR Medicago *FLS2*
Mt3	FLS2 3'end Fwd	TGCAAATGGAACGGAACAGC	qPCR Medicago *FLS2*
Mt4	FLS2 3'end Rev	AGGGTGCAGCACAATGAAAG	qPCR Medicago *FLS2*
Mt5	UBQ Fwd	GCAGATAGACACGCTGGGA	qPCR Medicago *Ubiquitin*
Mt6	UBQ Rev	CAGTCTTCAAAACTCTTGGGCAG	qPCR Medicago *Ubiquitin*
Mt7	PDF2 Fwd	GTGTTTTGCTTCCGCCGTT	qPCR Medicago *PDF2*

Mt8	PDF2 Rev	CCAAATCTTGCTCCCTCATCTG	qPCR Medicago *PDF2*
Mt9	UBQ gDNA Fwd	GCAGATAGACACGCTGGGA	Test for gDNA contamination in Medicago
Mt10	UBQ gDNA Rev	CTCTTGAGCTTGTGGCCAGT	Test for gDNA contamination in Medicago
Mt11	FLS2 gDNA Fwd	AAACCAGGCTCTTTGTGGAG	Test for gDNA contamination in Medicago
Mt12	FLS2 gDNA Rev	AGGGTGCAGCACAATGAAAG	Test for gDNA contamination in Medicago

2.4 Bacterial phenotypic tests

Colony morphologies were examined for 5 µL spots of *Pseudomonas* overnight cultures, after overnight incubation at 28°C on 1.3% agar minimal media (M9 salts, 0.4% pyruvate) plates containing 0.004% Congo Red dye. Pictures were taken with Leica M165 FC microscopy systems (Leica, Wetzlar, Germany). To measure swimming motility, 0.3% KB agar plates containing the appropriate antibiotics were poured and allowed to set and dry for 1 h in a sterile flow chamber. Plates were inoculated with 2 µL spots of *Pseudomonas* overnight cultures, and incubated for two days at room temperature.

Swimming motility in *S. meliloti* 1021 was assessed on TY media or SM media (K_2HPO_4, 100 mg/L, $KH_2PO_4 \cdot 3H_2O$, 400 mg/L, NaCl, 100 mg/L, yeast extract, 400 mg/L, $MgSO_4 \cdot 7H_2O$, 200 mg/L, $CaCl_2 \cdot 2H_2O$, 100 mg/L, glycerol, 0.2%) containing 0.3% agar and allowed to set and dry for 1 h in a sterile laminar flow chamber. One microliter bacterial suspension was stabbed into the agar plates and incubated for 2-4 days at 28°C.

2.5 Bacterial growth measurements

Pto DC3000 was grown in KB or L-medium overnight at 28°C. Growth curves were measured in a 96-well plate reader (Powerwave, BioTek, Swindon, UK) in 150 µL total volume KB or L-medium inoculated 1:50 with bacterial solution (diluted to OD_{600} = 0.1). Optical density measurements were recorded every hour after one minute agitation over a 48-h period at 28°C.

2.6 Preparation of bacterial extracts

Bacteria were grown on KB or LB plates (1.3% agar) containing the appropriate antibiotics. *Pto* DC3000 and *P. protegens* Pf-5 were grown at 28°C for 21 h and 18 h, respectively, and *P. aeruginosa* PAO1 at 37°C for 10 h. Bacteria were scraped off the plates and resuspended in

sterile demineralised ddH_2O. Cells were lysed by boiling at 95°C for 15 min with intermediate vortexing and immediately placed on ice. Bacterial extract was obtained by centrifugation of the lysed cells for 10 min at 13,000 rpm at 4°C, and the supernatant was collected for further analysis. Bacterial extracts were normalized to 5 µg/mL total protein concentration determined using a Bradford assay (BioRad, California, USA) or by NanoDrop (Thermo Fisher Scientific, Waltham, MA, USA) at λ280 nm.

2.7 *Pseudomonas syringae* infections on *Arabidopsis thaliana*

A. thaliana Col-0 and *fls2* plants were grown for 4-5 weeks. *Pto* DC3000 cultures were grown overnight at 28°C in liquid KB media containing 25 µg/mL kanamycin to OD_{600} between 0.6 and 1.0. Bacteria were resuspended in 10 mM $MgCl_2$ and adjusted to OD_{600} = 0.0002 [10^5 colony forming units (CFU) per mL] for syringe infiltration and to OD_{600} = 0.05 (2.5 x 10^7 CFU/mL) for spray inoculation. Shortly before spraying 0.02% Silwet L-77 (Lehle Seeds, Round Rock, USA) was added to the suspension. Plants were sprayed until run-off. Unless otherwise stated, infected plants were covered during the first day of infection with a plastic dome to increase humidity and promote infection. Four different plants per bacterial strain were infected and two leaf discs (7 mm diameter) per plant were collected two or three days post infection in 10 mM $MgCl_2$ and homogenized using a drill-adapted pestle. Serial dilutions were plated on KB or L-medium agar containing 25 µg/mL kanamycin and 25 µg/mL nystatin and colonies counted after two days incubation at 28°C. Equal inoculations with different bacterial strains were confirmed by serial dilution and colony counting of the initial infection suspensions.

2.8 Quantitation of cdG concentrations

The extraction and quantification of cdG was performed using high performance liquid chromatography-coupled tandem mass spectrometry (HPLC-MS/MS) analysis (Spangler et al., 2010). For cdG extraction bacteria were grown on plates, as described for the production of bacterial cell extracts. Cells were scraped off and resuspended in 300 µL of ice-cold extraction solvent, a mixture of acetonitrile/methanol/water (40/40/20, v/v/v) and incubated for 10 min at 4°C to extract nucleotides. The cell suspension was heated to 95°C for 10 min, cooled down and centrifuged at 13,000 x *g* for 5 min. Supernatant was stored and extraction of the resulting pellet was repeated twice with 200 µL of extraction solvent at 4°C, omitting the heating step. The combined supernatants were evaporated until dryness at 40°C in a miVac vacuum concentrator (Genevac, Ipswich, UK) and the dried residue

resuspended in 200 µL water. Protein content was determined by dissolving the cell pellet in 200 µL 0.1 M NaOH, then heating for 15 min at 95°C, before centrifugation and measurement of protein concentration in the supernatant using NanoDrop (Thermo Fisher Scientific, Waltham, MA, USA) at λ280 nm. Final cdG concentrations were expressed as pmol/mg of bacterial protein. Extractions were performed with two independent bacterial cultures as biological duplicates.

Nucleotide extracts were analysed by LC-MS using an Acquity UPLC System attached to a TQS tandem mass spectrometer (Waters, Milford, MA, USA). Separation was performed on a Kinetix XB-C18, 50 · 2.1 mm, 2.6 µm column (Phenomenex, CA, Torrance, USA) using the following gradient of acetonitrile (solvent B) versus 0.1% formic acid in water (solvent A), run at 600 µL/min and 30°C: 0 min, 1% B; 1 min, 1% B; 2.5 min, 25% B; 4 min, 70% B; 4.05 min, 1% B; 5.8 min, 1% B. The retention time for synthetic cdG was 1.21 min. Detection of cdG was by positive electrospray selected reaction monitoring (SRM) of the transition m/z 691/152 at a collision energy of 38 V and cone voltage of 50 V. Spray chamber conditions were 1.8 kV capillary voltage, 600°C desolvation temperature, 1000 L/h desolvation gas flow, 150 L/h cone gas flow, and 7.0 bar nebuliser pressure. Quantitation was done by external standard calibration using chemically synthesised cdG (BioLog, Bremen, Germany) standards from 10 to 5000 ng/mg.

2.9 Measurement of ROS burst

Generation of ROS was measured as previously described (Schwessinger et al., 2011). Eight leaf discs (4 mm diameter) per *A. thaliana* genotype or *N. benthamiana* plant were collected into 96-well plates and allowed to recover overnight in sterile water. The water was then replaced with a solution containing 17 mg/mL luminol (Sigma Aldrich), 200 µg/mL horseradish peroxidase (Sigma Aldrich), and either bacterial extracts with 50 ng/mL protein concentration or 1 µM cdG (BioLog, Bremen, Germany) or 100 nM flg22 peptide (EZBiolab, Westfield, IN, USA).

M. truncatula seedlings were grown sterile for 7 days under 16-h photoperiod at 21°C. Roots were cut into 3 mm segments and recovered in water overnight. Alternatively, leaf discs were sampled from soil-grown 4 to 5-week-old plants and recovered in water. The water was replaced with solution containing 200 µg/mL horseradish peroxidase (HRP) (Sigma-Aldrich) and 1 µM L-012 (Sigma-Aldrich), incubated for 5 min and topped up with solution containing flg22 or elf18 peptide (EZBiolab, Westfield, IN, USA) with 100 nM final concentration. Peptide sequences have been previously described (Felix et al., 1999, Zipfel et al., 2006).

Luminescence was recorded over a 45-60 min time period using a charge-coupled device camera (Photek Ltd., East Sussex, UK). Statistically significant differences between ROS output was determined by a two-tailed Mann-Whitney test.

2.10 Virus-induced gene silencing

Virus-induced gene silencing in *N. benthamiana* was performed using the *tobacco rattle virus* (TRV) system as described previously (Peart et al., 2002). The TRV-RNA1 construct is contained in a pBINTRA6 vector and the TRV-RNA2 constructs *TRV*:*GFP* and *TRV*:*SU* are in pTV00 vector (Peart et al., 2002). The *NbFls2* silencing construct was amplified from *N. benthamiana* cDNA using the primers 5'-CGACGACAAGACCCTTACCTTTTTCATACCTTTG and 5'-GAGGAGAAGAGCCCTGGTGGAATATTTCC and subsequently cloned into the pYY13 vector (Dong et al., 2007). *Agrobacterium tumefaciens* GV3101::*pMP90* carrying the binary TRV-RNA1 and the TRV-RNA2 constructs were resuspended in infiltration buffer consisting of 10 mM 2-(N-morpholino)ethanesulfonic acid (pH 5.5), 10 mM $MgCl_2$ and 150 mM acetosyringone and mixed in a 2:3 ratio (RNA1:RNA2) with a final OD_{600} of 1.0. Two-week-old *N. benthamiana* plants were infiltrated with the *Agrobacterium* solution. Infection and systemic spreading of the virus was monitored in *TRV:SU* plants, which are bleached due to reduced chlorophyll content upon silencing. Silenced plants were used for experiments three weeks after infiltration. Successful silencing of *NbFls2* was examined in a ROS assay applying 100 nM of flg22 peptide.

2.11 Immunoblot analysis

Bacterial extracts were separated on a 12% sodium dodecylsulfate polyacrylamide gel electrophoresis (SDS-PAGE) and blotted on polyvinylidene difluoride (PVDF) membrane (Thermo Fisher Scientific) blocked with 5% milk in TBS with 0.1% (v/v) Tween-20. The flagellin protein was detected with a monoclonal α-flagellin antibody specific against purified flagellin from *P. aeruginosa* (mabg-flapa, Invivogen, Toulouse, France) used in a 1:1000 dilution and α-mouse-HRP (Sigma Aldrich) used in 1:10,000 dilution as secondary antibody.

Plant tissue was ground in liquid nitrogen and protein was extracted using a buffer containing 100 mM Tris-HCl, pH 7.2, 150 mM NaCl, 5 mM EDTA, 5% SDS, 2 M urea, 10 mM DTT and 1% (v/v) Protease Inhibitor Cocktail (P9599, Sigma-Aldrich), boiled for 10 min and debris removed by centrifugation for 2 min at 13,900 g. Protein samples were separated on an 8% SDS-PAGE gel and blotted on PVDF membrane. Immunoblotting was performed with α-HA-horseradish peroxidase (HRP) antibody (3F10, Roche) diluted 1:2000 in 5% milk in TBS with

0.1% (v/v) Tween-20. Blots were developed with chemiluminescent Pierce ECL pico Western Blotting substrate (Thermo Fisher Scientific) and imaged with light-sensitive X-ray film (Super RX, Fujifilm) or with a LAS 4000 ImageQuant system (GE Healthcare, Little Chalfont, UK). Equal loading of protein was determined by Coomassie Brilliant Blue staining of the blotted membrane.

2.12 Stable transformation of *Medicago truncatula*

M. truncatula ecotype R108 was stably transformed by *A. tumefaciens* AGL1 carrying the recombinant binary vector *pBIN19-CaMV35S*::*EFR-HA* (Lacombe et al., 2010). Plant transformation was carried out as previously described (Cosson et al., 2006) with some minor, but important, changes; *in vitro* grown plants, only, were used for the transformations, excised leaves were sliced through with a scalpel and not vacuum infiltrated, the *A. tumefaciens* culture was used at OD_{600}=0.4 and re-suspended in SH3a broth with 300 µM acetosyringone, the leaflet explants were submerged in the bacterial suspension for 20 min only, shaking in the dark, leaves were co-cultivated and callus generated with their adaxial surface in contact with the media, explants were washed in SH3a media broth post co-cultivation, excess *Agrobacteria* was eliminated on solid media using 320 mg/L ticarcillin disodium/potassium clavulanate and finally, callus growth was carried out in the dark for 8 weeks rather than 6. Five transgenic plants were recovered by somatic embryogenesis, rescued and selected on kanamycin plates. Homozygous plants were identified by quantitative real-time PCR of a segregating T1 population and confirmed in the T2 stage by responsiveness to elf18 peptide. Two homozygous lines with only a single insertion locus carrying two *EFR* copies were identified and used for physiological and symbiotic characterizations. In addition, null segregants were isolated for each primary transformant and used as control lines. All experiments were performed with plants from the T3 population.

2.13 Rhizobial infection of *Medicago truncatula*

Plants were grown in pots (50 or 80 mL volume) in terragreen/sharp sand mix for 2 days (infection thread counting) or 7 days (nodule counting and acetylene reduction measurements) before inoculation with *Sm*1021-*lacZ*. Bacteria were grown in TY to OD_{600}=1.5, washed in 10 mM $MgCl_2$ and diluted to OD_{600}=0.0002. Plants were inoculated with 5 mL of *S. meliloti* suspension equally spread across the pot. Plants were harvested at

indicated time-points, carefully rinsed with water and stained with X-Gal for visualization of LacZ activity. Stained nodules were counted under a stereo microscope.

For late-time point experiments (*e.g.* 28 dpi), plants were grown in bigger pots (500 mL volume) to allow enough space for root development and were inoculated with 10 mL *S. meliloti* diluted to OD_{600}=0.0002. Plant nodules were scored visually and were not stained.

2.14 X-Gal staining of infection structures and nodules

For staining of infection threads on plants grown in terragreen/sand mixture, whole roots were detached from shoots and placed in fixing solution containing phosphate buffer, pH=7 (61 mM Na_2HPO_4, 39 mM NaH_2PO_4, 10 mM KCl, 1 mM $MgCl_2$) and 2.5% glutaraldehyde. Vacuum was applied for 5 min and roots were incubated for 1 h at room temperature. Roots were washed three times in phosphate buffer before staining solution (5 mM $K_4[Fe(CN)_6]$, 5 mM $K_3[Fe(CN)_6]$, 0.08 % X-Gal (Formedium, King's Lynn, UK) in phosphate buffer) was added and roots incubated in the dark at 30°C overnight. Roots were washed in phosphate buffer three times and stored at 4°C until analysis.

Stained infection structures were scored in brightfield mode using a Leica DMR microscope (Wetzlar, Germany). The infection events were classified into three categories: micro-colony formation at curled root hair, elongated and ramified infection threads, and nodule primordia.

2.15 *Ralstonia solanacearum* infection of *Medicago truncatula* roots

After germination, *M. truncatula* plants were transferred and grown in jiffy peat pellets. For inoculation, the 1/3 bottom half of the Jiffy pots was severed then soaked in a *R. solanacearum* solution at OD_{600}=0.1. Potting soil was used to absorb the remaining inoculum and spread on the bottom of the tray before putting Jiffy pots back on. Disease symptoms were scored daily. Statistical analysis was performed as previously outlined (Remigi et al., 2011).

2.16 Acetylene reduction measurements

Nitrogenase activity was determined by gas chromatography measuring the enzymatic conversion of acetylene gas to ethylene as previously described (Trinick et al., 1976). Infected plants at 28 dpi, placed in a 50-mL plastic vial and sealed with a rubber lid. Acetylene gas

(BOC, Manchester, UK) was injected into the vials with 2% (v/v) final concentration, incubated for 1 h at 23°C and 1 mL sample taken for analysis. Conversion of acetylene to ethylene by rhizobial nitrogenase was recorded on a Clarus 480 (Perkin Elmer) gas chromatograph with N_2 as the carrier gas set to a flow rate of 25 mL min^{-1}, a HayeSep N 80/100 mesh column, connected to a flame ionisation detector at 100°C. Acetylene was applied in excess and peak areas of ethylene were quantified using TotalChrom Workstation software (Perkin Elmer) and displayed as relative units.

2.17 RNA extraction, cDNA synthesis and qPCR of *M. truncatula* leaf tissue

For each *M. truncatula* line, approx. 50 mg leaf tissue has been harvested. Extraction of mRNA was done with RNeasy Plant Mini Kit (Qiagen) according to manufacturer's instructions. Genomic DNA was removed by DNAse treatment using Ambion Turbo DNA-free Kit (Thermo Fisher Scientific). Total RNA concentrations were measured by NanoDrop spectrophotometer (Thermo Fisher Scientific) and adjusted to approx. 280 ng/µL. RNA integrity was checked on a 1% agarose gel. Contamination with genomic DNA was tested by PCR using primers #Mt11 and #Mt12. cDNA synthesis was done with 3 µg total RNA, oligo-dT primers and SuperScript III reverse transcriptase (Invitrogen/ Thermo Fisher Scientific) according to the manufacturer's instructions. cDNA was amplified by quantitative PCR using SYBR Green JumpStart Taq ReadyMix (Sigma-Aldrich) and the PTC-200 Peltier Thermal Cycler (Bio-Rad Laboratories, Hercules, CA, USA). The relative expression values were determined using UBQ and PDF2 as reference and the comparative Ct method (2-ΔΔCt).

Chapter 3

High levels of cyclic-di-GMP in plant-associated *Pseudomonas* correlate with evasion of plant immunity

Parts of this chapter have been published in a manuscript (Pfeilmeier et al., 2016b), for which I performed all experimental work and wrote the first draft. The co-authors contributed by providing molecular tools and intellectually to project design and manuscript writing.

3.1 Summary

The plant innate immune system employs plasma membrane-localized receptors that specifically perceive pathogen/microbe-associated molecular patterns (PAMPs/MAMPs). This induces a defence response called pattern-triggered immunity (PTI) to fend off pathogen attack. Commensal bacteria are also exposed to potential immune recognition and must employ strategies to evade and/or suppress PTI to successfully colonize the plant. During plant infection the flagellum has an ambiguous role, acting as both a virulence factor and also as a potent immunogen due to the recognition of its main building block, flagellin, by plant pattern-recognition receptors (PRRs), including FLAGELLIN SENSING2 (FLS2). Therefore, strict control of flagella synthesis is especially important for plant-associated bacteria. In this chapter, I show that cyclic-di-GMP, a central regulator of bacterial lifestyle, is involved in the evasion of PTI. Elevated cyclic-di-GMP levels in the pathogen *Pseudomonas syringae* pv. *tomato* (*Pto*) DC3000, the opportunist *P. aeruginosa* PA01, and the commensal *P. protegens* Pf-5 inhibit flagellin synthesis, and help the bacteria to evade FLS2-mediated signalling in *Nicotiana benthamiana* and *Arabidopsis thaliana*. Despite this, high cellular cyclic-di-GMP concentrations were shown to drastically reduce the virulence of *Pto* DC3000 during plant infection. I propose that this is due to reduced flagellar motility and/or additional pleiotropic effects of cyclic-di-GMP signalling on bacterial behaviour.

3.2 Introduction

Plants rely on an innate immune system consisting of passive and active defences to resist potential attack by most microbial pathogens (Dangl et al., 2013). During infection, cell surface-localized pattern recognition receptors (PRRs) perceive pathogen/microbe-associated molecular patterns (PAMPs/MAMPs), and trigger local and systemic immune responses (Boller and Felix, 2009).

Plants are continuously exposed to a highly complex microbial community that contains not only pathogens but also commensal and beneficial species. Indeed, the microbiomes of the phyllosphere and rhizosphere most likely play critical roles in the adaption of a plant to its environment (Berendsen et al., 2012, Guttman et al., 2014). Flagellin and ELONGATION FACTOR-THERMO UNSTABLE (EF-Tu; or the immunogenic epitopes flg22 and elf18, respectively) are typical PAMPs, which are recognized by the *A. thaliana* PRRs FLAGELLIN SENSING2 (FLS2) and EF-TU RECEPTOR (EFR), respectively. Both PAMPs are widespread

among many bacterial species, abundant, and highly conserved, fulfilling important bacterial functions (Pel and Pieterse, 2013). While the PRRs for flg22 and elf18 ensure the reliable recognition of diverse bacterial pathogens, the universal nature of these PAMPs means that beneficial and commensal microbes are also potentially exposed to immune recognition (van Loon, 2007, Van Wees et al., 2008, Zamioudis and Pieterse, 2012). Yet, some symbiotic bacteria such as *Rhizobium* have evolved to evade flg22 recognition (Felix et al., 1999).

Pseudomonas is an important genus of plant-associated bacteria that contains both phytopathogenic and commensal species. *Pseudomonas syringae* pv. *tomato* (*Pto*) DC3000 is a foliar, hemibiotrophic plant pathogen that causes bacterial speck disease on tomato and *A. thaliana* (Xin and He, 2013). Primary infection sites are natural openings (such as stomata and hydathodes) and wounds, through which bacteria migrate into the apoplast before multiplying rapidly, leading to chlorosis and necrosis of plant tissue (Xin and He, 2013). *Pseudomonas aeruginosa* is an opportunistic pathogen that infects immune compromised humans and can also colonise and infect plants, although this ability is limited to specific hosts (Starkey and Rahme, 2009). Attachment, colonization and proliferation of *P. aeruginosa* in *A. thaliana* has been described as having similarities to the *Pto* DC3000 infection process (Plotnikova et al., 2000), although no specific plant virulence factor has yet been identified. *P. aeruginosa* growth in the intercellular space leads to systemic infection and ultimately to severe soft-rot symptoms (Plotnikova et al., 2000). Conversely, *Pseudomonas protegens* Pf-5 is a soil bacterium that colonizes the rhizosphere and promotes plant growth by suppression of a wide variety of plant diseases over a broad host range (Loper et al., 2007). *P. protegens* Pf-5 produces multiple secondary metabolites including pyoluteorin and 2, 4-diacetylphloroglucinol that underpin its biocontrol capacities (Loper et al., 2012). Beside the production of antibiotics, siderophore secretion and genetic features like broad catabolic pathways, an expanded array of efflux systems and numerous genes conferring tolerance to oxidative stress enable *P. protegens* Pf-5 to cope with environmental stress and microbial competition in the rhizosphere (Loper et al., 2012). Consistent with its commensal lifestyle, certain pathogenicity factors such as the type-III secretion system (T3SS) are not present in the Pf-5 genome (Loper et al., 2007, Loper et al., 2012). Like many Gram-negative bacteria, these three plant-associated *Pseudomonas* species (spp.) have polar flagella that confer directed mobility and enable both the spatial colonisation of plant surfaces and migration into the apoplast (Jackson, 2009). Another common feature between the three *Pseudomonas* species is the presence of a similar set of biosynthetic pathways for the production of exopolysaccharides (EPS), namely alginate, Psl and Wss or Pel, in their

genome (Whitney and Howell, 2013, Spiers et al., 2003, Franklin et al., 2011). EPS production is a common aspect of bacteria colonizing the phyllo- and rhizospheres (Davey and O'Toole G, 2000), and has been associated with evasion of plant immunity (D'Haeze and Holsters, 2004, Yun et al., 2006, Aslam et al., 2008).

The bacterial second messenger cyclic-di-GMP (cdG) is a key regulator of flagella expression and EPS production in *Pseudomonas* (Hickman and Harwood, 2008). In general, cdG controls processes involved in the switch between single-celled motile and communal sessile lifestyles in many bacterial species (Jenal et al., 2017). *Pseudomonas* and other bacteria integrate environmental cues and intracellular signals in cdG signalling pathways, which regulate a diverse range of behaviours including motility (Dasgupta et al., 2003), adhesion to surfaces (Newell et al., 2011), biofilm formation (Hickman et al., 2005), and virulence (Kulasakara et al., 2006). The level of intracellular cdG is coordinated by the opposing enzymatic activities of multiple diguanylate cyclases (DGCs) and phosphodiesterases (PDEs) (Jenal et al., 2017). In *P. aeruginosa*, flagella-driven motility and EPS production are reciprocally controlled by several cdG-dependent systems (Dasgupta et al., 2003, Lee et al., 2007), with the cdG-binding transcription factor FleQ playing a central role. FleQ is a σ^{54}-dependent master regulator that controls the expression of genes including the *fleSR* two-component system, flagella export apparatus loci, and genes involved in the initiation of flagella basal body assembly (Dasgupta et al., 2003, Robleto et al., 2003). When cdG levels are low, FleQ inhibits EPS production by repression of *pel* and *psl* EPS-operon transcription, but is required for transcription of multiple flagellar genes. Correspondingly, upon binding cdG, FleQ both releases EPS biosynthetic gene repression and abolishes flagella gene transcription, enabling the switch from motility to EPS production and biofilm formation (Hickman and Harwood, 2008, Baraquet and Harwood, 2013). Homologs of FleQ are present in most *Pseudomonas* spp., including *P. syringae* and *P. protegens* (Nogales et al., 2015).

While most of the work on virulence factors in pathogenic *Pseudomonas* bacteria focusses on type-3 effector proteins and the polyketide phytotoxin coronatine (Xin and He, 2013), little is known about the role of bacterial EPS during plant infection (Pfeilmeier et al., 2016a). Thus, I wanted to examine if the production of bacterial EPS is a common strategy of the pathogen *Pto* DC3000, the opportunist *P. aeruginosa* PA01, and the commensal *P. protegens* Pf-5 during plant colonization. As the production of EPS and biofilms is closely related to cdG signalling (Valentini and Filloux, 2016), I first characterized the impact of increased intracellular cdG levels in different *Pseudomonas* spp. on plant immune responses.

3.3 Results

3.3.1 Increased *Pseudomonas* cdG levels lead to suppressed PAMP-induced ROS response in *N. benthamiana* and *A. thaliana*

In order to examine the effect of increased cdG levels on the induction of plant immune responses by *Pseudomonas* spp., I first produced a broad-host-range expression vector for a constitutively active allele of the DGC *wspR* (pBBR2/5-*wspR19*), and transformed the three species included in this study (*Pto* DC3000, *P. protegens* Pf-5 and *P. aeruginosa* PA01). In agreement with previous findings, *wspR19* expression resulted in aggregative, wrinkled colony morphologies, enhanced Congo Red dye binding, which indicates production of polysaccharides such as cellulose (Spiers et al., 2002), and reduced motility (Figure 3.1A and B) (Goymer et al., 2006). Over-expression of genes encoding a DGC *in trans* leads to the intracellular accumulation of cdG in various bacterial species (Hengge, 2009). Accordingly, expression of *wspR19* led to increased cdG levels in all three *Pseudomonas* spp. as determined by LC-MS/MS analysis (Table 3.1). The cdG levels measured for the wild-type containing the empty vector (WT) and DGC-over-expression strains (*wspR19*) of *P. protegens* Pf-5 and *P. aeruginosa* PA01 were comparable to levels previously described for PA01 (Malone et al., 2010). Interestingly, *wspR19* expression increased cdG concentration to a much lesser extent in *Pto* DC3000 compared to the increases seen in *P. protegens* Pf-5 and *P. aeruginosa* PA01.

Table 3.1 Expression of *wspR19* in *Pseudomonas* elevates cellular cyclic-di-GMP concentrations.

Species		[c-di-GMP] (pmol/mg of bacterial protein)	
Pto DC3000	WT	1.97	± 1.66
	wspR19	32.85**	± 3.12
Pf-5	WT	1.70	± 0.06
	wspR19	206.02***	± 5.67
PA01	WT	2.45	± 0.67
	wspR19	223.49***	± 13.32

Data represent the means of two biological replicates with '±' representing the standard error (n= 2). Asterisks indicate statistical significance (**p< 0.01; *** p< 0.001) between wild-type (WT) and *wspR19* extracts based on an unpaired Mann–Whitney test.

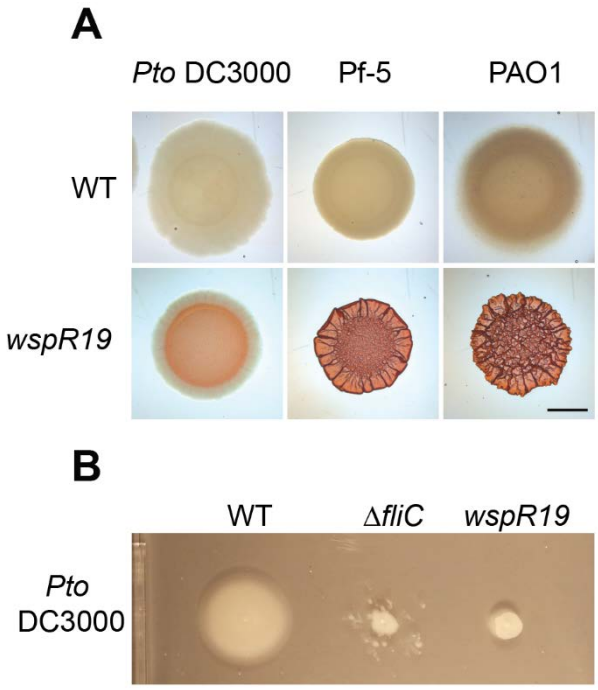

Figure 3.1. ***wspR19* overexpression enhances exopolysaccharide production and reduces motility.** (A) Congo red dye binding of WT and *wspR19*-expressing strain from *Pto* DC3000, *P. protegens* Pf-5 and *P. aeruginosa* PA01, respectively. (B) Swarming assay with *Pto* DC3000 WT, *wspR19* and Δ*fliC*.

Next, I investigated the effect of high cdG levels in *Pseudomonas* on the induction of PTI in different plants by measuring the ROS burst upon the application of bacterial extracts. The extracts of *Pto* DC3000 and *P. protegens* Pf-5 over-expressing the DGC *wspR19* triggered a reduced ROS burst in both *A. thaliana* and *N. benthamiana* compared to WT extracts (Figure 3.2A, B, Figure 3.3A, B), whereas extracts of *P. aeruginosa* PA01 expressing *wspR19* only caused a reduced ROS in *N. benthamiana* (Figure 3.3B) but not in *A. thaliana* (Figure 3.2C). To test if the cdG molecule itself is responsible for the suppression of ROS responses, I added chemically-synthesised cdG to the *Pto* DC3000 bacterial extract. No difference in *A. thaliana* ROS response was seen compared to the *Pto* DC3000 WT extract alone. Likewise, I saw no ROS response upon the addition of 1 µM cdG alone (Figure 3.3A). Bacterial extract from a previously characterized *P. aeruginosa* PA01 mutant with increased intracellular cdG levels, Δ*yfiR* (Malone et al., 2010), triggered a similarly reduced ROS response to the PA01 *wspR19* over-expression strain (Figure 3.3B). Thus, the intracellular activity of cdG in the bacterium leads to loss of ROS production triggered by the tested bacterial extracts in *N. benthamiana*, and in *A. thaliana* for *Pto* DC3000 and Pf-5 extracts.

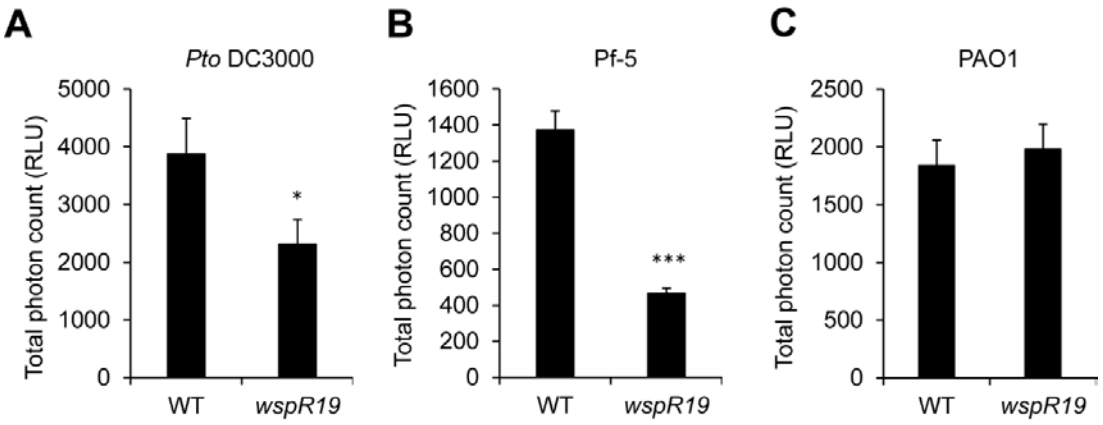

Figure 3.2. Extracts from *Pseudomonas* bacteria with high cyclic-di-GMP levels trigger reduced reactive oxygen species (ROS) burst in *Arabidopsis thaliana*. Total ROS accumulation in leaf discs after treatment with *Pseudomonas* extracts, expressed as relative light units (RLU) over 60 min. Leaf discs were treated with extracts from *Pseudomonas syringae* pv. *tomato* (*Pto*) DC3000 (A), *P. protegens* Pf-5 (B) or *P. aeruginosa* PA01 (C) carrying empty pBBR2 vector (WT), pBBR-*wspR19* (*wspR19*). Values are means ± standard error (n = 8). Asterisks indicate statistically significant difference (*p < 0.05; *** p < 0.001) between treatment of wild-type extracts and other samples based on a two-tailed Mann–Whitney test.

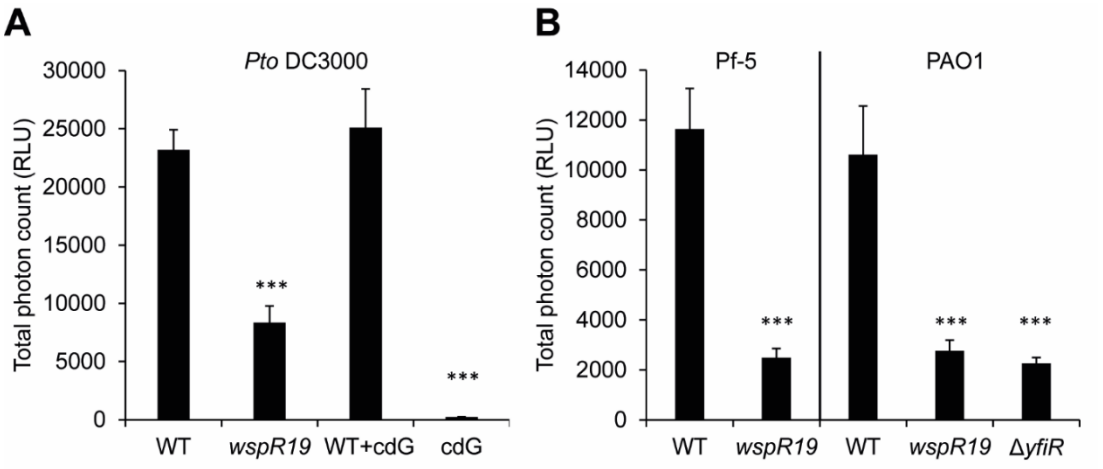

Figure 3.3. Extracts from *Pseudomonas* bacteria with high cyclic-di-GMP levels trigger reduced reactive oxygen species (ROS) burst in *Nicotiana benthamiana*. Total ROS accumulation in leaf discs after treatment with Pseudomonas extracts, expressed as relative light units (RLU) over 60 min. Leaf discs were treated with extracts from *Pseudomonas syringae* pv. *tomato* (*Pto*) DC3000 (A) or *P. protegens* Pf-5 and *P. aeruginosa* PA01 (B) carrying empty pBBR2 vector (WT), pBBR-*wspR19* (*wspR19*), PA01 Δ*yfiR* or 1 µM purified cdG. Values are means ± standard error (n = 8). Asterisks indicate statistically significant difference (*** p < 0.001) between treatment of wild-type extracts and other samples based on a two-tailed Mann–Whitney test.

3.3.2 FLS2-mediated ROS production is specifically reduced by *wspR19* expression

The ROS burst triggered by bacterial extracts can be initiated by the activation of several different PRRs (Boutrot and Zipfel, 2017). As the bacterial extracts used in the experiments are made from whole cell lysates, they may contain numerous different PAMPs.

Consequently, I tested whether the suppressed ROS bursts seen for the *wspR19* extracts depend on one or more specific plant receptors.

To identify the major eliciting agents in the bacterial extracts, I characterized the ROS response produced by *Pseudomonas* WT extracts on a series of different *A. thaliana* PRR knock-out mutants. The ROS response of *efr*, *cerk1-2* and *lym3-1* plants [CERK1 and LYM3 are involved in bacterial peptidoglycan perception (Willmann et al., 2011)] to all tested extracts was comparable to that of Col-0 (Figure 3.4). Conversely, total ROS accumulation was drastically reduced in *fls2* and even more so in *efr fls2* and *bak1-5 bkk1* plant lines (relative to Col-0) after application of WT extracts from *Pto* DC3000 and *P. protegens* Pf-5 (Figure 3.4A and B). This suggests that ROS production is mainly triggered by flagellin and to a lesser extent by EF-Tu for these two extracts. Wild-type *P. aeruginosa* PA01 extract triggered equally high ROS production in Col-0, *efr* and *fls2* plants, while ROS response was strongly diminished in *efr fls2* and *bak1-5 bkk1* (Figure 3.4C). Previous work showed that flg22- or elf18-triggered ROS production is drastically reduced in *bak1-5 bkk1* due to the role of BAK1 and BKK1 as co-receptors for FLS2 and EFR (Chinchilla et al., 2007, Roux et al., 2011, Heese et al., 2007, Sun et al., 2013). Furthermore, the signal transduction pathways of both receptors converge into the same signalling pathway (Couto and Zipfel, 2016), which means that the intensity of FLS2 and EFR activation is not additive and both elicitors can compensate for each other. The results suggest that under the culture conditions used here the main elicitor in *Pto* DC3000 and *P. protegens* Pf-5 extracts is flagellin, while in the *P. aeruginosa* PA01 extract flagellin and EF-Tu are equally strong elicitors.

Next, I repeated the ROS burst experiments for the *A. thaliana* PRR knock-out mutants with extracts from *wspR19*-over-expressing strains. Over-expression of *wspR19* in *Pto* DC3000 and *P. protegens* Pf-5 suppresses the ROS burst elicited by their extracts in *A. thaliana* Col-0 and the *efr* knock-out mutant (Figure 3.5A and B). Because the major elicitor of ROS production in the extracts of those two species is probably flagellin (Figure 3.4A and B), this suggests that suppression of the ROS response by *wspR19* expression is due to decreased flagellin perception by FLS2. Extracts from a *Pto* DC3000 Δ*fliC* strain were tested as a control. ROS production induced by *Pto* DC3000 *wspR19* extracts induced slightly higher ROS production in Col-0 and *efr* plants compared to extracts from the Δ*fliC* strain, but ROS was equally low in *fls2* and *efr fls2* (Figure 3.5A). The slightly higher ROS production for *wspR19* extracts in plants containing the functional FLS2 receptor is probably the consequence of residual flagellin levels in these strains. *P. aeruginosa* PA01 *wspR19*-expressing extracts induced equally strong ROS production in Col-0 and *fls2*, while the ROS response was reduced in *efr*

plants, in which ROS production mainly derives from activation of the FLS2 pathway (Figure 3.5C).

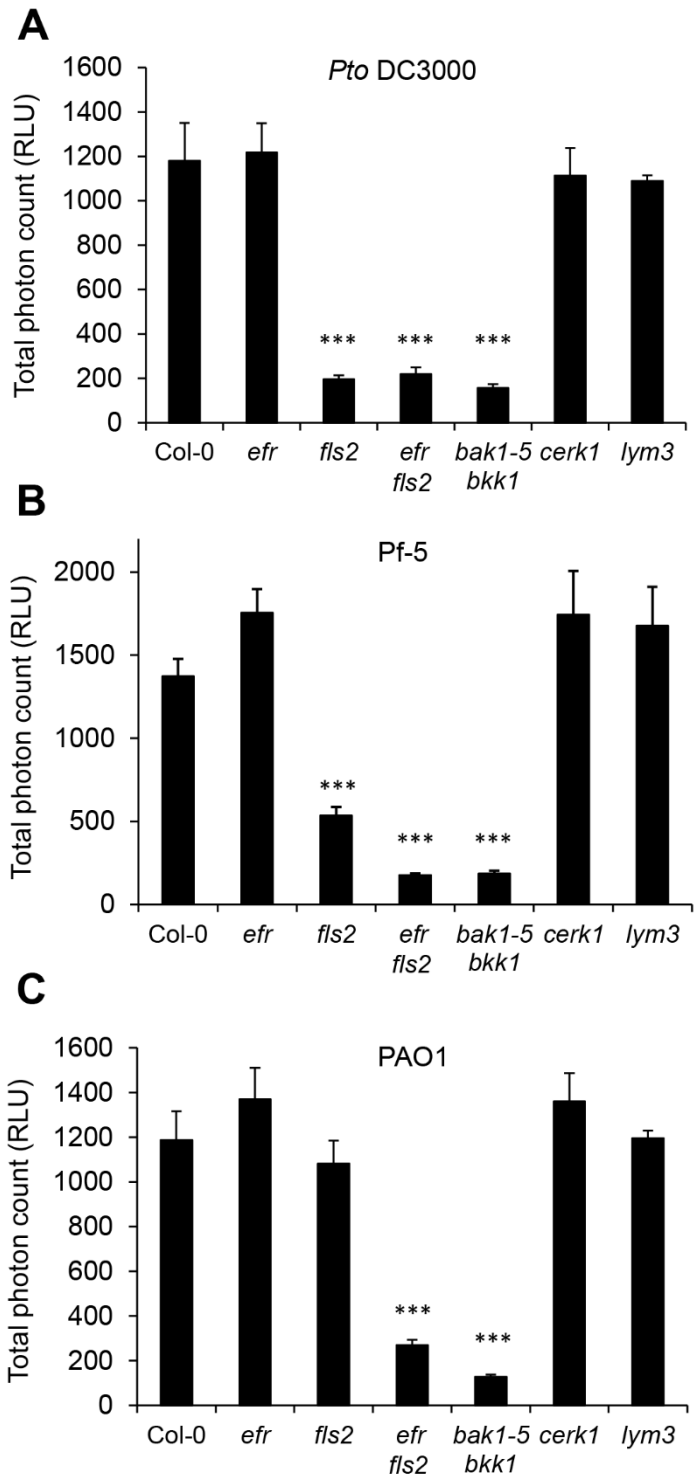

Figure 3.4. Flagellin and elongation factor thermo-unstable (EF-Tu) in *Pseudomonas* extracts are the main elicitors of reactive oxygen species (ROS) production in *A. thaliana*. Total ROS accumulation was measured in *A. thaliana* genotypes Col-0, *efr*, *fls2*, *efr fls2*, *bak1-5 bkk1*, *cerk1-2* and *lym3-1* (A–C). The ROS burst was induced by extracts from *Pseudomonas syringae* pv. *tomato* (*Pto*) DC3000 (A), *P. protegens* Pf-5 (B) or *P. aeruginosa* PA01 (C). Values are means ± standard error (n = 8). Asterisks indicate statistically significant difference (***p < 0.001) between the treatment of wild-type extracts and other samples based on a two-tailed Mann–Whitney test. RLU, relative light units.

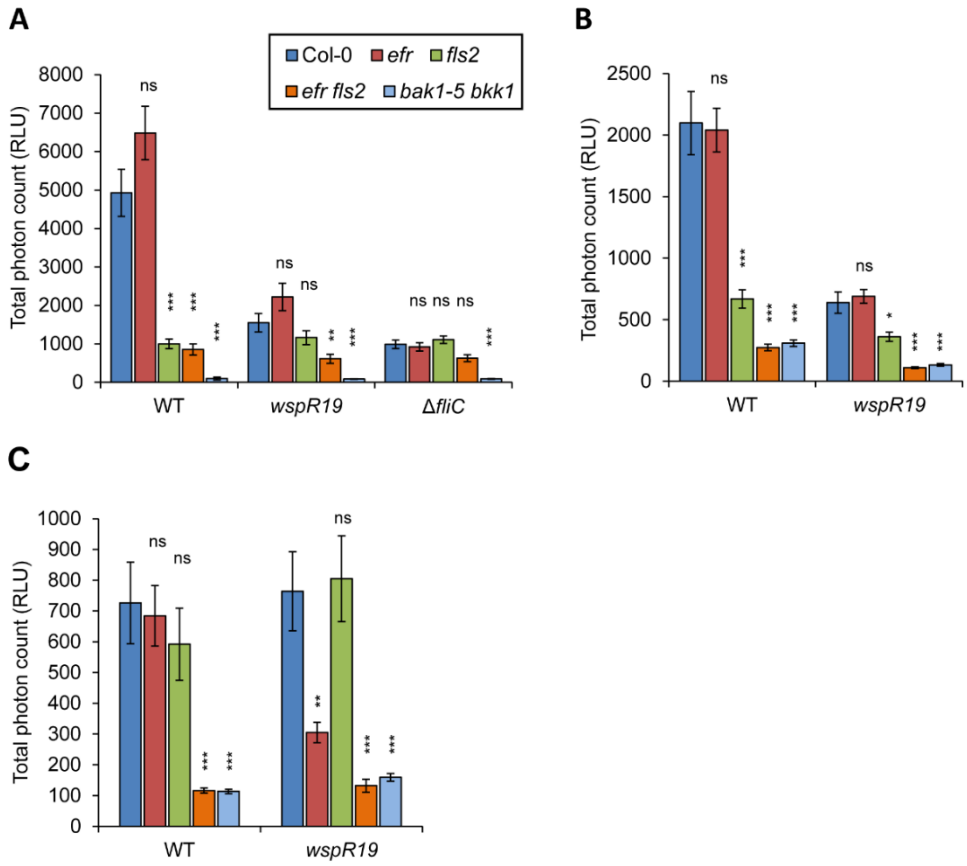

Figure 3.5. Reduced reactive oxygen species (ROS) burst triggered by *Pseudomonas* extracts with high cyclic-di-GMP is FLAGELLIN SENSING2 (FLS2) dependent. Total ROS accumulation was measured in *Arabidopsis thaliana* genotypes Col-0, *efr*, *fls2*, *efr fls2*, *bak1-5 bkk1* (A–C). The ROS burst was induced by extracts from *Pseudomonas syringae* pv. *tomato* (*Pto*) DC3000 (A), *P. protegens* Pf-5 (B) or *P. aeruginosa* PA01 (C) expressing *wspR19* and their respective control strains carrying empty pBBR2 vector (WT) or *Pto* DC3000 Δ*fliC*. Values are means ± standard error (n = 8). Asterisks indicate statistically significant difference (*p < 0.05; **p < 0.01; ***p < 0.001) between *A. thaliana* Col-0 and other transgenic or mutant lines, based on a two-tailed Mann–Whitney test. RLU, relative light units.

Perception of flagellin and EF-Tu by FLS2 and EFR respectively, has been extensively studied in *A. thaliana* (Boller and Felix, 2009); there is no current evidence for other *A. thaliana* receptors recognizing flagellin or EF-Tu, nor for the existence of additional FLS2 or EFR ligands. As the presence of either flagellin or EF-Tu in the PA01 extracts seems to be sufficient to trigger the full ROS response in the plant (Figure 3.4C), ROS production is only reduced if elements of both recognition systems are simultaneously absent. Thus, the reduction in ROS production upon *wspR19* expression in *P. aeruginosa* PA01 also appears to be FLS2-dependent.

To examine whether the effect of *wspR19* expression on ROS accumulation also depends on FLS2 in *N. benthamiana*, I silenced *NbFls2* using virus-induced gene silencing. *NbFls2* silencing was confirmed by abolished ROS production upon application of 10 nM flg22 peptide (Figure 3.6A). ROS accumulation upon treatment with WT extracts from all three *Pseudomonas* spp.

was strongly reduced in *NbFls2*-silenced plants (*TRV*:*NbFls2*) compared to mock-silenced control plants (*TRV*:*GFP*) (Figure 3.6A to C), indicating that within the bacterial extracts, flagellin is the major elicitor of ROS burst in *N. benthamiana*. *N. benthamiana* is unable to perceive EF-Tu, as it lacks a functional EFR homologue (Zipfel et al., 2006). The suppressive effect of *wspR19* expression is dependent on FLS2, as there was no significant difference in the ROS signal between *TRV*:*NbFls2* and *TRV*:*GFP* plants when the *wspR19*-expressing extracts were tested (Figure 3.6A to C). Together, these results indicate that the reduced *A. thaliana* and *N. benthamiana* ROS responses induced by extracts of *Pseudomonas* spp. with increased cdG levels depend on signalling through the FLS2 receptor. The *TRV:NbFLS2* construct has been designed and provided by Isabel Saur[1].

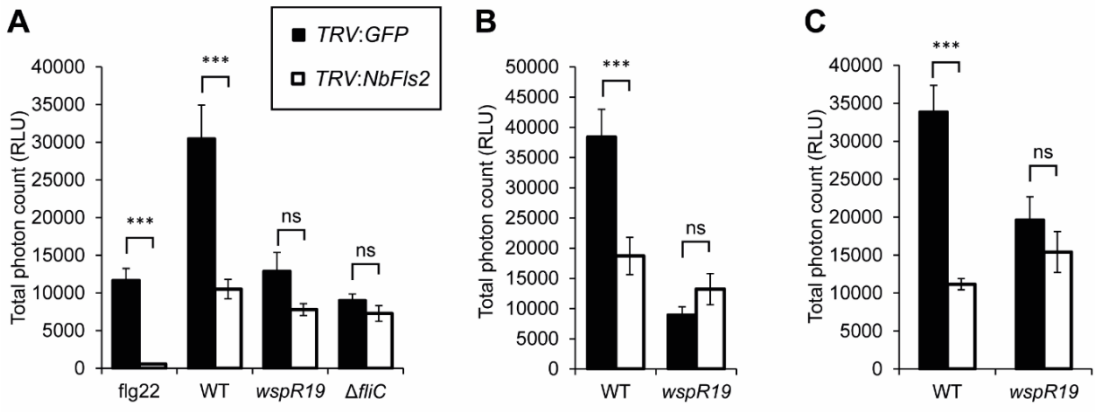

Figure 3.6. Reduced reactive oxygen species (ROS) burst triggered by *Pseudomonas* extracts with high cyclic-di-GMP is FLAGELLIN SENSING 2 (FLS2)-dependent. Total ROS accumulation was measured in *NbFls2*-silenced (TRV:*NbFls2*) or control silenced (TRV:*GFP*) *Nicotiana benthamiana* plants (A–C). The ROS burst was induced by extracts from *Pseudomonas syringae* pv. *tomato* (Pto) DC3000 (A), *P. protegens* Pf-5 (B) or *P. aeruginosa* PA01 (C) expressing *wspR19* and their respective control strains carrying empty pBBR2 vector (WT) or *Pto* DC3000 Δ*fliC*. Values are means ± standard error (n = 8). Asterisks indicate statistically significant difference (***p < 0.001) between *N. benthamiana* control plants and *NbFls2*-silenced plants, based on a two-tailed Mann–Whitney test. RLU, relative light units.

3.3.3 Expression of *wspR19* leads to impaired accumulation of flagellin

The data from the ROS assays in *A. thaliana* and *N. benthamiana* indicated that *wspR19* expression in the three tested *Pseudomonas* spp. affected the amount of the PAMP flagellin in the extracts, thus reducing the FLS2-induced ROS burst relative to WT. I tested the accumulation of flagellin in the bacterial extracts by western blot analysis using a commercial

1 Research School of Biology, The Australian National University, Canberra, Australia (Present address: Department of Plant-Microbe Interactions, Max Planck Institute for Plant Breeding Research, Cologne, Germany).

anti-FliC antibody. Flagellin accumulation was drastically reduced in *Pto* DC3000 and *P. protegens* Pf-5 (Figure 3.7A and B) and undetectable in *P. aeruginosa* PA01 (Figure 3.7C) upon *wspR19* expression compared to the respective wild-type extracts. Studies in *P. aeruginosa* have shown that cdG negatively affects expression of flagella genes by binding to FleQ, a master regulator of flagella gene transcription (Dasgupta et al., 2003, Hickman and Harwood, 2008, Baraquet and Harwood, 2013). This would explain the reduced accumulation of flagellin in the *wspR19*-expressing extracts compared to WT strains, and the correspondingly weaker ROS response due to reduced FLS2 activation (Figure 3.8).

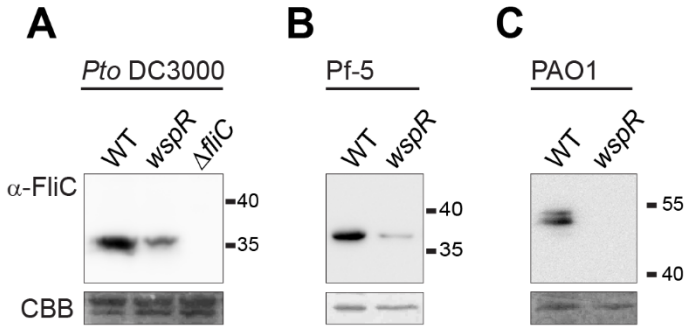

Figure 3.7. High cyclic-di-GMP levels suppress FliC accumulation in *Pseudomonas*. Extracts from *Pseudomonas syringae* pv. *tomato* (*Pto*) DC3000 (A), *P. protegens* Pf-5 (B) and *P. aeruginosa* PA01 (C) carrying the empty pBBR2 vector (WT) or pBBR-*wspR19* (*wspR19*) and *Pto* DC3000 Δ*fliC* were analysed by western blot using α-flagellin antibody. Membranes were stained with Coomassie Brilliant Blue (CBB) as loading controls.

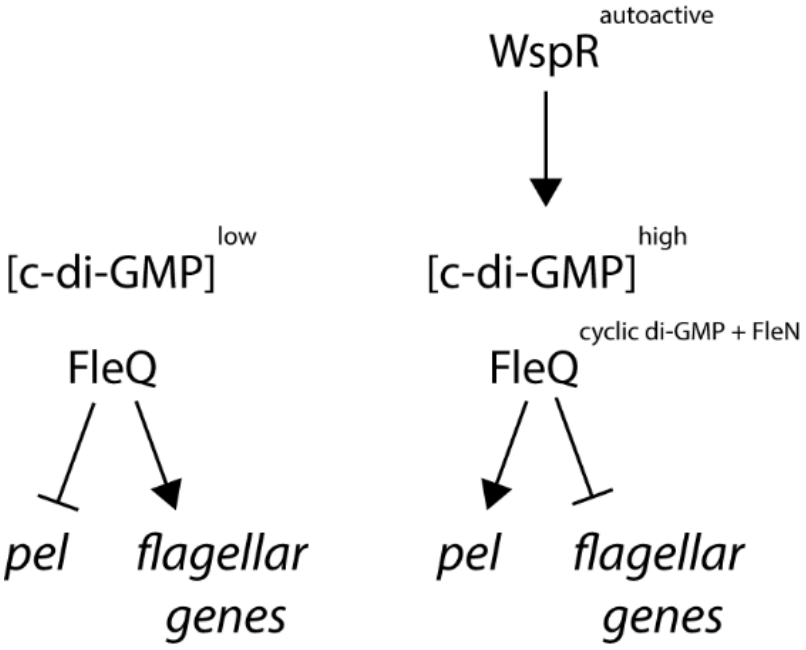

Figure 3.8. Illustration of the FleQ-mediated regulation of flagellar and *pel* genes transcription by *wspR19* expression.

To examine whether down-regulation of flagella synthesis through elevation of cdG levels is a strategy adopted by *Pto* DC3000 upon plant colonization, I attempted to extract and measure cdG from *Pto* DC3000 growing *in planta*. Unfortunately, despite my best efforts and the examination of large amounts of infected plant tissue I was unable to reliably quantify *in planta* cdG levels. While this remains a highly interesting question, it appears that *in planta* cdG measurements are currently beyond the limit of the technical capabilities available.

3.3.4 *P. aeruginosa* was non-pathogenic on *A. thaliana* under tested infection conditions

As FLS2-mediated flg22 perception impedes the success of bacterial infection (Zipfel et al., 2004, Hann and Rathjen, 2007, Forsyth et al., 2010, Zeng and He, 2010), I wanted to test the effect of *wspR19* expression on the virulence of the adapted pathogen *Pto* DC3000 and the non-adapted opportunistic pathogen *P. aeruginosa*. It has been previously reported that *P. aeruginosa* is able to infect plants and a plant infection model with *P. aeruginosa* has been described for roots of sweet basil (*Ocimum basilicum*) and *A. thaliana* (Walker et al., 2004), as well as *A. thaliana* and detached Romaine lettuce leaves (Starkey and Rahme, 2009, Rahme et al., 1997). I tested the effect of high cdG levels on the virulence of *P. aeruginosa* PA01 during infection of *A. thaliana*. However, *P. aeruginosa* PA01 wild-type and *wspR19*-expressing strain did not proliferate or cause any disease symptoms within 5 days post-infection (dpi) on Col-0 (Figure 3.9) or on the *A. thaliana* ecotypes Wassilewskija (Ws-0), Llagostera (Ll-0) and Landsberg *erecta* (L*er*-0) under the tested growth conditions (24°C, 12 hour light cycle, 95% relative humidity) (Figure 3.10A). Previously, plant infections with *P. aeruginosa* were described for strain PA14, which contains additional pathogenicity islands that might enable its virulence in *A. thaliana* (Plotnikova et al., 2000, He et al., 2004). However, *P. aeruginosa* strain PA14 also could not cause disease after infiltration infection of various *A. thaliana* ecotypes, including Col-0 and an *fls2* mutant (Figure 3.10B). The enhanced proliferation seen on Col-0 was not reproducible in repeat experiments.

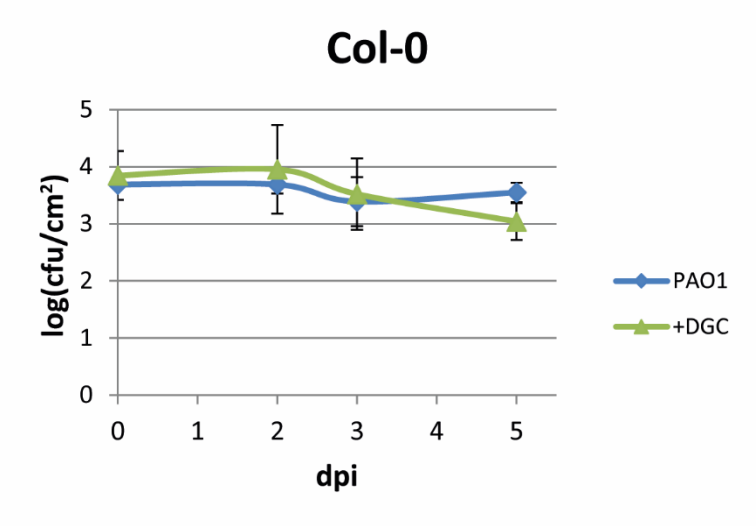

Figure 3.9. *P. aeruginosa* PA01 infection on *A. thaliana* Col-0. Growth of .*P. aeruginosa* PA01 wild-type and *wspR19*-expressing strain (+DGC) were monitored for 5 days on *A. thaliana* Col-0 after leaf infiltration with 2.5 × 10^6 cfu/mL. Values are means ± standard error (*n* = 4).

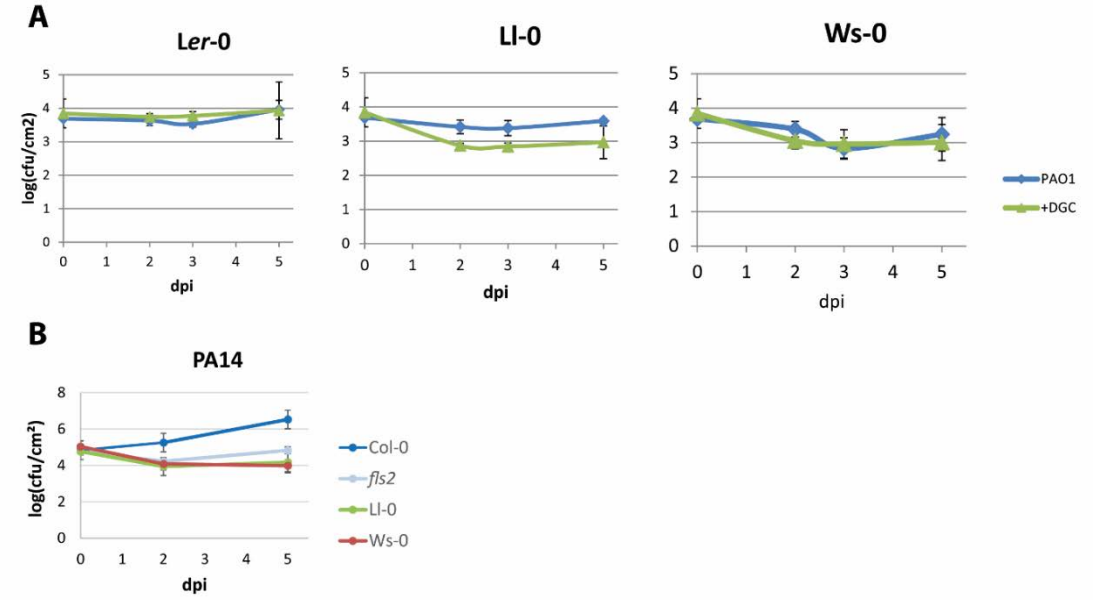

Figure 3.10. *P. aeruginosa* infection on various *A. thaliana* ecotypes. Growth of .*P. aeruginosa* PA01 wild-type and *wspR19*-expressing strain (+DGC) (A) and *P. aeruginosa* PA14 (B) was monitored for 5 days on *A. thaliana* ecotypes L*er*-0, Ll-0, Ws-0, Col-0 and fls2 mutant after leaf infiltration with 2.5 × 10^6 cfu/mL. Values are means ± standard error (*n* = 4).

3.3.5 Virulence of *Pto* DC3000 during infection is drastically reduced by *wspR19* expression

I next tested the effect of *wspR19* expression on the virulence of *Pto* DC3000 during infection of *A. thaliana* plants. The growth of *Pto* DC3000 *wspR19* was drastically reduced after spray-infection of *A. thaliana* Col-0 (Figure 3.11). This suggests that high intracellular cdG levels

exert a strong negative effect on *Pto* DC3000 virulence, which in turn cancels out any benefit from the evasion of FLS2-triggered immunity. FLS2-induced defences against the virulent *Pto* DC3000 may only be effective when the flagellin-triggered immune responses are activated in the early stages of the colonisation process (Zipfel et al., 2004). In order to dissect the different effects of *wspR19* over-expression on plant infection, I syringe-infiltrated *Pto* DC3000 WT and the *wspR19*-expressing strains directly into the apoplast, bypassing the critical initial colonisation steps. Interestingly, the *Pto* DC3000 WT and *wspR19* over-expression strains were equally virulent after infection by infiltration (Figure 3.11), suggesting that the infectious disadvantage arising from increased cdG levels is associated exclusively with the initial stages of plant colonisation and migration into the apoplast.

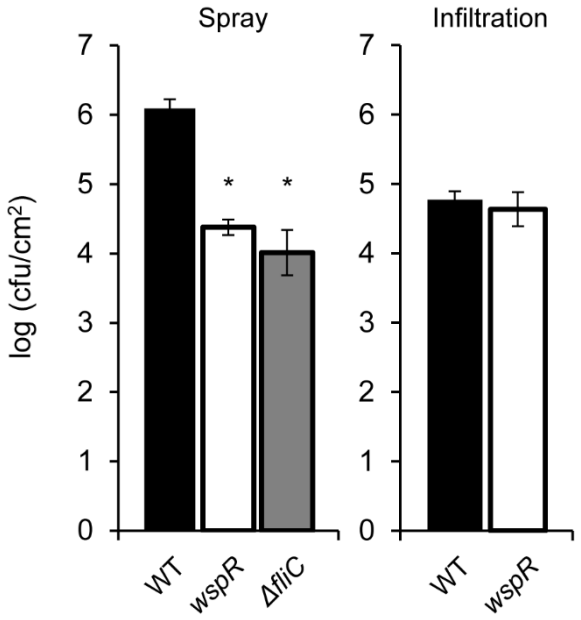

Figure 3.11. *wspR19* expression reduces the virulence of *Pseudomonas syringae* pv. *tomato* (*Pto*) DC3000 during plant infection after spray inoculation, but not after infiltration. Growth of *Pto* DC3000 carrying empty pBBR2 vector (WT), pBBR-wspR19 (*wspR19*) or Δ*fliC* at 2 days post-infection of *Arabidopsis thaliana* Col-0 plants. Bacteria were either sprayed onto [inoculum 2.5×10^7 colony-forming units (cfu)/mL] or syringe-infiltrated into (inoculum 10^5 cfu/mL) the plant. Values are means ± standard error ($n = 4$). Significant differences (*$p < 0.05$) based on two-tailed Mann–Whitney test.

3.4 Discussion

Plants sense and respond to the presence of microbes by recognition of PAMPs, ubiquitous microbe-associated molecules, using plasma membrane-localised PRRs. PAMP perception triggers an intracellular signal transduction cascade and a subsequent defence response (Boller and Felix, 2009). Flagellin, the central structural unit of the flagellum filament, is a

strong immunogen that elicits PTI in plants (Boller and Felix, 2009). The experiments described in this chapter, measuring ROS production in *A. thaliana* and *N. benthamiana* leaves after application of whole cell extracts revealed that flagellin from *Pto* DC3000, *P. protegens* Pf-5 and *P. aeruginosa* PA01 substantially contributes to the induction of this early plant immune response.

The flagellum is an important bacterial organelle, enabling the bacterium to sense and explore its environment, and contributing to initial attachment to surfaces (Rossez et al., 2015). Flagella-driven motility plays critical roles both in effective plant infection and commensal rhizosphere colonisation. It facilitates colonization of plant surfaces, migration into the apoplast and movement through the soil towards the nutrient-rich environment of the plant root (Lugtenberg et al., 2001). The role of flagella during plant interactions is therefore somewhat ambiguous. Plant-associated bacteria must balance the requirement for flagella-driven motility in colonisation and infection with the downside of potential immune recognition.

To successfully colonize and infect plants, both pathogenic and commensal bacteria need to evade recognition, or to suppress host immune responses. Bacteria have evolved a variety of mechanisms to evade flg22-triggered immunity (Rossez et al., 2015). One important strategy for evading plant immune recognition is the control of flagella synthesis. Bacteria can down-regulate or switch off flagella expression during infection when motility is unnecessary. While expression of flagella genes is controlled by a number of different signal inputs, the transcriptional regulator FleQ plays a central role in this process via cdG (Hickman and Harwood, 2008, Baraquet and Harwood, 2013), with FleQ inactivation by cdG-binding leading to the down-regulation of flagella gene expression in *Pseudomonas* spp. (Baraquet and Harwood, 2013). The results of this study suggest a direct link between cdG-regulated flagella synthesis and evasion of plant immunity. This relationship is widespread, and applies to commensal as well as specific and non-specific plant pathogens. Elevated cdG levels in *Pto* DC3000, *P. protegens* Pf-5 and *P. aeruginosa* PA01 reduce extracellular flagellin levels, and thus help the bacteria to evade the FLS2-mediated immune response in *N. benthamiana* and *A. thaliana* plants. Reduced flagellin levels appear to explain most, if not all of the ROS-suppressive effect of cdG overproduction, as little or no additional effect was observed upon *wspR19* expression in either *fls2* or *efr fls2* plants. While flagellin is a major elicitor in the bacterial extracts from all three *Pseudomonas* spp., EF-Tu appears to be a stronger elicitor in *P. aeruginosa* PA01 extracts compared to *Pto* DC3000 and *P. protegens* Pf-5. PAMPs from different species generally vary in their eliciting potential (Lacombe et al., 2010, Clarke et al.,

2013) due to allelic variation in the recognized epitope. The immunogenic elf18 sequence from *P. protegens* Pf-5 and *P. aeruginosa* PA01 are identical, which suggests that the difference in their ability to trigger a ROS burst might be due to post-translational modifications or protein abundance in the extract.

CdG regulates various phenotypic output pathways that define the bacterial lifestyle, and is consequently likely to play an important role in controlling the association of bacteria with plants. This relationship is indirect, and relates entirely to the control of bacterial phenotypes. In contrast to the mammalian innate immune system where a specific immune receptor for cdG has been found (Burdette et al., 2011), to my knowledge no direct effect of cdG on plant immunity has been reported, and purified cdG did not affect plant ROS production in these experiments. Recently, researchers have started to examine the role of cdG signalling in the interactions of commensal and pathogenic *Pseudomonas* spp. with their host plants. For example, the DGCs WspR and Rup4959 play important roles in effective wheat rhizosphere colonisation by the commensal species *P. fluorescens* F113 and *P. putida* KT2440 respectively (Matilla et al., 2011, Barahona et al., 2011). In *P. syringae*, artificially elevating cdG levels by over-expressing a DGC gene induces pleiotropic responses including reduced motility, increased EPS production and enhanced biofilm formation, which together produce aberrant plant interaction phenotypes (Perez-Mendoza et al., 2014). More specifically, the DGC DgcP is conserved in *Pseudomonas* and inversely controls motility and biofilm in *P. savastanoi* and is required for full virulence in olive plants (Aragon et al., 2015b). Also, deletion of the putative PDE gene *bifA* results in both decreased motility and reduced virulence in *Pto* DC3000 (Aragon et al., 2015a). Highlighting the relevance of cdG for bacterial virulence, the DGC Chp8 is part of the *hrp* regulon, a gene cluster containing the T3SS and expressed in response to plant signals in *Pto* DC3000 (Engl et al., 2014). Over-expression of Chp8 produces high cellular cdG levels, once again leading to EPS production and reduced flagella expression (Engl et al., 2014).

Over-expressing a DGC *in trans* drastically changed the global cdG concentration in all three bacterial species tested here. In turn, increased cdG levels trigger significant changes in the various signalling networks controlled by this important second messenger (Hengge, 2009). This is borne out by the major shifts in colony morphology, polysaccharide production and motility seen for the *wspR19* over-expression strains. Despite these pleiotropic effects, this study shows that the suppressive effect of cdG on the plant immune response depends almost entirely on the reduced signal transduction through the FLS2 receptor, as a consequence of reduced flagellin production in the cdG over-producing strains.

Infections of *P. aeruginosa* on *A. thaliana* did not show any disease symptoms or bacterial proliferation on various *A. thaliana* accessions including the FLS2-defective genotypes Ws-0 and *fls2* (Figures 3.9 and 3.10) (Gomez-Gomez and Boller, 2000, Zipfel et al., 2004). Successful infections of *A. thaliana* have been described by incubating the plants at a temperature of 30°C compared to 24°C used in my experiments (Starkey and Rahme, 2009). This drastic rise in temperature could explain the enhanced susceptibility of *A. thaliana* and/or increased virulence and growth of *P. aeruginosa* (Alcázar and Parker, 2011, Cheng et al., 2013, Wurtzel et al., 2012).

Although cdG overproduction enables bacteria to evade FLS2-mediated immunity, high levels of cdG actually led to drastically reduced *Pto* DC3000 virulence during *A. thaliana* infection. I propose that the reduction in virulence upon *wspR19* expression is largely due to the loss of flagella-driven motility. Restriction of bacterial growth due to flagellin recognition in *A. thaliana* is highly effective against non-adapted pathogens (Li et al., 2005, de Torres et al., 2006, Forsyth et al., 2010, Zeng and He, 2010). Conversely, against adapted pathogens like *Pto* DC3000 FLS2-mediated immunity is only effective when the bacteria are detected in the early stages of infection (Zipfel et al., 2004, Zeng and He, 2010, Hann and Rathjen, 2007). During these initial infection steps, bacteria must trade-off evasion of FLS2-mediated immune responses with the loss of flagellar motility. It has been reported that the virulence of a *Pto* DC3000 Δ*fliC* mutant is compromised upon spray infection in *A. thaliana* Col-0, but that the mutant grows as well as wild-type when the bacteria are syringe-infiltrated into the apoplast (Li et al., 2005, Clarke et al., 2013). Likewise, in my experiments over-expression of *wspR19* negatively affected bacterial growth only during spray infections, where bacteria have to attach to the plant surface and migrate into the apoplast, but had no effect on virulence following leaf infiltration.

Besides the loss of flagellar motility, other pleiotropic effects of cdG signalling may contribute to the compromised virulence of *Pto* DC3000 over-expressing *wspR19*. Thus, infiltrating bacteria directly into the apoplast might also bypass these virulence-associated cdG pathways. These include a reduction in pili-driven motility (Kazmierczak et al., 2006), interference with the correct deployment and function of the T3SS (Kulasakara et al., 2006), overproduction of EPS or other attachment factors in an inappropriate context (Gal et al., 2003), and as-yet undefined effects on secondary metabolism and small molecule secretion (Malone et al., 2010). AmrZ is a transcriptional regulator of several proteins involved in cdG metabolism and a *Pto* DC3000 *amrZ* insertion mutant shows the typical cdG phenotypes, including wrinkly colony morphology, increased cellulose production and loss of motility

(Prada-Ramírez et al., 2016). The *amrZ* strain, but not a cellulose-deficient mutant, is impaired in virulence on spray-infected tomato plants, which could be due to effects of AmrZ-regulated motility and/or other bacterial processes during pathogenesis (Prada-Ramírez et al., 2016). Clearly the negative effects of high cdG levels are far less severe during an established infection, although whether the lifestyle transition from colonisation and initial infection to apoplastic proliferation is accompanied by a significant increase in the intracellular level of cdG in *Pto* DC3000 remains to be determined.

A ground-breaking discovery has been made in a study that illustrates in picturesque Mickey-Mouse-plates a stable phenotypic transition in multiple *X. campestris* strains cultivated on artificial growth media from non-motile, EPS producing to motile, non-mucoid cells with reduced virulence (Kamoun and Kado, 1990). Although the molecular determinants have not been investigated, this switch of bacterial behaviour strongly resembles cdG-associated phenotypes.

In this chapter, I established a potential role for the bacterial second messenger cdG in plant immune evasion, and showed that this effect is mediated by a reduction in the levels of the PAMP flagellin, and consequently reduced FLS2-mediated host immune response. However, bacteria cannot simply over-produce cdG whenever they encounter host plants; the complex intracellular signalling networks controlled by cdG play important roles in mediating the initial stages of plant infection, and flagella driven motility appears to be at least as important to infection as immune system evasion, at least until the infection is established.

Chapter 4

The role of bacterial exopolysaccharides during plant infection

4.1 Summary

To study the specific role of bacterial exopolysaccharides (EPS) during plant colonization and infection, deletion mutants of multiple EPS biosynthesis operons were generated in *Pto* DC3000 and *P. protegens* Pf-5. Indeed, *Pto* DC3000 EPS deletion mutants showed significantly reduced virulence on *A. thaliana*, with a combination of at least two different types of EPS required for normal proliferation in the apoplast. Next, a series of experiments was conducted to try defining the mechanism of action of EPS in the apoplast. Besides surface adhesion and stress protection, a role has also been suggested for EPS in evasion of pattern-triggered immunity (PTI). Extracts from these EPS-deficient strains were tested for their capacity to elicit or suppress PAMP-induced ROS burst. However, extracts from the EPS mutant strains induced similar ROS burst as the respective wild-type strain in *A. thaliana*. Morphology of bacterial 'macrocolonies' and EPS staining experiments suggested that *Pto* DC3000 and *P. protegens* Pf-5 do not produce large amounts of EPS during *in vitro* growth under the tested conditions. Nonetheless, EPS seems to be important during infection of *A. thaliana* by *Pto* DC3000. I examined the presence of a genetic link between EPS and PTI by infecting PTI-compromised *A. thaliana* mutant lines. However, the experiments were inconclusive regarding the role of EPS in suppression of PTI and indicate that EPS has multiple functions during the infection process. EPS are key components of bacterial biofilms and contribute to water retention and nutrient accumulation. To test a role of EPS for maintaining a wet growth environment, plants were infected under different humidity conditions. However, the reduced growth *in planta* could not be compensated by high humidity. Thus, further experiments are underway to address the structural role of EPS during colony formation and expansion during apoplast colonization.

4.2 Introduction

The production of exopolysaccharides (EPS) is a common factor of bacteria colonizing the phyllo- and rhizosphere of plants (Davey and O'Toole G, 2000). EPS molecules are carbohydrate polymers that are secreted by bacteria, and form a highly viscous extracellular slime or build a capsule layer around the cell (Flemming and Wingender, 2010). The production of oligosaccharide polymers is generally associated with biofilm formation, a macro structure composed of bacterial cells embedded in a matrix containing further polymeric substances such as proteins, extracellular DNA and lipids (Flemming and

Wingender, 2010, Petrova and Sauer, 2012). Biofilms define the sessile lifestyle of a bacterial community and form the immediate environment, providing multiple functions including adherence to surfaces, absorption of water, accumulation of nutrients and protection from hydrophobic and toxic substances (Petrova and Sauer, 2012, Flemming et al., 2016).

EPS can vary in their chemical and physical properties not only between bacterial species but also between strains of a single species (Petrova and Sauer, 2012). EPS from the opportunistic human pathogen *P. aeruginosa* are well studied, and comprise at least three different polysaccharides, namely alginate, Psl, and Pel (Wozniak et al., 2003, Friedman and Kolter, 2004, Jackson et al., 2004). The biosynthesis pathway of alginate, a high molecular weight co-polymer of β-1,4-linked acetylated D-mannuronic acid and L-guluronic acid subunits has been first described in *P. aeruginosa* (Franklin et al., 2011, Evans and Linker, 1973), and seems to be conserved in other *Pseudomonas*, including *P. syringae* (Penaloza-Vazquez et al., 1997, Whitney and Howell, 2013, Osman et al., 1986). Psl is composed of a repeating pentamer of D-mannose, L-rhamnose and D-glucose (Byrd et al., 2009), while the detailed structure of the glucose-rich polymer Pel is currently unknown (Franklin et al., 2011, Friedman and Kolter, 2004, Friedman and Kolter, 2003). Bacterial cellulose is a homopolymer of β-1,4-linked D-glucose and is produced by many *Pseudomonas* (Römling and Galperin, 2015). While cellulose biosynthesis is encoded by the *bcs* gene cluster in some *Pseudomonas* (Nielsen et al., 2011), other species including *Pto* DC3000 produce an acetylated form of cellulose whose synthesis requires the *wss* operon, which has been first described in *P. fluorescens* SBW25 (Spiers et al., 2003, Prada-Ramírez et al., 2016). Additionally, *P. syringae* is known to produce a high molecular mass β-2,6 polyfructan with extensive branching through β-2,1 linkages (Fett and Dunn, 1989, Osman et al., 1986, Laue et al., 2006). The poly-β-1,6-linked N-acetylglucosamine (PNAG) has been found in various Gram-negative bacteria and is presumably involved in biofilm formation of *P. protegens* Pf-5 (Kidarsa et al., 2013, Wang et al., 2004). Other EPS from *Pseudomonas* without known composition or structure are Pea (Nielsen et al., 2011) and Peb (Nilsson et al., 2011), which have been described in *P. putida*.

Although there seem to be specific differences for transcriptional activation of EPS biosynthesis genes between *Pseudomonas* species (Penaloza-Vazquez et al., 1997, Keith et al., 2003), regulation of EPS production is controlled by the same intracellular signalling molecule, cyclic-di-GMP (cdG), in regulatory networks that are present in *P. syringae* and *P. aeruginosa* (Chapter 3) (Hickman et al., 2005, Prada-Ramírez et al., 2016, Hickman and Harwood, 2008, Moscoso et al., 2014, Records and Gross, 2010, Vakulskas et al., 2015). It has

been shown in *P. aeruginosa* that cdG-binding by Alg44, a cytoplasmic membrane protein of the alginate biosynthesis complex, is essential for alginate production (Merighi et al., 2007). The functional equivalent protein in Pel biosynthesis in *P. aeruginosa* is PelD, which regulates Pel production in a cdG-dependent manner (Lee et al., 2007). Additionally, Pel and Psl production are positively regulated at the transcriptional level by cdG produced by the diguanylate cyclase WspR (Hickman et al., 2005) and the cdG-responsive transcription factor FleQ (Hickman and Harwood, 2008). These aspects indicate a potential role of cdG as a common transcriptional and/or post-translational regulator of EPS production.

Bacterial EPS are an important factor for many processes, including adhesion to surfaces, stress protection and creating an optimal growth environment (Flemming et al., 2016). Cystic fibrosis lung disease caused by the human opportunistic pathogen *P. aeruginosa* is strongly associated with the production of EPS and biofilm formation, including alginate, Pel and Psl (Sousa and Pereira, 2014, Kirisits et al., 2005, Malone et al., 2010). A role for EPS as a virulence factor of *P. syringae* during plant infection has also been suggested (Aslam et al., 2008, Fett and Dunn, 1989, Yu et al., 1999), but the specific role of the different types of EPS and their contribution to pathogenesis is not well understood. A mechanistic explanation for the role of EPS in virulence has been suggested in a study showing that EPS molecules can interfere with PTI signalling by chelating calcium ions in the apoplast (Aslam et al., 2008). Infiltration of purified EPS from different species into *A. thaliana* leaves also inhibits the PAMP-induced Ca^{2+} influx, ROS burst and defence-related gene expression (Aslam et al., 2008).

The plant-associated species *Pto* DC3000, *P. aeruginosa* PA01 and *P. protegens* Pf-5 encode the enzymes for the production of alginate, Psl, and Pel or the equivalent cellulosic polymer Wss (Whitney and Howell, 2013). Moreover, the genomic arrangement of the structural biosynthetic genes is almost identical in all three species (Winsor et al., 2016). The work described in this chapter aims to test a role of EPS during plant colonisation, and to examine the contribution of these EPS molecules to modulate immune responses during plant infection. As my attempt to manupulate cdG-dependent regulation of EPS led to various pleiotropic effects due to other cdG-controlled factors (see Chapter 3), I here rather focused on strains with loss-of-function mutations in the EPS production pathways.

4.3 Results

4.3.1 Generation of EPS deletion strains

The three *Pseudomonas* species *Pto* DC3000, *P. aeruginosa* PA01 and *P. protegens* Pf-5 encode a similar set of biosynthetic genes for EPS production in their genomes (Figure 4.1) (Winsor et al., 2016). All three species are able to produce alginate and Psl, and *P. aeruginosa* PA01 and *P. protegens* Pf-5 additionally carry the genes of the Pel pathway, while *Pto* DC3000 has the *wss* operon for production of acetylated cellulose (Figure 4.1).

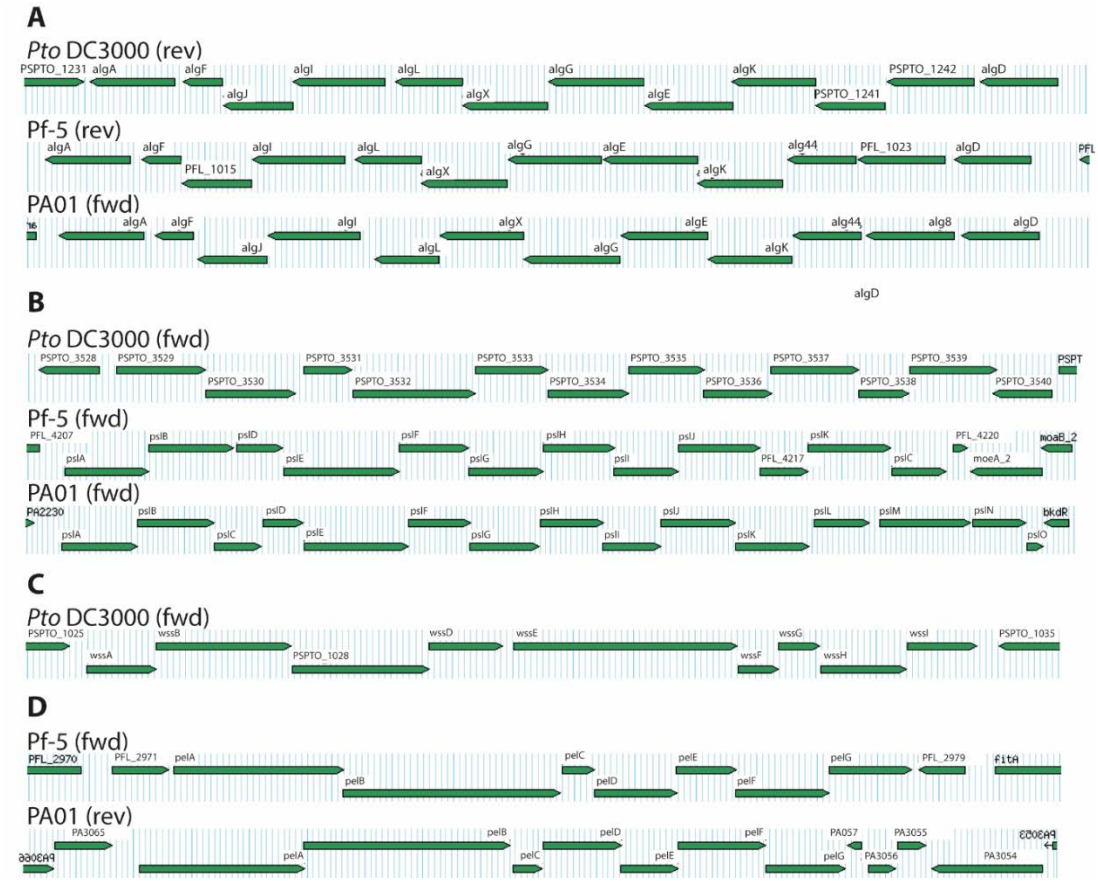

Figure 4.1. Exopolysaccharide biosynthesis gene cluster on the chromosomal loci of the *Pseudomonas* species *Pto* DC3000, *P. protegens* Pf-5 and *P. aeruginosa* PA01. Gene structure of the pathway for the production of alginate (A), Psl (B), Wss (C) and Pel (D). The depicted genomic regions are obtained from GBrowse of the *Pseudomonas Genome Database* (Winsor et al. 2016) and show approximately 19 kb. Orientation on the chromosomal DNA strands is indicated by forward (fwd) and reverse (rev) notation after species name.

The deletion of individual genes in these pathways in different *Pseudomonas spp*. abolishes the production of the respective EPS. *P. aeruginosa* PA01 Δ*pslD* is unable to produce Psl polymer (Byrd et al., 2009), and non-polar deletions of *algG* and *algX* result in a lack of alginate secretion (Jain et al., 2003, Robles-Price et al., 2004). Similarly, biofilm and pellicle formation is impaired in non-polar disruptions of *pelB* and *pelC* in *P. aeruginosa* PA14

(Vasseur et al., 2007, Friedman and Kolter, 2003). Production of the acetylated cellulose polymer encoded in the *wss* pathway is abolished in a *wssB::Tn5* mutant of *P. fluorescens* SBW25 (Spiers et al., 2002). The core cellulose synthase complex comprising *WssBCDE* of *P. fluorescens* SBW25 is also conserved in *Pto* DC3000 (Spiers et al., 2003). Based on the required genes for EPS synthesis and export described in the literature, I engineered in-frame deletions of two genes required for production of the respective EPS in *Pto* DC3000 and *P. protegens* Pf-5 (Table 4.1). The deleted genes are part of an operon, and expression of downstream genes is presumably unaffected as the deletions were done in-frame. Additionally, it has been suggested that intermediate products of EPS biosynthesis that do not get secreted across the outer membrane get degraded in the periplasm (Franklin et al., 2011). Beside the deletion mutants, which are defective in a single EPS pathway, I made double and triple mutants to obtain EPS-deficient strains (Table 2.1). The in-frame deletions were created by a two-step homologous recombination process using a suicide plasmid (Chapter 2.3), and were confirmed by PCR and by sequencing the transitions to the adjacent regions in the genome. The mutations in the EPS pathways did not affect *Pto* DC3000 growth in rich media (Figure 4.2).

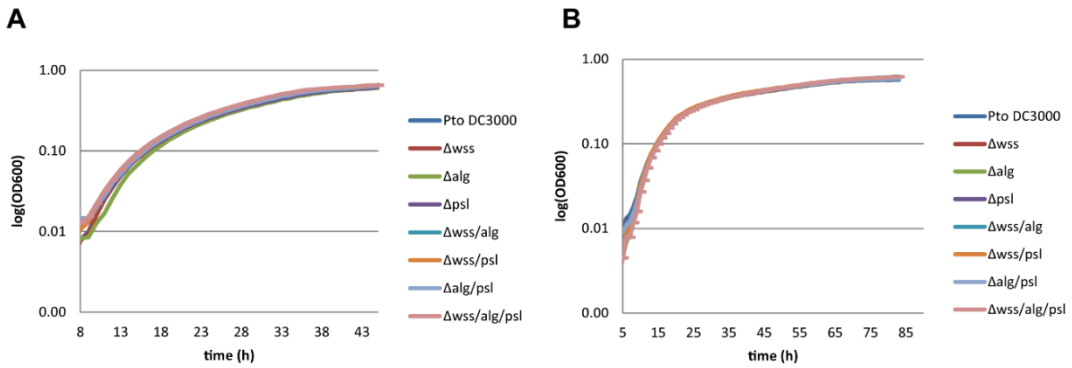

Figure 4.2. Growth of EPS-deficient *Pto* DC3000. Growth of *Pto* DC3000 wild-type and isogenic EPS mutant strains was measured in L- medium (A) and KB medium (B). Values are means ± standard error (n = 6). The experiment was performed once.

A *P. aeruginosa* PA01 *pelG::Tn5*/Δ*pslAB* double mutant, which lacks Pel and Psl production, was already available for further analysis (Malone et al., 2010). However, *P. aeruginosa* did not infect *A. thaliana* under the tested conditions (Figure 3.9 and 3.10), so I did not proceed with the characterization of the biological role of EPS from *P. aeruginosa* during the interaction with plants.

4.3.2 EPS production in *Pto* DC3000 is important for bacterial virulence during plant infection

I was interested in the role of EPS during the interaction of *Pseudomonas* with plants, and focussed mainly on the model system of *A. thaliana* and the pathogenic *Pto* DC3000. EPS biosynthesis appears to be important for *Pto* DC3000 virulence, as the triple EPS mutant *Pto* Δ*alg/psl/wss* (also described as Δ*eps*) showed reduced growth 3 dpi *in planta* and reduced disease symptoms compared to the wild-type strain on *A. thaliana* Col-0 (Figure 4.3). Growth of *Pto* DC3000 Δ*alg/psl/wss* was impaired after infiltrating bacterial directly into the intercellular space of the leaf (Figure 4.3A) or after spraying the solution on the leaf surface (Figure 4.3B). Although it was not clear from these infection experiments which processes are affected by the lack of EPS, the reduced virulence after infiltration suggested a role of EPS during the establishment of infection in the apoplast.

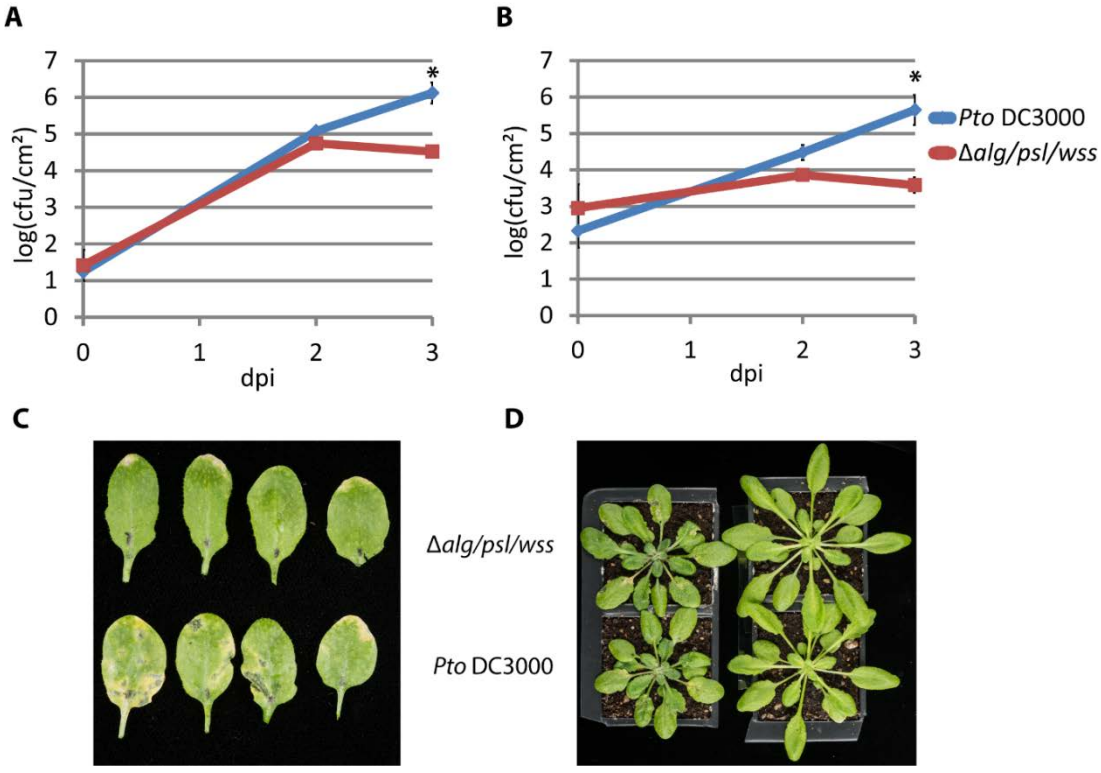

Figure 4.3. Infection of *A. thaliana* with EPS-deficient *Pto* DC3000. Four-week-old *A. thaliana* plants were infected with *Pto* DC3000 wild-type or Δ*alg*/*psl*/*wss* by infiltration with 10^5 cfu/mL (A and C) or spray infection with 10^8 cfu/mL (B and D). Bacterial growth *in planta* was monitored over time by leaf sampling, serial dilutions and colony counting (A and B). Pictures of plants with disease symptoms were taken at 7 dpi (C and D). Values are means ± standard error (n = 4). Significant differences (*p < 0.05) based on two-tailed Mann–Whitney test. The experiment was done at least two times.

EPS production in *Pto* DC3000 appeared to play an important role during infection (Figure 4.3). To dissect which EPS contributes to virulence, I performed *A. thaliana* leaf infiltrations of single, double and triple EPS mutants. The bacterial growth of wild-type and the deletion mutant strains in the plant tissue was monitored over 5 days. According to the bacterial

proliferation data *in planta*, the strains separated into two virulence groups (Figure 4.4A). While *Pto* Δ*wss, Pto* Δ*alg, Pto* Δ*psl* and *Pto* Δ*alg/psl* showed similar virulence as the wild-type, *Pto* Δ*wss/alg, Pto* Δ*alg/psl and Pto* Δ*alg/psl/wss* were impaired during infection. Hence, wild-type-like virulence seemed to require Wss production, but a combination of Alg and Psl could compensate for the lack of Wss. The enhanced growth of *Pto* Δ*psl* strain at 3 dpi was not reproducible upon repeating the experiment (Figure A8.1). The growth data is also reflected in the disease symptoms on *A. thaliana* leaves, as enhanced growth correlated with stronger necrosis at 5 dpi (Figure 4.4B).

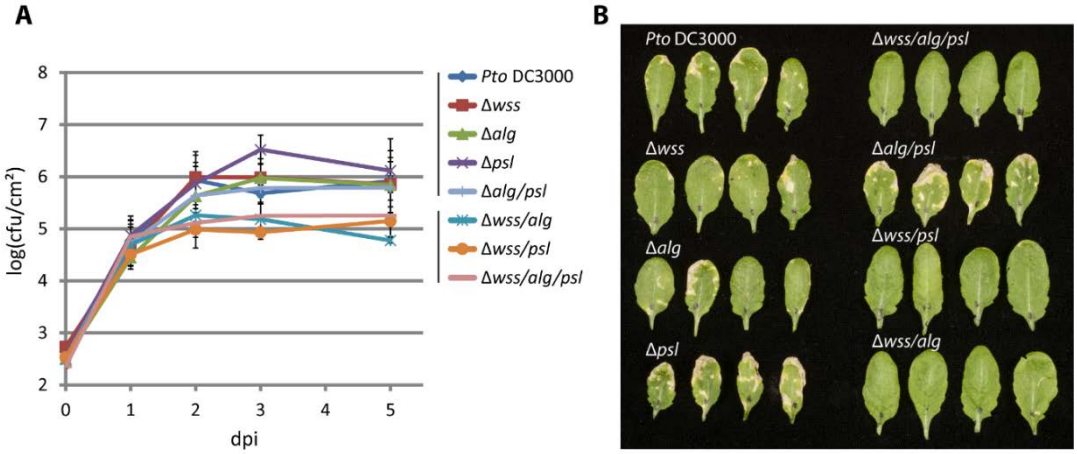

Figure 4.4. Infection of *A. thaliana* with EPS-deficient *Pto* DC3000 strains. Four-week-old *A. thaliana* plants were infected with *Pto* DC3000 wild-type or indicated EPS mutant strains by infiltration with 10^5 cfu/mL. Bacterial growth in planta was monitored over time by leaf sampling, serial dilutions and colony counting (A). Pictures of leaves with disease symptoms were taken at 5 dpi (B). Values are means ± standard error (n = 4). The experiment was done three times.

4.3.3 Crude bacterial extracts of EPS deletion mutants did not affect plant PAMP-induced ROS burst

To study the effect of EPS on PTI, I made crude bacterial extracts of the *P. protegens* Pf-5 and *Pto* DC3000 EPS-deficient strains, and tested their potential to elicit or suppress the PAMP-induced ROS burst. Extracts from EPS-deficient *P. protegens* Δ*alg/pel/psl* and *Pto* DC3000 Δalg/*wss/psl* triggered a similar ROS burst in Col-0 leaf discs as an extract from the respective wild-type strains (Figure 4.5A and C). Similarly, extracts from the EPS-deficient *P. protegens* Pf-5 mutants did not affect flg22-induced ROS production (Figure 4.5B and D). Crude extracts were normalized based on total protein levels of the final extract. However, the plant ROS burst induced by the bacterial extract was quite variable and EPS-deficient extracts occasionally triggered an enhanced (Figure A8.2B) or reduced ROS response (Figure A8.2E). This variability might be due to the complex mixture of the crude extract or small changes of

components with a strong impact on the ROS burst, such as the PAMP flagellin (see Chapter 3). However, the reduction of ROS production after application of extract from *P. protegens* Δ*alg/pel/psl*. (Figure A8.2E and F) was independent of *fls2* (Figure A8.2G and H), which thus excludes flagellin levels as source of variability in this case.

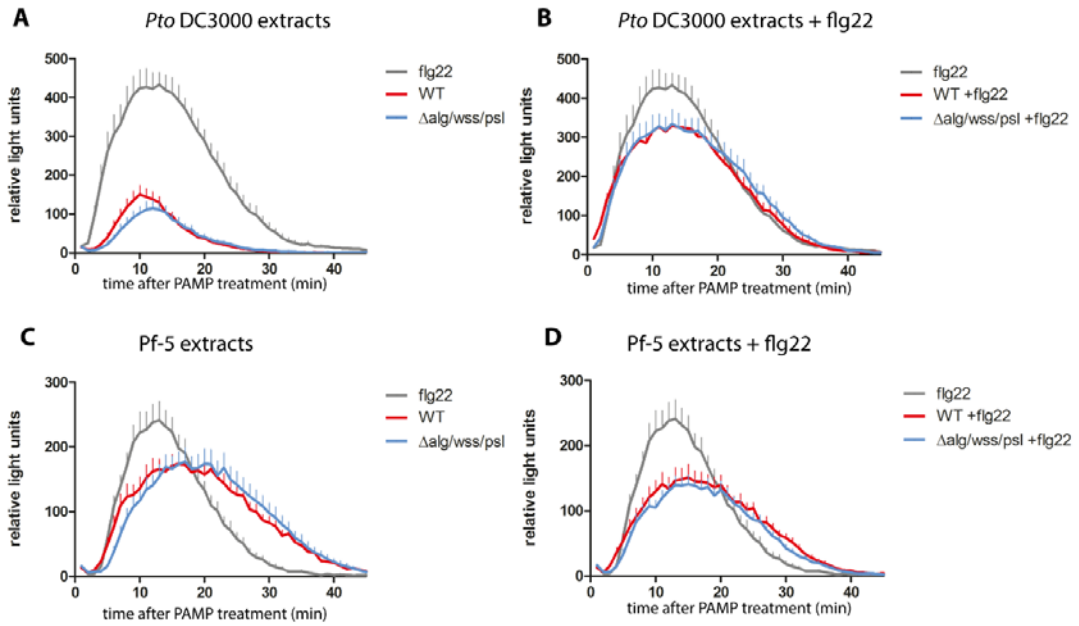

Figure 4.5. Extracts from *Pseudomonas* wild-type strains and respective EPS-deficient mutants trigger similar ROS burst in *Arabidopsis thaliana*. Leaf discs were treated with extracts from *Pto* DC3000 wild-type and Δ*alg*/*psl*/*wss* (A and B) and *P. protegens* Pf-5 wild-type (WT) and Δ*alg*/*psl*/*pel* (C and D) to assess the ability to induce a ROS burst (A and C) or to suppress a ROS burst elicited by co-application of 100 nM flg22 with the extracts (B and D). Values are means ± standard error (n = 8). ROS production is expressed as relative light units. The experiment was done at least two times.

The amount of EPS in the bacterial extract preparations was unknown. To visualize EPS production by the different strains, I tested various polysaccharide-binding dyes, including Calcofluor White, Ruthenium Red, Toluidine Blue-O and Congo Red, which have been described to stain specific types of EPS during bacterial growth on solid medium (Ferrieres et al., 2007, Spiers et al., 2002). Unfortunately, I did not observe any difference in colour intensity between wild-type and the EPS deletion mutant strains of *Pto* DC3000 and *P. protegens* Pf-5, respectively, under standard growth conditions on L-medium or LB medium agar plates supplemented with Congo Red (Figure 4.6) or other dyes (data not shown).

Wild-type strains *P. protegens* Pf-5 and *Pto* DC3000 did not seem to produce large amounts of EPS under standard culturing conditions, as both strains only showed considerable binding of the cellulose-binding dye Congo Red after expression of the diguanylate cyclase *wspR19* (Figure 4.6 and Figure 3.1A). This might be due to lack of EPS production in the tested

cultivation media and growth conditions. To enhance production of the different types of EPS, I thus decided to express *wspR19* in the individual EPS mutation backgrounds and to test different growth media. Certain media such as KB and SFM media were identified to promote EPS production according to the colony morphology when bacteria expressed *wspR19* (Figure 4.6 and 4.7). Using these culturing conditions and *wspR19*-expressing strains to make the bacterial crude extracts may lead to a stronger effect of the EPS in the ROS burst assays; however, previous experiments showed that the major elicitor of ROS burst in these extracts is the PAMP flagellin, and thus small changes in flagellin levels can have a strong effect, and therefore may mask any contribution of EPS to the ROS burst (see Chapter 3).

4.3.4 Optimizing bacterial growth condition for EPS production

To exclude additional effects from the bacterial crude extract and to directly test the ability of EPS to suppress the PAMP-induced ROS burst, I purified the different types of EPS, namely aceylated cellulose (Wss), Pel, Psl and alginate. As the double deletion strains have only one functional EPS biosynthesis pathway left, they are a useful tool to facilitate purification of a single EPS. Additionally, I transiently expressed the diguanylate cyclase *wspR19* to increase cdG levels in the production strains, as many EPS biosynthetic clusters are transcriptionally or allosterically controlled by cdG (Hengge, 2009, Starkey et al., 2009, Franklin et al., 2011). *wspR19* expression markedly enhanced staining of the cellulose-binding dye Congo Red (Figure 3.1A and Figure 4.6). Solid growth media was preferred over liquid media as it allows easy assessment of colony morphology, and a transcriptional reporter study of alginate biosynthetic genes in *P. aeruginosa* suggested that surface contact is a cue for inducing alginate production (Davies and Geesey, 1995). To find suitable conditions for EPS production, I spotted 5 µL of the bacterial solution onto solid growth media and assessed typical features of (macro-)colony morphology (*e.g.* mucoid or wrinkled) as an indication for EPS production (Figure 4.7).

A mucoid colony surface is an indicator for alginate production in *P. aeruginosa* and *P. syringae* (Ramsey and Wozniak, 2005, Schreiber and Desveaux, 2011). This feature could be observed by growing the double mutant strain *Pto* DC3000 under constitutive *wspR19* expression on SFM medium. This colony morphology is likely due to alginate production, because the mucoid phenotype is even more pronounced in the *Pto* Δ*psl/wss* (Alg+) strain, but absent in the other mutants lacking alginate production. Typically, *Pseudomonas* strains with high cdG levels, for example due to expression of a DGC, have a small colony variant phenotype with wrinkled structures (Malone et al., 2007, D'Argenio et al., 2002, Hickman et al., 2005). The wrinkled colony phenotype was only mildly expressed during growth on L-,

M9 minimal and SFM medium (Figure 4.6). However, on KB medium w*spR19* expression turns *Pto* Δ*alg/psl* colonies wrinkly, probably due to Wss production (Figure 4.7A). *P. protegens* Pf-5 expressing *wspR19* showed the wrinkly colony phenotype (Figure 4.7B).

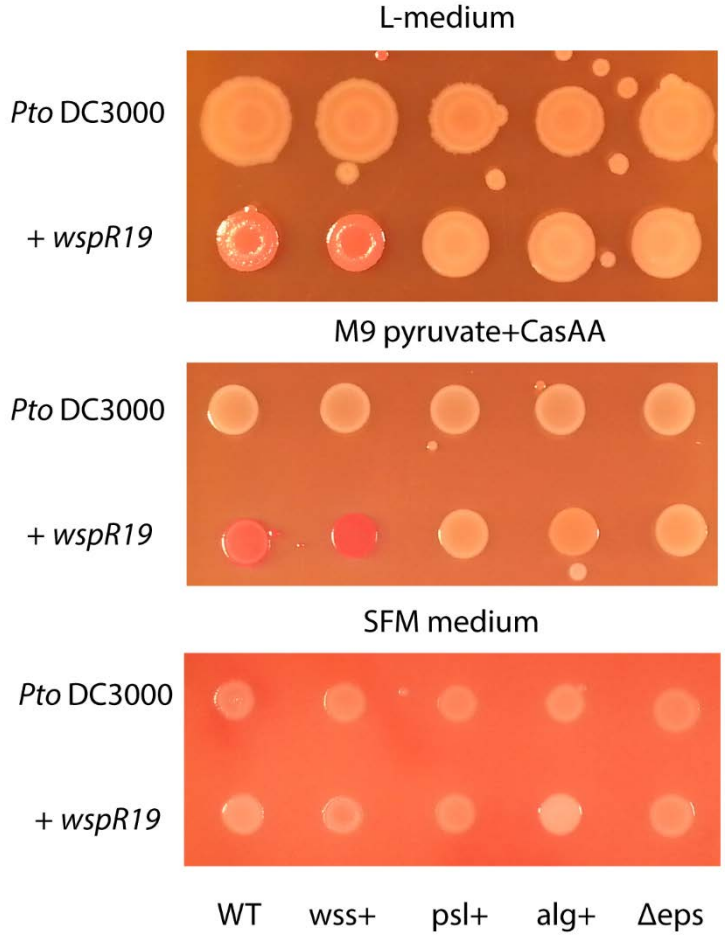

Figure 4.6. Exopolysaccharide production of *Pto* DC3000 expressing *wspR19.* Congo Red dye binding of wild-type and EPS mutant strains from *Pto* DC3000, Wss+ (*Pto* Δ*alg*/*psl*), Psl+ (*Pto* Δ*alg*/*wss*), Alg+ (*Pto* psl/*wss*), ΔΔΔ (*Pto* Δ*alg*/*psl*/*wss*) without and with expression of *wspR19.* Bacterial solution (5 µL) were spotted on L-medium, M9 medium with 0.2% pyruvate and 0.2% Cas amino acids, and SFM medium agar plates and incubated for 3 days at 30°C.

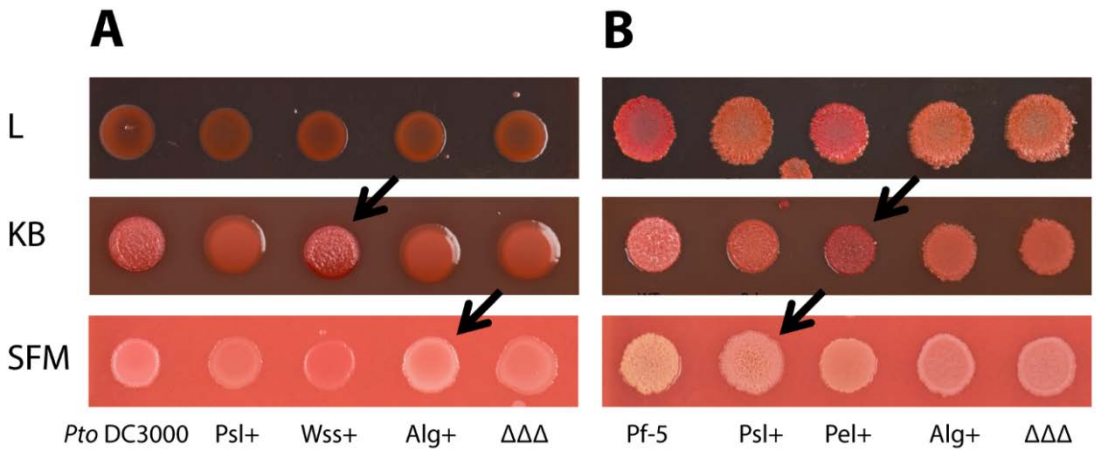

Figure 4.7. Exopolysaccharide production of *Pto* DC3000 and *P. protegens* Pf-5 expressing *wspR19.* Congo Red dye binding of wild-type and EPS mutant strains from (A) *wspR19*-expressing *Pto* DC3000, Psl+ (*Pto* Δ*alg*/*wss*), Wss+ (*Pto* Δ*alg*/*psl*), Alg+ (*Pto psl*/*wss*), ΔΔΔ (*Pto* Δ*alg*/*psl*/*wss*) and (B) *wspR19*-expressing *P. protegens* Pf-5, Psl+ (Pf-5 Δ*alg*/*wss*), Pel+ (Pf-5 Δ*alg*/*psl*), Alg+ (Pf-5 *psl*/*pel*), ΔΔΔ (Pf-5 Δ*alg*/*psl*/*pel*). Bacterial solution (5 µL) were spotted on L-medium, KB medium and SFM medium agar plates and incubated for 3 days at 30°C. Black arrows mark characteristic colony morphology phenotypes.

The wrinkly colony phenotypes were dependent on certain media, *e.g.* Psl production of *P. protegens* Pf-5 on SFM or Pel production of *Pto* DC3000 on KB medium. These growth media were used to culture different strains for alginate, Psl and Pel purification from *Pto* Δ*psl/wss-wspR19*, *P. protegens* Δ*alg/pel-wspR19* and *P. protegens* Δ*alg/psl-wspR19*, respectively.

Provisional EPS purification attempts from bacterial growth on solid agar plates were based on protocols described in the literature (Byrd et al., 2009, Ferrieres et al., 2007). Quantification of purified EPS was performed according to the previously described phenol-sulfuric acid method (Masuko et al., 2005). However, the purification process was not successful, as final aliquots contained very low EPS concentrations and could not be used for further analysis (data not shown). During the purification efforts, I realized that each type of EPS has different physio-chemical properties, and it would require substantial amount of time and effort to optimize the EPS purification protocols, as previously noted (Flemming and Wingender, 2010). Given that initial tests with bacterial crude extracts did not indicate a specific EPS-dependent plant response (*e.g*. ROS burst), I decided not pursue further EPS purification.

Overall, both strains *Pto* DC3000 and *P. protegens* Pf-5 did not appear to be strong producers of EPS under the used laboratory culture conditions (Figure 4.7), which has been noted before (Freeman et al., 2013, Keith et al., 2003, Aslam et al., 2008). The morphology of colony growth indicated that certain growth media and expression of the cyclase *wspR19* resulted in slightly enhanced EPS production.

A notable aspect from the growth experiments on different media was that the morphology of *P. protegens* Δ*alg/pel/psl-wspR19* colonies were still wrinkly (Figure 4.7B), suggesting the presence of additional types of EPS. The genome of *P. protegens* Pf-5 contains the EPS operon *pgaABCD*, which was first identified for PNAG production in *E. coli* and is expressed in *P. protegens* Pf-5 during biofilm formation (Wang et al., 2004, Kidarsa et al., 2013). In addition, *P. protegens* Pf-5 encodes the *pea* gene cluster, which has been first described in *P. putida* (Nielsen et al., 2011, Winsor et al., 2016). Production of both types of EPS, PNAG and Pea, is controlled by cdG (Nielsen et al., 2011, Steiner et al., 2013), and thus represent promising candidates to be the additional EPS responsible for the wrinkly colony phenotype during *wspR19* expression. A *pgaCD* deletion construct has been cloned, but the corresponding mutant has not yet been generated, due to lack of time.

4.3.5 Reduced bacterial growth of *Pto* Δ*alg/psl/wss* is not recovered in PTI-compromised plants.

As all three types of EPS contribute to virulence (Figure 4.4), the triple mutant *Pto* Δ*alg/psl/wss* was used for the following infection experiments. To address whether EPS has a function in the suppression of PTI, I tested if PTI contributes to the impaired growth of the *Pto* Δ*alg/psl/wss* strain. I infected Col-0 and the PTI-compromised mutant lines *fls2/efr/cerk1* (*fec*) (Gimenez-Ibanez et al., 2009b) and *bak1-5*/*bkk1-1*/*cerk1* (*bbc*) (Xin et al., 2016), which are lacking major PRRs and co-receptors. According to the bacterial growth data, the impaired virulence of *Pto* Δ*alg/psl/wss* (Δ*eps*) was not recovered on PTI-compromised *fec* and *bbc* plants (Figure 4.8 and Figure A8.3). These experiments do not allow to exclude a role of EPS for suppression of PTI, and do not support it either. The data rather suggests that EPS has multiple functions during plant infection beside PTI suppression. It is easy to imagine that biofilm formation could be required before or in parallel to immune evasion for optimal infection. In such a case, the PTI-deficient mutants would not complement the lack of biofilm formation.

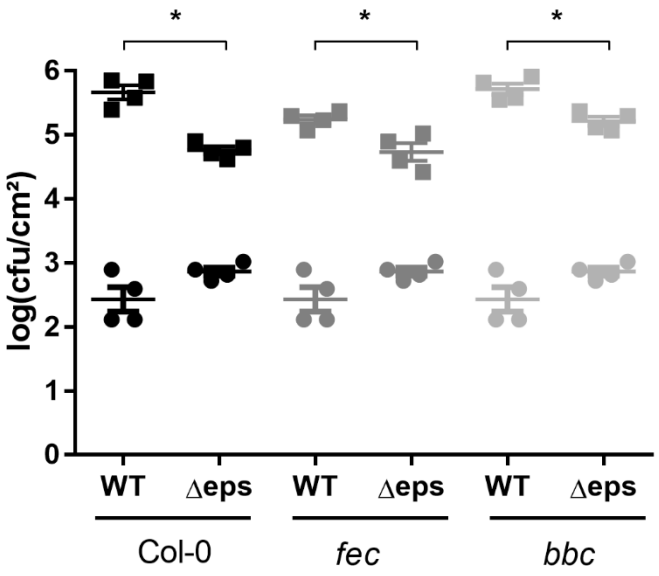

Figure 4.8. Infection of PTI-compromised *A. thaliana* plants with EPS-deficient *Pto* DC3000. Four-week-old *A. thaliana* Col-0 and mutant genotypes *fec* (*fls2/efr/cerk1*) and *bbc* (*bak1-5*/*bkk1-1*/*cerk1*) were infiltrated with 10^5 cfu/mL *Pto* DC3000 wild-type or Δ*eps* (*Pto* Δ*alg/psl/wss*). Bacterial growth *in planta* was assessed at 0 dpi (round symbols) and 3 dpi (square symbol) by leaf sampling, serial dilutions and colony counting. Values are means ± standard error ($n = 4$). Asterisks indicate statistically significant difference (* $p < 0.05$) between treatment of wild-type and Δ*eps* based on a two-tailed Mann–Whitney test. The experiment was done three times.

4.3.6 High humidity does not rescue impaired bacterial growth of Δ*eps*

Bacterial biofilms constitute a micro-environment for bacterial growth and EPS is a major component of the biofilm matrix (Davey and O'Toole G, 2000, Danhorn and Fuqua, 2007). High air humidity promotes the plant infection of *P. syringae,* and water-soaking spots are characteristic disease symptoms on infected plant leaves (Xin and He, 2013, Xin et al., 2016). As EPS molecules, predominantly alginate, form a hydrogel, which is able to retain large amounts of water (Chang et al., 2007, Hall-Stoodley et al., 2004), EPS might be involved in the maintenance of a humid living environment for the bacteria during plant infection. In collaboration with Xiu-Fang Xin from the laboratory of Sheng Yang He[2], who has a suitable experimental set-up to control air humidity in plant growth rooms, we tested whether the proliferation of the EPS-deficient strain is restored under high air humidity conditions during an infection. Water-soaking spots could be observed under high humidity after 1 dpi on leaves infected with *Pto* DC3000, and reduced spots on the *Pto* Δ*alg/psl/wss* mutant (Figure 4.9A). However, growth of *Pto* Δ*alg/psl/wss* was still reduced in Col-0 plants compared to

[2] Department of Energy, Plant Research Laboratory, Michigan State University, East Lansing, Michigan 48824, USA.

wild-type and could not be recovered due to high humidity levels (Figure 4.9B). This experiment did not support the hypothesis that high air humidity can compensate for the lack of EPS.

Interestingly, increasing levels of humidity seem to enhance bacterial growth *in planta* (Xin et al., 2016) and this growth-promoting effect was stronger in the wild-type compared to the *Pto* Δ*alg/psl/wss* strain (Figure 4.9B).

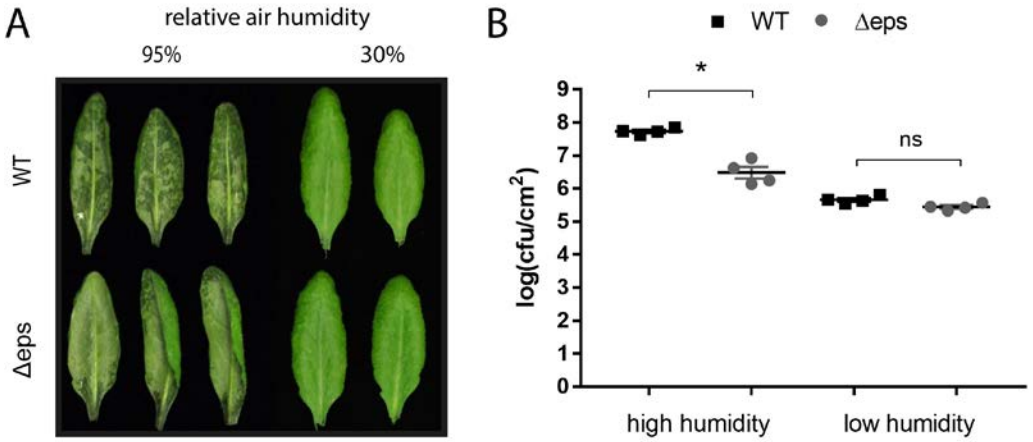

Figure 4.9. Infection of *A. thaliana* plants with EPS-deficient *Pto* DC3000 under high and low humidity. Four-week-old *A. thaliana* Col-0 were infiltrated with 10^5 cfu/mL *Pto* DC3000 wild-type or *Pto* Δ*alg*/*psl*/*wss* (Δ*eps*). After infection, plants were kept under high (95%) and low (30%) relative air humidity. Disease symptoms (A) and bacterial growth *in planta* (B) was assessed at 2 dpi. Values are means ± standard error (n = 4). Asterisks indicate statistical significance (*p< 0.05) between wild-type and Δeps based on an unpaired Mann–Whitney test. The experiment was performed by Xiu-Fang Xin and has been repeated once.

4.4 Discussion

EPS is an important factor for different processes during host colonization including surface adhesion, stress protection and biofilm formation. In *P. aeruginosa*, three types of EPS; namely alginate, Pel and Psl, have been identified as part of the biofilm matrix and as important virulence factors (Hentzer et al., 2001, Friedman and Kolter, 2004, Friedman and Kolter, 2003). Other plant-associated *Pseudomonas* species, such as the pathogenic *Pto* DC3000 and the commensal *P. protegens* Pf-5 also encode a similar set of EPS biosynthetic pathways (Figure 4.1) (Whitney and Howell, 2013).

Infection of *A. thaliana* with *Pto* DC3000 wild-type and the EPS deficient *Pto* Δ*alg/psl/wss* suggested that EPS is a major virulence factor, as bacterial proliferation and plant disease symptoms were strongly reduced (Figure 4.3). Virulence was not only impaired after spray inoculating the leaf surface (Figure 4.3B), but also after infiltration of the bacteria directly

into the intercellular space (Figure 4.3A). This suggests that EPS has an important function during colonization of the apoplast.

To dissect the contribution of individual types of EPS, I infected *A. thaliana* Col-0 with *Pto* DC3000 single, double and triple mutants of the different EPS pathways. Although the *wss* biosynthetic pathway appeared to be particularly important for the virulence of *Pto* DC3000, as the *Pto* Δ*alg/psl* strain still displayed wild-type-like growth *in planta*, a combination of functional alginate and Psl could compensate for the lack of Wss in the *Pto* Δ*wss* strain (Figure 4.4). It thus appears that all three EPS pathways can contribute to maximal virulence of *Pto* DC3000.

Compared to other *P. syringae* strains, *Pto* DC3000 does not produce excessive amounts of EPS during growth on agar plates (Figure 4.6 and 4.7A), and has been described as a weak epiphyte with low osmotolerance (Freeman et al., 2013). The epiphytic fitness of an alginate-deficient *P. syringae* pv. *syringae* strain, is severely compromised, in part due to increased susceptibility to oxidative stress (Yu et al., 1999). Interestingly, alginate biosynthesis in *Pto* DC3000 is stimulated by ROS, which is produced by the plant during bacterial colonization of the apoplast in *A. thaliana* (Keith et al., 2003, Keith and Bender, 1999) and in tomato (*Solanum lycopersicum*) (Boch et al., 2002). However, a *Pto* Δ*alg* mutant was not compromised during *A. thaliana* infection after infiltration into the apoplast (Figure 4.4), but only in combination with the deletion of *psl* or *wss* genes.

Acetylated cellulose produced by the *wss* biosynthetic gene cluster is an important component of biofilm formation and surface attachment in *P. fluorescens* SBW25 (Spiers et al., 2002, Spiers et al., 2003) and other *P. syringae* species (Ude et al., 2006, Arrebola et al., 2015). While there are strong links between production of acetylated cellulose and cdG regulation in *Pseudomonas* (Spiers et al., 2002, Spiers et al., 2003, Morgan et al., 2014, Prada-Ramírez et al., 2016), the environmental signals triggering *wss* gene transcription have not yet been identified. In agreement with my results for infection of *A. thaliana* (Figure 4.4), the cellulose-deficient *Pto* Δ*wssBC* mutant is not affected in virulence on tomato plants after spray infection (Prada-Ramírez et al., 2016). The role of cellulose as a virulence factor has been previously mentioned in various studies with different plant-pathogen model systems, but evidence is mostly indirect and inconclusive. Induced EPS production, including acetylated cellulose, due to DGC expression in *Pto* DC3000 and other *P. syringae* strains had no significant impact on virulence after spray infection on tomato (Perez-Mendoza et al., 2014, Arrebola et al., 2015) and infiltration in *A. thaliana* (Figure 3.11). Furthermore, EPS-compromised *Tn5* insertion mutants of *P. syringae* pv. *syringae* B728a behaved like the wild-

type regarding epiphytic growth and survival on bean leaves (Lindow et al., 1993). Similarly, cellulose-deficient mutants of the distantly related plant pathogen *Agrobacterium tumefaciens* remained fully virulent (Barnhart et al., 2013). All these studies suggesting that cellulose is not a virulence factor are based on genetic data or rely mostly on indirect evidence, but do not take compensatory effects by other EPS molecules into account.

Nevertheless, my data indicates that there seems to be partial functional redundancy among the different types of EPS and potentially compensatory EPS production. This has been reported for Pel and Psl polysaccharides in *P. aeruginosa* (Colvin et al., 2011). Both Pel and Psl can serve as primary scaffolds for biofilm formation, and genetic adaptation occurs during biofilm cultivation to compensate for lack of individual EPS types (Colvin et al., 2011). Overall, my infection data indicate that EPS production is an important factor for *Pto* DC3000 infection of *A. thaliana* (Figures 4.3 and 4.4).

It has been suggested that bacterial EPS can suppress plant immune responses during infection (Aslam et al., 2008, Girija et al., 2017). Various types of EPS from different plant-associated bacteria were able to interfere with PTI by chelating Ca^{2+} in the apoplast, thereby suppressing PAMP-induced calcium influx (Aslam et al., 2008). Pre-treatment with purified EPS from various bacterial species including *Xanthomonas campestris* pv. *campestris*, *Erwinia amylovora*, *P. syringae* pv. *syringae*, *Ralstonia solanacearum*, *Sinorhizobium meliloti* and *P. aeruginosa*, suppressed PAMP-induced Ca^{2+} influx, ROS burst and defence gene activation (Aslam et al., 2008). Furthermore, the suppression of PTI was not due to blocking PAMP binding to the receptor or limited PAMP diffusion in the apoplast, but rather due to scavenging of Ca^{2+} by EPS in the apoplast (Aslam et al., 2008). To examine whether EPS from *Pto* DC3000 and *P. protegens* Pf-5 affects plant immunity, I tested bacterial extracts from *Pto* DC3000 and *P. protegens* Pf-5 wild-type and EPS deficient *Pto* Δ*alg/psl/wss* and *P. protegens* Δ*alg/psl/pel* strains, respectively, for their capacity to elicit a ROS burst in *A. thaliana*. Wild-type and EPS-deficient strains triggered a similar ROS response in the plant (Figure 4.5). The levels of EPS in the extracts were unknown and staining of the bacterial colonies suggested that neither strain produced large amounts of polysaccharides under the tested culture conditions. The negative result that the EPS mutant strain showed no effect could be explained by the absence of EPS in the wild-type extract. Unfortunately, EPS purification attempts were unsuccessful, hence the suppression of Ca^{2+} and ROS burst by EPS could not be directly tested.

A complementary approach to examine the function of EPS for immune suppression is to genetically test if the EPS-deficient strain recovers virulence on PTI-compromised *A. thaliana*

genotypes, such as *fec* and *bbc*. Bacterial growth of *Pto* Δ*alg/psl/wss* (Δ*eps*) was still strongly reduced in *fec* and *bbc* lines compared to wild-type. This suggests that suppression of PTI is not the only function of EPS, as other important processes would still be affected in the PTI-compromised lines and would result in reduced growth of the EPS-deficient strain. Hence, no final conclusion could be drawn from these experiments regarding the question whether EPS suppresses PTI.

The timing of PAMP recognition and EPS production might be important for effective immune responses. PAMP recognition presumably happens during invasion of plant tissue, while EPS, as a constituent of biofilms, are produced for surface attachment and during colony expansion in the apoplast. In that respect, EPS plays a role in various processes that are happening in parallel or are required for its function PTI suppression. In addition, flagellin, EF-Tu and peptidoglycan are major bacterial PAMPs and presumably not recognized in the *fec* line, whereas other PRRs are still present and could be affected by EPS. Similarly, some PRRs function independently of the co-receptors BAK1, BKK1 or CERK1 and are therefore still capable of signalling in the *bbc* line. In addition, PTI provides quantitative, basal resistance against adapted pathogens and is most effective during spray infection experiments (Zipfel et al., 2004); therefore, the effect of EPS on PTI might not be observed after infiltration inoculation. Spray infection on PTI-compromised lines has not been tested as EPS production can influence epiphytic survival, and the reduced virulence phenotype was observed also for infiltration infections (Figure 4.3).

It has been reported that an insertional *algD*$^{-}$ mutant of *Pto* DC3000 is compromised in virulence during *A. thaliana* infection (Aslam et al., 2008), which was not observed with the *Pto* Δ*algGX* mutant in my experiments. This inconsistency could be due to the different modes of gene inactivation or infection method/conditions used.

Various glycopolymeric compounds have been associated with the elicitation and suppression of plant immune responses (Silipo et al., 2010). The bacterial root pathogen *R. solanacearum* triggers enhanced ROS and defence-associated gene transcription in a resistant, but not in a susceptible tomato cultivar, compared to its isogenic EPS-deficient mutant strain (Milling et al., 2011). Application of purified EPS from different plant pathogenic *Pseudomonas* to tobacco suspension cells induced immune-associated responses (de Pinto et al., 2003). Multiple types of EPS contribute to the formation of biofilms and their contribution varies not only between bacterial species but also between strains of a single species. For example, while *P. aeruginosa* is able to produce at least alginate, Psl, and Pel, individual strains or isolates only produce a subset of these EPS (Franklin et al., 2011). Indeed,

diversification of bacterial subpopulations in biofilms that produce different EPS has been observed and is hypothesised to be a survival strategy to withstand rapid changes in environmental conditions (Boles et al., 2004). In the context of host-microbe interaction, genetic diversification within a population can be imposed by the host immune system due to PAMP recognition (Cai et al., 2011). Recently, a receptor for EPS detection has been identified in the legume *Lotus japonicus* that specifically recognizes EPS from its symbiont *Mesorhizobium loti* (Muszynski et al., 2016, Kawaharada et al., 2015). However, in the present study the absence of EPS in the *Pto* Δ*alg/psl/wss* did not promote virulence and did not enhance the ROS burst compared to wild-type (Figure 4.3 and Figure 4.5), suggesting that there is no PRR for either of these three EPS from *Pto* DC3000 in *A. thaliana* (Aslam et al., 2008).

The sessile lifestyle within a biofilm provides multiple advantages and allows bacteria to thrive in a favorable environmental niche. Beside its protective function from biotic and abiotic stresses and the accumulation of nutrients (Davey and O'Toole G, 2000, Petrova and Sauer, 2012), the biofilm matrix absorbs and retains water (Chang et al., 2007, Hall-Stoodley et al., 2004). An aqueous growth environment is especially important for *P. syringae* during plant infection (Xin et al., 2016). Recently, the molecular basis for the characteristic water-soaking spots and enhanced bacterial infection under high air humidity has been demonstrated (Xin et al., 2016). For successful plant infection, it is crucial for *Pto* DC3000 to suppress PTI and to create and maintain an aqueous living environment in the intercellular space of the plant. The two type 3-secreted effector proteins HopM1 and AvrE contribute to create an aqueous apoplast and high air humidity is required to maintain this condition (Xin et al., 2016). Even though high humidity did not compensate for the lack of EPS in our experiments, *Pto* DC3000 wild-type benefited from air humidity to a greater extent than *Pto* Δ*alg/psl/wss* as it is reflected in stronger bacterial growth promotion (Figure 4.9B). However, this is only true under the assumption of a linear relationship between growth promotion and humidity. The fact that there is still a small difference between wild-type and *Pto* Δ*alg/psl/wss* under low humidity conditions might indicate that the growth defect due to lack of EPS is independent of humidity, and due to other processes. In this respect, it would be interesting to compare the growth of *Pto* Δ*alg/psl/wss* with a non-virulent control, such as the T3SS deficient *hrcC*$^{-}$ mutant. The non-virulent *hrcC*$^{-}$ strain regains its ability to proliferate in *A. thaliana* plants with a compromised immune system and under high humidity (Xin et al., 2016). Thus, the contribution of EPS to this humidity-dependent growth

promotion could be tested in the future with a *hrcC⁻*/Δ*alg/psl/wss* quadruple mutant on immune-compromised *A. thaliana*.

Another emergent property of biofilms conferred by hydrated EPS molecules is the protection from desiccation (Flemming and Wingender, 2010). Previous studies indicate a role of alginate during water-limiting conditions in *P. putida* and *P. syringae* (Freeman et al., 2013, Chang et al., 2007, Li et al., 2010). EPS might work in conjunction with other protectants for survival under water-limiting conditions, such as trehalose (Freeman et al., 2013, Freeman et al., 2010). The contribution of EPS to withstand desiccation stress could also be tested *in vitro* by measuring the survival rate under low humidity.

Stress protection and persistence in the host tissue is often associated with the production of EPS during animal infection of *P. aeruginosa* and is a key requisite for chronic infections (Starkey et al., 2009). Compared to free-living cells, biofilms are better adapted to cope with pH changes, oxygen radicals and antimicrobial agents (Flemming and Wingender, 2010). The PAMP-induced ROS burst in the plant apoplast is initiated by the NADPH oxidase RbohD in *A. thaliana*, and represents an early response during pathogen infection (Boller and Felix, 2009, Torres, 2010). While it has been demonstrated that PAMP-induced ROS has a signalling role and is important for stomatal closure to limit pathogen entry (Kadota et al., 2014, Li et al., 2014), apoplastic ROS could also directly harm bacterial cells (Lamb and Dixon, 1997).

Interestingly, ROS seems to be a cue for the production of EPS in *Pto* DC3000 (Keith et al., 2003). The bactericidal effect of ROS may be direct through local exposure in the host or indirect via the action of antimicrobial compounds inducing oxidative stress intracellularly leading to cell death (Kohanski et al.). A *P. syringae* pv. *syringae* B728a mutant compromised in quorum sensing produces less alginate and has increased sensitivity to ROS, indicating a role for EPS in tolerating oxidative stress (Quiñones et al., 2005). The reduced *in planta* growth of *Pto* Δ*alg/psl/wss* compared to wild-type could be due to higher sensitivity towards ROS or other antimicrobial compounds. The contribution of EPS to protect against ROS could be tested *in vitro* by assessing the sensitivity to H_2O_2. Although the tested PTI-compromised lines trigger a reduced ROS towards bacterial crude extracts (Figure 3.4), there is still the possibility that other PAMPs contribute to ROS production during the infection.

EPS play an important role in the pathogenesis of many bacteria as a structural component of biofilms mediating the direct interaction with the host and cell-cell contact. The contribution and properties of individual types of EPS to biofilms varies between bacterial

species (Flemming and Wingender, 2010, Petrova and Sauer, 2012). The structure of biofilms has been extensively studied in *P. aeruginosa*, where the major EPS components are alginate, Pel and Psl (Franklin et al., 2011). Accumulating evidence suggests that individual types of EPS are involved in different stages of the *P. aeruginosa* infection process (Schurr, 2013). *P. aeruginosa* with deletions in *pel* and *psl* genes lose their ability to form a biofilm (Friedman and Kolter, 2004, Jackson et al., 2004) suggesting that Pel and Psl serve as the main structural EPS components of the biofilm matrix. More specific functions have been reported for Pel and Psl, such as cell-to-cell interactions (Colvin et al., 2011, Ma et al., 2009) and crosslinking of extracellular DNA strands (Jennings et al., 2015), but clear functional differences could not be established and may be strain-specific and depend on the experimental approach. Although alginate is not essential for *P. aeruginosa* biofilm formation (Wozniak et al., 2003), it contributes to specific physical biofilm properties and biological function (Hentzer et al., 2001, Flemming and Wingender, 2010). In addition, the three EPS molecules are not produced simultaneously, suggesting different roles of EPS types in adaption to the plant environment (Franklin et al., 2011, Petrova and Sauer, 2012). Therefore, Pel and Psl seem to be especially important in the early stages of biofilm formation to form a structural scaffold, while alginate might be involved in stress protection during later stages of infection.

Monitoring the colonization pattern of fluorescently tagged *Pto* DC3000 wild-type and EPS mutant strains during plant infection by confocal microscopy could provide more insights into the structural role of EPS. For example, it would be interesting to analyse the contribution of EPS to colony formation and colony expansion during plant infection. Furthermore, it is unclear whether EPS contribute to cooperation or competition of bacterial cells during infection. EPS could confer either a competitive advantage for the producing cells or function as a common good. It has been suggested that Psl from *P. aeruginosa* is a social trait, but preferentially shared with other Psl-producing cells (Irie et al., 2017). Confocal microscopy of mixed infections with varying inoculum densities reveals spatial dynamics and interaction of different bacterial strains during plant colonization (Rufian et al., 2017). Following the spatial and temporal dynamics of wild-type and EPS mutant strains during mixed infections could provide valuable insights into the role of EPS for cooperative or competitive behavior of *Pto* DC3000 during plant infections.

Chapter 5

Influence of a heterologous pattern recognition receptor on symbiotic and pathogenic bacterial interactions in *Medicago truncatula*

Parts of this chapter have been published in a pre-print manuscript (Pfeilmeier et al., 2017), for which I performed the experimental work (unless otherwise stated in the text) and wrote the first draft. The co-authors provided technical help, performed individual experiments or contributed intellectually to project design and manuscript writing.

5.1 Summary

Interfamily transfer of plant pattern recognition receptors (PRRs) represents a promising biotechnological approach to engineer broad-spectrum, and potentially durable, disease resistance in crops. It is however unclear whether new recognition specificities to given pathogen-associated molecular patterns (PAMPs) affect the interaction of the recipient plant with beneficial microbes. To test this in a direct reductionist approach, I transferred the *Brassicaceae*-specific PRR ELONGATION FACTOR-THERMO UNSTABLE (EF-Tu) RECEPTOR (EFR) from *Arabidopsis thaliana* to the legume *Medicago truncatula*, conferring recognition of the bacterial EF-Tu protein. Constitutive *EFR* expression led to EFR accumulation and activation of immune responses upon treatment with the EF-Tu-derived elf18 peptide in leaves and roots. The interaction of *M. truncatula* with the bacterial symbiont *Sinorhizobium meliloti* is characterized by the formation of root nodules that fix atmospheric nitrogen, and its elf18 epitope is recognized by EFR. Although nodule numbers were slightly reduced at an early stage of the infection in *EFR-Medicago* when compared to control lines, nodulation was similar in all lines at later stages. Furthermore, nodule colonization by rhizobia, and nitrogen fixation were not compromised by *EFR* expression. Importantly, the *M. truncatula* lines expressing *EFR* were substantially more resistant to the root bacterial pathogen *Ralstonia solanacearum*. My data suggest that the transfer of EFR to *M. truncatula* does not impede root nodule symbiosis, but has a positive impact on disease resistance against a bacterial pathogen. In addition, the results indicate that *Rhizobium* can either avoid PAMP recognition during the infection process, or is able to actively suppress immune signalling. In addition, a complementary approach to study the relevance of PAMP recognition during symbiosis has been initiated by engineering an eliciting PAMP in *Sinorhizobium meliloti.*

5.2 Introduction

Plant pattern recognition receptors (PRRs) perceive conserved characteristic microbial features, termed pathogen- or microbe-associated molecular patterns (PAMPs or MAMPs), and trigger an immune response commonly referred to as PAMP- or pattern-triggered immunity (PTI). This confers basal disease resistance against adapted pathogens and plays a major role in non-host resistance against non-adapted pathogens (Boutrot and Zipfel, 2017, Lee et al., 2017). Plants recognise a wide variety of PAMPs, and it is becoming increasingly clear that many PRRs have evolved in a family- or even species-specific manner (Boutrot and

Zipfel, 2017). While some PRRs, such as FLAGELLIN SENSING 2 (FLS2, which detects the PAMP epitope flg22 from bacterial flagellin) are present in all higher plant species, others have only evolved in certain plant families (Boller and Felix, 2009, Boutrot and Zipfel, 2017). For example, the ELONGATION FACTOR-TU RECEPTOR (EFR), which recognizes the highly abundant and conserved bacterial protein EF-Tu (or the PAMP epitope elf18) and was first identified in *Arabidopsis thaliana*, seems to be present only in *Brassicaceae* (Boller and Felix, 2009). Based on these observations, the ability to transfer novel PAMP recognition capabilities across plant species, families or even classes represents a promising biotechnological strategy to engineer broad-spectrum (and potentially durable) disease resistance in crops (Boutrot and Zipfel, 2017, Michelmore et al., 2017, Dangl et al., 2013, Rodriguez-Moreno et al., 2017). For example, the transgenic expression of *EFR* in other plant species, such as tomato (*Solanum lycopersicum*), *Nicotiana benthamiana*, wheat (*Triticum aestivum*), or rice (*Oryza sativa*) confers elf18 recognition and quantitative resistance to a range of bacterial pathogens including *Ralstonia solanacearum*, *Pseudomonas syringae*, *Xanthomonas perforans*, *X. oryzae* and *Acidovorax avenae* (Lacombe et al., 2010, Schwessinger et al., 2015, Schoonbeek et al., 2015, Zipfel et al., 2006, Lu et al., 2015). In addition, the PRR XA21 (which recognises the tyrosine-sulfated peptide RaxX; (Pruitt et al., 2015)) from the wild rice *O. longistaminata* confers increased resistance against *Xanthomonas spp.* when expressed in banana (*Musa sp.*), sweet orange (*Citrus sinensis*) or *N. benthamiana* (Mendes et al., 2010, Tripathi et al., 2014, Holton et al., 2015). Similarly, the PRR ELICITIN RECEPTOR (ELR) from the wild potato *S. microdontum* or the *A. thaliana* PRR RECEPTOR-LIKE PROTEIN 23 (RLP23, which recognises the taxonomically conserved peptide nlp20) confer increased resistance to the oomycete *Phytophthora infestans* when expressed in cultivated potato (*S. tuberosum*) (Albert et al., 2015, Du et al., 2015). These selected recent examples illustrate that PRRs normally restricted to specific plant taxonomic lineages remain functional when expressed in other plant species. Beyond the biotechnological usefulness of this property, this also illustrates that immune signalling components acting downstream of PRRs must be (at least partially) functionally conserved.

While plants must constantly defend themselves against potential invaders, they also form close interactions with beneficial microbes, in what is commonly referred to as the plant microbiome (Müller et al., 2016, Hacquard et al., 2017). While all plants express PRRs as part of their innate immune system, it is however still unclear whether the engineering of novel PAMP recognition specificities through heterologous PRR expression affects the beneficial interaction of plants with commensal microbes.

The symbiosis between rhizobia and legumes is a defined and well understood interaction involving mutual communication. The symbiotic interaction starts with plant roots secreting chemical signals, including flavonoids, to attract host-compatible rhizobia. In turn, rhizobia produce symbiosis-inducing Nod factors, which are perceived by the plant and trigger two independent, yet coordinated, developmental processes: nodule organogenesis and bacterial infection (Oldroyd and Downie, 2008, Madsen et al., 2010). Bacteria attach to the root hair tip and form micro-colonies, from which they invade the plant tissue by growing inside a tubular structure called an infection thread. In parallel to the root hair infection, plant cortical cells divide and develop a new organ, known as a nodule, which ultimately accommodates the rhizobia. In mature nodules, bacteria live as membrane encased bacteroids and fix atmospheric nitrogen making it available to the plant (Oldroyd and Downie, 2008). The harmonious interplay between both organisms requires continuous signal exchange and can be terminated at various stages (Gibson et al., 2008, Cao et al., 2017).

Although the role of PAMP perception and immune signalling during symbiosis has not been extensively studied, there is accumulating evidence to suggest that rhizobia are initially perceived as potential invaders (Cao et al., 2017). The apparent overlap of components and concepts between immunity and symbiosis signalling pathways in legumes is both intriguing, and relevant to the question about the importance of PAMP recognition during these contrasting processes (Zipfel and Oldroyd, 2017). Rhizobia are capable of eliciting PTI, because suspension cultures of *Mesorhizobium loti* can trigger defence-associated responses in the legume *Lotus japonicus*, such as ethylene production, mitogen-activated protein kinase (MAPK) activation and immune gene transcription in a similar way to the flg22 peptide (Lopez-Gomez et al., 2012). In addition, PTI signalling triggered by exogenous application of the *Pseudomonas aeruginosa*-derived flg22 peptide delays nodulation and reduces nodule numbers during the symbiosis between *L. japonicus* and *M. loti* (Lopez-Gomez et al., 2012). Transcriptional studies in different legume species also revealed the transient upregulation of immune-related genes upon first encounter with its rhizobial symbiont, followed by a downregulation during the onset of symbiosis. For example, immune and stress-related genes in *M. truncatula* roots were upregulated 1 hour post-inoculation (hpi) and subsequently downregulated to a minimal level at 12 hpi in response to *S. meliloti* inoculation (Lohar et al., 2006). Similarly, transcriptome analysis of root hair cells from soybean and *M. truncatula* showed induction of defence genes 24 hpi with *Bradyrhizobium japonicum* and *S. meliloti*, respectively, then a marked reduction at later time-points (Libault et al., 2010,

Breakspear et al., 2014) . Interestingly, the early activation of plant defence may play a role in the selection of symbionts and endophytes versus pathogens during the early stages of the rhizobia-legume interaction (Zgadzaj et al., 2015).

5.3 Results

5.3.1 Transgenic expression of *EFR* in *Medicago truncatula* conferred elf18 recognition in leaves and roots

To test directly in a reductionist approach whether a novel PAMP recognition ability affects the symbiotic interaction between legumes and rhizobia, I expressed the *A. thaliana EFR* (*EFR*) gene in *M. truncatula* to engineer the perception of EF-Tu (or derived elf18 peptide) from its symbiont *S. meliloti*.

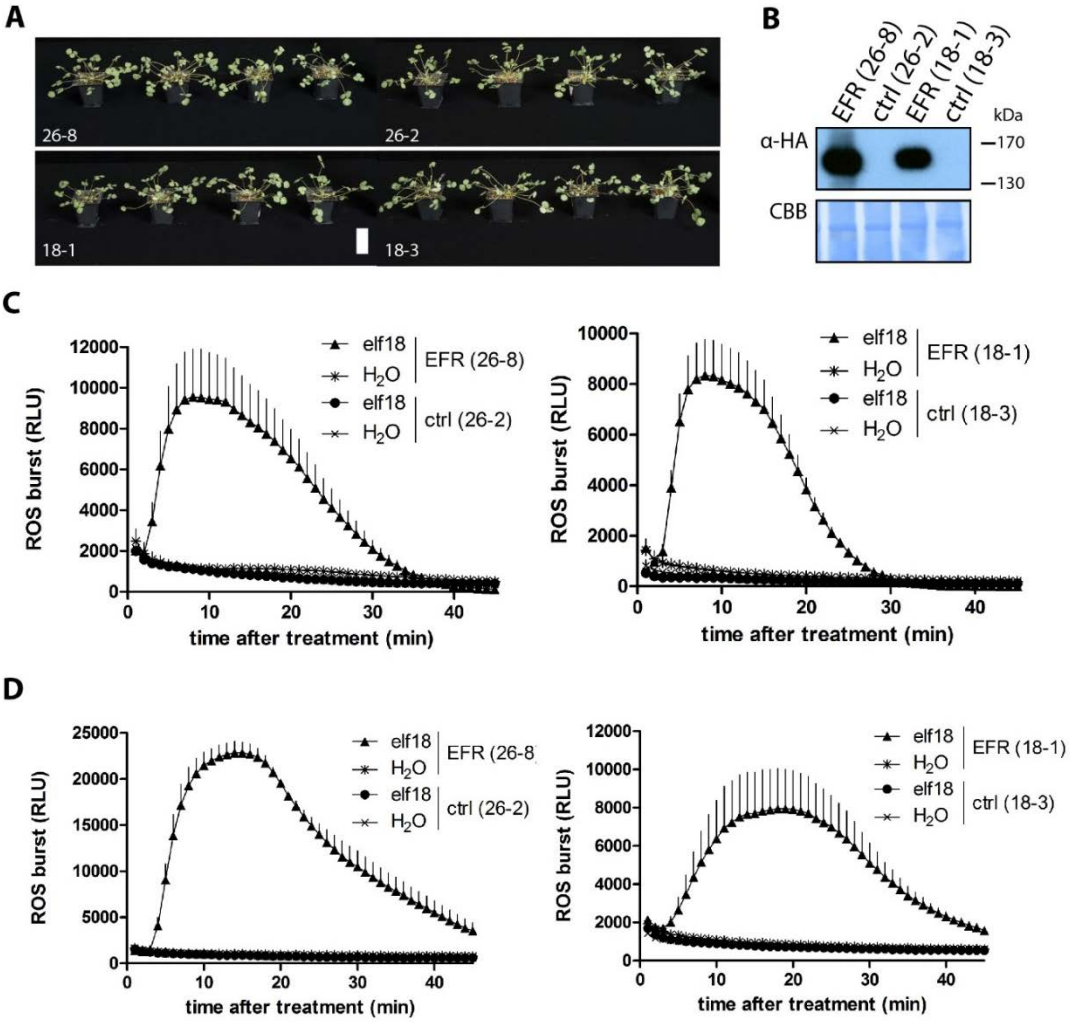

Figure 5.1. Transgenic *EFR-Medicago* responds to elf18 peptide. (A) Phenotype of two independent stable *EFR* expressing *M. truncatula* lines, 26-8 and 18-1, and their null segregant control lines 26-2 and 18-3, respectively. White scale bar represents 5 cm. (B) Western blot of leaf material from *EFR-Medicago* lines (26-8 and 18-1) and control lines (26-2 and 18-3) using α-HA antibody to detect AtEFR-HA. Membrane was stained with Coomassie Brilliant Blue (CBB) as loading control. ROS burst was

monitored in (C) leaf discs and (D) root segments from line 26-8 (left panels) and from line 18-1 (right panels) after application of 100 nM elf18 peptide and displayed as relative light units (RLU). Values are means ± standard error (*n*=8). The experiments were performed three times with similar results.

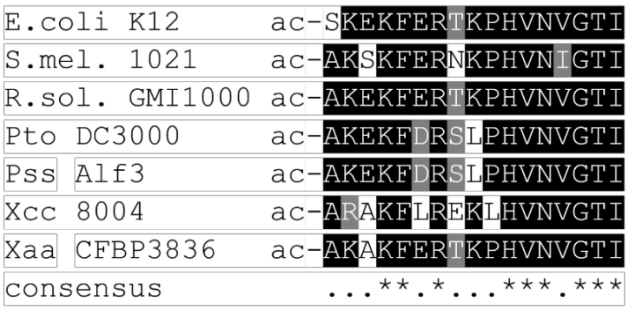

Figure 5.2. Alignment of elf18 peptide sequences. Peptide sequences are displayed with N-terminal acetylation (ac-) from following species: *Xanthomonas alfalfae* subsp. *alfalfae* CFBP3836, *X. campestris* pv. *campestris* 8004, *S. meliloti* 1021, *Escherichia coli* K12, *R. solanacearum* GMI1000, *Pseudomonas syringae* pv. *syringae* ALF3, *P. syringae* pv. *tomato* DC3000. Elf18 peptide sequences belong to seven groups with different eliciting activity according to Lacombe *et al.* 2010. Multiple sequence alignment has been created with Boxshade v3.21. Shadings indicate different degrees of conservation. Asterisk (*) in consensus indicates identity across all sequences.

With the help of Matthew Smoker[3], *M. truncatula* ecotype R108 was stably transformed with p*CaMV35S*::*EFR-HA* by *Agrobacterium tumefaciens*-mediated transformation (Cosson et al., 2006). Two independently transformed lines with a single insertion event were isolated (lines 26-8 and 18-1) and characterized alongside their respective null segregants as control (lines 26-2 and 18-3). Transgenic *EFR*-Medicago plants showed similar growth and development as their control lines (Figure 5.1A), and EFR accumulation could be detected in leaf tissue by western blot analysis (Figure 5.1B). EFR specifically perceives the PAMP elf18 from various bacterial species (Figure 5.2), including the *M. truncatula* symbiont *S. meliloti*, and initiates immune signalling (Kunze et al., 2004, Lacombe et al., 2010). Transgenic *EFR-Medicago* plants responded to local treatment with the elf18 peptide by production of a transient burst of reactive oxygen species (ROS) in leaves (Figure 5.1C) and roots (Figure 5.1D). I also tested responsiveness to the PAMP flg22, and confirmed that all lines responded to the peptide (Figure 5.3), showing that the presence of EFR does not interfere with the function of an endogenous PRR (*i.e.* FLS2). These results show that EFR is functional in *M. truncatula* as it provides responsiveness to the PAMP elf18.

[3] The Sainsbury Laboratory, Norwich Research Park, Norwich, NR4 7UH, UK.

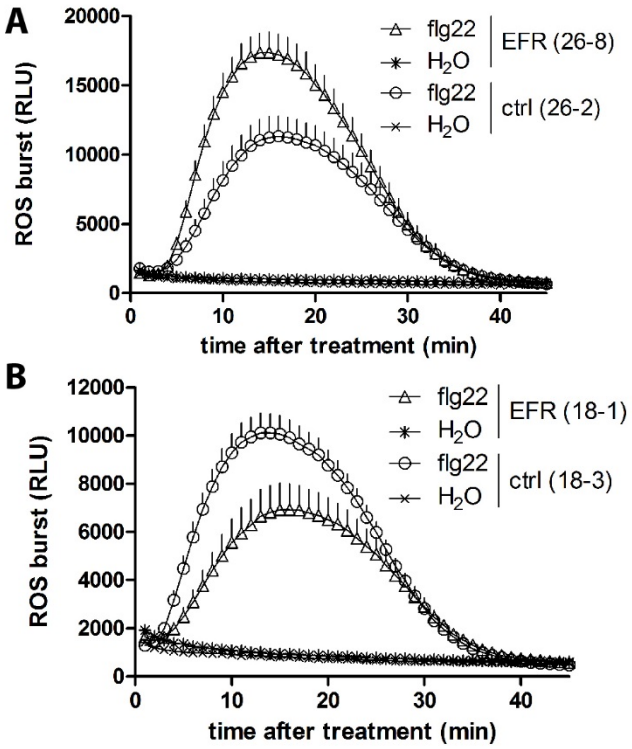

Figure 5.3. *M. truncatula* responds to flg22 peptide. ROS burst was monitored in root segments from line 26-8 and 26-2 (A) and from line 18-1 and 18-3 (B) after application of 100 nM flg22 peptide and displayed as relative light units (RLU). Values are means ± standard error (*n*=8). Experiment was done twice with similar results.

5.3.2 *EFR* expression did not affect the long-term symbiosis between *S. meliloti* and *M. truncatula*

I tested whether heterologous expression of EFR affects the symbiosis between *S. meliloti* and *M. truncatula*. Expression of *EFR* in *M. truncatula* did not have a negative effect on plant growth after inoculation with *S. meliloti*, as the plant phenotype and fresh weight were similar in *EFR*-expressing and control plants when symbiosis was established at four weeks after infection (Figure 5.4A and B). *EFR* expression was driven by the ubiquitous *CaMV35S* promoter, and I was able to detect EFR accumulation in different root tissues, such as the main root, lateral roots and nodules (Figure 5.5).

Next, different stages of the rhizobial infection and the nodulation process were examined. Perception of PAMPs and the initiation of PTI signalling presumably happens at the beginning of infection, when the plant first encounters the microbe. I therefore tested whether EF-Tu recognition affects symbiotic interaction at this early stage. The formation of micro-colonies at the root hair tip, the number of infection threads and nodule primordia were similar between *EFR-Medicago* and the control lines (Figure 5.6). Together with Sonali

Roy[4] and Jeoffrey George[5], I looked at the formation of nodules at various time-points. Scoring total nodule numbers of the root at an early time-point (10 dpi) we observed a small, but significant, reduction in *EFR-Medicago* lines compared to control lines (Figure 5.7). Total nodule numbers were reduced by 25% in line 18-1 and by 35% in line 26-8 at this early time-point. Importantly, all nodules were colonized by rhizobia, as detected by staining for β-galactosidase activity in nodules colonized by the *S. meliloti* strain 1021-*lacZ*, and the spectrum of nodule morphology was similar for all lines. Notably, we observed a small, but significant difference between the transformed null segregant control line 18-3 and the untransformed wild-type (Figure 5.7), which encouraged us to use the null segregants as an appropriate control to avoid artefacts that could be linked to the genetic transformation and/or the associated *in vitro* culture process.

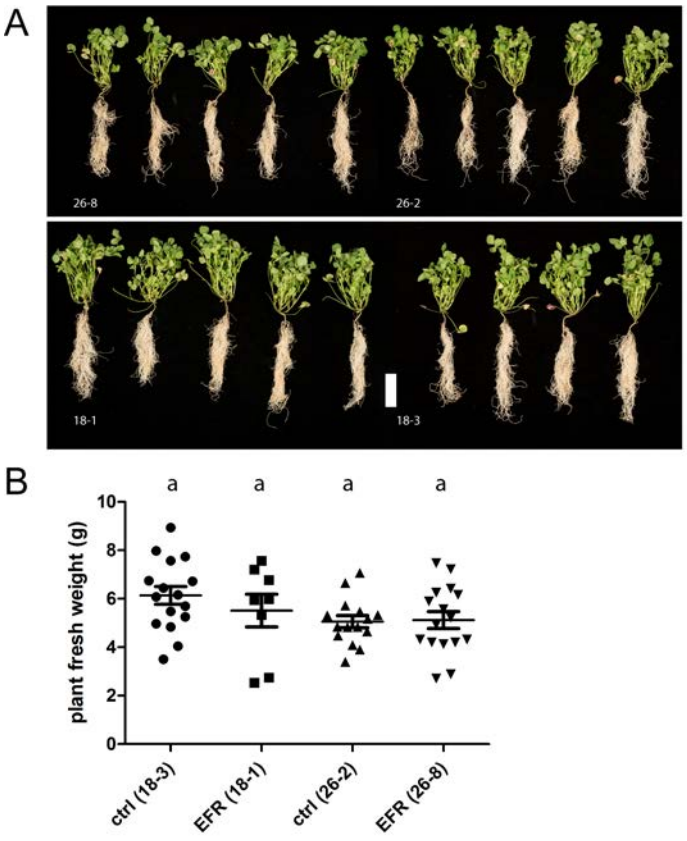

Figure 5.4. *EFR* expression does not effect development and fresh weight of *M. truncatula* infected with *S. meliloti*. (A) Plant pictures and (B) fresh weight were assessed of five-week old *M. truncatula* plants expressing *EFR* (26-8 and 18-1) and respective control lines (26-2 and 18-3) inoculated with *Sm*1021-*lacZ* and harvested at 28 dpi. White scale bar represents 5 cm. The experiment was done three times with similar results.

[4] John Innes Centre, Norwich Research Park, Norwich, NR4 7UH, UK. (Present address: Noble Research Institute, Ardmore, OK73401, USA.)

[5] The Sainsbury Laboratory, Norwich Research Park, Norwich, NR4 7UH, UK.

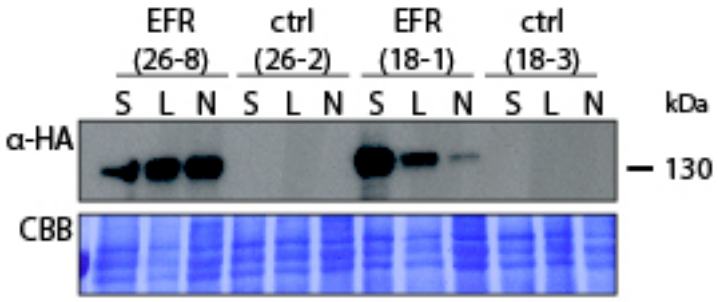

Figure 5.5. *M. truncatula* roots and nodules stably express *EFR*. Accumulation of EFR can be detected in stem root (S), lateral roots (L) and nodules (N) by western blot using α-HA antibody. Root material and nodules were harvested after infection with *Sm*1021-*lacZ* at 28 dpi. Membrane was stained with Coomassie Brilliant Blue (CBB) as loading control. The experiment was done twice with similar results.

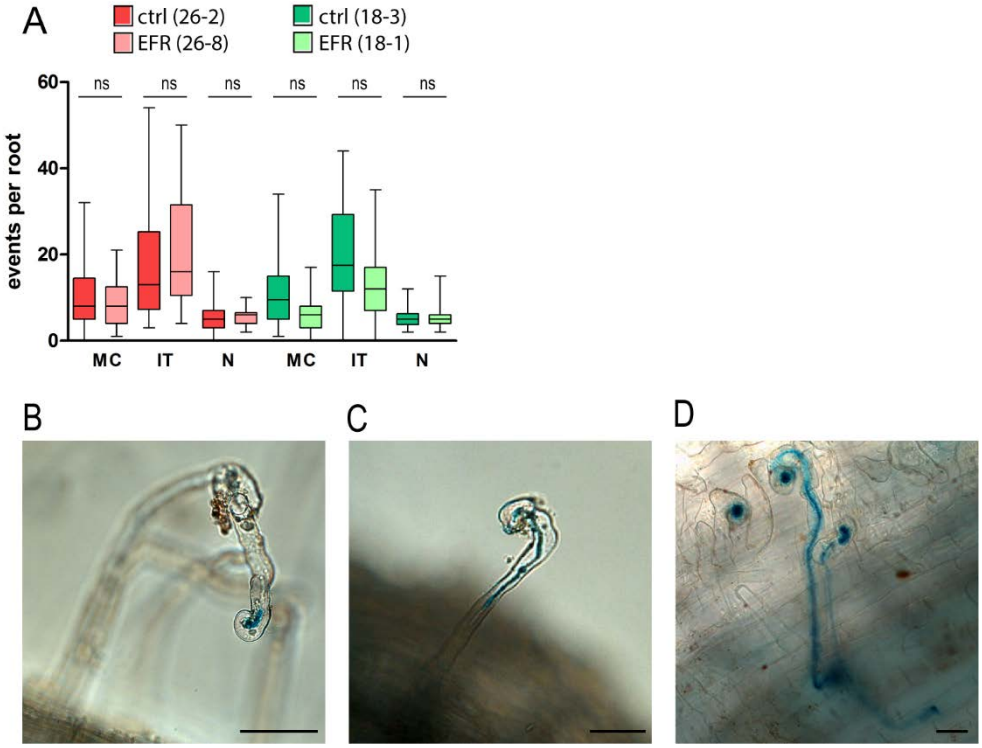

Figure 5.6. Infection events between *M. truncatula* and *S. meliloti* are not affected by *EFR* expression. (A) Infection events were scored at 7 dpi on roots of *M. truncatula* lines expressing *EFR* (26-8 and 18-1) and control lines (26-2 and 18-3) infected with *Sm*1021-*lacZ*. MC: micro-colony. IT: infection threads. N: nodule primordia. Data from three independent experiments (each n=10) were combined. One-way ANOVA with p<0.05 did not indicate statistical significant differences (ns) between ctrl and *EFR* expressing lines. Representative images of *Sm*1021-*lacZ* micro-colony (B), elongated infection thread (C) and ramified infection thread (D). Scale bar represents 25 µm.

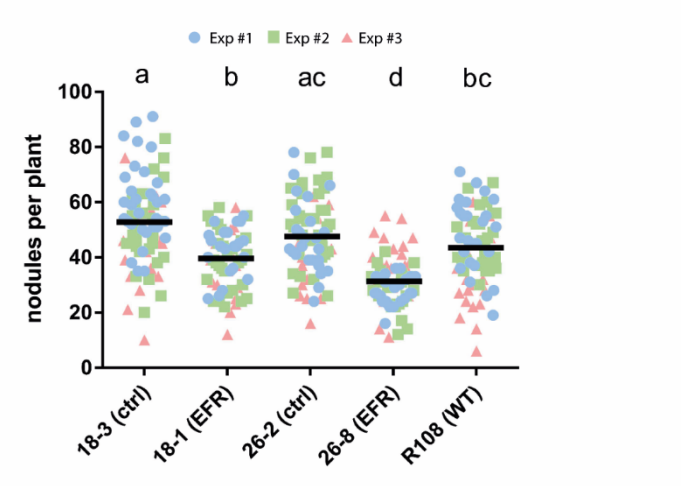

Figure 5.7. Nodulation between *M. truncatula* and *S. meliloti* is affected by *EFR* expression at 10 dpi. Total nodules were scored at 10 dpi on roots of *M. truncatula* lines expressing *EFR* (26-8 and 18-1), control lines (26-2 and 18-3) and untransformed wild-type R108 infected with *Sm*1021-*lacZ*. Data from three independent experiments (each *n*=25) were combined. Colours indicate three independent experiments: Exp#1 (blue), Exp#2 (green) and Exp#3 (red). Letters indicate statistical significance groups with p<0.05 after One-way ANOVA (Kruskal-Wallis's test and Dunn's multiple comparison).

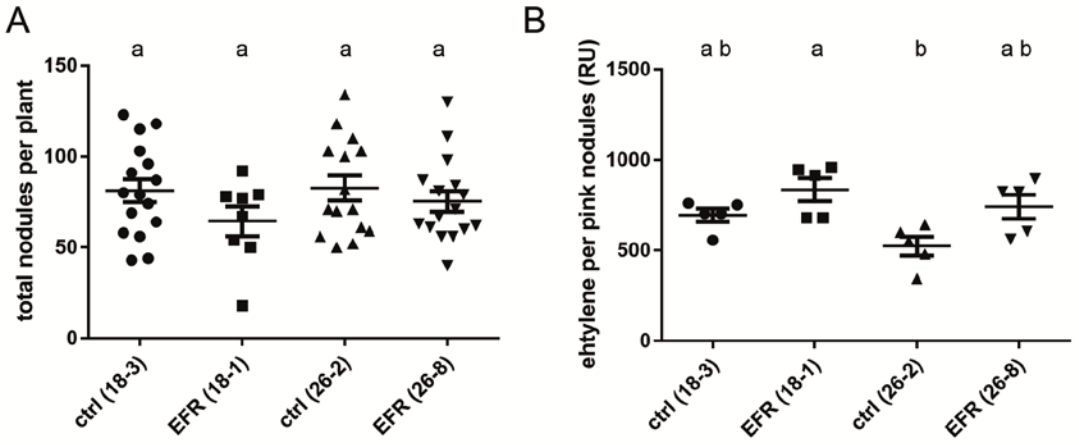

Figure 5.8. Nodulation and nitrogen fixation between *M. truncatula* and *S. meliloti* are not affected by *EFR* expression at 28 dpi. (A) Total nodules were scored at 28 dpi on roots of *M. truncatula* lines expressing *EFR* (26-8 and 18-1) and control lines (26-2 and 18-3) infected with *Sm*1021-*lacZ*. One-way ANOVA with p<0.05 did not indicate statistical significant differences. (B) Acetylene reduction to ethylene was measured on whole plants of *M. truncatula* lines expressing *EFR* (26-8 and 18-1) and control lines (26-2 and 18-3) infected with *Sm*1021 *hemA::lacZ* at 28 dpi. Production of ethylene is displayed as relative units (RU) per pink nodules of each root system. Letters indicate statistical significance groups with p<0.05 after one-way ANOVA and did not indicate statistical significant differences between ctrl and *EFR* expressing lines. The experiments were performed three times with similar results.

I next assessed nodulation during the later stages of symbiosis. Four weeks after infection, symbiosis is well established and nodules are actively fixing atmospheric nitrogen (Oldroyd and Downie, 2008). There was no difference in total nodule numbers between both *EFR*-*Medicago* lines and their respective controls (Figure 5.8A). In addition, acetylene reduction to ethylene has been measured to examine the enzymatic activity of rhizobial nitrogenase

inside nodules; this can be used as an indicator of the nitrogen fixation rate (Price et al., 2015). Notably, root systems from *EFR-Medicago* and from the control lines reduced acetylene at similar rates (Figure 5.8B). In addition, the nodule morphology was similar in all lines, and no macroscopic signs of defence phenotypes or early senescence could be observed.

Together, my results thus indicate that *EFR* expression in *M. truncatula* may cause a slight initial delay in nodule formation, but overall does not negatively affect either rhizobial infection or long term-nitrogen-fixing symbiosis.

5.3.3 *EFR* expression increased the resistance of *M. truncatula* to the bacterial root pathogen *R. solanacearum*

The β-proteobacterium *R. solanacearum* is a root pathogen that causes bacterial wilt disease in different plant species including *M. truncatula* (Vailleau et al., 2007, Mansfield et al., 2012). *M. truncatula* plants infected with *R. solanacearum* develop disease symptoms such as chlorosis and wilting, ultimately leading to plant death (Vailleau et al., 2007). *M. truncatula* was infected with *R. solanacearum* by my collaborators Alice Morel and Nemo Peeters[6]. To test whether EFR can protect *M. truncatula* against bacterial pathogens, they infected *EFR-Medicago* and control lines with *R. solanacearum* GMI1000, and monitored disease progression and survival of the plants over several days. *EFR*-expressing plants displayed a consistently higher survival rate than plants from the control lines (Figure 5.9A and B). Although these results were only statistically significant for line 26-8 (based on Mantel-Cox test), they reproducibly observed a tendency for higher disease resistance in line 18-1 across six independent experiments (Figure A8.4). A possible explanation for the enhanced disease resistance of line 26-8 compared to 18-3 may be the different EFR accumulation levels in these plants (Figures 5.1B and 5.5), which also translate into stronger elf18-induced ROS production in the root of line 26-8 compared to the line 18-1 (Figure 5.10).

Overall, as previously observed with other *EFR*-expressing plant species infected with bacterial pathogens (Lacombe et al., 2010, Schwessinger et al., 2015, Schoonbeek et al., 2015, Zipfel et al., 2006, Lu et al., 2015), EFR conferred increased quantitative resistance, delayed disease progression and increased survival under the used experimental conditions.

[6] INRA/CNRS, Laboratoire des Interactions Plantes Micro-organismes (LIPM), UMR441, 31326, Castanet-Tolosan, France.

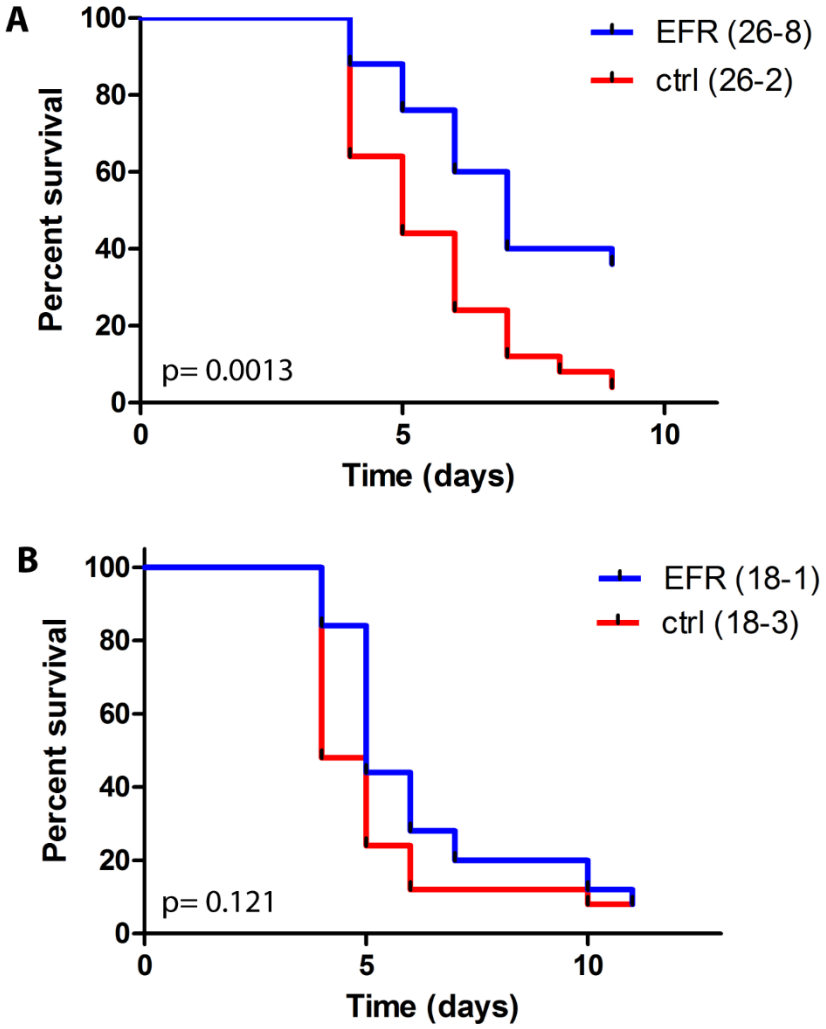

Figure 5.9. *EFR* expression in *M. truncatula* provides quantitative resistance against the pathogen *R. solanacearum*. (A) *M. truncatula* lines expressing *EFR* 26-8 and control line 26-2 were infected with *R. solanacearum* GMI1000 and disease symptoms assessed daily. Survival rate is displayed over 12 days and statistical analysis performed with Mantel-Cox test, p=0.0013 (*n*=25). Experiments were repeated four times with similar results. (B) *M. truncatula* lines expressing *EFR* 18-1 and control line 18-3 were infected with *R. solanacearum* GMI1000 and disease symptoms assessed daily. Survival rate is displayed over time and statistical analysis performed with Mantel-Cox test, *p*=0.121 (*n*=25). Experiments were done six times with similar tendency.

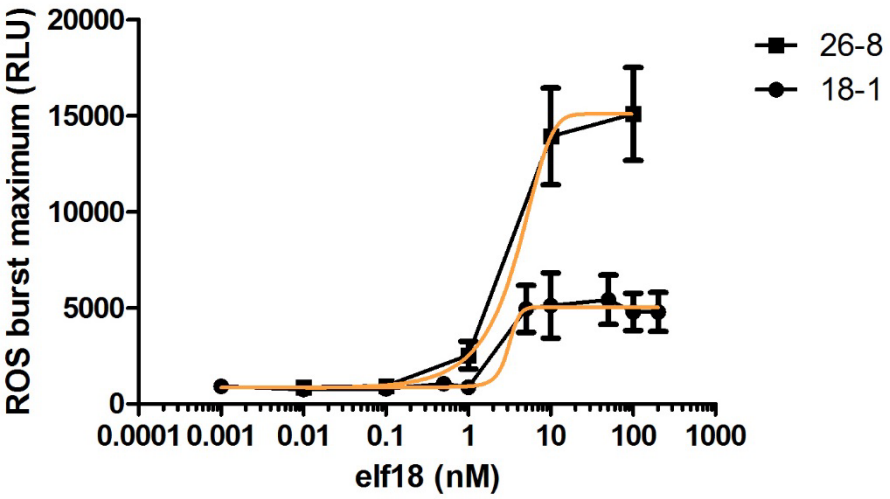

Figure 5.10. Dose-dependent ROS response of *M. truncatula* roots from *EFR*-expressing lines 26-8 and 18-1 to elf18 peptide. ROS burst maximum (displayed as relative light units) was monitored in root segments of lines 26-8 and 18-1 and plotted against elf18 peptide concentration. Orange line was calculated by the sigmoidal non-linear fit function in GraphPad Prism 5. Values are means ± standard error (*n*=8). Experiment was done three times with similar results.

5.4 Discussion

Several PRRs have been successfully expressed in heterologous hosts across taxonomically diverse plant species to improve disease resistance, and PRRs have thus become attractive tools to use as part of the biotechnological arsenal to genetically engineer disease resistance in crops (Boutrot and Zipfel, 2017, Rodriguez-Moreno et al., 2017, Michelmore et al., 2017, Dangl et al., 2013). It was however still unclear whether such PRR transfer may negatively impact the association of the recipient plants with symbiotic microbes.

In this chapter, I discuss the study of transgenic *M. truncatula* lines that express the heterologous PRR *EFR* to confer recognition of the endogenous PAMP EF-Tu from the symbiotic bacterium *S. meliloti*. These *EFR-Medicago* plants recognized elf18 peptide and initiated a PAMP-induced ROS burst in both leaves and roots (Figure 5.1C and D). As previously reported (Holton et al., 2015, Schwessinger et al., 2015), these results indicate that components involved in the PTI signalling pathway (and in PRR biogenesis) are also present and conserved in the root and leaves of *M. truncatula*, as they enable the functionality of EFR.

Legumes benefit from the symbiosis with rhizobia during growth in nitrogen-limited soil due to the additional bioavailable nitrogen supplied by the bacteria. The growth and development of plants with an established symbiosis was similar between transgenic *EFR-Medicago* and control lines. Therefore, I concluded that *EFR* expression did not exert a

negative effect on growth of infected plants, or on long-term symbiosis (Figure 5.4A and B). Likewise, early interaction events were unaltered by *EFR* expression. There was no major difference in the occurrence of micro-colonies, infection threads and nodule primordia formation between *EFR-Medicago* and control lines (Figure 5.6A). Although infection and nodulation are triggered simultaneously, both processes belong to different developmental programs (Murray et al., 2007, Tirichine et al., 2006). Interestingly, at an early time-point after rhizobial infection nodule numbers were slightly reduced in *EFR* expressing lines (Figure 5.7). However, at later stages of symbiosis nodule numbers were similar in all lines (Figure 5.8A). These data indicate that while nodulation might be delayed at early stages, the expression of *EFR* did not impede long-term nodulation. Importantly, the nitrogen-fixation capacity of nodules was unaffected by *EFR* expression (Figure 5.8B).

The absence of detrimental effects of *EFR* expression on rhizobial nitrogen-fixing symbiosis may at first appear counterintuitive. Indeed, the EF-Tu-derived EFR ligand elf18 from *S. meliloti* is able to induce immune responses (Kunze et al., 2004, Lacombe et al., 2010), and it has previously been shown that elicitation of PTI using exogenous PAMP treatment can affect the interaction between rhizobia and legumes. For example, application of flg22 peptide or *M. loti* cells to *L. japonicus* triggered similar PTI responses leading to a delay in nodule formation and reduced nodule numbers (Lopez-Gomez et al., 2012). Furthermore, co-inoculation experiments in *M. truncatula* recently showed that the pathogenic bacterium *P. syringae* pv. *tomato* (*Pto*) DC3000 induces immune responses and suppresses the establishment of the symbiosis with *S. meliloti* (Chen et al., 2017). In addition, constitutive activation of immune responses in *M. truncatula* in specific mutants or over-expression lines impairs nodule formation and symbiosis (Ryu et al., 2017, Berrabah et al., 2014, Berrabah et al., 2015, Domonkos et al., 2013, Wang et al., 2016, Bourcy et al., 2013). Interestingly, nodulation in *M. truncatula* was only impaired when plants were co-treated with the PAMP peptide flg22 together with *M. loti*, but not when flg22 was applied after symbiosis was established (Lopez-Gomez et al., 2012). Also, PAMP treatment seems to delay nodule development rather than impairing rhizobial fitness, as spontaneously nodulating *snf1* mutant plants were similarly affected by flg22 treatment (Lopez-Gomez et al., 2012). It thus appears that the timing of PTI activation and symbiotic signalling may be important to observe the impact of PAMP recognition on symbiosis. In this context, it is important to note that *EFR* expression in recipient transgenic plants does not seem associated with constitutive activation of immune responses, as no detrimental effects on plant growth or development have ever been observed in these plants in either axenic or non-sterile soil conditions

(Lacombe et al., 2010, Schwessinger et al., 2015, Schoonbeek et al., 2015, Lu et al., 2015) (Figures 5.1A and 5.4). Thus, my findings that *EFR* expression negatively affects early nodulation but not infection events or nodule numbers, as well as the observation that nitrogen fixation was unchanged at later stages of symbiosis, support the notion that the perception of rhizobial PAMPs might have an early transient effect on plant nodulation but does not compromise rhizobial fitness, infection, or the ultimate establishment of a functional nitrogen-fixing symbiosis during the natural infection process.

My data therefore suggest that during a natural infection process, *S. meliloti* either evades EF-Tu recognition, actively suppresses PTI in the host, or that it is in a protected compartment within the plant. While rhizobia are known to carry a flg22 allele of the flagellin gene that is not recognized by the plant FLS2 receptor (Felix et al., 1999), the EF-Tu-derived elf18 peptide from *S. meliloti* is recognised by EFR (Lacombe et al., 2010, Kunze et al., 2004), suggesting that an immune evasion strategy is not conceivable here. Despite the manifold evidence that *EFR* expression provides efficient disease resistance, it is still unclear how the intracellular EF-Tu protein (and by extension the elf18 epitope) gets exposed to the EFR receptor during infection (Zipfel et al., 2006). EF-Tu has however been found in the cell-free supernatant from cultures of different bacterial species (Kazemi-Pour et al., 2004, Watt et al., 2005), and an active role for EF-Tu has been suggested during effector translocation via the type-6 secretion system (T6SS) in *P. aeruginosa* (Whitney et al., 2015). Interestingly, EF-Tu was recently identified in bacterial outer membrane vesicles, which was linked to the ability of these vesicles to induce EFR-dependent immune responses in *A. thaliana* (Bahar et al., 2016), illustrating a possible mechanism by which this potent PAMP can be released. Although the leguminous hosts of rhizobia do not carry EFR, members of the *Rhizobiales* family have been found in the *A. thaliana* rhizosphere (Bai et al., 2015). I cannot therefore completely exclude the possibility that rhizobia have evolved strategies to control EF-Tu secretion.

Previous transcriptomic studies indicate that rhizobia initially elicit an immune response, which is then suppressed as symbiosis proceeds (Lohar et al., 2006, Libault et al., 2010, Breakspear et al., 2014). In addition, co-inoculation with *S. meliloti* suppresses immune responses normally triggered by *Pto* DC3000 in *M. truncatula* (Chen et al., 2017). These results suggest that rhizobia have active mechanisms to suppress PTI. Plant pathogenic bacteria can suppress host immunity by secretion of effectors, many of which interfere with the canonical PTI pathway at different stages (Macho and Zipfel, 2015). Many of these PTI-suppressing effectors are translocated within plant cells via the T3SS. While there is evidence suggesting that rhizobia also use effectors to suppress plant immunity, only a few rhizobial

effectors (Nop proteins) have been characterized (Staehelin and Krishnan, 2015). Rhizobial genomes encode several different secretion pathways, and the importance of T3SS, type-4 secretion system (T4SS) and T6SS for symbiosis has been demonstrated genetically in certain rhizobial species (Sugawara et al., 2013, Nelson and Sadowsky, 2015, Bladergroen et al., 2003). *Sinorhizobium* sp. NGR234 translocates multiple type-3 secreted effectors, including NopM, NopL, NopP and NopT, to interfere with immune signaling (Skorpil et al., 2005, Dai et al., 2008, Xin et al., 2012b, Ge et al., 2016b). However, the *S. meliloti* strain 1021 used in this study, *Sm*1021, only carries a T4SS gene cluster for translocation of effectors into host cytoplasm, and deletion mutant studies showed no impact of mutating the T4SS on nodulation (Jones et al., 2007, Nelson et al., 2016).

Other bacterial mechanisms have been suggested to suppress PTI (Cao et al., 2017). For example, Nod factors not only play a role in initiating and maintaining symbiosis signaling, but also in suppression of plant immunity (Liang et al., 2013). Application of *B. japonicum* Nod factor to the non-host plant *A. thaliana* resulted in reduced accumulation of the immune receptors FLS2 and EFR at the plasma membrane (Liang et al., 2013). Although this partial suppression of PTI seems to be conserved in legume and non-legume plants, the impact on rhizobial-legume root infection has not been directly tested. Contrary to these findings, I detected EFR accumulation in the nodules of my transgenic *M. truncatula* plants (Figure 5.5). Exopolysaccharide (EPS) production is a common factor among plant-associated bacteria and has been previously associated with evasion of PTI (D'Haeze and Holsters, 2004, Aslam et al., 2008). While EPS from rhizobia is absolutely essential for plant infection (Gibson et al., 2008), other cell surface polysaccharides such as lipopolysaccharides (LPS), glucomannan and cyclic β-glucans have been implicated in facilitating symbiotic interaction (Tellstroem et al., 2007, Williams et al., 2008, Niehaus et al., 1993, Mithofer et al., 1996). Notably, the EPS receptor EPR3 from *L. japonicus* specifically detects EPS from its symbiont and acts as a positive regulator of infection (Kawaharada et al., 2015, Muszynski et al., 2016). Mutant strains defective in cell surface polysaccharides result in impaired infections or ineffective nitrogen-fixing nodules (D'Haeze and Holsters, 2004). For example, the succinoglycan-deficient *Sm*1021 *exoY* mutant induces immune-related genes more strongly than wild-type, indicating a possible involvement of succinoglycan in the suppression of immunity (Jones et al., 2008). Additionally, purified LPS from *S. meliloti* can suppress ROS burst in *M. truncatula* suspension cells treated with invertase (Tellstroem et al., 2007). However, the phenotypes of cell surface polysaccharide mutants are often difficult to interpret, because they seem to be specific for the type of polysaccharides, the rhizobial species and the host plant. It is

therefore likely that cell surface polysaccharides contribute to the symbiotic interaction in multiple ways in addition to facilitating immune evasion (Gourion et al., 2015). Legumes and rhizobia appear to be well adapted to each other for the specific and intimate symbiotic interaction (Gourion et al., 2015). As EFR shares the same components for signal transduction as other PRRs (Couto and Zipfel, 2016), rhizobia may have evolved mechanisms for evasion of PAMP detection and/or efficient suppression of PTI signaling downstream of the receptor. It will be thus interesting in future studies to investigate the exact mechanisms employed by rhizobia to suppress PTI. It is also conceivable that legumes themselves specifically suppress PTI in a local and timely manner in response to rhizobial signals (*i.e.* Nod factor or EPS) to facilitate infection by their symbionts. For example, localized immune tolerance could be achieved by limiting trafficking of PRRs into the infection thread and/or peribacteroid membranes to restrict recognition of those PAMPs.

The transfer of EFR has already been shown to confer increased quantitative resistance against different bacterial pathogens in a wide range of plant species, including tomato, *N. benthamiana*, wheat and rice (Lacombe et al., 2010, Schwessinger et al., 2015, Schoonbeek et al., 2015, Zipfel et al., 2006, Lu et al., 2015). The study described in this chapter expands this list, and reveals that *EFR* is also functional when expressed in legumes (at least as demonstrated here for *M. truncatula*) and increases the survival of *M. truncatula* plants upon infection by the root bacterial pathogen *R. solanacearum* (Figure 5.9A and B). Thus, together, the data demonstrate that *EFR* expression can protect *M. truncatula* from the destructive root pathogen *R. solanacearum*, without compromising the overall symbiotic interaction with *S. meliloti*, which allows fixation of atmospheric nitrogen. My results suggest that legumes can be engineered with novel PRRs without affecting the nitrogen-fixing symbiosis, and may be relevant in the future as attempts to transfer this important symbiosis into non-legume plants are currently ongoing (Zipfel & Oldroyd, 2017). More generally, it also illustrates that the transfer of PRRs across plant species does not necessarily come at a cost to the plant, but can actually increase its fitness when faced with aggressive pathogens. It will be interesting in the future to expand the reductionist approach used in this study to test whether heterologous PRR expression affects the composition and function of other commensals in the plant microbiome. A potential effect on the microbiome would then however need to be reconciled with the absence of obvious growth defects of transgenic plants expressing PRRs in non-sterile soil, and counterbalanced in an agricultural context against the benefit conferred by PRR transfer in terms of disease resistance under strong pathogen pressure.

5.5 Additional research approach: Engineering of an eliciting flg22 epitope in *Sinorhizobium meliloti*

The heterologous expression of a PRR conferring a novel detection capability in the plant is a valuable tool to study the relevance of PAMP recognition during symbiosis. A complementary approach to address this question is to engineer an additional immunogenic epitope into the symbiont that would activate the plant immune system. Several plant-associated bacteria, including the symbiont *S. meliloti*, have variants of the flg22 epitope that are not recognized by the plant receptor FLS2 (Sun et al., 2006, Felix et al., 1999, Pfund et al., 2004) (Figure 5.11). To test whether recognition of flagellin via flg22 engineering affects the outcome of the symbiosis between legumes and rhizobia, I replaced the non-eliciting flg22 in *S. meliloti* with an eliciting version, then characterised the rhizobial strains carrying novel flg22 variants for their capacity to elicit a ROS burst in plant and for bacterial motility.

```
                        1234567890123456789012
P.aer. PA01       (+)   QRLSTGSRINSAKDDAAGLQIA
Pto DC3000        (+)   TRLSSGLKINSAKDDAAGLQIA
Xcc B186          (-)   QQLSSGKRITSASVDAAGLAIS
S.mel. 1021       (-)   AHVSSGLRVGQAADNAAYWSIA
A.fab. C58        (-)   ARVSSGLRVGDASDNAAYWSIA
R.sol. K60        (-)   QRLSTGMRVNSAQDDAAAYASA
Pcal/Psm ES4326   (-)   ERLSTGKKINTASDDAGGSVTQ
```

Figure 5.11. Alignment of flg22 sequences from plant-associated bacteria. Sequences of eliciting (+) and non-eliciting (-) flg22 alleles derived from *Pseudomonas aeruginosa* PA01, *P. syringae* pv. *tomato* (*Pto*) DC3000, *Xanthomonas campestris* pv. *campestris* (*Xcc*) B186, *Sinorhizobium meliloti* 1021, *Agrobacterium fabrum* C58 (formerly *A. tumefaciens*), *Ralstonia solanacearum* K60, and *P. canabina* pv. *alisalensis* (formerly *P. syringae* pv. *maculicola*) ES4326. Red letters indicate variation compared to the two eliciting sequence on top.

5.5.1 Results

5.5.1.1 Engineering a Sm1021 flaA deletion strain

*Sm*1021 has four chromosomal copies of the *fla* gene encoding flagellin (Figure 5.12A and B), which constitute the structural component of the flagellum filament. Genetic and functional studies in the related strain *Sm* MV II-1 suggest that the flagellum is composed of at least two different flagellin proteins forming a heterodimer, with FlaA as the major component (Scharf et al., 2001). Deletion of *flaA* completely abolishes swarming motility in *Sm* MV II-1, while deletions of either *flaB*, *flaC* or *flaD* only reduced swarming (Scharf et al., 2001). As PTI-

eliciting activity of flagellin is a dominant trait, it should be sufficient to engineer the *fla* gene with the highest abundance to obtain a mutant strain carrying a flg22 epitope capable of triggering PTI.

I decided to first make a *Sm*1021 *flaA* deletion strain, *Sm* Δ*flaA*, to facilitate the screening by PCR of cells with a successfully introduced *flaA* gene encoding an eliciting flg22 variant. An in-frame deletion of *flaA*, leaving only 15 base pairs between the intact start and stop codons, was made in *Sm*1021 by a two-step homologous recombination process and confirmed by sequencing of a PCR product obtained with primers annealing to the chromosomal DNA outside of the recombinant plasmid (primers #1007 and #1008). Surprisingly, *Sm* Δ*flaA* was still motile, and swimming was reduced by only 25% compared to *Sm*1021 wild-type (Figure 5.13). This is in contrast to the complete abolition of motility reported in the literature for *flaA* deletion in the related strains *Sm* MV II-1 and *Rhizobium lupini* H13-3 (Scharf et al., 2001).

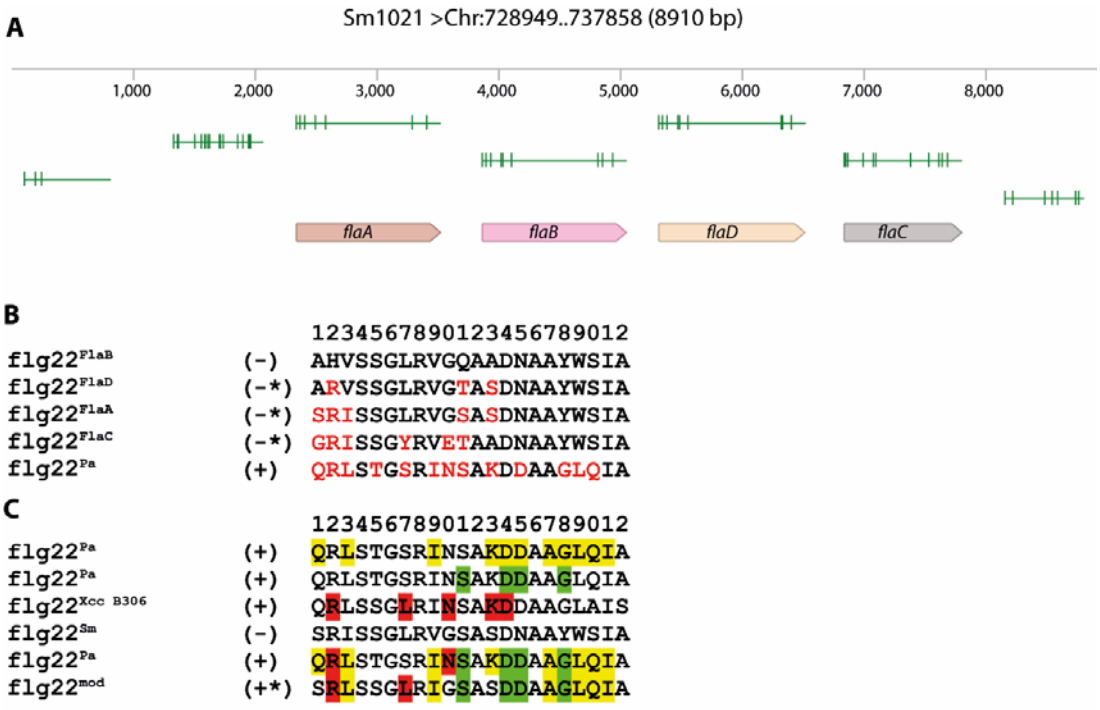

Figure 5.12. flg22 sequences encoded by fla genes from *Sm*1021 and flg22 variants. (A) Chromosomal locus of fla genes on *Sm*1021 genome (JBrowser, http://lipm-bioinfo.toulouse.inra.fr/). Thin green line shows open reading frames with potential start codons. Arrow-shaped boxes represent annotated *fla* genes *flaA*, *flaB*, *flaD* and *flaC* (B) Sequences of flg22 derived from *fla* genes from *S. meliloti* (Sm) 1021 and *fliC* gene from *P. aeruginosa* (Pa) PA01. (-*) or (+*) indicates that eliciting activity of peptide has not been directly shown, but is likely to be as indicated. (C) Sequences of flg22 from *P. aeruginosa* (Pa) PA01 *fliC*, *X. campestris* pv. *campestris* B306 *fliC*, *Sm*1021 *flaA* and flg22 variants $flg22^{Pa}$ and $flg22^{mod}$ replacing chromosomal allele of *Sm*1021. Yellow colour highlights residues important for interaction with FLS2-BAK1 receptor complex (Sun et al. 2013), green and red colour mark residues important for eliciting activity (Felix et al. 1999, Sun et al. 2013).

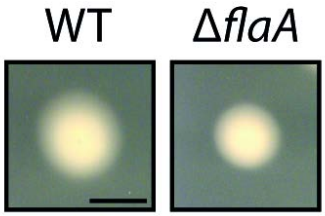

Figure 5.13. Swimming motility of *Sm*1021 and *Sm* Δ*flaA*. *Sm*1021 wild-type (WT) and *Sm* Δ*flaA* were stabbed into TY media containing 0.3% agar and incubated for 2 days at 30°C. Scale bar represents 1 cm. The experiment has been performed at least three times with similar results.

5.5.1.2 Design of eliciting flg22 alleles in the flaA gene and their impact on motility

I next tried to complement *Sm* Δ*flaA* with the full length *flaA* gene containing an eliciting flg22 variant, flg22^{Pa}, which is derived from the *P. aeruginosa* PA01 sequence (Felix et al., 1999) and has 11 amino acid residue changes compared to the flg22 sequence of FlaA from *Sm*1021 (Figure 5.12C). Notably, the flg22^{Sm} variant, which has been previously identified to be an inactive PAMP (Felix et al., 1999), is derived from the FlaB protein sequence. The flg22 epitope of FlaA has not been tested for eliciting activity, but based on structural and functional studies (Sun et al., 2006, Felix et al., 1999, Sun et al., 2013). I assumed that the six amino acid residue substitutions compared to FlaB are not important for receptor binding or activity of the peptide (Figure 5.12B and C). A chromosomal complementation was conducted in the *Sm* Δ*flaA* background with the full-length *flaA* gene containing the flg22^{Pa} variant. I then screened for recombinant strains carrying *flaA-flg22^{Pa}* but without any aberrant chromosomal rearrangements in the *fla* gene locus. As FlaB, FlaD and FlaC share a high degree of sequence identity with FlaA (Figure 5.14A), the integrity of the entire *fla* gene locus was tested by PCR with three different primer combinations amplifying *flaA* (primer #1346 and #1347, blue colour in Figure 5.14A), *flaB* to *flaC* (primer #1348 and #1349 red colour in Figure 5.14A) and *flaA* to *flaC* (primer #1346 and #1349, green colour in Figure 5.14A), respectively. While I obtained four colonies containing *flg22^{Pa}* as shown by PCR amplification (with primer #1007 binding outside and primer #1008 binding inside the recombinant construct) and sequencing, only one colony, *Sm flaA-flg22^{Pa}* c5, had the right sizes of PCR products spanning across the *fla* gene locus as seen in the PCR amplification pattern of wild-type *Sm*1021 (Figure 5.14B and Figure A8.5). No PCR products were obtained with different primers sets spanning across the *fla* locus from the other three colonies, which were subsequently discarded (Figure A8.5). One colony, *Sm flaA-flg22^{Pa}* c1, reverted back to its original state, *Sm* Δ*flaA*, in the second cross-over event of the homologous recombination during the allele replacement process as shown by PCR amplification of a shortened *flaA* gene (blue colour in Figure 5.14B) and shortened *fla* locus (green colour in Figure 5.14B).

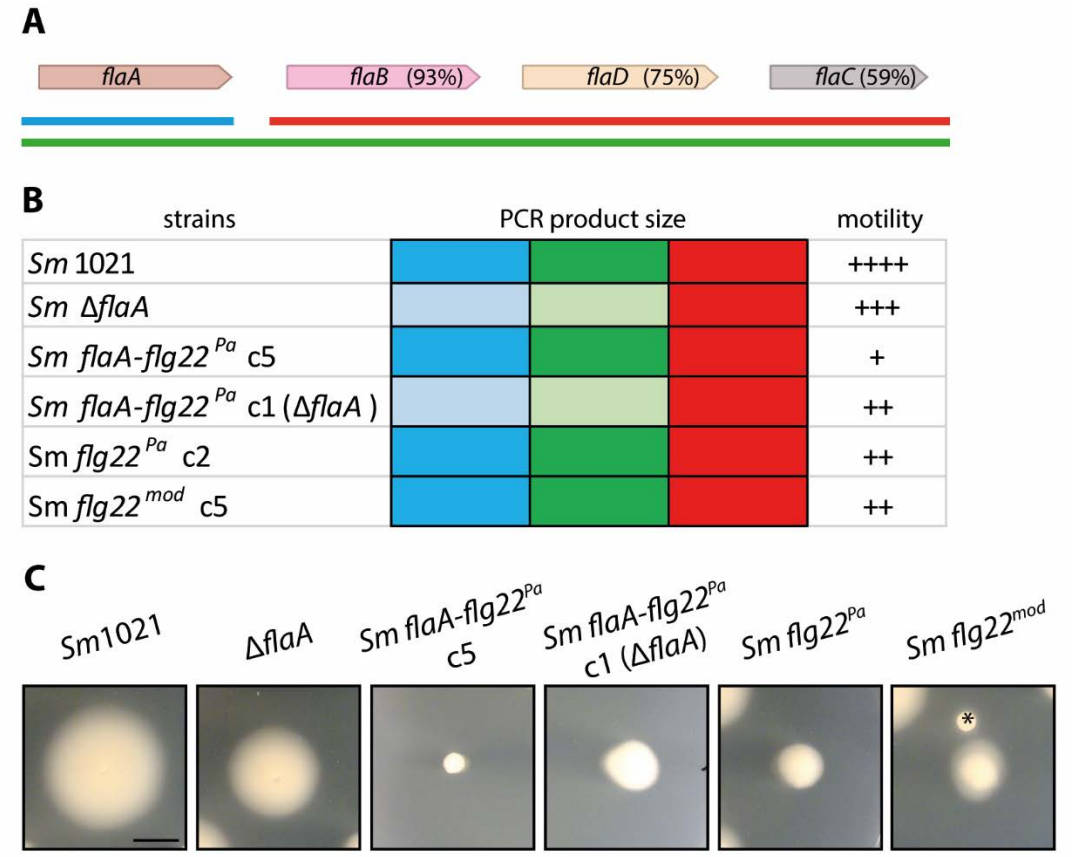

Figure 5.14. Chromosomal engineering of flaA alleles in *Sm*1021. (A) Arrow shaped boxes represent chromosomal *fla* gene locus. Thick coloured lines show PCR amplification product with primers #1346 and #1347 (blue), #1348 and #1349 (red), #1346 and #1349 (green). BLAST Needleman-Wunsch global alignment revealed sequence identity (and gaps) between the query *flaA* with *flaB* 93% (0%), with *flaD* 75% (2%) and with *flaC* 59% (21%). (B) List of *Sm*1021 wild-type, *Sm* Δ*flaA* mutant and strains transformed with *flaA* encoding the flg22 variants *Sm flaA-flg22*^{Pa} c5, *Sm flaA-flg22*^{Pa} c1, *Sm flg22*^{Pa} c2 and *Sm flg22*^{mod} c5. Coloured boxes show presence PCR product indicated in (A). Colony diameter of swimming motility test shown in (C) was grouped in different categories from highest (++++) to lowest (+) motility. (C) Swimming motility was assessed after stabbing strains from (B) into TY 0.3% agar plates, incubated for 4 days at 30°C. Asteriks * marks unrelated colony on medium surface. Scale bar represents 1 cm. The experiment has been performed twice with similar results.

To test if the novel flg22 alleles affect motility of the strains, I assayed bacterial swimming by measuring the diameter of the colony stabbed into growth medium with 0.3% agar concentration. While swimming was slightly reduced in *Sm* Δ*flaA*, it was drastically impaired in *Sm flaA-flg22*^{Pa} c5 carrying the novel flg22^{Pa} epitope (Figure 5.14C). Unexpectedly, motility of *Sm flaA-flg22*^{Pa} c1 was reduced compared to *Sm* Δ*flaA* (Figure 5.14C) although both strains should have the same genetic background (Figure 5.14B).

In parallel, I followed an alternative approach by engineering eliciting flg22 epitopes in the *Sm*1021 wild-type background, as this intragenic recombination approach is likely to be less invasive as introducing the complete *flaA* gene. I designed two independent constructs replacing only the flg22 sequence of the *flaA* gene with the *P. aeruginosa*-derived flg22^{Pa}

sequence containing eleven altered amino acid residues and with a modified flg22^{mod} version containing six altered amino acid residues (Figure 5.12C). The sequence design of flg22^{mod} was guided by previous studies of systematic mutations of the flg22 peptide (Sun et al., 2006, Felix et al., 1999) and structural analysis of the FLS2-BAK1 ectodomains in complex with flg22 (Sun et al., 2013). Although the eliciting activity of flg22^{mod} peptide remains to be experimentally tested, it is likely to be active, because critical residues for binding and activation were maintained (Figure 5.12C). The resulting *Sm flg22^{Pa}* c2 and *Sm flg22^{mod}* c5 strains were validated by sequencing to carry the novel flg22 variants and used for further analysis. Furthermore, both strains with novel flg22 variants showed the same pattern as *Sm*1021 wild-type in terms of PCR products obtained with primers spanning the *fla* gene locus (Figure 5.14B and Figure A8.5).

Interestingly, the novel flg22 variants seemed to have a dominant negative effect on motility, as *Sm flg22^{Pa}* and *Sm flg22^{mod}* swimming was reduced by 50%, while *Sm* Δ*flaA* was only reduced by 25% compared to wild-type (Figure 5.14B and C). Although the strains *Sm flaA-flg22^{Pa}* c5 and *Sm flg22^{Pa}* c2 should have the identical *flaA* allele and *fla* gene locus based on sequencing and PCR amplification pattern, both showed different degrees of motility, that is reduced compared to their parental strain *Sm* Δ*flaA* and *Sm*1021, respectively (Figure 5.14B and C). Overall, the data suggest that *flaB*, *flaD* and/or *flaC* partially compensate for lack of FlaA, which leads to only slightly reduced motility in *Sm* Δ*flaA*. The dominant-negative effect of the introduced novel flg22 variants in *flaA* implies their interference with flagellum assembly and/or function, which may be caused by structural changes induced in the FlaA protein by the introduced mutations.

5.5.1.3 Immunogenic activity of Sm1021 strains with eliciting flg22 variants

Next, I made crude extracts from the different rhizobial strains to examine the capacity of the novel flg22 variants to elicit plant immunity. Bacterial extracts from neither *Sm flg22^{Pa}* or *Sm flg22^{mod}* triggered a FLS2-dependent ROS burst when applied to *A. thaliana* Col-0 and *fls2* plants (Figure 5.15). This suggests that *flaA* is probably not or only marginally expressed or that FlaA does not accumulate in these mutants. In that case, impaired flagellum assembly could not explain the dominant-negative effect observed on swimming motility.

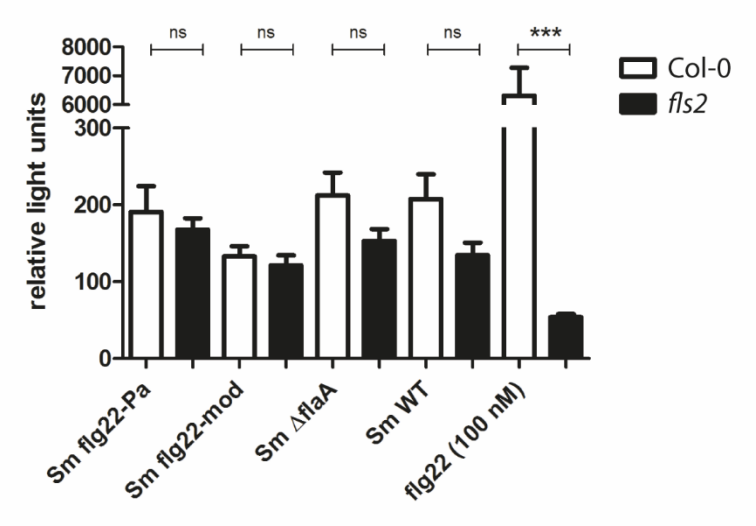

Figure 5.15. *Sm*1021 strains with novel flg22 alleles do not trigger FLS2-dependent ROS burst. Total ROS production was measured in *A. thaliana* Col-0 and *fls2* mutants after treatment with bacterial extracts from *Sm*1021, *Sm* Δ*flaA*, *Sm flg22*^{Pa} c2, *Sm flg22*^{mod} c5, or flg22 peptide for 60 min. Error bars are standard errors (n = 8) and statistical analysis by Mann-Whitney test with p<0.05 (***). The experiment has been performed once.

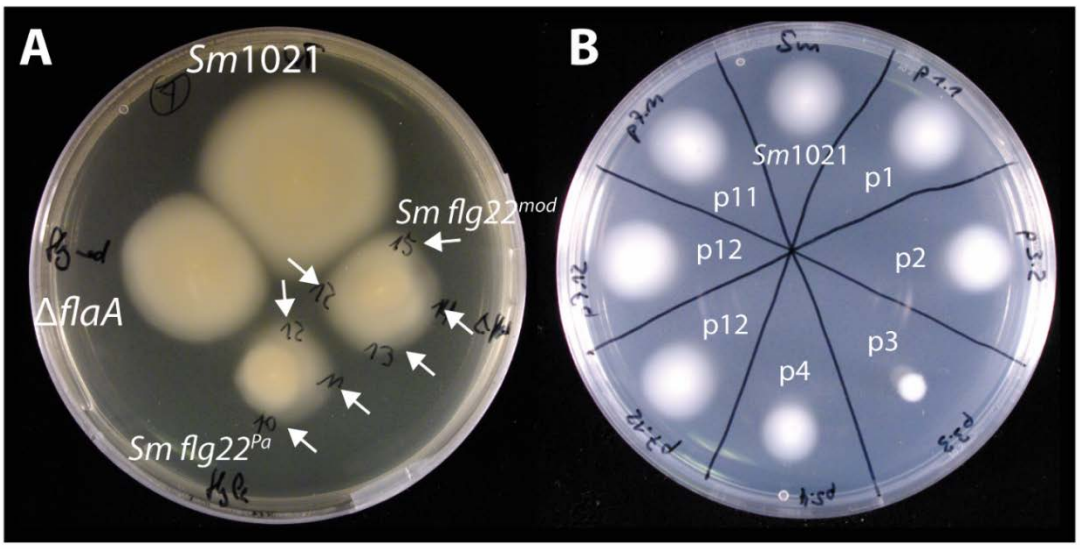

Figure 5.16. Illustration of swimming plates with bacterial flares representing cells with restored motility. (A) Exemplary swimming plate to illustrate restoration of motility. *Sm*1021, *Sm* Δ*flaA*, *Sm flg22*^{Pa} c2, and *Sm flg22*^{mod} c5 were stabbed into TY media containing 0.3% agar, and incubated for 7 days at 30°C. White arrows mark flares from which cells have been isolated (C) Isolated cells were tested for motility by stabbing strains in SM medium containing 0.3% agar and incubated for 4 days at 30°C. The experiment has been performed twice with similar results.

Previously, flagellin was engineered in pathogenic bacteria from plants and mammals (Sun et al., 2006, Andersen-Nissen et al., 2005). Site-specific mutagenesis in *fliC* – the *flaA* homologue in *Salmonella typhimurium* – resulted in loss of motility due to incorrect assembly and function of the flagellum (Andersen-Nissen et al., 2005). Therefore, it has been suggested that compensatory mutations in other domains of the flagellin protein are

necessary to allow multimerization for proper filament formation (Andersen-Nissen et al., 2005).

After seven days incubation at 30°C, flares started to appear at the edge of the Sm *flg22*^{Pa} and Sm *flg22*^{mod} colonies (Figure 5.16A) suggesting evolutionary adaptation leading to increased motility of individual cells. Some of the bacteria isolated from these flares had regained swimming motility to a similar extent as wild-type *Sm*1021 (Figure 5.16B and 5.17A). I made crude extracts of selected isolates, and tested them for ROS burst eliciting activity in plants. Before lysis of cells in the exponential growth phase (OD_{600} = 0.5-1.2), I confirmed flagella-driven motility by light microscopy. However, the motile strains carrying novel flg22 variants did not trigger an enhanced ROS burst compared to wild-type *Sm*1021 (Figure 5.17B). Lysate from *P. aeruginosa* PA01 with the endogenous flg22^{Pa} and synthesised flg22^{Pa} peptide were used as positive controls. This finding suggests that the engineered FlaA proteins are not expressed in *Sm*1021, and that the reverted motility was probably independent of *flaA*.

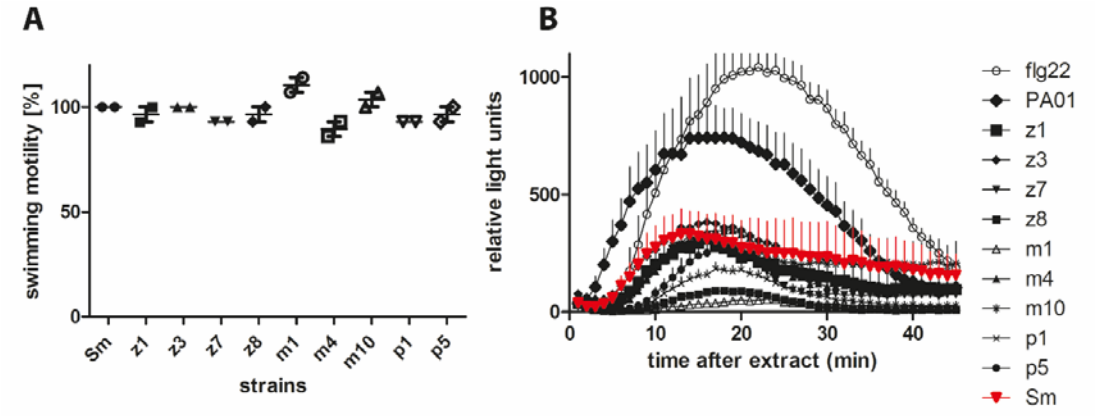

Figure 5.17. *Sm*1021 with novel flg22 alleles that regained motility did not trigger ROS burst. (A) *Sm*1021 wild-type and isolated suppressor cells with regained motility were stabbed into SM medium containing 0.3% agar and incubated for 4 days at 30°C. Swimming colony diameter is presented relative to that of wild-type *Sm*1021. (B) ROS burst in *N. benthamiana* leaf disc was measured after application of bacterial crude extracts from *P. aeruginosa* PA01, wild-type *Sm*1021, or *Sm*1021 suppressor cells with regained motility (z1, z3, z7, z8, m1, m4, m10, p1, and p5), or 100 nM flg22 peptide. Values are means ± standard error (n = 8). The experiment has been performed once.

5.5.1.4 Characterization of a M. truncatula fls2 Tnt1 insertion line

In parallel, a *M. truncatula* mutant line (NF15434) with a predicted *Tnt1* insertion in the *FLS2* locus was obtained, as it could be used as a control alongside wild-type *M. truncatula* R108 for nodulation experiments with the *Sm*1021 strains carrying eliciting flg22 variants. The *Mtfls2 Tnt1* insertion line was identified in the collection of the Samuel Roberts Noble Foundation, which hosts a collection with over 21,000 *M. truncatula Tnt1* retrotransposon

insertion lines (Cheng et al., 2014). Tobacco *Tnt1* is a DNA-retrotransposon, which mobilizes in *M. truncatula* during regeneration in tissue culture but is otherwise stable (D'Erfurth et al., 2003). The *Tnt1* insertion (5.2 kb) in the *MtFLS2* gene in the line NF15434 was localized by sequencing the *Tnt1* flanking sequence tags to a position 2,605 bp after the start codon, which is in an exon just before the kinase domain (Figure A8.6). Homozygous *Mtfls2 Tnt1* insertion lines were identified by PCR-genotyping. *Mtfls2 Tnt1* insertion lines did not express full-length *MtFLS2* transcripts and were unable to produce a flg22^{Pa}-induced ROS burst (Figure 5.18A and B). As *Tnt1* lines typically contain several background insertion events in the *M. truncatula* genome (Tadege et al., 2008), the characterized *Mtfls2* lines were backcrossed once to the parental wild-type R108 line, and the resulting heterozygous *FLS2*/*fls2* lines subsequently self-fertilized to obtain homozygous *Mtfls2* knock-out lines. Three independently backcrossed *Mtfls2* lines have been isolated, and they do not show any unusual phenotypic variations compared to wild-type R108 during growth in soil in controlled environment chambers. The symbiotic infection efficiency with rhizobia has not yet been tested on these lines.

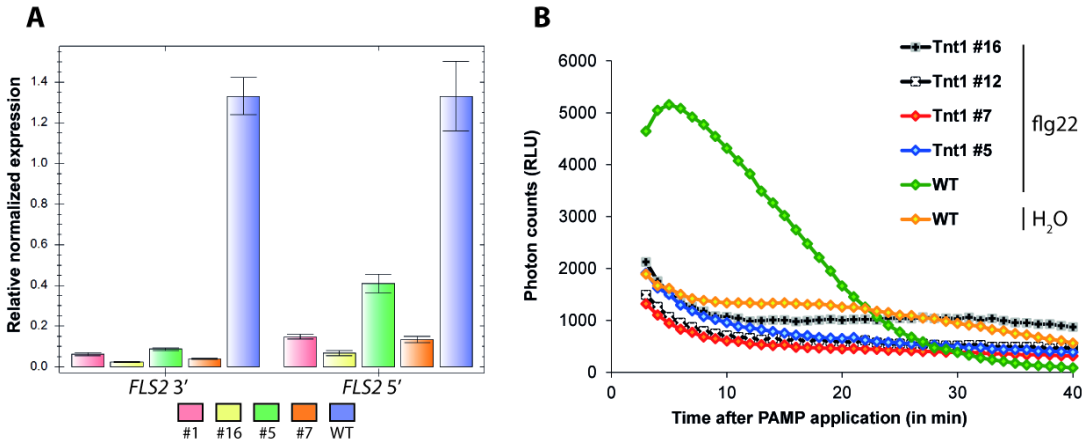

Figure 5.18. Identification of *M. truncatula Tnt1* insertion lines *Mtfls2* with non-functional FLS2. (A) qPCR analysis has been performed with mRNA isolated from leaves of four homozygous *Tnt1* insertion lines (NF15434) Tnt1 #1, #16, #5, #7 and wild-type R108 after cDNA synthesis. qPCR primers were designed at FLS2 3' (#Mt3 and #Mt4) and 5' (#Mt1 and #Mt2) ends at either side of the Tnt1 insertion. Expression was normalized with transcripts of the housekeeping genes UBQ (#Mt5 and #Mt6) and PDF2 (#Mt7 and #Mt8). Values are means ± standard error (n = 3). (B) ROS burst was measured in leaf discs of *M. truncatula* lines Tnt1 #16, #12, #7, #5 and wild-type R108 after flg22 (100 nM) application. Values are means ± standard error (n = 8). These experiments were performed once.

5.5.2 Discussion

Accumulating evidence suggests that evasion of plant immunity is crucial for rhizobia infecting their host legumes (Cao et al., 2017). The flg22 epitope of the legume symbiont *S.*

meliloti is divergent in the otherwise conserved domain and does not elicit typical defence responses in plants (Felix et al., 1999).

I generated *Sm*1021 mutant strains with chromosomal replacements of the flg22 sequence in the *flaA* gene with the aim to creating a new PAMP recognition capability by the *M. truncatula* PRR FLS2. However, bacterial crude extracts of the strains with novel flg22 variants, *Sm flg22*^{Pa} and *Sm flg22*^{mod}, did not trigger a FLS2-dependent ROS burst (Figure 5.15) indicating a lack of eliciting-flagellin gene expression or protein accumulation. Additionally, the introduced flg22 variants seem to have a strong dominant-negative effect on motility, as it was more strongly impaired in *Sm flg22*^{Pa} and *Sm flg22*^{mod} than in the *Sm* Δ*flaA* deletion mutant (Figure 5.14B and C).

Flagellin engineering has been done previously in mammalian and plant pathogenic bacteria (Clarke et al., 2013, Andersen-Nissen et al., 2005, Sun et al., 2006). Plant and mammalian innate immune systems recognize different epitopes of the flagellin protein, but in both cases the immunogenic epitope is located within a conserved domain of the protein (Fliegmann and Felix, 2016). Replacement of a sequence of eight amino acids in the immunogenic flagellin epitope of *Salmonella typhimurium* with a non-eliciting allele from *Helicobacter pylori* enables the pathogen to evade TOLL-LIKE RECEPTOR 5 (TLR5) recognition (Andersen-Nissen et al., 2005). However, these amino acid replacements severely impaired motility, which confers a disadvantage during host infection. Based on structural information of the molecular interaction between flagellin from *S. typhimurium*, Andersen-Nissen *et al*. demonstrated that compensatory mutations in other parts of the flagellin subunit are able to preserve a functional flagellum (Andersen-Nissen et al., 2005). However, the authors did not show this for the chimeric, non-eliciting flagellin variant, but for another non-motile mutant with reduced TLR5 activation.

A natural *Xanthomonas campestris pv. campestris* (*Xcc*) strain has been isolated, which has a single amino acid substitution, V43D, in the flg22 epitope leading to evasion of FLS2 recognition (Sun et al., 2006). Isogenic gene replacements, introducing the V43D variant into related *Xcc* strains, did not constrain motility and allowed the bacteria to evade FLS2 detection (Sun et al., 2006). Similarly, the flg22 variant of *Pseudomonas cannabina* pv. *alisalensis* (*Pcal*) ES4326 is not recognized by FLS2, and complementation of the flagellin-encoding gene *fliC* in *Pto* DC3000 with different *fliC* alleles from related *Pto* strains, including *fliC*^{Pcal}, remained motile (Clarke et al., 2013). Furthermore, sequence variations of flg22 were found in different natural populations of *Pto* exhibiting lower elicitation potential compared to the known eliciting flg22 epitope of *Pto* DC3000 (Cai et al., 2011). These studies highlight

that mutations in the immunogenic flagellin encoding gene can allow immune evasion while preserving motility.

While previous *fliC* engineering has been done in bacterial species with a single flagellin gene copy [*e.g. Salmonella*, *Xanthomonas* and *P. syringae* (Andersen-Nissen et al., 2005, Sun et al., 2006, Clarke et al., 2013)], *S. meliloti* contains four *fla* homologues, which seem to function in a partially redundant manner (Scharf et al., 2001). Although *flaA* seems to be required for motility in *Sm* MV II-1 and *Rhizobium lupini* H13-3 (Scharf et al., 2001), there might be differences between strains, as *flaA* deletion in *Sm*1021 resulted in only a slight reduction of swimming motility (Figure 5.13). The dominant-negative effect of the novel flg22 variant on motility is difficult to explain. Indeed, the complete absence of FlaA had less effect on motility than the presence of a *flaA* variant with mutations in the flg22 encoding sequence (Figure 5.14B and C). However, my preliminary data suggest that FlaA proteins with the eliciting flg22 might not be present, because the bacterial extract did not trigger a FLS2-dependent ROS burst (Figure 5.15). The absence of FlaA could be explained by disturbances on the post-transcriptional level, in a situation where FlaA with a novel flg22 variant induces a structural change and disrupts flagellum assembly (interfering with motility) and is subsequently degraded (so the extract does not trigger a ROS burst). In that case, *Sm*1021 would need efficient protein degradation mechanisms for rapid clearing of the 'defective' flagellin protein. Although the integrity of gene synteny in the *fla* gene locus has been confirmed by PCR after the allele replacements, individual strains with similar gene synteny showed different degrees of motility. This indicates that other events could have happened during the gene replacement process that are not major chromosomal rearrangements, but have an impact on motility.

Various bacterial cells with suppressor mutations could be isolated from the strains with reduced motility after several days of incubation. Individual cells recovered the ability to swim to a similar extent as wild-type (Figure 5.16). However, the fact that bacterial extracts from motile cells of these strains did not trigger a stronger ROS burst than wild-type (Figure 5.17B) suggests that the *flaA* gene with the novel flg22 variant is not expressed or the introduced mutations (partially) reverted. There are multiple hypotheses to explain the recovered motility of the isolated cells without having eliciting activity: i) although it is very unlikely, point mutations in *flaA* could have reconstituted the original flg22 allele; ii) gene fusion of *fla* homologues and/or deletion of the novel *flaA* allele; iii) mutations in the promoter region leading to transcriptional changes favouring other *fla* homologues over *flaA* – these possibilities could be tested by analysing the integrity and sequence of the whole *fla*

gene locus by PCR and sequencing; and iv) regain of motility could also be achieved independently of *flaA* and/or *fla* locus by another mechanism, such as pili-dependent motility. Whole genome sequencing of several independent isolates could indicate common genetic markers responsible for the recovery of motility. As my attempt with chromosomal replacements of the fl22 sequence did not provide conclusive results, a rapid approach to study *Sm*1021 with an eliciting flg22 variant could be to transform various *flaA* alleles expressed from a plasmid under the native promoter in a Δ*flaA*/*flaB*/*flaD*/*flaC* background. This could also reveal whether a single *fla* gene is sufficient for flagellum assembly.

A *Mtfls2 Tnt1* insertion line has been obtained, which does not respond to flg22^{Pa} (Figure 5.18B), and thus represents a useful control line that could be use in the future alongside wild-type *M. truncatula* R108 to examine the effect of *Sm*1021 strains carrying eliciting flg22 variants on the symbiotic interaction.

Overall, genetically engineering the specific residues in bacterial PAMPs that determine the recognition by the plant is a valuable approach to understand the role of plant immunity during symbiosis in more detail and can provide insights into the evolutionary adaptation of rhizobia to establish symbiotic interactions.

Chapter 6

General discussion and future perspectives

In nature, plants are colonized by a plethora of microorganisms living as epiphytes on surfaces or as endophytes within the plant tissue. These microbes can be either in a commensal, mutualistic or pathogenic relationship with their host. While the majority behave rather neutrally towards the plant, specialized microbes can have a beneficial or detrimental effect on the host. To defend themselves against pathogenic attack, plants have evolved a multi-layered immune system comprising an array of extra- and intra-cellular receptors to detect microbes, and initiate immune responses orchestrated by an intricate network of phytohormones to ultimately restrict pathogenic growth (Dodds and Rathjen, 2010). Cell surface-localized pattern recognition receptors (PRRs) perceive characteristic microbial features, termed pathogen (or microbe)-associated molecular patterns (PAMPs/MAMPs) and trigger an immune response leading to resistance against non-adapted pathogens and to basal resistance against adapted pathogens (Boutrot and Zipfel, 2017). Successful pathogens have evolved ways to colonize plants by overcoming these defence mechanisms. While plants must constantly defend themselves against harmful invaders, they also form close interactions with beneficial microbes and it is unclear whether PAMP recognition influences the beneficial interaction with commensals or symbionts (Trdá et al., 2015, Hacquard et al., 2017).

Colonization of plants is a complex process and bacteria need to respond to changing environmental conditions in a rapid and robust way to ensure survival and infection of the host. A central regulator of intracellular signalling pathways balancing a planktonic and motile versus a communal and biofilm-associated lifestyle is the secondary messenger cyclic-di-GMP (cdG) (Jenal et al., 2017). Various studies in different bacteria indicate that high levels of cdG generally stimulate exopolysaccharide (EPS) production and biofilm formation, whereas lower levels promote motility and the expression of virulence factors in bacterial pathogens (Hengge, 2009).

The central subject of this thesis is to understand how pathogenic and beneficial bacteria cope with plant immunity. To this end, I have investigated the role of bacterial EPS from different *Pseudomonas* species during plant infection. In a related project, I have addressed the question of whether perception of immunogenic PAMPs changes the outcome of the legume-rhizobia symbiosis.

6.1 The role of cyclic-di-GMP signalling in immune evasion and plant infection

In Chapter 3, I examined the role of high cdG levels in commensal, beneficial and pathogenic *Pseudomonas* on evasion of plant immunity. I was able to show that both production of EPS and flagella-driven motility are important factors in *P. syringae* pv. *tomato* (*Pto*) DC3000 during different stages of the infection process on *Arabidopsis thaliana*. During infection, the flagellum has a complex role, acting as a virulence factor and as an immunogen due to the recognition of its main structural component, flagellin, by the PRR FLAGELLIN SENSING 2 (FLS2). Therefore, strict control of flagella synthesis is important for plant-associated bacteria. Elevated cdG levels due to expression of a recombinant diguanylate cyclase in the pathogen *Pto* DC3000, the opportunist *P. aeruginosa* PA01 and the commensal *P. protegens* Pf-5 helped the bacteria to evade FLS2-mediated defence. While elevated cdG levels promoted EPS production, they also inhibited flagellin synthesis and reduced accumulation of the PAMP flagellin, which could fully explain the observed evasion of FLS2-mediated immunity. However, during infection, *Pto* DC3000 did not benefit from this immune evasion, as high cellular cdG levels drastically reduced its virulence. This negative effect on virulence was probably a result of reduced flagellar motility and/or additional pleiotropic effects of cdG signalling on bacterial behaviour.

cdG is an important intracellular signalling molecule controlling many bacterial traits including adhesion to surfaces, cell aggregation, biofilm formation, developmental transitions and virulence of pathogens, highlighting its central role for bacterial adaption to environmental conditions. Most bacterial species rely on intricate cdG signalling networks and carry multiple cdG metabolic enzymes. Cellular cdG levels are controlled by diguanylate cyclases (DGCs; characterized by GGDEF domains) producing cdG and phosphodiesterases (PDEs; characterized by EAL or HD-GYP domains) degrading the signalling molecule. Bacterial cells contain multiple cdG-binding components including proteins and RNA molecules that perceive cdG and trigger cellular downstream responses (Hengge, 2009). While the number of DGCs and PDEs for a given bacterial species can be predicted by genome analysis due to the conservation of characteristic domains, cdG-binding domains are highly diverse and many cdG-perceiving proteins with unusual binding domains have been discovered (Jenal et al., 2017). Given the multitude of cdG binding proteins, the regulatory activity can occur at the transcriptional, posttranscriptional or posttranslational level (Sondermann et al., 2012).

While an important role of cdG signalling has been established for virulence factors of *P. aeruginosa* infecting mammals (Malone et al., 2010, Tamayo et al., 2007), it has only been addressed in selected plant pathogens such as *Xanthomonas campestris* (Ryan, 2013), *Erwinia amylovora* (Edmunds et al., 2013), and recently also in *P. syringae* (Engl et al., 2014, Prada-Ramírez et al., 2016, Perez-Mendoza et al., 2014). Various studies, including the results presented in Chapter 3, showed that studying cdG signalling during plant pathogenesis by increasing total cdG levels in the cell (*e.g.* by recombinant DGC expression) (Perez-Mendoza et al., 2014) or by mutating global regulators of cdG-controlled pathways (*e.g.* Gac-Rsm network) (Vakulskas et al., 2015, Records and Gross, 2010, Kong et al., 2012, Grenga et al., 2017) can lead to pleiotropic phenotypes including the typical features of cdG signalling (*e.g.* motility and biofilm formation, but may mask other effects on virulence. Hence, deletion or overexpression of specific DGCs and/or PDEs might affect virulence in an unpredictable fashion. A systematic screen for virulence phenotypes in *X. campestris* pv. *campestris* did not identify a simple relationship between the predicted changes in cdG concentrations and virulence (Kulasakara et al., 2006, Ryan et al., 2007). These findings might indicate that finely tuned cdG signalling is required during individual stages of the complex plant infection process (Romling et al., 2013).

Focussing on the identification of cdG binding proteins expressed during plant infection can be a valuable approach to elucidate the molecular mechanisms for how cdG controls specific cellular features of bacterial virulence. For example, pull-down experiments with biotinylated cdG found that cdG binds to the T3SS component HrcN, and may control T3SS assembly or activity (Trampari et al., 2015, Nesper et al., 2012). This finding could indicate a role of this signalling molecule in the modulation of type-3-secreted effector translocation dynamics.

Different genetic repertoires of cdG signalling modules have been identified by genome comparison analysis of pathogenic, commensal and probiotic isolates of *E. coli*, indicating an cdG-mediated adaptive mechanism to host-specific and environmental niches (Povolotsky and Hengge, 2016). Similar results have also been observed for *Pto* DC3000 and *P. fluorescens* grown in rich media versus nutrient-limiting conditions (Malone and Trampari, *unpublished data*). Interestingly, the results presented in Chapter 3 showed that overexpression of the DGC *wspR19* in three *Pseudomonas* species led to distinct Congo Red-binding phenotypes due to differences in EPS production. Congo Red-binding and the typical wrinkly colony morphology was more pronounced in *P. aeruginosa* PA01 and *P. protegens* Pf-5 compared to *Pto* DC3000, and this was also reflected in distinctive cellular cdG levels.

This could indicate that cdG signalling is under tighter control in *Pto* DC3000 compared to the other two species. A preliminary BLAST search for proteins containing the canonical motifs for DGC (GGDEF) and for PDE (EAL or HD-GYP) enzymes in the genomes of *P. aeruginosa* PA01, *P. protegens* Pf-5 and *Pto* DC3000 revealed similar numbers of proteins with GGDEF (31 to 39 proteins), EAL (21 to 30 proteins) and HD-GYP (1 to 4 proteins) domains, suggesting complex regulatory systems control cellular cdG levels in all three species.

Importantly, cdG binding proteins show varying affinity to the ligand indicating that the effective cellular cdG level and the receptor sensitivity together are crucial for triggering cdG-dependent outputs (Pultz et al., 2012). Furthermore, a considerable fraction of cdG molecules in a given cell seem to be bound, which may result in high local concentrations that differ from the global concentration in the cell (Hengge, 2009). Multiple fluorophore-based tools have been developed to quantify cdG levels within living cells, and on a single cell as well as on the population level (Rybtke et al., 2012, Christen et al., 2010, Strack et al., 2014, Kellenberger et al., 2013). Recent studies have measured distinctive features of bacterial biofilms comparing wild-type and mutant strains under different environmental conditions. This led to the identification of extracellular cues that initiate cdG signalling and biofilm formation, such as mechanical stress (Rodesney et al., 2017), as well as the spatial and temporal distribution of cdG in a developing biofilm of *P. aeruginosa* (Nair et al., 2017). Combined use of genetic and microscopy tools revealed that *E. coli* 'macrocolonies' developed a biofilm with clearly separated zones showing different physiological states and forming complex supracellular structures with wrinkles and ridges. The formation of this particular biofilm architecture is most likely guided by finely tuned cdG signalling involving multiple DGCs and PDEs responding to microenvironmental conditions to control the synthesis of cellulose, curli, flagella and additional matrix components (Serra et al., 2013, Serra and Hengge, 2014, Serra et al., 2015).

During plant infection, *P. syringae* is exposed to different environmental conditions on the surface and inside the plant tissue. Bacterial cells need to adapt to these conditions and perform a switch from a planktonic living mode during colonization and acute infection phase to the formation of colonies and biofilms during later infection stages inside the leaves. The tools described above to quantitatively monitor cdG levels of bacterial cells in a spatial and temporal manner, could be applied to visualize the impact of this important signalling molecule during different steps of plant infection.

6.2 The role of bacterial exopolysaccharides during plant infection

In Chapter 4, I addressed the role of EPS during plant infection. Besides surface adhesion, stress protection and biofilm formation (Arrebola et al., 2015, Quiñones et al., 2005), a role has also been suggested for EPS in suppression of PTI (Aslam et al., 2008, Silipo et al., 2010). To study whether EPS contributes to *P. syringae* infection of *A. thaliana*, deletion mutants of multiple EPS operons (alginate, acetylated cellulose [Wss] and Psl) were generated and have been tested for virulence. EPS-deficient *Pto* DC3000 mutants showed reduced virulence during infection of *A. thaliana*. A combination of at least two different types of EPS seemed to be required for normal proliferation in the apoplast. I tested whether there is a genetic link between EPS and PTI by infecting PTI-compromised *A. thaliana* lines. However, EPS-deficient *Pto* DC3000 did not recover its virulence on the PTI-compromised mutants. This suggests that EPS has other roles independent of PTI suppression during the infection process, and does not exclude that EPS can suppress PTI.

Biofilms represent a ubiquitous and abundant form of life for many microorganisms. Beside lipids, proteins and extracellular DNA, EPS are a major component of bacterial biofilms. These polymeric substances form a matrix that provides the architecture of biofilms with particular physical and hydrodynamic properties. In addition, biofilms also comprise microenvironments with spatial distribution of microbial populations and compounds, such as nutrients, communal signalling molecules and toxic metabolites. High cell densities and diversity in biofilms drive 'social phenotypes' (Nadell et al., 2009) that are characterised by cooperative or competitive behaviour between cells. Cooperative behaviour includes secretion of nutrient chelators, metabolic enzymes, surface-attaching adhesins, structural polymers and signalling molecules, and provides substantial advantages compared to a living mode as singular cells. But strains and species within the biofilm also compete with each other for limited space and resources. Secretion of antibiotic compounds, injection of toxins into adjacent cells and displacement of neighbouring cells are different ways to directly reduce the fitness of competitors (Nadell et al., 2009). The spatial arrangement of different strains and species within biofilms affects their cooperative and competitive behaviour. In turn, this social behaviour can alter the population structure and the spatial arrangement through interaction with neighbouring cells and local modification of matrix components that organize the biofilm architecture (Nadell et al., 2016). The secreted matrix has a crucial role in organising local and global biofilm architecture and proliferation of clonal cell

populations. For example, secretion of the protein RbmA by *Vibrio cholerae* enhances the bonds between cells and to the surrounding EPS (Berk et al., 2012, Smith et al., 2015). Pel and Psl are the main structural polysaccharides in *P. aeruginosa* biofilms and promote cell-cell interactions as well as cross-linking of extracellular DNA molecules (Ma et al., 2009, Jennings et al., 2015). It has been suggested that the secretion of matrix components builds a scaffold with structural cavities that create growth space and define the spatial arrangement of cell lineages (Nadell et al., 2016). During growth of *P. fluorescens* in biofilms on agar plates, individual cells rapidly evolved mutations in the Rsm pathway providing them an evolutionary advantage as these cells are able to push themselves to the surface of the biofilm, probably due to enhanced secretion of EPS (Kim et al., 2014). A similar phenomenon could be observed in *V. cholerae* biofilms, in which strains secreting matrix components displace non-secreting competitor cells (Schluter et al., 2015, Nadell and Bassler, 2011).

The study of model organisms, such as *E. coli*, *V. cholerae*, or *P. aeruginosa*, in experimental systems using *in vitro* cultures has revealed the genetic pathways, physiological responses and molecular signalling pathways underlying biofilm development (Flemming et al., 2016, Flemming and Wingender, 2010). In general, reductionist approaches using *in vitro* cultures helped identifying principles underlying biofilm structure and function, but have clear limitations as specific biofilm properties are strongly dependent on environmental conditions. Recently, a combined experimental and computational study analysed biofilm growth of *E. coli* populations in a porous medium with a microfluidic device, mimicking a soil environment (Coyte et al., 2017). In contrast to previous observations with growth experiments on planar agar surfaces, the results suggest that slow growing cells within a biofilm under the tested hydrodynamic conditions can have a competitive advantage compared to fast growing cells (Coyte et al., 2017).

Natural biofilms can comprise various organisms such as bacteria, viruses, archaea, protozoa and fungi. Understanding the interaction in mixed-species communities will help to explain the emergent properties of biofilms such as stress tolerance and communal metabolic activities. Synthetic community experiments have been designed to study mixed-species biofilms and have provided insights into emergent community properties (Fredrickson, 2015, Zelezniak et al., 2015, Mee et al., 2014). Together, these studies highlight the complexity of biological, chemical and physical interactions within a biofilm. However, the emergent biological properties and functional capacities of the biofilm matrix are still largely unclear (Flemming et al., 2016).

Technological advances in microfluidics and microscopy have greatly improved the ability to study complex biofilms (Rusconi et al., 2014). However, most studies of spatial organisation in bacterial biofilms have relied on laboratory assays and do not always replicate in ecologically realistic settings (Roberts et al., 2015). Nonetheless, knowledge about the structure and function of microbial interactions in biofilms is steadily increasing, albeit predominantly focused on mammal-associated microbial biofilms (Stacy et al., 2016, Mark Welch et al., 2016, Earle et al., 2015).

The colonization and infection of plants represent a valuable experimental system to study biofilm formation and function during pathogenesis. Quantitative metabolomics techniques, such as imaging high-resolution mass spectrometry and nuclear magnetic resonance methods have been used to analyse the *in situ* distribution of metabolites in the microbiota on the leaf surface (Ryffel et al., 2016). Furthermore, biofilm development can be monitored *in planta* in a spatial and temporal manner with fluorescence microscopy. For example, plant root colonization by fluorescently labelled bacteria can be accurately traced in microfluidic devices to understand the interaction between the root and bacteria as well as within bacterial communities (Massalha et al., 2017). Colonization of *A. thaliana* roots by a *Bacillus subtilis* EPS-deficient mutant was reduced compared to wild-type (Massalha et al., 2017). A study looking at virulent, avirulent and non-pathogenic variants of *P. syringae* during apoplast co-colonization experiments found multiple interactions between the different populations and with the host, affecting the spread and proliferation of pathogens, and host immune suppression (Rufian et al., 2017). An experimental system similar to those described above could provide further insights into the role of EPS during plant colonization. Mixed infection experiments with wild-type and EPS-deficient strain could reveal whether secreted EPS is a social good that could be shared between cells of different genotypes growing within the same biofilm. Alternatively, EPS production could also represent a barrier for non-producing cells and exclude them from the biofilm microhabitat. Studying these interactions in the context of different host factors by using plant genotypes with changes in host immunity, metabolite secretion or apoplast structure would contribute greatly to our understanding of the spatial interaction between plants and bacterial pathogens.

6.3 Symbiotic infection process might comprise mechanisms for accommodation of rhizobia in an immune-compromised niche

Crop engineering helps to reduce the economic and environmental costs of plant disease. The genetic transfer of immune receptors across plant species is a promising biotechnological approach to increase disease resistance. Surface-localized PRRs, which detect conserved characteristic microbial features, are functional in heterologous taxonomically-diverse plant species, and can confer broad-spectrum disease resistance (Boutrot and Zipfel, 2017). However, it is unclear whether PRR transfer negatively impacts the association of the recipient plants with symbiotic microbes. In a reductionist approach, I studied if PAMP recognition affects the symbiotic model interaction between the legume *Medicago truncatula* and the bacterium *Sinorhizobium meliloti*. To test this, I transferred the PRR ELONGATION FACTOR-TU RECEPTOR (EFR) from *Arabidopsis thaliana* to the legume *M. truncatula*, conferring recognition of the bacterial EF-Tu protein (or elf18 peptide). EFR perceives the PAMP elf18 from various bacterial species, including *S. meliloti*, and initiates immune signalling (Kunze et al., 2004, Lacombe et al., 2010). I then tested the impact of EFR on the interaction with pathogenic and beneficial bacteria. Constitutive *EFR* expression led to activation of immune responses upon elf18 treatment in leaves and roots. The interaction of *M. truncatula* with the rhizobial symbiont is characterized by the formation of root nodules that fix atmospheric nitrogen. Although nodule numbers were slightly reduced at an early stage of the infection in *EFR-Medicago* when compared to control lines, nodulation was similar in all lines in later stages. Furthermore, nodule colonization by rhizobia, and nitrogen fixation were not compromised by *EFR* expression. Importantly, the *M. truncatula* lines expressing *EFR* were significantly more resistant to the root bacterial pathogen *Ralstonia solanacearum*. The data described in Chapter 5 indicate that the transfer of EFR to *M. truncatula* does not impede root nodule symbiosis, but has a positive impact on disease resistance against a bacterial pathogen. This finding is of particular relevance as attempts to transfer this important symbiosis into non-legume plants are ongoing. This suggest that legumes can be engineered with novel immune receptors, as a biotechnological approach for disease resistance that nonetheless maintains their full symbiosis potential.

In addition, as discussed in Chapter 5, the results indicate that rhizobia can either avoid PAMP recognition during the infection process or actively suppress immune signalling. Another possibility is that the plant accommodates the rhizobia in a compartment with

reduced immune capacity. The symbiotic process between legumes and rhizobia is based on the common symbiotic pathway, which dates back to the emergence of early land plants resulting in thorough adaptation of both interaction partners (Oldroyd, 2013). It is conceivable that the plant evolved specialized structures or mechanisms for the accommodation of the symbiotic partner that minimize its potential to elicit disadvantageous immune responses. Hence, it would be interesting to examine the subcellular localization and tissue-specific accumulation of EFR in the membranes of infection threads and bacteroids by confocal or electron-microscopy. Although *EFR* expression was driven by the ubiquitous CaMV35S promoter and high EFR accumulation could be detected in nodule tissue by western blot analysis, the host may have evolved a mechanism to specifically reduce PTI signalling in subcellular symbiotic compartments that could also affect EFR, as its biogenesis and signal transduction relies on other components of the PTI pathway. Localized immune suppression in plant-derived membranes of the infection thread and bacteroid could reduce PTI signalling capacity, for example due to depletion or exclusion of PRRs. Legumes could have evolved to provide such an immune-compromised niche as a core part of the symbiotic process. Alternatively, this could be achieved *via* an active signalling mechanism triggered by rhizobial signals, such as the perception of Nod factors by the NFP-LYK3 receptor complex (Oldroyd, 2013). An additional signal contributing to successful infections is the perception of EPS from the symbiont by the plant receptor-like kinase EPR3 (Kawaharada et al., 2015). Sequential signal perception is thought to control compatibility and colonization of the symbiotic partner (Zipfel and Oldroyd, 2017) and may provide sufficient stringency to select for a compatible symbiont to allow the plant to reduce immune surveillance in specific compartments. Interestingly, Nod factor perception reduces PRR levels at the plasma membrane and suppresses PTI signalling in the leaves of legume and non-legume plants (Liang et al., 2013). Transcriptome analysis have been performed on isolated root hair cells and the data suggest a transient reduction of defence-associated gene transcription after rhizobial infection (Breakspear et al., 2014, Libault et al., 2010). Recent technical advancements allow to study gene transcription on a single cell level (Papalexi and Satija, 2017, Guillaume-Gentil et al., 2016). This could be an insightful approach to analyse the cellular states of infected and non-infected root hairs. In addition, several studies have addressed suppression of immune signalling by pathogenic microbes. Degradation of PRRs at the plasma membrane is triggered by bacterial effectors employed by pathogens (Gohre et al., 2008, Gimenez-Ibanez et al., 2009a) and exclusion of PRRs from the specialised

extrahaustorial membrane encasing the haustorium has been reported for oomycetes (Lu et al., 2012).

Studies have shown that plant tissues and organs differ in their ability to elicit immune responses upon PAMP treatment. FLS2 is expressed throughout the entire plant, but transcription seems to be higher in cells and tissues vulnerable to bacterial colonization, such as stomata, hydatodes and lateral roots (Beck et al., 2014). While some PAMPs/DAMPs are perceived throughout the entire *A. thaliana* plant, such as flg22, chitin, PGN and Pep1, the root seems to be insensitive for elf18 (Poncini et al., 2017, Wyrsch et al., 2015, Millet et al., 2010). A study analysing LRR-RLK expression patterns with promoter-fusion reporter lines, revealed that EFR is predominantly expressed in reproductive tissues, but not in roots, wheras FLS2 is ubiquitously expressed in almost all tissues (Wu et al., 2016). It is interesting to speculate about the evolutionary forces driving expression of PRRs specifically in certain cells. Among others, the spatial distribution and colonization pattern of pathogens and commensals on the plant could be a determining factor to evolve tissue-specific PRRs in order to ensure immune competence where it is crucial for survival, but to prevent unnecessary activation and allowing colonization of commensals.

An example for a ligand-induced host mechanism to facilitate colonization by commensal or beneficial microbes comes from a study of the gut microbiota in mice (Round et al., 2011). The gut commensal *Bacteroides fragilis* releases a polysaccharide A (PSA) factor, which activates TOLL-LIKE RECEPTOR 2 (TLR2) signalling. In contrast to ligands of TLR2 from pathogenic bacteria, PSA leads to TLR2-dependent local immune suppression in epithelial cells, which is required to accommodate *B. fragilis* in the intestinal mucosa and to establish an immunosuppressed niche (Round et al., 2011).

The work described in Chapter 5 focused on the binary interaction between a host and a symbiont. While the transfer of EFR to *M. truncatula* did not impede symbiosis with its rhizobial partner, the impact of heterologous PRRs on the overall microbiota colonizing the rhizosphere and phyllosphere is unclear. This is particularly relevant as many laboratories are currently looking to exploit the capacity of beneficial microbes to increase plant health and promote agricultural systems (Michelmore et al., 2017, Busby et al., 2017). PRR transfer has been demonstrated to be a valuable tool to increase disease resistance (Boutrot and Zipfel, 2017, Rodriguez-Moreno et al., 2017), as such any potential effect on the microbiota needs to be balanced for a deliberate decision about its use in agriculture depending on disease pressure and other relevant environmental conditions. Nonetheless, little is

currently known about the interaction of PTI with commensal and beneficial microbes (Hacquard et al., 2017).

6.4 Interplay between pattern-triggered immunity and the plant microbiota

Plants live in close association with microbes, which form stable communities and critically affect plant physiology and performance. The functional repertoire of the microbiome expands the plant's capacity to adapt to its environment, as some microbes increase plant growth and tolerance for biotic and abiotic stresses (Müller et al., 2016, Pieterse et al., 2014). This poses a fundamental question about plant-microbe interactions: How do plants discriminate between beneficial and pathogenic microbes? The work of this thesis contributes to the molecular understanding of binary host-pathogen and host-symbiont interactions by analysing the impact of bacterial traits and plant immune receptors during infection. Recent technical advances in next generation sequencing methods in combination with computational tools for 16S rRNA phylogenetic and metagenomics analysis have facilitated research into plant-microbiota interactions at a community level (Vorholt et al., 2017, Bulgarelli et al., 2013). Marker gene amplicon sequencing studies revealed the microbiota composition and major factors explaining the community structure. The bacterial microbiota on the plant root and leaf share a similar taxonomic distribution of species at the phylum-level comprising Proteobacteria, Actinobacteria, Bacteroidetes, and Firmicutes. (Bai et al., 2015, Hacquard et al., 2015). Numerous studies have shown that the main factors driving microbiota assemblages are environmental conditions and soil type, plant age and plant species/genotype (Agler et al., 2016, Dombrowski et al., 2017, Edwards et al., 2015, Coleman-Derr et al., 2016, Wagner et al., 2016).

Recently, the plant immune system has been suggested as a prime candidate to dynamically shape the composition of the microbial community (Hacquard et al., 2017). Previous studies analysing the microbiota indicated that plant immunity has a significant impact on the community composition (Bodenhausen et al., 2014, Horton et al., 2014, Lebeis et al., 2015). The main function of plant immunity is to restrict pathogenic growth and ultimately stop pathogenic attack. As such, PRRs are part of a surveillance system to detect harmful activities due to perception of molecules indicating 'non-self' or 'damaged-self' that initiate quantitative immune responses to limit microbial proliferation. PAMP-induced immune

responses play an important role in restricting the growth of adapted and non-adapted pathogens (Boutrot and Zipfel, 2017, Cook et al., 2015). PRRs are able to perceive PAMPs from commensal and beneficial microbes and can monitor and control the microbial load in the apoplast. As such, the interaction between an array of PRRs and diverse PAMPs has the potential to actively and selectively shape host-microbiota associations.

Evolutionary adaptation and modification of PAMP epitopes is an effective process to evade PTI (Trdá et al., 2015). For example, the immunogenic epitopes elf18, flg22, flgII-28 and xup25 diversified among different phytopathogenic species and strains at a higher rate than other domains of their respective proteins (McCann et al., 2012, Cai et al., 2011, Sun et al., 2006, Mott et al., 2016). Interestingly, preliminary gene sequence comparison of more than 400 members of the *A. thaliana* microbiota revealed that there is a higher variability in the flg22 and elf18 epitopes, which are perceived by *A. thaliana* FSL2 and EFR, respectively, compared to the csp22 epitope, which is not perceived by *A. thaliana,* but by the *Solanacea*-specific PRRs CORE and CSPR (Hacquard et al., 2017). It remains to be validated experimentally whether core members of the plant microbiota adapted to evade immunity. Together, these examples illustrate how plant-associated bacteria are able to diversify immunogenic PAMP epitopes and reduce immune recognition. Beside modification of PAMPs, inhibition of biosynthesis or accumulation of PAMP-containing molecules, such as flagellin (see Chapter 3), effector secretion and host hormone modulation are additional ways to evade plant immunity. While these strategies have been mostly characterized for host-adapted pathogens and symbionts, it is conceivable that similar mechanisms are employed by endophytic commensal and beneficial microbes, which also associate closely with their respective hosts (Pel and Pieterse, 2013, Gourion et al., 2015, Trdá et al., 2015, Zamioudis and Pieterse, 2012). Recently, it has been shown that the plant-growth promoting rhizobacterium *P. simiae* WCS417 suppresses many transcriptional changes induced by the PAMP flg22 (Stringlis et al., 2018). The symbiotic *Sinorhizobium* sp. NGR234 translocates multiple type-3 secreted effectors including NopM, NopL, NopP and NopT into the legume host to interfere with immune signaling (Skorpil et al., 2005, Dai et al., 2008, Xin et al., 2012a, Ge et al., 2016a). Mycorrhizal fungi and endophytic fungi secrete small proteins during the interaction with their host. For example, the effector SP7 from arbuscular mycorrhiza *Rhizofagus irregularis* attenuates ethylene-mediated immune responses and the effector MiSSP7 from the mutualistic fungus *Laccaria bicolor* suppresses JA signalling in the host plant to foster the symbiotic interaction (Kloppholz et al., 2011, Plett et al., 2014). The mutualistic endophyte *Piriformospora indica* expresses a plethora of putative small secreted proteins

and effectively suppresses host immunity during colonization (Zuccaro et al., 2011, Jacobs et al., 2011). These examples indicate that mutualistic microbes actively manipulate their host to promote colonization. Especially in the context of a diverse plant-associated microbial community, suppression of host immunity might be a more successful strategy than immune evasion for the individual microbe, as the former also prevents potential harm due to immune activation by neighboring microbes.Nonetheless, some members of the microbiota probably still activate plant immunity. An *A. thaliana* transcriptome analysis revealed that colonization with the commensal leaf bacteria *Sphingomonas melonis* Fr1 induced a set of approximately 400 genes that partly overlaps with genes induced by the pathogenic *Pto* DC3000 (Vogel et al., 2016). *S. melonis* Fr1 can protect the *A. thaliana* against *Pto* DC3000 infection (Innerebner et al., 2011) and this plant protection appears to be partially dependent on the PRR complex co-receptors BAK1 and BKK1 indicating that PTI signalling is required for the protective activity mediated by *S. melonis* Fr1 (Vogel et al., 2016).

Gene families encoding receptor-like kinases (RLKs) and receptor-like proteins (RLPs) are expanding over time in plant genomes (Shiu et al., 2004) and hundreds of RLKs/RLPs are upregulated upon microbial colonization (Postel et al., 2009, Zipfel et al., 2006, Vogel et al., 2016, Lewis et al., 2015, Yadeta et al., 2017). To date, only a small fraction of these have been functionally characterized or their corresponding ligands identified (Boutrot and Zipfel, 2017). Interestingly, several studies reported that plant responses, such as ROS burst, in response to treatment with various PAMPs including flg22, flgII-28, csp22 and elf18 varied across different plant species or ecotypes (Albert et al., 2010, Vetter et al., 2012, Veluchamy et al., 2014). Furthermore, a study assessing PAMP-induced seedling growth inhibition in multiple *A. thaliana* accessions indicated that despite a common PTI signalling pathway, responses to individual PAMPs might evolve independently in plant populations (Vetter et al., 2016).

Together, this suggests that PTI signalling in the host can be modulated at different levels and from the plant as well as the microbial side. It is intriguing to speculate that host immunity shapes the microbiota structure and composition (Hacquard et al., 2017). Plant immunity has been mostly studied in the laboratory with binary interactions of a host plant and a pathogenic microbe. It is a major challenge to understand the evolutionary and molecular principles of plant immunity in natural environments and in the context of complex microbial communities. Many questions remain yet to be answered: To what extent are microbiota members with eliciting PAMP epitopes sensed by plant PRRs? What drives evolution and diversification of PAMPs on the population- and the community-level? Do

PRRs play a role in sensing and shaping the overall microbial community? Are there ecological and evolutionary mechanisms driving adaptation of plants to local microbiota populations? Future studies will reveal whether the mechanistic principles of plant immunity that govern individual plant-pathogen interactions also hold true for the overall microbial community.

References

AGLER, M. T., RUHE, J., KROLL, S., MORHENN, C., KIM, S.-T., WEIGEL, D. & KEMEN, E. M. 2016. Microbial Hub Taxa Link Host and Abiotic Factors to Plant Microbiome Variation. *PLOS Biology,* 14**,** e1002352.

ALBERT, I., BOHM, H., ALBERT, M., FEILER, C. E., IMKAMPE, J., WALLMEROTH, N., BRANCATO, C., RAAYMAKERS, T. M., OOME, S., ZHANG, H., KROL, E., GREFEN, C., GUST, A. A., CHAI, J., HEDRICH, R., VAN DEN ACKERVEKEN, G. & NURNBERGER, T. 2015. An RLP23-SOBIR1-BAK1 complex mediates NLP-triggered immunity. *Nat Plants,* 1**,** 15140.

ALBERT, M., JEHLE, A. K., LIPSCHIS, M., MUELLER, K., ZENG, Y. & FELIX, G. 2010. Regulation of cell behaviour by plant receptor kinases: Pattern recognition receptors as prototypical models. *Eur J Cell Biol,* 89**,** 200-7.

ALCÁZAR, R. & PARKER, J. E. 2011. The impact of temperature on balancing immune responsiveness and growth in *Arabidopsis*. *Trends in Plant Science,* 16**,** 666-675.

ANDERSEN-NISSEN, E., SMITH, K. D., STROBE, K. L., BARRETT, S. L., COOKSON, B. T., LOGAN, S. M. & ADEREM, A. 2005. Evasion of Toll-like receptor 5 by flagellated bacteria. *Proc Natl Acad Sci U S A,* 102**,** 9247-52.

ARAGON, I. M., PEREZ-MENDOZA, D., GALLEGOS, M. T. & RAMOS, C. 2015a. The c-di-GMP phosphodiesterase BifA is involved in the virulence of bacteria from the *Pseudomonas syringae* complex. *Mol Plant Pathol,* 16**,** 604-15.

ARAGON, I. M., PEREZ-MENDOZA, D., MOSCOSO, J. A., FAURE, E., GUERY, B., GALLEGOS, M. T., FILLOUX, A. & RAMOS, C. 2015b. Diguanylate cyclase DgcP is involved in plant and human *Pseudomonas* spp. infections. *Environ Microbiol,* 17**,** 4332-51.

ARREBOLA, E., CARRION, V. J., GUTIERREZ-BARRANQUERO, J. A., PEREZ-GARCIA, A., RODRIGUEZ-PALENZUELA, P., CAZORLA, F. M. & DE VICENTE, A. 2015. Cellulose production in *Pseudomonas syringae* pv. *syringae*: A compromise between epiphytic and pathogenic lifestyles. *FEMS Microbiol Ecol,* 91.

ASAI, T., TENA, G., PLOTNIKOVA, J., WILLMANN, M. R., CHIU, W. L., GOMEZ-GOMEZ, L., BOLLER, T., AUSUBEL, F. M. & SHEEN, J. 2002. MAP kinase signalling cascade in *Arabidopsis* innate immunity. *Nature,* 415**,** 977-83.

ASLAM, S. N., NEWMAN, M. A., ERBS, G., MORRISSEY, K. L., CHINCHILLA, D., BOLLER, T., JENSEN, T. T., DE CASTRO, C., IERANO, T., MOLINARO, A., JACKSON, R. W., KNIGHT, M. R. & COOPER, R. M. 2008. Bacterial polysaccharides suppress induced innate immunity by calcium chelation. *Curr Biol,* 18**,** 1078-83.

BAHAR, O., MORDUKHOVICH, G., LUU, D. D., SCHWESSINGER, B., DAUDI, A., JEHLE, A. K., FELIX, G. & RONALD, P. C. 2016. Bacterial outer membrane vesicles induce plant immune responses. *Molecular Plant-Microbe Interactions,* 29**,** 374-384.

BAI, Y., MÜLLER, D. B., SRINIVAS, G., GARRIDO-OTER, R., POTTHOFF, E., ROTT, M., DOMBROWSKI, N., MÜNCH, P. C., SPAEPEN, S., REMUS-EMSERMANN, M., HÜTTEL, B., MCHARDY, A. C., VORHOLT, J. A. & SCHULZE-LEFERT, P. 2015. Functional overlap of the *Arabidopsis* leaf and root microbiota. *Nature,* 528**,** 364-369.

BARAHONA, E., NAVAZO, A., MARTINEZ-GRANERO, F., ZEA-BONILLA, T., PEREZ-JIMENEZ, R. M., MARTIN, M. & RIVILLA, R. 2011. *Pseudomonas fluorescens* F113 mutant with enhanced competitive colonization ability and improved biocontrol activity against fungal root pathogens. *Appl Environ Microbiol,* 77**,** 5412-9.

BARAQUET, C. & HARWOOD, C. S. 2013. Cyclic diguanosine monophosphate represses bacterial flagella synthesis by interacting with the Walker A motif of the enhancer-binding protein FleQ. *Proc Natl Acad Sci U S A,* 110**,** 18478-83.

BARDOEL, B. W., VAN KESSEL, K. P. M., VAN STRIJP, J. A. G. & MILDER, F. J. 2012. Inhibition of pseudomonas aeruginosa virulence: Characterization of the apra-apri interface and species selectivity. *Journal of Molecular Biology,* 415**,** 573-583.

BARNHART, D. M., SU, S., BACCARO, B. E., BANTA, L. M. & FARRAND, S. K. 2013. Celr, an ortholog of the diguanylate cyclase pled of caulobacter, regulates cellulose synthesis in agrobacterium tumefaciens. *Appl Environ Microbiol,* 79**,** 7188-202.

BAUER, Z., GOMEZ-GOMEZ, L., BOLLER, T. & FELIX, G. 2001. Sensitivity of different ecotypes and mutants of arabidopsis thaliana toward the bacterial elicitor flagellin correlates with the presence of receptor-binding sites. *J Biol Chem,* 276**,** 45669-76.

BEATTIE, G. A. & LINDOW, S. E. 1995. The secret life of foliar bacterial pathogens on leaves. *Annu Rev Phytopathol,* 33**,** 145-72.

BECK, M., WYRSCH, I., STRUTT, J., WIMALASEKERA, R., WEBB, A., BOLLER, T. & ROBATZEK, S. 2014. Expression patterns of FLAGELLIN SENSING 2 map to bacterial entry sites in plant shoots and roots. *Journal of Experimental Botany,* 65**,** 6487-6498.

BENDER, C. L., ALARCON-CHAIDEZ, F. & GROSS, D. C. 1999. *Pseudomonas syringae* phytotoxins: Mode of action, regulation, and biosynthesis by peptide and polyketide synthetases. *Microbiol Mol Biol Rev,* 63**,** 266-92.

BERENDSEN, R. L., PIETERSE, C. M. & BAKKER, P. A. 2012. The rhizosphere microbiome and plant health. *Trends Plant Sci,* 17**,** 478-86.

BERK, V., FONG, J. C. N., DEMPSEY, G. T., DEVELIOGLU, O. N., ZHUANG, X., LIPHARDT, J., YILDIZ, F. H. & CHU, S. 2012. Molecular Architecture and Assembly Principles of Vibrio cholerae Biofilms. *Science,* 337**,** 236-239.

BERRABAH, F., BOURCY, M., ESCHSTRUTH, A., CAYREL, A., GUEFRACHI, I., MERGAERT, P., WEN, J., JEAN, V., MYSORE, K. S., GOURION, B. & RATET, P. 2014. A nonRD receptor-like kinase prevents nodule early senescence and defense-like reactions during symbiosis. *New Phytologist,* 203**,** 1305-1314.

BERRABAH, F., RATET, P. & GOURION, B. 2015. Multiple steps control immunity during the intracellular accommodation of rhizobia. *Journal of Experimental Botany,* 66**,** 1977-1985.

BLADERGROEN, M. R., BADELT, K. & SPAINK, H. P. 2003. Infection-blocking genes of a symbiotic *Rhizobium leguminosarum* strain that are involved in temperature-dependent protein secretion. *Mol Plant-Microbe Interact,* 16.

BLOCK, A. & ALFANO, J. R. 2011. Plant targets for pseudomonas syringae type iii effectors: Virulence targets or guarded decoys? *Curr Opin Microbiol,* 14**,** 39-46.

BOCH, J., JOARDAR, V., GAO, L., ROBERTSON, T. L., LIM, M. & KUNKEL, B. N. 2002. Identification of pseudomonas syringae pv. Tomato genes induced during infection of arabidopsis thaliana. *Molecular Microbiology,* 44**,** 73-88.

BODENHAUSEN, N., BORTFELD-MILLER, M., ACKERMANN, M. & VORHOLT, J. A. 2014. A synthetic community approach reveals plant genotypes affecting the phyllosphere microbiota. *PLOS Genetics,* 10**,** e1004283.

BOLES, B. R., THOENDEL, M. & SINGH, P. K. 2004. Self-generated diversity produces "insurance effects" in biofilm communities. *Proc Natl Acad Sci U S A,* 101**,** 16630-5.

BOLLER, T. & FELIX, G. 2009. A renaissance of elicitors: Perception of microbe-associated molecular patterns and danger signals by pattern-recognition receptors. *Annu Rev Plant Biol,* 60**,** 379-406.

BOURCY, M., BROCARD, L., PISLARIU, C. I., COSSON, V., MERGAERT, P., TADEGE, M., MYSORE, K. S., UDVARDI, M. K., GOURION, B. & RATET, P. 2013. *Medicago truncatula* DNF2 is a PI-PLC-XD-containing protein required for bacteroid persistence and prevention of nodule early senescence and defense-like reactions. *New Phytolog,* 197.

BOUTROT, F. & ZIPFEL, C. 2017. Function, discovery, and exploitation of plant pattern recognition receptors for broad-spectrum disease resistance. *Annu Rev Phytopathol,* 55**,** 257-286.

BREAKSPEAR, A., LIU, C., ROY, S., STACEY, N., ROGERS, C., TRICK, M., MORIERI, G., MYSORE, K. S., WEN, J., OLDROYD, G. E., DOWNIE, J. A. & MURRAY, J. D. 2014. The root hair "infectome" of medicago truncatula uncovers changes in cell cycle genes and reveals a requirement for auxin signaling in rhizobial infection. *Plant Cell,* 26**,** 4680-701.

BROWN, I., MANSFIELD, J., IRLAM, I., CONRADSSTRAUCH, J. & BONAS, U. 1993. Ultrastructure of interactions between *Xanthomonas campestris* pv *vesicatoria* and pepper, including immunocytochemical localization of extracellular polysaccharides and the AvrBs3 protein. *Molecular Plant-Microbe Interactions,* 6**,** 376-386.

BRUTUS, A., SICILIA, F., MACONE, A., CERVONE, F. & DE LORENZO, G. 2010. A domain swap approach reveals a role of the plant wall-associated kinase 1 (WAK1) as a receptor of oligogalacturonides. *Proc Natl Acad Sci U S A,* 107**,** 9452-7.

BULGARELLI, D., SCHLAEPPI, K., SPAEPEN, S., THEMAAT, E. V. L. V. & SCHULZE-LEFERT, P. 2013. Structure and Functions of the Bacterial Microbiota of Plants. *Annual Review of Plant Biology,* 64**,** 807-838.

BURDETTE, D. L., MONROE, K. M., SOTELO-TROHA, K., IWIG, J. S., ECKERT, B., HYODO, M., HAYAKAWA, Y. & VANCE, R. E. 2011. STING is a direct innate immune sensor of cyclic di-GMP. *Nature,* 478**,** 515-8.

BUSBY, P. E., SOMAN, C., WAGNER, M. R., FRIESEN, M. L., KREMER, J., BENNETT, A., MORSY, M., EISEN, J. A., LEACH, J. E. & DANGL, J. L. 2017. Research priorities for harnessing plant microbiomes in sustainable agriculture. *PLOS Biology,* 15**,** e2001793.

BYRD, M. S., SADOVSKAYA, I., VINOGRADOV, E., LU, H., SPRINKLE, A. B., RICHARDSON, S. H., MA, L., RALSTON, B., PARSEK, M. R., ANDERSON, E. M., LAM, J. S. & WOZNIAK, D. J. 2009. Genetic and biochemical analyses of the *Pseudomonas aeruginosa* Psl exopolysaccharide reveal overlapping roles for polysaccharide synthesis enzymes in Psl and LPS production. *Mol Microbiol,* 73**,** 622-38.

CAI, R., LEWIS, J., YAN, S., LIU, H., CLARKE, C. R., CAMPANILE, F., ALMEIDA, N. F., STUDHOLME, D. J., LINDEBERG, M., SCHNEIDER, D., ZACCARDELLI, M., SETUBAL, J. C., MORALES-LIZCANO, N. P., BERNAL, A., COAKER, G., BAKER, C., BENDER, C. L., LEMAN, S. & VINATZER, B. A. 2011. The plant pathogen *Pseudomonas syringae* pv. *tomato* is genetically monomorphic and under strong selection to evade tomato immunity. *PLoS Pathog,* 7**,** e1002130.

CAO, Y., HALANE, M. K., GASSMANN, W. & STACEY, G. 2017. The role of plant innate immunity in the legume-rhizobium symbiosis. *Annu Rev Plant Biol,* 68**,** 535-561.

CAO, Y., LIANG, Y., TANAKA, K., NGUYEN, C. T., JEDRZEJCZAK, R. P., JOACHIMIAK, A. & STACEY, G. 2014. The kinase LYK5 is a major chitin receptor in *Arabidopsis* and forms a chitin-induced complex with related kinase CERK1. *Elife,* 3**,** e03766.

CHANG, J. H., DESVEAUX, D. & CREASON, A. L. 2014. The ABCs and 123s of bacterial secretion systems in plant pathogenesis. *Annu Rev Phytopathol,* 52**,** 317-45.

CHANG, W.-S., VAN DE MORTEL, M., NIELSEN, L., NINO DE GUZMAN, G., LI, X. & HALVERSON, L. J. 2007. Alginate production by pseudomonas putida creates a hydrated microenvironment and contributes to biofilm architecture and stress tolerance under water-limiting conditions. *Journal of Bacteriology,* 189**,** 8290-8299.

CHAPARRO-GARCIA, A., WILKINSON, R. C., GIMENEZ-IBANEZ, S., FINDLAY, K., COFFEY, M. D., ZIPFEL, C., RATHJEN, J. P., KAMOUN, S. & SCHORNACK, S. 2011. The receptor-like kinase SERK3/BAK1 is required for basal resistance against the late blight pathogen *Phytophthora infestans* in *Nicotiana benthamiana*. *PLoS One,* 6**,** e16608.

CHEN, T., DUAN, L., ZHOU, B., YU, H., ZHU, H., CAO, Y. & ZHANG, Z. 2017. Interplay of pathogen-induced defense responses and symbiotic establishment in *Medicago truncatula*. *Frontiers in Microbiology,* 8.

CHENG, C., GAO, X., FENG, B., SHEEN, J., SHAN, L. & HE, P. 2013. Plant immune response to pathogens differs with changing temperatures. *Nature communications,* 4**,** 2530.

CHENG, X., WANG, M., LEE, H. K., TADEGE, M., RATET, P., UDVARDI, M., MYSORE, K. S. & WEN, J. 2014. An efficient reverse genetics platform in the model legume *Medicago truncatula*. *New Phytol,* 201**,** 1065-76.

CHINCHILLA, D., ZIPFEL, C., ROBATZEK, S., KEMMERLING, B., NURNBERGER, T., JONES, J. D., FELIX, G. & BOLLER, T. 2007. A flagellin-induced complex of the receptor FLS2 and BAK1 initiates plant defence. *Nature,* 448**,** 497-500.

CHOI, J., TANAKA, K., CAO, Y., QI, Y., QIU, J., LIANG, Y., LEE, S. Y. & STACEY, G. 2014. Identification of a plant receptor for extracellular ATP. *Science,* 343**,** 290-4.

CHRISTEN, M., KULASEKARA, H. D., CHRISTEN, B., KULASEKARA, B. R., HOFFMAN, L. R. & MILLER, S. I. 2010. Asymmetrical Distribution of the Second Messenger c-di-GMP upon Bacterial Cell Division. *Science,* 328**,** 1295-1297.

CLARKE, C. R., CHINCHILLA, D., HIND, S. R., TAGUCHI, F., MIKI, R., ICHINOSE, Y., MARTIN, G. B., LEMAN, S., FELIX, G. & VINATZER, B. A. 2013. Allelic variation in two distinct *Pseudomonas syringae* flagellin epitopes modulates the strength of plant immune responses but not bacterial motility. *New Phytol,* 200**,** 847-60.

COLEMAN-DERR, D., DESGARENNES, D., FONSECA-GARCIA, C., GROSS, S., CLINGENPEEL, S., WOYKE, T., NORTH, G., VISEL, A., PARTIDA-MARTINEZ, L. P. & TRINGE, S. G. 2016. Plant compartment and biogeography affect microbiome composition in cultivated and native Agave species. *New Phytologist,* 209**,** 798-811.

COLLMER, A., BADEL, J. L., CHARKOWSKI, A. O., DENG, W. L., FOUTS, D. E., RAMOS, A. R., REHM, A. H., ANDERSON, D. M., SCHNEEWIND, O., VAN DIJK, K. & ALFANO, J. R. 2000. *Pseudomonas syringae hrp* type III secretion system and effector proteins. *Proc Natl Acad Sci U S A,* 97**,** 8770-7.

COLVIN, K. M., GORDON, V. D., MURAKAMI, K., BORLEE, B. R., WOZNIAK, D. J., WONG, G. C. L. & PARSEK, M. R. 2011. The Pel polysaccharide can serve a structural and protective role in the biofilm matrix of *Pseudomonas aeruginosa*. *Plos Pathogens,* 7.

COOK, D. E., MESARICH, C. H. & THOMMA, B. P. 2015. Understanding plant immunity as a surveillance system to detect invasion. *Annu Rev Phytopathol,* 53**,** 541-63.

COSSON, V., DURAND, P., D'ERFURTH, I., KONDOROSI, A. & RATET, P. 2006. *Medicago truncatula* transformation using leaf explants. *Methods Mol Biol,* 343**,** 115-27.

COUTO, D. & ZIPFEL, C. 2016. Regulation of pattern recognition receptor signalling in plants. *Nat Rev Immunol,* 16**,** 537-52.

COYTE, K. Z., TABUTEAU, H., GAFFNEY, E. A., FOSTER, K. R. & DURHAM, W. M. 2017. Microbial competition in porous environments can select against rapid biofilm growth. *Proceedings of the National Academy of Sciences,* 114**,** E161-E170.

CUI, H., TSUDA, K. & PARKER, J. E. 2015. Effector-triggered immunity: from pathogen perception to robust defense. *Annu Rev Plant Biol,* 66**,** 487-511.

CUPPELS, D. A. 1986. Generation and Characterization of Tn5 Insertion Mutations in Pseudomonas syringae pv. tomato. *Applied and Environmental Microbiology,* 51**,** 323-327.

D'ARGENIO, D. A., CALFEE, M. W., RAINEY, P. B. & PESCI, E. C. 2002. Autolysis and autoaggregation in *Pseudomonas aeruginosa* colony morphology mutants. *Journal of Bacteriology,* 184**,** 6481-6489.

D'ERFURTH, I., COSSON, V., ESCHSTRUTH, A., LUCAS, H., KONDOROSI, A. & RATET, P. 2003. Efficient transposition of the *Tnt1* tobacco retrotransposon in the model legume *Medicago truncatula*. *The Plant Journal,* 34**,** 95-106.

D'HAEZE, W. & HOLSTERS, M. 2004. Surface polysaccharides enable bacteria to evade plant immunity. *Trends Microbiol,* 12**,** 555-61.

DAI, W. J., ZENG, Y., XIE, Z. P. & STAEHELIN, C. 2008. Symbiosis-promoting and deleterious effects of NopT, a novel type 3 effector of *Rhizobium* sp. strain NGR234. *J Bacteriol,* 190**,** 5101-10.

DANGL, J. L., HORVATH, D. M. & STASKAWICZ, B. J. 2013. Pivoting the plant immune system from dissection to deployment. *Science,* 341**,** 746-751.

DANHORN, T. & FUQUA, C. 2007. Biofilm formation by plant-associated bacteria. *Annual Review of Microbiology,* 61**,** 401-422.

DARRASSE, A., CARRERE, S., BARBE, V., BOUREAU, T., ARRIETA-ORTIZ, M. L., BONNEAU, S., BRIAND, M., BRIN, C., COCIANCICH, S., DURAND, K., FOUTEAU, S., GAGNEVIN, L., GUERIN, F., GUY, E., INDIANA, A., KOEBNIK, R., LAUBER, E., MUNOZ, A., NOEL, L. D., PIERETTI, I., POUSSIER, S., PRUVOST, O., ROBENE-SOUSTRADE, I., ROTT, P., ROYER, M., SERRES-GIARDI, L., SZUREK, B., VAN SLUYS, M. A., VERDIER, V., VERNIERE, C., ARLAT, M., MANCEAU, C. & JACQUES, M. A. 2013. Genome sequence of *Xanthomonas fuscans* subsp. *fuscans* strain 4834-R reveals that flagellar motility is not a general feature of xanthomonads. *BMC Genomics,* 14**,** 761.

DASGUPTA, N., WOLFGANG, M. C., GOODMAN, A. L., ARORA, S. K., JYOT, J., LORY, S. & RAMPHAL, R. 2003. A four-tiered transcriptional regulatory circuit controls flagellar biogenesis in *Pseudomonas aeruginosa*. *Mol Microbiol,* 50**,** 809-24.

DAVEY, M. E. & O'TOOLE G, A. 2000. Microbial biofilms: from ecology to molecular genetics. *Microbiol Mol Biol Rev,* 64**,** 847-67.

DAVIES, D. G. & GEESEY, G. G. 1995. Regulation of the alginate biosynthesis gene *algC* in *Pseudomonas aeruginosa* during biofilm development in continuous culture. *Applied and Environmental Microbiology,* 61**,** 860-7.

DE PINTO, M. C., LAVERMICOCCA, P., EVIDENTE, A., CORSARO, M. M., LAZZARONI, S. & DE GARA, L. 2003. Exopolysaccharides produced by plant pathogenic bacteria affect ascorbate metabolism in *Nicotiana tabacum*. *Plant Cell Physiol,* 44**,** 803-10.

DE TORRES, M., MANSFIELD, J. W., GRABOV, N., BROWN, I. R., AMMOUNEH, H., TSIAMIS, G., FORSYTH, A., ROBATZEK, S., GRANT, M. & BOCH, J. 2006. *Pseudomonas syringae* effector AvrPtoB suppresses basal defence in *Arabidopsis*. *Plant J,* 47**,** 368-82.

DEAKIN, W. J. & BROUGHTON, W. J. 2009. Symbiotic use of pathogenic strategies: Rhizobial protein secretion systems. *Nat Rev Microbiol,* 7**,** 312-20.

DODDS, P. N. & RATHJEN, J. P. 2010. Plant immunity: Towards an integrated view of plant-pathogen interactions. *Nature Reviews Genetics,* 11**,** 539-548.

DOMBROWSKI, N., SCHLAEPPI, K., AGLER, M. T., HACQUARD, S., KEMEN, E., GARRIDO-OTER, R., WUNDER, J., COUPLAND, G. & SCHULZE-LEFERT, P. 2017. Root microbiota dynamics of perennial Arabis alpina are dependent on soil residence time but independent of flowering time. *ISME J,* 11**,** 43-55.

DOMONKOS, A., HORVATH, B., MARSH, J. F., HALASZ, G., AYAYDIN, F., OLDROYD, G. E. & KALO, P. 2013. The identification of novel loci required for appropriate nodule development in *Medicago truncatula*. *BMC Plant Biology,* 13**,** 157.

DONG, Y., BURCH-SMITH, T. M., LIU, Y., MAMILLAPALLI, P. & DINESH-KUMAR, S. P. 2007. A ligation-independent cloning tobacco rattle virus vector for high-throughput virus-induced gene silencing identifies roles for nbmads4-1 and -2 in floral development. *Plant Physiol,* 145**,** 1161-70.

DOWNIE, J. A. 2010. The roles of extracellular proteins, polysaccharides and signals in the interactions of rhizobia with legume roots. *FEMS Microbiol Rev,* 34**,** 150-70.

DU, J., VERZAUX, E., CHAPARRO-GARCIA, A., BIJSTERBOSCH, G., KEIZER, L. C., ZHOU, J., LIEBRAND, T. W., XIE, C., GOVERS, F., ROBATZEK, S., VAN DER VOSSEN, E. A., JACOBSEN, E., VISSER, R. G., KAMOUN, S. & VLEESHOUWERS, V. G. 2015. Elicitin recognition confers enhanced resistance to *Phytophthora infestans* in potato. *Nat Plants,* 1**,** 15034.

DUNGER, G., RELLING, V. M., TONDO, M. L., BARRERAS, M., IELPI, L., ORELLANO, E. G. & OTTADO, J. 2007. Xanthan is not essential for pathogenicity in citrus canker but contributes to *Xanthomonas* epiphytic survival. *Arch Microbiol,* 188**,** 127-35.

DUNNING, F. M., SUN, W., JANSEN, K. L., HELFT, L. & BENT, A. F. 2007. Identification and mutational analysis of Arabidopsis FLS2 leucine-rich repeat domain residues that contribute to flagellin perception. *Plant Cell,* 19**,** 3297-313.

EARLE, KRISTEN A., BILLINGS, G., SIGAL, M., LICHTMAN, JOSHUA S., HANSSON, GUNNAR C., ELIAS, JOSHUA E., AMIEVA, MANUEL R., HUANG, KERWYN C. & SONNENBURG, JUSTIN L. 2015. Quantitative Imaging of Gut Microbiota Spatial Organization. *Cell Host & Microbe,* 18**,** 478-488.

EDMUNDS, A. C., CASTIBLANCO, L. F., SUNDIN, G. W. & WATERS, C. M. 2013. Cyclic Di-GMP modulates the disease progression of *Erwinia amylovora*. *J Bacteriol,* 195**,** 2155-65.

EDWARDS, J., JOHNSON, C., SANTOS-MEDELLÍN, C., LURIE, E., PODISHETTY, N. K., BHATNAGAR, S., EISEN, J. A. & SUNDARESAN, V. 2015. Structure, variation, and assembly of the root-associated microbiomes of rice. *Proceedings of the National Academy of Sciences,* 112**,** E911-E920.

ENGL, C., WAITE, C. J., MCKENNA, J. F., BENNETT, M. H., HAMANN, T. & BUCK, M. 2014. Chp8, a diguanylate cyclase from *Pseudomonas syringae* pv. *tomato* DC3000, suppresses the pathogen-associated molecular pattern flagellin, increases extracellular polysaccharides, and promotes plant immune evasion. *MBio,* 5**,** e01168-14.

ERBS, G. & NEWMAN, M. A. 2012. The role of lipopolysaccharide and peptidoglycan, two glycosylated bacterial microbe-associated molecular patterns (MAMPs), in plant innate immunity. *Mol Plant Pathol,* 13**,** 95-104.

ERBS, G., SILIPO, A., ASLAM, S., DE CASTRO, C., LIPAROTI, V., FLAGIELLO, A., PUCCI, P., LANZETTA, R., PARRILLI, M., MOLINARO, A., NEWMAN, M. A. & COOPER, R. M. 2008. Peptidoglycan and muropeptides from pathogens *Agrobacterium* and *Xanthomonas* elicit plant innate immunity: Structure and activity. *Chem Biol,* 15**,** 438-48.

EVANS, L. R. & LINKER, A. 1973. Production and characterization of the slime polysaccharide of *Pseudomonas aeruginosa*. *J Bacteriol,* 116**,** 915-24.

FELIX, G., DURAN, J. D., VOLKO, S. & BOLLER, T. 1999. Plants have a sensitive perception system for the most conserved domain of bacterial flagellin. *Plant J,* 18**,** 265-76.

FENG, F., YANG, F., RONG, W., WU, X., ZHANG, J., CHEN, S., HE, C. & ZHOU, J. M. 2012. A *Xanthomonas* uridine 5′-monophosphate transferase inhibits plant immune kinases. *Nature,* 485.

FERRIERES, L., ASLAM, S. N., COOPER, R. M. & CLARKE, D. J. 2007. The *yjbEFGH* locus in *Escherichia coli* K-12 is an operon encoding proteins involved in exopolysaccharide production. *Microbiology,* 153**,** 1070-80.

FETT, W. F. & DUNN, M. F. 1989. Exopolysaccharides produced by phytopathogenic *Pseudomonas syringae* pathovars in infected leaves of susceptible hosts. *Plant Physiology,* 89**,** 5-9.

FINLAY, B. B. & FALKOW, S. 1997. Common themes in microbial pathogenicity revisited. *Microbiol Mol Biol Rev,* 61**,** 136-69.

FLEMMING, H.-C. & WINGENDER, J. 2010. The biofilm matrix. *Nat Rev Micro,* 8**,** 623-633.

FLEMMING, H.-C., WINGENDER, J., SZEWZYK, U., STEINBERG, P., RICE, S. A. & KJELLEBERG, S. 2016. Biofilms: an emergent form of bacterial life. *Nat Rev Micro,* 14**,** 563-575.

FLIEGMANN, J. & FELIX, G. 2016. Immunity: Flagellin seen from all sides. *Nat Plants,* 2**,** 16136.

FLOR, H. H. 1971. Current status of gene-for-gene concept. *Annual Review of Phytopathology,* 9**,** 275-+.

FORSYTH, A., MANSFIELD, J. W., GRABOV, N., DE TORRES, M., SINAPIDOU, E. & GRANT, M. R. 2010. Genetic Dissection of Basal Resistance to Pseudomonas syringae pv. phaseolicola in Accessions of Arabidopsis. *Molecular Plant-Microbe Interactions,* 23**,** 1545-1552.

FRANKLIN, M. J., NIVENS, D. E., WEADGE, J. T. & HOWELL, P. L. 2011. Biosynthesis of the *Pseudomonas aeruginosa* extracellular polysaccharides, alginate, Pel, and Psl. *Front Microbiol,* 2**,** 1-16.

FREDRICKSON, J. K. 2015. Ecological communities by design. *Science,* 348**,** 1425-1427.

FREEMAN, B. C., CHEN, C. & BEATTIE, G. A. 2010. Identification of the trehalose biosynthetic loci of *Pseudomonas syringae* and their contribution to fitness in the phyllosphere. *Environmental Microbiology,* 12**,** 1486-1497.

FREEMAN, B. C., CHEN, C., YU, X., NIELSEN, L., PETERSON, K. & BEATTIE, G. A. 2013. Physiological and transcriptional responses to osmotic stress of two *Pseudomonas syringae* strains that differ in epiphytic fitness and osmotolerance. *Journal of Bacteriology,* 195**,** 4742-4752.

FRIEDMAN, L. & KOLTER, R. 2003. Genes involved in matrix formation in *Pseudomonas aeruginosa* PA14 biofilms. *Molecular Microbiology,* 51**,** 675-690.

FRIEDMAN, L. & KOLTER, R. 2004. Two genetic loci produce distinct carbohydrate-rich structural components of the *Pseudomonas aeruginosa* biofilm matrix. *J Bacteriol,* 186**,** 4457-65.

FU, Z. Q. & DONG, X. 2013. Systemic acquired resistance: Turning local infection into global defense. *Annu Rev Plant Biol,* 64**,** 839-63.

GAL, M., PRESTON, G. M., MASSEY, R. C., SPIERS, A. J. & RAINEY, P. B. 2003. Genes encoding a cellulosic polymer contribute toward the ecological success of *Pseudomonas fluorescens* SBW25 on plant surfaces. *Molecular Ecology,* 12**,** 3109-3121.

GE, Y.-Y., XIANG, Q.-W., WAGNER, C., ZHANG, D., XIE, Z.-P. & STAEHELIN, C. 2016a. The type 3 effector NopL of *Sinorhizobium* sp. strain NGR234 is a mitogen-activated protein kinase substrate. *Journal of Experimental Botany,* 67**,** 2483-2494.

GE, Y. Y., XIANG, Q. W., WAGNER, C., ZHANG, D., XIE, Z. P. & STAEHELIN, C. 2016b. The type 3 effector nopl of sinorhizobium sp. Strain ngr234 is a mitogen-activated protein kinase substrate. *J Exp Bot,* 67**,** 2483-94.

GIBSON, K. E., KOBAYASHI, H. & WALKER, G. C. 2008. Molecular determinants of a symbiotic chronic infection. *Annu Rev Genet,* 42**,** 413-41.

GIMENEZ-IBANEZ, S., HANN, D. R., NTOUKAKIS, V., PETUTSCHNIG, E., LIPKA, V. & RATHJEN, J. P. 2009a. AvrPtoB Targets the LysM Receptor Kinase CERK1 to Promote Bacterial Virulence on Plants. *Current Biology,* 19**,** 423-429.

GIMENEZ-IBANEZ, S., NTOUKAKIS, V. & RATHJEN, J. P. 2009b. The LysM receptor kinase CERK1 mediates bacterial perception in *Arabidopsis*. *Plant Signaling & Behavior,* 4**,** 539-541.

GIRIJA, A. M., KINATHI, B. K., MADHAVI, M. B., RAMESH, P., VUNGARALA, S., PATEL, H. K. & SONTI, R. V. 2017. Rice leaf transcriptional profiling suggests a functional interplay between *Xanthomonas oryzae* pv. *oryzae* lipopolysaccharide and extracellular polysaccharide in modulation of defense responses during infection. *Mol Plant Microbe Interact,* 30**,** 16-27.

GLAZEBROOK, J. 2005. Contrasting mechanisms of defense against biotrophic and necrotrophic pathogens. *Annu Rev Phytopathol,* 43**,** 205-27.

GOHRE, V., SPALLEK, T., HAWEKER, H., MERSMANN, S., MENTZEL, T., BOLLER, T., DE TORRES, M., MANSFIELD, J. W. & ROBATZEK, S. 2008. Plant pattern-recognition receptor FLS2 is directed for degradation by the bacterial ubiquitin ligase AvrPtoB. *Curr Biol,* 18**,** 1824-32.

GOMEZ-GOMEZ, L. & BOLLER, T. 2000. FLS2: An LRR receptor-like kinase involved in the perception of the bacterial elicitor flagellin in *Arabidopsis*. *Molecular Cell,* 5**,** 1003-1011.

GOMEZ-GOMEZ, L., FELIX, G. & BOLLER, T. 1999. A single locus determines sensitivity to bacterial flagellin in *Arabidopsis thaliana*. *Plant Journal,* 18**,** 277-284.

GOURION, B., BERRABAH, F., RATET, P. & STACEY, G. 2015. *Rhizobium*-legume symbioses: The crucial role of plant immunity. *Trends Plant Sci,* 20**,** 186-94.

GOYMER, P., KAHN, S. G., MALONE, J. G., GEHRIG, S. M., SPIERS, A. J. & RAINEY, P. B. 2006. Adaptive divergence in experimental populations of *Pseudomonas fluorescens*. II. Role of the GGDEF regulator WspR in evolution and development of the wrinkly spreader phenotype. *Genetics,* 173**,** 515-26.

GREENBERG, J. T. & YAO, N. 2004. The role and regulation of programmed cell death in plant-pathogen interactions. *Cell Microbiol,* 6**,** 201-11.

GRENGA, L., LITTLE, R. H. & MALONE, J. G. 2017. Quick change: post-transcriptional regulation in Pseudomonas. *FEMS Microbiology Letters,* 364**,** fnx125-fnx125.

GUILLAUME-GENTIL, O., GRINDBERG, R. V., KOOGER, R., DORWLING-CARTER, L., MARTINEZ, V., OSSOLA, D., PILHOFER, M., ZAMBELLI, T. & VORHOLT, J. A. 2016. Tunable single-cell extraction for molecular analyses. *Cell,* 166**,** 506-516.

GUST, A. A., BISWAS, R., LENZ, H. D., RAUHUT, T., RANF, S., KEMMERLING, B., GOTZ, F., GLAWISCHNIG, E., LEE, J., FELIX, G. & NURNBERGER, T. 2007. Bacteria-derived peptidoglycans constitute pathogen-associated molecular patterns triggering innate immunity in *Arabidopsis*. *J Biol Chem,* 282**,** 32338-48.

GUTTMAN, D. S., MCHARDY, A. C. & SCHULZE-LEFERT, P. 2014. Microbial genome-enabled insights into plant-microorganism interactions. *Nat Rev Genet,* 15**,** 797-813.

HAAS, D. & DEFAGO, G. 2005. Biological control of soil-borne pathogens by fluorescent pseudomonads. *Nat Rev Microbiol,* 3**,** 307-19.

HACQUARD, S., GARRIDO-OTER, R., GONZÁLEZ, A., SPAEPEN, S., ACKERMANN, G., LEBEIS, S., MCHARDY, ALICE C., DANGL, JEFFREY L., KNIGHT, R., LEY, R. & SCHULZE-LEFERT, P. 2015. Microbiota and Host Nutrition across Plant and Animal Kingdoms. *Cell Host & Microbe,* 17**,** 603-616.

HACQUARD, S., SPAEPEN, S., GARRIDO-OTER, R. & SCHULZE-LEFERT, P. 2017. Interplay between innate immunity and the plant microbiota. *Annual Review of Phytopathology,* 55**,** 565-589.

HALL-STOODLEY, L., COSTERTON, J. W. & STOODLEY, P. 2004. Bacterial biofilms: From the natural environment to infectious diseases. *Nat Rev Micro,* 2**,** 95-108.

HAMMOND-KOSACK, K. E. & JONES, J. D. 1997. Plant disease resistance genes. *Annu Rev Plant Physiol Plant Mol Biol,* 48**,** 575-607.

HANN, D. R. & RATHJEN, J. P. 2007. Early events in the pathogenicity of *Pseudomonas syringae* on *Nicotiana benthamiana*. *Plant J,* 49**,** 607-18.

HE, J., BALDINI, R. L., DEZIEL, E., SAUCIER, M., ZHANG, Q., LIBERATI, N. T., LEE, D., URBACH, J., GOODMAN, H. M. & RAHME, L. G. 2004. The broad host range pathogen *Pseudomonas aeruginosa* strain PA14 carries two pathogenicity islands harboring plant and animal virulence genes. *Proc Natl Acad Sci U S A,* 101**,** 2530-5.

HE, K., GOU, X., YUAN, T., LIN, H., ASAMI, T., YOSHIDA, S., RUSSELL, S. D. & LI, J. 2007. BAK1 and BKK1 regulate brassinosteroid-dependent growth and brassinosteroid-independent cell-death pathways. *Curr Biol,* 17**,** 1109-15.

HEESE, A., HANN, D. R., GIMENEZ-IBANEZ, S., JONES, A. M., HE, K., LI, J., SCHROEDER, J. I., PECK, S. C. & RATHJEN, J. P. 2007. The receptor-like kinase serk3/bak1 is a central regulator of innate immunity in plants. *Proc Natl Acad Sci U S A,* 104**,** 12217-22.

HENGGE, R. 2009. Principles of c-di-GMP signalling in bacteria. *Nat Rev Microbiol,* 7**,** 263-73.

HENTZER, M., TEITZEL, G. M., BALZER, G. J., HEYDORN, A., MOLIN, S., GIVSKOV, M. & PARSEK, M. R. 2001. Alginate overproduction affects *Pseudomonas aeruginosa* biofilm structure and function. *Journal of Bacteriology,* 183**,** 5395-5401.

HICKMAN, J. W. & HARWOOD, C. S. 2008. Identification of fleq from pseudomonas aeruginosa as a c-di-gmp-responsive transcription factor. *Mol Microbiol,* 69**,** 376-89.

HICKMAN, J. W., TIFREA, D. F. & HARWOOD, C. S. 2005. A chemosensory system that regulates biofilm formation through modulation of cyclic diguanylate levels. *Proc Natl Acad Sci U S A,* 102**,** 14422-7.

HIND, S. R., STRICKLER, S. R., BOYLE, P. C., DUNHAM, D. M., BAO, Z., O'DOHERTY, I. M., BACCILE, J. A., HOKI, J. S., VIOX, E. G., CLARKE, C. R., VINATZER, B. A., SCHROEDER, F. C. & MARTIN, G. B. 2016. Tomato receptor FLAGELLIN-SENSING 3 binds flgII-28 and activates the plant immune system. *Nat Plants,* 2**,** 16128.

HIRAI, H., TAKAI, R., IWANO, M., NAKAI, M., KONDO, M., TAKAYAMA, S., ISOGAI, A. & CHE, F. S. 2011. Glycosylation regulates specific induction of rice immune responses by *Acidovorax avenae* flagellin. *J Biol Chem,* 286**,** 25519-30.

HMELO, L. R., BORLEE, B. R., ALMBLAD, H., LOVE, M. E., RANDALL, T. E., TSENG, B. S., LIN, C., IRIE, Y., STOREK, K. M., YANG, J. J., SIEHNEL, R. J., HOWELL, P. L., SINGH, P. K., TOLKER-NIELSEN, T., PARSEK, M. R., SCHWEIZER, H. P. & HARRISON, J. J. 2015. Precision-engineering the Pseudomonas aeruginosa genome with two-step allelic exchange. *Nat. Protocols,* 10**,** 1820-1841.

HOLTON, N., NEKRASOV, V., RONALD, P. C. & ZIPFEL, C. 2015. The phylogenetically-related pattern recognition receptors EFR and XA21 recruit similar immune signaling components in monocots and dicots. *PLOS Pathogens,* 11**,** e1004602.

HORTON, M. W., BODENHAUSEN, N., BEILSMITH, K., MENG, D., MUEGGE, B. D., SUBRAMANIAN, S., VETTER, M. M., VILHJALMSSON, B. J., NORDBORG, M., GORDON, J. I. & BERGELSON, J. 2014. Genome-wide association study of *Arabidopsis thaliana* leaf microbial community. *Nat Commun,* 5**,** 5320.

HOWELL, C. R. & STIPANOVIC, R. D. 1979. Control of *Rhizoctonia solani* on cotton seedlings with *Pseudomonas fluorescens* and with an antibiotic produced by the bacterium. *Phytopathology,* 69**,** 480-482.

IAVICOLI, A., BOUTET, E., BUCHALA, A. & METRAUX, J. P. 2003. Induced systemic resistance in *Arabidopsis thaliana* in response to root inoculation with *Pseudomonas fluorescens* CHA0. *Mol Plant Microbe Interact,* 16**,** 851-8.

ICHINOSE, Y., SHIMIZU, R., TAGUCHI, F., TAKEUCHI, K., MARUTANI, M., MUKAIHARA, T., INAGAKI, Y., TOYODA, K. & SHIRAISHI, T. 2003. Role of flagella and flagellin in plant - pseudomonas syringae interactions. *Pseudomonas Syringae and Related Pathogens: Biology and Genetics***,** 311-318.

ICHINOSE, Y., TAGUCHI, F. & MUKAIHARA, T. 2013. Pathogenicity and virulence factors of pseudomonas syringae. *Journal of General Plant Pathology,* 79**,** 285-296.

INNEREBNER, G., KNIEF, C. & VORHOLT, J. A. 2011. Protection of Arabidopsis thaliana against Leaf-Pathogenic Pseudomonas syringae by Sphingomonas Strains in a Controlled Model System. *Applied and Environmental Microbiology,* 77**,** 3202-3210.

IRIE, Y., ROBERTS, A. E. L., KRAGH, K. N., GORDON, V. D., HUTCHISON, J., ALLEN, R. J., MELAUGH, G., BJARNSHOLT, T., WEST, S. A. & DIGGLE, S. P. 2017. The *Pseudomonas aeruginosa* PSL polysaccharide is a social but noncheatable trait in biofilms. *MBio,* 8.

JACKSON, K. D., STARKEY, M., KREMER, S., PARSEK, M. R. & WOZNIAK, D. J. 2004. Identification of psl, a locus encoding a potential exopolysaccharide that is essential for pseudomonas aeruginosa pao1 biofilm formation. *J Bacteriol,* 186**,** 4466-75.

JACKSON, R. W. 2009. *Plant pathogenic bacteria: Genomics and molecular biology*, Caister Academic Press.

JACOBS, S., ZECHMANN, B., MOLITOR, A., TRUJILLO, M., PETUTSCHNIG, E., LIPKA, V., KOGEL, K.-H. & SCHÄFER, P. 2011. Broad-Spectrum Suppression of Innate Immunity Is Required for Colonization of Arabidopsis Roots by the Fungus Piriformospora indica. *Plant Physiology,* 156**,** 726-740.

JAIN, S., FRANKLIN, M. J., ERTESVÅG, H., VALLA, S. & OHMAN, D. E. 2003. The dual roles of AlgG in C-5-epimerization and secretion of alginate polymers in *Pseudomonas aeruginosa*. *Molecular Microbiology,* 47**,** 1123-1133.

JENAL, U., REINDERS, A. & LORI, C. 2017. Cyclic di-GMP: second messenger extraordinaire. *Nat Rev Micro,* 15**,** 271-284.

JENNINGS, L. K., STOREK, K. M., LEDVINA, H. E., COULON, C., MARMONT, L. S., SADOVSKAYA, I., SECOR, P. R., TSENG, B. S., SCIAN, M., FILLOUX, A., WOZNIAK, D. J., HOWELL, P. L. & PARSEK, M. R. 2015. Pel is a cationic exopolysaccharide that cross-links extracellular DNA in the *Pseudomonas aeruginosa* biofilm matrix. *Proc Natl Acad Sci U S A,* 112**,** 11353-8.

JONES, J. D. G. & DANGL, J. L. 2006. The plant immune system. *Nature,* 444**,** 323-329.

JONES, K. M., LLORET, J., DANIELE, J. R. & WALKER, G. C. 2007. The type IV secretion system of *Sinorhizobium meliloti* strain 1021 is required for conjugation but not for intracellular symbiosis. *J Bacteriol,* 189.

JONES, K. M., SHAROPOVA, N., LOHAR, D. P., ZHANG, J. Q., VANDENBOSCH, K. A. & WALKER, G. C. 2008. Differential response of the plant *Medicago truncatula* to its symbiont *Sinorhizobium meliloti* or an exopolysaccharide-deficient mutant. *Proc Natl Acad Sci U S A,* 105**,** 704-9.

KADOTA, Y., SKLENAR, J., DERBYSHIRE, P., STRANSFELD, L., ASAI, S., NTOUKAKIS, V., JONES, J. D., SHIRASU, K., MENKE, F., JONES, A. & ZIPFEL, C. 2014. Direct regulation of the nadph oxidase rbohd by the prr-associated kinase bik1 during plant immunity. *Mol Cell,* 54**,** 43-55.

KAMOUN, S. & KADO, C. I. 1990. Phenotypic switching affecting chemotaxis, xanthan production, and virulence in *Xanthomonas campestris*. *Appl Environ Microbiol,* 56**,** 3855-60.

KANDA, E., TATSUTA, T., SUZUKI, T., TAGUCHI, F., NAITO, K., INAGAKI, Y., TOYODA, K., SHIRAISHI, T. & ICHINOSE, Y. 2011. Two flagellar stators and their roles in motility and virulence in Pseudomonas syringae pv. tabaci 6605. *Mol Genet Genomics,* 285**,** 163-74.

KATSURAGI, Y., TAKAI, R., FURUKAWA, T., HIRAI, H., MORIMOTO, T., KATAYAMA, T., MURAKAMI, T. & CHE, F. S. 2015. CD2-1, the C-terminal region of flagellin, modulates the induction of immune responses in rice. *Mol Plant Microbe Interact,* 28**,** 648-58.

KAWAHARADA, Y., KELLY, S., NIELSEN, M. W., HJULER, C. T., GYSEL, K., MUSZYNSKI, A., CARLSON, R. W., THYGESEN, M. B., SANDAL, N., ASMUSSEN, M. H., VINTHER, M., ANDERSEN, S. U., KRUSELL, L., THIRUP, S., JENSEN, K. J., RONSON, C. W., BLAISE, M., RADUTOIU, S. & STOUGAARD, J. 2015. Receptor-mediated exopolysaccharide perception controls bacterial infection. *Nature,* 523**,** 308-12.

KAZEMI-POUR, N., CONDEMINE, G. & HUGOUVIEUX-COTTE-PATTAT, N. 2004. The secretome of the plant pathogenic bacterium *Erwinia chrysanthemi*. *PROTEOMICS,* 4**,** 3177-3186.

KAZMIERCZAK, B. I., LEBRON, M. B. & MURRAY, T. S. 2006. Analysis of FimX, a phosphodiesterase that governs twitching motility in Pseudomonas aeruginosa. *Mol Microbiol,* 60**,** 1026-43.

KEITH, L. M. W. & BENDER, C. L. 1999. AlgT (ς22) controls alginate production and tolerance to environmental stress in *Pseudomonas syringae*. *Journal of Bacteriology,* 181**,** 7176-7184.

KEITH, R. C., KEITH, L. M., HERNANDEZ-GUZMAN, G., UPPALAPATI, S. R. & BENDER, C. L. 2003. Alginate gene expression by *Pseudomonas syringae* pv. *tomato* DC3000 in host and non-host plants. *Microbiology,* 149**,** 1127-38.

KELLENBERGER, C. A., WILSON, S. C., SALES-LEE, J. & HAMMOND, M. C. 2013. RNA-Based Fluorescent Biosensors for Live Cell Imaging of Second Messengers Cyclic di-GMP and Cyclic AMP-GMP. *Journal of the American Chemical Society,* 135**,** 4906-4909.

KEMMERLING, B., SCHWEDT, A., RODRIGUEZ, P., MAZZOTTA, S., FRANK, M., QAMAR, S. A., MENGISTE, T., BETSUYAKU, S., PARKER, J. E., MUSSIG, C., THOMMA, B. P., ALBRECHT, C., DE VRIES, S. C., HIRT, H. & NURNBERGER, T. 2007. The bri1-associated kinase 1, bak1, has a brassinolide-independent role in plant cell-death control. *Curr Biol,* 17**,** 1116-22.

KEMP, B. P., HORNE, J., BRYANT, A. & COOPER, R. M. 2004. Xanthomonas axonopodis pv. Manihotis gumd gene is essential, for eps production and pathogenicity and enhances epiphytic survival on cassava (manihot esculenta). *Physiological and Molecular Plant Pathology,* 64**,** 209-218.

KIDARSA, T. A., SHAFFER, B. T., GOEBEL, N. C., ROBERTS, D. P., BUYER, J. S., JOHNSON, A., KOBAYASHI, D. Y., ZABRISKIE, T. M., PAULSEN, I. & LOPER, J. E. 2013. Genes expressed by the biological control bacterium Pseudomonas protegens Pf-5 on seed surfaces under the control of the global regulators GacA and RpoS. *Environmental Microbiology,* 15**,** 716-735.

KIM, M. G., DA CUNHA, L., MCFALL, A. J., BELKHADIR, Y., DEBROY, S., DANGL, J. L. & MACKEY, D. 2005. Two Pseudomonas syringae type III effectors inhibit RIN4-regulated basal defense in Arabidopsis. *Cell,* 121**,** 749-59.

KIM, W., RACIMO, F., SCHLUTER, J., LEVY, S. B. & FOSTER, K. R. 2014. Importance of positioning for microbial evolution. *Proceedings of the National Academy of Sciences,* 111**,** E1639-E1647.

KIM, Y. C., LEVEAU, J., MCSPADDEN GARDENER, B. B., PIERSON, E. A., PIERSON, L. S., 3RD & RYU, C. M. 2011. The multifactorial basis for plant health promotion by plant-associated bacteria. *Appl Environ Microbiol,* 77**,** 1548-55.

KIRISITS, M. J., PROST, L., STARKEY, M. & PARSEK, M. R. 2005. Characterization of colony morphology variants isolated from *Pseudomonas aeruginosa* biofilms. *Appl Environ Microbiol,* 71**,** 4809-21.

KLOPPHOLZ, S., KUHN, H. & REQUENA, N. 2011. A Secreted Fungal Effector of Glomus intraradices Promotes Symbiotic Biotrophy. *Current Biology,* 21**,** 1204-1209.

KOHANSKI, M. A., DWYER, D. J., HAYETE, B., LAWRENCE, C. A. & COLLINS, J. J. 2007. A common mechanism of cellular death induced by bactericidal antibiotics. *Cell,* 130**,** 797-810.

KONG, H. S., ROBERTS, D. P., PATTERSON, C. D., KUEHNE, S. A., HEEB, S., LAKSHMAN, D. K. & LYDON, J. 2012. Effect of Overexpressing rsmA from Pseudomonas aeruginosa on Virulence of Select Phytotoxin-Producing Strains of P. syringae. *Phytopathology,* 102**,** 575-587.

KOVACH, M. E., ELZER, P. H., HILL, D. S., ROBERTSON, G. T., FARRIS, M. A., ROOP, R. M., 2ND & PETERSON, K. M. 1995. Four new derivatives of the broad-host-range cloning vector pBBR1MCS, carrying different antibiotic-resistance cassettes. *Gene,* 166**,** 175-6.

KULASAKARA, H., LEE, V., BRENCIC, A., LIBERATI, N., URBACH, J., MIYATA, S., LEE, D. G., NEELY, A. N., HYODO, M., HAYAKAWA, Y., AUSUBEL, F. M. & LORY, S. 2006. Analysis

of Pseudomonas aeruginosa diguanylate cyclases and phosphodiesterases reveals a role for bis-(3'-5')-cyclic-GMP in virulence. *Proc Natl Acad Sci U S A,* 103**,** 2839-44.

KUNZE, G., ZIPFEL, C., ROBATZEK, S., NIEHAUS, K., BOLLER, T. & FELIX, G. 2004. The N terminus of bacterial elongation factor Tu elicits innate immunity in *Arabidopsis* plants. *Plant Cell,* 16**,** 3496-507.

KWAAITAAL, M., HUISMAN, R., MAINTZ, J., REINSTÄDLER, A. & PANSTRUGA, R. 2011. Ionotropic glutamate receptor (iGluR)-like channels mediate MAMP-induced calcium influx in *Arabidopsis thaliana*. *Biochemical Journal,* 440**,** 355-373.

LACOMBE, S., ROUGON-CARDOSO, A., SHERWOOD, E., PEETERS, N., DAHLBECK, D., VAN ESSE, H. P., SMOKER, M., RALLAPALLI, G., THOMMA, B. P., STASKAWICZ, B., JONES, J. D. & ZIPFEL, C. 2010. Interfamily transfer of a plant pattern-recognition receptor confers broad-spectrum bacterial resistance. *Nat Biotechnol,* 28**,** 365-9.

LALUK, K., LUO, H., CHAI, M., DHAWAN, R., LAI, Z. & MENGISTE, T. 2011. Biochemical and genetic requirements for function of the immune response regulator BOTRYTIS-INDUCED KINASE1 in plant growth, ethylene signaling, and PAMP-triggered immunity in *Arabidopsis*. *Plant Cell,* 23**,** 2831-49.

LAMB, C. & DIXON, R. A. 1997. The oxidative burst in plant disease resistance. *Annual Review of Plant Physiology and Plant Molecular Biology,* 48**,** 251-275.

LAUE, H., SCHENK, A., LI, H., LAMBERTSEN, L., NEU, T. R., MOLIN, S. & ULLRICH, M. S. 2006. Contribution of alginate and levan production to biofilm formation by *Pseudomonas syringae*. *Microbiology,* 152**,** 2909-18.

LEBEIS, S. L., PAREDES, S. H., LUNDBERG, D. S., BREAKFIELD, N., GEHRING, J., MCDONALD, M., MALFATTI, S., GLAVINA DEL RIO, T., JONES, C. D., TRINGE, S. G. & DANGL, J. L. 2015. Salicylic acid modulates colonization of the root microbiome by specific bacterial taxa. *Science,* 349**,** 860-864.

LEE, H. A., LEE, H. Y., SEO, E., LEE, J., KIM, S. B., OH, S., CHOI, E., CHOI, E., LEE, S. E. & CHOI, D. 2017. Current understandings of plant nonhost resistance. *Mol Plant Microbe Interact,* 30**,** 5-15.

LEE, J., ESCHEN-LIPPOLD, L., LASSOWSKAT, I., BOTTCHER, C. & SCHEEL, D. 2015. Cellular reprogramming through mitogen-activated protein kinases. *Front Plant Sci,* 6**,** 940.

LEE, V. T., MATEWISH, J. M., KESSLER, J. L., HYODO, M., HAYAKAWA, Y. & LORY, S. 2007. A cyclic-di-GMP receptor required for bacterial exopolysaccharide production. *Mol Microbiol,* 65**,** 1474-84.

LEHMAN, A. P. & LONG, S. R. 2013. Exopolysaccharides from *Sinorhizobium meliloti* can protect against H_2O_2-dependent damage. *J Bacteriol,* 195**,** 5362-9.

LEONG, S. A., WILLIAMS, P. H. & DITTA, G. S. 1985. Analysis of the 5' regulatory region of the gene for delta-aminolevulinic acid synthetase of *Rhizobium meliloti*. *Nucleic Acids Res,* 13**,** 5965-76.

LEWIS, L. A., POLANSKI, K., DE TORRES-ZABALA, M., JAYARAMAN, S., BOWDEN, L., MOORE, J., PENFOLD, C. A., JENKINS, D. J., HILL, C., BAXTER, L., KULASEKARAN, S., TRUMAN, W., LITTLEJOHN, G., PRUSINSKA, J., MEAD, A., STEINBRENNER, J., HICKMAN, R., RAND, D., WILD, D. L., OTT, S., BUCHANAN-WOLLASTON, V., SMIRNOFF, N., BEYNON, J., DENBY, K. & GRANT, M. 2015. Transcriptional dynamics driving MAMP-triggered immunity and pathogen effector-mediated immunosuppression in *Arabidopsis* leaves following infection with *Pseudomonas syringae* pv *tomato* DC3000. *The Plant Cell,* 27**,** 3038-3064.

LI, J., WEN, J., LEASE, K. A., DOKE, J. T., TAX, F. E. & WALKER, J. C. 2002. BAK1, an *Arabidopsis* LRR receptor-like protein kinase, interacts with BRI1 and modulates brassinosteroid signaling. *Cell,* 110**,** 213-22.

LI, L., LI, M., YU, L. P., ZHOU, Z. Y., LIANG, X. X., LIU, Z. X., CAI, G. H., GAO, L. Y., ZHANG, X. J., WANG, Y. C., CHEN, S. & ZHOU, J. M. 2014. The fls2-associated kinase bik1 directly phosphorylates the nadph oxidase rbohd to control plant immunity. *Cell Host & Microbe,* 15**,** 329-338.

LI, X., KAPOS, P. & ZHANG, Y. 2015. NLRs in plants. *Current Opinion in Immunology,* 32**,** 114-121.

LI, X., LIN, H., ZHANG, W., ZOU, Y., ZHANG, J., TANG, X. & ZHOU, J. M. 2005. Flagellin induces innate immunity in nonhost interactions that is suppressed by *Pseudomonas syringae* effectors. *Proc Natl Acad Sci U S A,* 102**,** 12990-5.

LI, X., NIELSEN, L., NOLAN, C. & HALVERSON, L. J. 2010. Transient alginate gene expression by *Pseudomonas putida* biofilm residents under water-limiting conditions reflects adaptation to the local environment. *Environmental Microbiology,* 12**,** 1578-1590.

LIANG, Y., CAO, Y. R., TANAKA, K., THIBIVILLIERS, S., WAN, J. R., CHOI, J., KANG, C. H., QIU, J. & STACEY, G. 2013. Nonlegumes respond to rhizobial Nod factors by suppressing the innate immune response. *Science,* 341**,** 1384-1387.

LIBAULT, M., FARMER, A., BRECHENMACHER, L., DRNEVICH, J., LANGLEY, R. J., BILGIN, D. D., RADWAN, O., NEECE, D. J., CLOUGH, S. J., MAY, G. D. & STACEY, G. 2010. Complete transcriptome of the soybean root hair cell, a single-cell model, and its alteration in response to *Bradyrhizobium japonicum* infection. *Plant Physiol,* 152**,** 541-52.

LIN, N. C. & MARTIN, G. B. 2007. Pto- and Prf-mediated recognition of AvrPto and AvrPtoB restricts the ability of diverse *Pseudomonas syringae* pathovars to infect tomato. *Mol Plant Microbe Interact,* 20**,** 806-15.

LINDEBERG, M., CUNNAC, S. & COLLMER, A. 2009. The evolution of *Pseudomonas syringae* host specificity and type III effector repertoires. *Mol Plant Pathol,* 10**,** 767-75.

LINDEBERG, M., CUNNAC, S. & COLLMER, A. 2012. *Pseudomonas syringae* type III effector repertoires: Last words in endless arguments. *Trends Microbiol,* 20**,** 199-208.

LINDOW, S. E., ANDERSEN, G. & BEATTIE, G. A. 1993. Characteristics of insertional mutants of *Pseudomonas syringae* with reduced epiphytic fitness. *Applied and Environmental Microbiology,* 59**,** 1593-1601.

LIU, Z., WU, Y., YANG, F., ZHANG, Y., CHEN, S., XIE, Q., TIAN, X. & ZHOU, J. M. 2013. BIK1 interacts with PEPRs to mediate ethylene-induced immunity. *Proc Natl Acad Sci U S A,* 110**,** 6205-10.

LOHAR, D. P., SHAROPOVA, N., ENDRE, G., PENUELA, S., SAMAC, D., TOWN, C., SILVERSTEIN, K. A. & VANDENBOSCH, K. A. 2006. Transcript analysis of early nodulation events in *Medicago truncatula*. *Plant Physiol,* 140**,** 221-34.

LOPER, J. E., HASSAN, K. A., MAVRODI, D. V., DAVIS, E. W., 2ND, LIM, C. K., SHAFFER, B. T., ELBOURNE, L. D., STOCKWELL, V. O., HARTNEY, S. L., BREAKWELL, K., HENKELS, M. D., TETU, S. G., RANGEL, L. I., KIDARSA, T. A., WILSON, N. L., VAN DE MORTEL, J. E., SONG, C., BLUMHAGEN, R., RADUNE, D., HOSTETLER, J. B., BRINKAC, L. M., DURKIN, A. S., KLUEPFEL, D. A., WECHTER, W. P., ANDERSON, A. J., KIM, Y. C., PIERSON, L. S., 3RD, PIERSON, E. A., LINDOW, S. E., KOBAYASHI, D. Y., RAAIJMAKERS, J. M., WELLER, D. M., THOMASHOW, L. S., ALLEN, A. E. & PAULSEN, I. T. 2012. Comparative genomics of plant-associated *Pseudomonas* spp.: Insights into diversity and inheritance of traits involved in multitrophic interactions. *PLoS Genet,* 8**,** e1002784.

LOPER, J. E., KOBAYASHI, D. Y. & PAULSEN, I. T. 2007. The genomic sequence of *Pseudomonas fluorescens* Pf-5: Insights into biological control. *Phytopathology,* 97**,** 233-238.

LOPEZ-GOMEZ, M., SANDAL, N., STOUGAARD, J. & BOLLER, T. 2012. Interplay of flg22-induced defence responses and nodulation in lotus japonicus. *Journal of Experimental Botany,* 63**,** 393-401.

LU, D., WU, S., GAO, X., ZHANG, Y., SHAN, L. & HE, P. 2010. A receptor-like cytoplasmic kinase, BIK1, associates with a flagellin receptor complex to initiate plant innate immunity. *Proc Natl Acad Sci U S A,* 107**,** 496-501.

LU, F., WANG, H., WANG, S., JIANG, W., SHAN, C., LI, B., YANG, J., ZHANG, S. & SUN, W. 2015. Enhancement of innate immune system in monocot rice by transferring the dicotyledonous elongation factor Tu receptor EFR. *J Integr Plant Biol,* 57**,** 641-52.

LU, Y.-J., SCHORNACK, S., SPALLEK, T., GELDNER, N., CHORY, J., SCHELLMANN, S., SCHUMACHER, K., KAMOUN, S. & ROBATZEK, S. 2012. Patterns of plant subcellular responses to successful oomycete infections reveal differences in host cell reprogramming and endocytic trafficking. *Cellular Microbiology,* 14**,** 682-697.

LUGTENBERG, B. & KAMILOVA, F. 2009. Plant-growth-promoting rhizobacteria. *Annual Review of Microbiology.*

LUGTENBERG, B. J., DEKKERS, L. & BLOEMBERG, G. V. 2001. Molecular determinants of rhizosphere colonization by *Pseudomonas*. *Annu Rev Phytopathol,* 39**,** 461-90.

MA, L., CONOVER, M., LU, H., PARSEK, M. R., BAYLES, K. & WOZNIAK, D. J. 2009. Assembly and development of the *Pseudomonas aeruginosa* biofilm matrix. *PLoS Pathog,* 5**,** e1000354.

MACHO, A. P., SCHWESSINGER, B., NTOUKAKIS, V., BRUTUS, A., SEGONZAC, C., ROY, S., KADOTA, Y., OH, M. H., SKLENAR, J., DERBYSHIRE, P., LOZANO-DURAN, R., MALINOVSKY, F. G., MONAGHAN, J., MENKE, F. L., HUBER, S. C., HE, S. Y. & ZIPFEL, C. 2014. A bacterial tyrosine phosphatase inhibits plant pattern recognition receptor activation. *Science,* 343**,** 1509-1512.

MACHO, A. P. & ZIPFEL, C. 2015. Targeting of plant pattern recognition receptor-triggered immunity by bacterial type-III secretion system effectors. *Curr Opin Microbiol,* 23**,** 14-22.

MADSEN, L. H., TIRICHINE, L., JURKIEWICZ, A., SULLIVAN, J. T., HECKMANN, A. B., BEK, A. S., RONSON, C. W., JAMES, E. K. & STOUGAARD, J. 2010. The molecular network governing nodule organogenesis and infection in the model legume *Lotus japonicus*. *Nat Comm,* 1.

MALONE, J. G., JAEGER, T., SPANGLER, C., RITZ, D., SPANG, A., ARRIEUMERLOU, C., KAEVER, V., LANDMANN, R. & JENAL, U. 2010. YfiBNR mediates cyclic di-GMP dependent small colony variant formation and persistence in *Pseudomonas aeruginosa*. *PLoS Pathog,* 6**,** e1000804.

MALONE, J. G., WILLIAMS, R., CHRISTEN, M., JENAL, U., SPIERS, A. J. & RAINEY, P. B. 2007. The structure-function relationship of WspR, a *Pseudomonas fluorescens* response regulator with a GGDEF output domain. *Microbiology,* 153**,** 980-94.

MANSFIELD, J., GENIN, S., MAGORI, S., CITOVSKY, V., SRIARIYANUM, M., RONALD, P., DOW, M., VERDIER, V., BEER, S. V., MACHADO, M. A., TOTH, I., SALMOND, G. & FOSTER, G. D. 2012. Top 10 plant pathogenic bacteria in molecular plant pathology. *Mol Plant Pathol,* 13**,** 614-29.

MARIE, C., DEAKIN, W. J., VIPREY, V., KOPCINSKA, J., GOLINOWSKI, W., KRISHNAN, H. B., PERRET, X. & BROUGHTON, W. J. 2003. Characterization of Nops, nodulation outer proteins, secreted via the type III secretion system of NGR234. *Mol Plant Microbe Interact,* 16**,** 743-51.

MARK WELCH, J. L., ROSSETTI, B. J., RIEKEN, C. W., DEWHIRST, F. E. & BORISY, G. G. 2016. Biogeography of a human oral microbiome at the micron scale. *Proceedings of the National Academy of Sciences,* 113**,** E791-E800.

MASSALHA, H., KORENBLUM, E., MALITSKY, S., SHAPIRO, O. H. & AHARONI, A. 2017. Live imaging of root–bacteria interactions in a microfluidics setup. *Proceedings of the National Academy of Sciences,* 114**,** 4549-4554.

MASUKO, T., MINAMI, A., IWASAKI, N., MAJIMA, T., NISHIMURA, S.-I. & LEE, Y. C. 2005. Carbohydrate analysis by a phenol–sulfuric acid method in microplate format. *Analytical Biochemistry,* 339**,** 69-72.

MATILLA, M. A., TRAVIESO, M. L., RAMOS, J. L. & RAMOS-GONZALEZ, M. I. 2011. Cyclic diguanylate turnover mediated by the sole GGDEF/EAL response regulator in *Pseudomonas putida*: Its role in the rhizosphere and an analysis of its target processes. *Environ Microbiol,* 13**,** 1745-66.

MAVRODI, D. V., JOE, A., MAVRODI, O. V., HASSAN, K. A., WELLER, D. M., PAULSEN, I. T., LOPER, J. E., ALFANO, J. R. & THOMASHOW, L. S. 2011. Structural and functional analysis of the type III secretion system from *Pseudomonas fluorescens* Q8r1-96. *J Bacteriol,* 193**,** 177-89.

MCCANN, H. C., NAHAL, H., THAKUR, S. & GUTTMAN, D. S. 2012. Identification of innate immunity elicitors using molecular signatures of natural selection. *Proceedings of the National Academy of Sciences of the United States of America,* 109**,** 4215-4220.

MCGARVEY, J. A., DENNY, T. P. & SCHELL, M. A. 1999. Spatial-temporal and quantitative analysis of growth and EPS I production by *Ralstonia solanacearum* in resistant and susceptible tomato cultivars. *Phytopathology,* 89**,** 1233-9.

MEADE, H. M., LONG, S. R., RUVKUN, G. B., BROWN, S. E. & AUSUBEL, F. M. 1982. Physical and genetic characterization of symbiotic and auxotrophic mutants of *Rhizobium meliloti* induced by transposon Tn5 mutagenesis. *Journal of Bacteriology,* 149**,** 114-122.

MEE, M. T., COLLINS, J. J., CHURCH, G. M. & WANG, H. H. 2014. Syntrophic exchange in synthetic microbial communities. *Proceedings of the National Academy of Sciences,* 111**,** E2149-E2156.

MEINDL, T. 2000. The bacterial elicitor flagellin activates its receptor in tomato cells according to the address-message concept. *The Plant Cell Online,* 12**,** 1783-1794.

MELOTTO, M., UNDERWOOD, W. & HE, S. Y. 2008. Role of stomata in plant innate immunity and foliar bacterial diseases. *Annu Rev Phytopathol,* 46**,** 101-22.

MELOTTO, M., UNDERWOOD, W., KOCZAN, J., NOMURA, K. & HE, S. Y. 2006. Plant stomata function in innate immunity against bacterial invasion. *Cell,* 126**,** 969-80.

MENDES, B. M. J., CARDOSO, S. C., BOSCARIOL-CAMARGO, R. L., CRUZ, R. B., MOURÃO FILHO, F. A. A. & BERGAMIN FILHO, A. 2010. Reduction in susceptibility to *Xanthomonas axonopodis* pv. *citri* in transgenic *Citrus sinensis* expressing the rice *Xa21* gene. *Plant Pathology,* 59**,** 68-75.

MENG, X. & ZHANG, S. 2013. MAPK cascades in plant disease resistance signaling. *Annu Rev Phytopathol,* 51**,** 245-66.

MERIGHI, M., LEE, V. T., HYODO, M., HAYAKAWA, Y. & LORY, S. 2007. The second messenger bis-(3'-5')-cyclic-GMP and its PilZ domain-containing receptor Alg44 are required for alginate biosynthesis in *Pseudomonas aeruginosa*. *Mol Microbiol,* 65**,** 876-95.

MICHELMORE, R., COAKER, G., BART, R., BEATTIE, G., BENT, A., BRUCE, T., CAMERON, D., DANGL, J., DINESH-KUMAR, S., EDWARDS, R., EVES-VAN DEN AKKER, S., GASSMANN, W., GREENBERG, J. T., HANLEY-BOWDOIN, L., HARRISON, R. J., HARVEY, J., HE, P., HUFFAKER, A., HULBERT, S., INNES, R., JONES, J. D. G., KALOSHIAN, I., KAMOUN, S., KATAGIRI, F., LEACH, J., MA, W., MCDOWELL, J., MEDFORD, J., MEYERS, B., NELSON, R., OLIVER, R., QI, Y., SAUNDERS, D., SHAW, M., SMART, C., SUBUDHI, P., TORRANCE, L., TYLER, B., VALENT, B. & WALSH, J. 2017. Foundational and translational research opportunities to improve plant health. *Molecular Plant-Microbe Interactions,* 30**,** 515-516.

MILLER, J. B., PRATAP, A., MIYAHARA, A., ZHOU, L., BORNEMANN, S., MORRIS, R. J. & OLDROYD, G. E. 2013. Calcium/calmodulin-dependent protein kinase is negatively and positively regulated by calcium, providing a mechanism for decoding calcium responses during symbiosis signaling. *Plant Cell,* 25**,** 5053-66.

MILLET, Y. A., DANNA, C. H., CLAY, N. K., SONGNUAN, W., SIMON, M. D., WERCK-REICHHART, D. & AUSUBEL, F. M. 2010. Innate immune responses activated in *Arabidopsis* roots by microbe-associated molecular patterns. *Plant Cell,* 22**,** 973-90.

MILLING, A., BABUJEE, L. & ALLEN, C. 2011. *Ralstonia solanacearum* extracellular polysaccharide is a specific elicitor of defense responses in wilt-resistant tomato plants. *PLoS One,* 6**,** e15853.

MITHOFER, A., BHAGWAT, A. A., FEGER, M. & EBEL, J. 1996. Suppression of fungal beta-glucan-induced plant defence in soybean (*Glycine max* l) by cyclic 1,3-1,6-beta-glucans from the symbiont *Bradyrhizobium japonicum*. *Planta,* 199**,** 270-275.

MIYA, A., ALBERT, P., SHINYA, T., DESAKI, Y., ICHIMURA, K., SHIRASU, K., NARUSAKA, Y., KAWAKAMI, N., KAKU, H. & SHIBUYA, N. 2007. CERK1, a LysM receptor kinase, is essential for chitin elicitor signaling in *Arabidopsis*. *Proc Natl Acad Sci U S A,* 104**,** 19613-8.

MONAGHAN, J., MATSCHI, S., ROMEIS, T. & ZIPFEL, C. 2015. The calcium-dependent protein kinase CPK28 negatively regulates the BIK1-mediated PAMP-induced calcium burst. *Plant Signaling & Behavior,* 10**,** e1018497.

MORGAN, J. L. W., MCNAMARA, J. T. & ZIMMER, J. 2014. Mechanism of activation of bacterial cellulose synthase by cyclic di-GMP. *Nat Struct Mol Biol,* 21**,** 489-496.

MOSCOSO, J. A., JAEGER, T., VALENTINI, M., HUI, K., JENAL, U. & FILLOUX, A. 2014. The diguanylate cyclase SadC is a central player in Gac/Rsm-mediated biofilm formation in *Pseudomonas aeruginosa*. *J Bacteriol,* 196**,** 4081-8.

MOTT, G. A., THAKUR, S., SMAKOWSKA, E., WANG, P. W., BELKHADIR, Y., DESVEAUX, D. & GUTTMAN, D. S. 2016. Genomic screens identify a new phytobacterial microbe-associated molecular pattern and the cognate *Arabidopsis* receptor-like kinase that mediates its immune elicitation. *Genome Biology,* 17**,** 98.

MUELLER, K., BITTEL, P., CHINCHILLA, D., JEHLE, A. K., ALBERT, M., BOLLER, T. & FELIX, G. 2012. Chimeric FLS2 receptors reveal the basis for differential flagellin perception in *Arabidopsis* and tomato. *Plant Cell,* 24**,** 2213-24.

MÜLLER, D. B., VOGEL, C., BAI, Y. & VORHOLT, J. A. 2016. The plant microbiota: Systems-level insights and perspectives. *Annual Review of Genetics,* 50**,** 211-234.

MURRAY, J. D., KARAS, B. J., SATO, S., TABATA, S., AMYOT, L. & SZCZYGLOWSKI, K. 2007. A cytokinin perception mutant colonized by *Rhizobium* in the absence of nodule organogenesis. *Science,* 315**,** 101-104.

MUSZYNSKI, A., HEISS, C., HJULER, C. T., SULLIVAN, J. T., KELLY, S. J., THYGESEN, M. B., STOUGAARD, J., AZADI, P., CARLSON, R. W. & RONSON, C. W. 2016. Structures of exopolysaccharides involved in receptor-mediated perception of *Mesorhizobium loti* by *Lotus japonicus*. *J Biol Chem,* 291**,** 20946-20961.

NADELL, C. D. & BASSLER, B. L. 2011. A fitness trade-off between local competition and dispersal in Vibrio cholerae biofilms. *Proceedings of the National Academy of Sciences,* 108**,** 14181-14185.

NADELL, C. D., DRESCHER, K. & FOSTER, K. R. 2016. Spatial structure, cooperation and competition in biofilms. *Nat Rev Micro,* 14**,** 589-600.

NADELL, C. D., XAVIER, J. B. & FOSTER, K. R. 2009. The sociobiology of biofilms. *FEMS Microbiology Reviews,* 33**,** 206-224.

NAIR, H. A. S., PERIASAMY, S., YANG, L., KJELLEBERG, S. & RICE, S. A. 2017. Real Time, Spatial, and Temporal Mapping of the Distribution of c-di-GMP during Biofilm Development. *Journal of Biological Chemistry,* 292**,** 477-487.

NAM, K. H. & LI, J. 2002. BRI1/BAK1, a receptor kinase pair mediating brassinosteroid signaling. *Cell,* 110**,** 203-12.

NELSON, M. S., CHUN, C. L. & SADOWSKY, M. J. 2016. Type IV effector proteins involved in the medicago-sinorhizobium symbiosis. *Molecular Plant-Microbe Interactions,* 30**,** 28-34.

NELSON, M. S. & SADOWSKY, M. J. 2015. Secretion systems and signal exchange between nitrogen-fixing rhizobia and legumes. *Frontiers in Plant Science,* 6.

NESPER, J., REINDERS, A., GLATTER, T., SCHMIDT, A. & JENAL, U. 2012. A novel capture compound for the identification and analysis of cyclic di-GMP binding proteins. *Journal of Proteomics,* 75**,** 4874-4878.

NEWELL, P. D., BOYD, C. D., SONDERMANN, H. & O'TOOLE, G. A. 2011. A c-di-GMP effector system controls cell adhesion by inside-out signaling and surface protein cleavage. *PLoS Biol,* 9**,** e1000587.

NIEHAUS, K., KAPP, D. & PÜHLER, A. 1993. Plant defence and delayed infection of pseudonodules induced by an exopolysaccharide (EPS I)-deficient *Rhizobium meliloti* mutant. *Planta,* 190.

NIELSEN, L., LI, X. & HALVERSON, L. J. 2011. Cell–cell and cell–surface interactions mediated by cellulose and a novel exopolysaccharide contribute to *Pseudomonas putida* biofilm formation and fitness under water-limiting conditions. *Environmental Microbiology,* 13**,** 1342-1356.

NILSSON, M., CHIANG, W.-C., FAZLI, M., GJERMANSEN, M., GIVSKOV, M. & TOLKER-NIELSEN, T. 2011. Influence of putative exopolysaccharide genes on *Pseudomonas putida* KT2440 biofilm stability. *Environmental Microbiology,* 13**,** 1357-1369.

NOGALES, J., VARGAS, P., FARIAS, G. A., OLMEDILLA, A., SANJUAN, J. & GALLEGOS, M. T. 2015. FleQ coordinates flagellum-dependent and -independent motilities in *Pseudomonas syringae* pv. *tomato* DC3000. *Appl Environ Microbiol,* 81**,** 7533-45.

NÜHSE, T. S., BOTTRILL, A. R., JONES, A. M. E. & PECK, S. C. 2007. Quantitative phosphoproteomic analysis of plasma membrane proteins reveals regulatory mechanisms of plant innate immune responses. *The Plant Journal,* 51**,** 931-940.

OGASAWARA, Y., KAYA, H., HIRAOKA, G., YUMOTO, F., KIMURA, S., KADOTA, Y., HISHINUMA, H., SENZAKI, E., YAMAGOE, S., NAGATA, K., NARA, M., SUZUKI, K., TANOKURA, M. & KUCHITSU, K. 2008. Synergistic activation of the *Arabidopsis* NADPH oxidase AtRBOHD by Ca^{2+} and phosphorylation. *Journal of Biological Chemistry,* 283**,** 8885-8892.

OLDROYD, G. E. 2013. Speak, friend, and enter: Signalling systems that promote beneficial symbiotic associations in plants. *Nat Rev Microbiol,* 11**,** 252-63.

OLDROYD, G. E. & DOWNIE, J. A. 2008. Coordinating nodule morphogenesis with rhizobial infection in legumes. *Annu Rev Plant Biol,* 59**,** 519-46.

OLDROYD, G. E., MURRAY, J. D., POOLE, P. S. & DOWNIE, J. A. 2011. The rules of engagement in the legume-rhizobial symbiosis. *Annu Rev Genet,* 45**,** 119-44.

OSMAN, S. F., FETT, W. F. & FISHMAN, M. L. 1986. Exopolysaccharides of the phytopathogen *Pseudomonas syringae* pv. *glycinea*. *Journal of Bacteriology,* 166**,** 66-71.

PANDEY, S. P. & SOMSSICH, I. E. 2009. The role of WRKY transcription factors in plant immunity. *Plant Physiology,* 150**,** 1648-1655.

PAPALEXI, E. & SATIJA, R. 2017. Single-cell RNA sequencing to explore immune cell heterogeneity. *Nat Rev Immunol,* advance online publication.

PAULSEN, I. T., PRESS, C. M., RAVEL, J., KOBAYASHI, D. Y., MYERS, G. S. A., MAVRODI, D. V., DEBOY, R. T., SESHADRI, R., REN, Q. H., MADUPU, R., DODSON, R. J., DURKIN, A. S., BRINKAC, L. M., DAUGHERTY, S. C., SULLIVAN, S. A., ROSOVITZ, M. J., GWINN, M. L., ZHOU, L. W., SCHNEIDER, D. J., CARTINHOUR, S. W., NELSON, W. C., WEIDMAN, J., WATKINS, K., TRAN, K., KHOURI, H., PIERSON, E. A., PIERSON, L. S., THOMASHOW, L. S. & LOPER, J. E. 2005. Complete genome sequence of the plant commensal *Pseudomonas fluorescens* Pf-5. *Nature Biotechnology,* 23**,** 873-878.

PEART, J. R., COOK, G., FEYS, B. J., PARKER, J. E. & BAULCOMBE, D. C. 2002. An *EDS1* orthologue is required for *N*-mediated resistance against tobacco mosaic virus. *Plant J,* 29**,** 569-79.

PEL, M. J., VAN DIJKEN, A. J., BARDOEL, B. W., SEIDL, M. F., VAN DER ENT, S., VAN STRIJP, J. A. & PIETERSE, C. 2014. *Pseudomonas syringae* evades host immunity by degrading flagellin monomers with alkaline protease AprA. *Mol Plant Microbe Interact*.

PEL, M. J. C. & PIETERSE, C. M. J. 2013. Microbial recognition and evasion of host immunity. *Journal of Experimental Botany,* 64**,** 1237-1248.

PENALOZA-VAZQUEZ, A., KIDAMBI, S. P., CHAKRABARTY, A. M. & BENDER, C. L. 1997. Characterization of the alginate biosynthetic gene cluster in *Pseudomonas syringae* pv. *syringae*. *J Bacteriol,* 179**,** 4464-72.

PEREZ-MENDOZA, D., ARAGON, I. M., PRADA-RAMIREZ, H. A., ROMERO-JIMENEZ, L., RAMOS, C., GALLEGOS, M. T. & SANJUAN, J. 2014. Responses to elevated c-di-GMP levels in mutualistic and pathogenic plant-interacting bacteria. *PLoS One,* 9**,** e91645.

PETROVA, O. E. & SAUER, K. 2012. Sticky situations: Key components that control bacterial surface attachment. *Journal of Bacteriology,* 194**,** 2413-2425.

PETUTSCHNIG, E. K., JONES, A. M., SERAZETDINOVA, L., LIPKA, U. & LIPKA, V. 2010. The lysin motif receptor-like kinase (LysM-RLK) CERK1 is a major chitin-binding protein in *Arabidopsis thaliana* and subject to chitin-induced phosphorylation. *J Biol Chem,* 285**,** 28902-11.

PFEILMEIER, S., CALY, D. L. & MALONE, J. G. 2016a. Bacterial pathogenesis of plants: Future challenges from a microbial perspective: Challenges in bacterial molecular plant pathology. *Molecular Plant Pathology,* 17**,** 1298-1313.

PFEILMEIER, S., GEORGE, J., MOREL, A., ROY, S., SMOKER, M., STRANSFELD, L., DOWNIE, A., PEETERS, N., MALONE, J. & ZIPFEL, C. 2017. Heterologous expression of the immune receptor *EFR* in *Medicago truncatula* reduces pathogenic infection, but not rhizobial symbiosis. *bioRxiv*.

PFEILMEIER, S., SAUR, I. M., RATHJEN, J. P., ZIPFEL, C. & MALONE, J. G. 2016b. High levels of cyclic-di-GMP in plant-associated *Pseudomonas* correlate with evasion of plant immunity. *Mol Plant Pathol,* 17**,** 521-31.

PFUND, C., TANS-KERSTEN, J., DUNNING, F. M., ALONSO, J. M., ECKER, J. R., ALLEN, C. & BENT, A. F. 2004. Flagellin is not a major defense elicitor in *Ralstonia solanacearum* cells or extracts applied to *Arabidopsis thaliana*. *Mol Plant Microbe Interact,* 17**,** 696-706.

PIETERSE, C. M., VAN DER DOES, D., ZAMIOUDIS, C., LEON-REYES, A. & VAN WEES, S. C. 2012. Hormonal modulation of plant immunity. *Annu Rev Cell Dev Biol,* 28**,** 489-521.

PIETERSE, C. M., ZAMIOUDIS, C., BERENDSEN, R. L., WELLER, D. M., VAN WEES, S. C. & BAKKER, P. A. 2014. Induced systemic resistance by beneficial microbes. *Annu Rev Phytopathol,* 52**,** 347-75.

PLETT, J. M., DAGUERRE, Y., WITTULSKY, S., VAYSSIÈRES, A., DEVEAU, A., MELTON, S. J., KOHLER, A., MORRELL-FALVEY, J. L., BRUN, A., VENEAULT-FOURREY, C. & MARTIN, F. 2014. Effector MiSSP7 of the mutualistic fungus Laccaria bicolor stabilizes the Populus JAZ6 protein and represses jasmonic acid (JA) responsive genes. *Proceedings of the National Academy of Sciences,* 111**,** 8299-8304.

PLOTNIKOVA, J. M., RAHME, L. G. & AUSUBEL, F. M. 2000. Pathogenesis of the human opportunistic pathogen *Pseudomonas aeruginosa* PA14 in *Arabidopsis*. *Plant Physiol,* 124**,** 1766-74.

PONCINI, L., WYRSCH, I., DÉNERVAUD TENDON, V., VORLEY, T., BOLLER, T., GELDNER, N., MÉTRAUX, J.-P. & LEHMANN, S. 2017. In roots of Arabidopsis thaliana, the damage-associated molecular pattern AtPep1 is a stronger elicitor of immune signalling than flg22 or the chitin heptamer. *PLOS ONE,* 12**,** e0185808.

POPLAWSKY, A. R. & CHUN, W. 1998. *Xanthomonas campestris* pv. *campestris* requires a functional pigB for epiphytic survival and host infection. *Molecular Plant-Microbe Interactions,* 11**,** 466-475.

POSTEL, S., KUFNER, I., BEUTER, C., MAZZOTTA, S., SCHWEDT, A., BORLOTTI, A., HALTER, T., KEMMERLING, B. & NURNBERGER, T. 2009. The multifunctional leucine-rich repeat receptor kinase BAK1 is implicated in Arabidopsis development and immunity. *Eur J Cell Biol,* 89.

POVOLOTSKY, T. L. & HENGGE, R. 2016. Genome-Based Comparison of Cyclic Di-GMP Signaling in Pathogenic and Commensal Escherichia coli Strains. *Journal of Bacteriology,* 198**,** 111-126.

PRADA-RAMÍREZ, H. A., PÉREZ-MENDOZA, D., FELIPE, A., MARTÍNEZ-GRANERO, F., RIVILLA, R., SANJUÁN, J. & GALLEGOS, M.-T. 2016. AmrZ regulates cellulose production in *Pseudomonas syringae* pv. *tomato* DC3000. *Molecular Microbiology,* 99**,** 960-977.

PRESTON, G. M., BERTRAND, N. & RAINEY, P. B. 2001. Type III secretion in plant growth-promoting *Pseudomonas fluorescens* SBW25. *Mol Microbiol,* 41**,** 999-1014.

PRICE, P. A., TANNER, H. R., DILLON, B. A., SHABAB, M., WALKER, G. C. & GRIFFITTS, J. S. 2015. Rhizobial peptidase HrrP cleaves host-encoded signaling peptides and mediates symbiotic compatibility. *Proc Natl Acad Sci U S A,* 112**,** 15244-15249.

PRUITT, R. N., SCHWESSINGER, B., JOE, A., THOMAS, N., LIU, F., ALBERT, M., ROBINSON, M. R., CHAN, L. J. G., LUU, D. D., CHEN, H., BAHAR, O., DAUDI, A., DE VLEESSCHAUWER, D., CADDELL, D., ZHANG, W., ZHAO, X., LI, X., HEAZLEWOOD, J. L., RUAN, D., MAJUMDER, D., CHERN, M., KALBACHER, H., MIDHA, S., PATIL, P. B., SONTI, R. V., PETZOLD, C. J., LIU, C. C., BRODBELT, J. S., FELIX, G. & RONALD, P. C. 2015. The rice immune receptor XA21 recognizes a tyrosine-sulfated protein from a Gram-negative bacterium. *Science Advances,* 1.

PULTZ, I. S., CHRISTEN, M., KULASEKARA, H. D., KENNARD, A., KULASEKARA, B. & MILLER, S. I. 2012. The response threshold of salmonella pilz domain proteins is determined by their binding affinities for c-di-gmp. *Mol Microbiol,* 86**,** 1424-40.

QUANDT, J. & HYNES, M. F. 1993. Versatile suicide vectors which allow direct selection for gene replacement in Gram-negative bacteria. *Gene,* 127**,** 15-21.

QUIÑONES, B., DULLA, G. & LINDOW, S. E. 2005. Quorum sensing regulates exopolysaccharide production, motility, and virulence in *Pseudomonas syringae*. *Molecular Plant-Microbe Interactions,* 18**,** 682-693.

RAHME, L. G., TAN, M. W., LE, L., WONG, S. M., TOMPKINS, R. G., CALDERWOOD, S. B. & AUSUBEL, F. M. 1997. Use of model plant hosts to identify *Pseudomonas aeruginosa* virulence factors. *Proceedings of the National Academy of Sciences of the United States of America,* 94**,** 13245-13250.

RAMOS, H. C., RUMBO, M. & SIRARD, J. C. 2004. Bacterial flagellins: Mediators of pathogenicity and host immune responses in mucosa. *Trends Microbiol,* 12**,** 509-17.

RAMSEY, D. M. & WOZNIAK, D. J. 2005. Understanding the control of *Pseudomonas aeruginosa* alginate synthesis and the prospects for management of chronic infections in cystic fibrosis. *Molecular Microbiology,* 56**,** 309-322.

RANF, S., ESCHEN-LIPPOLD, L., FRÖHLICH, K., WESTPHAL, L., SCHEEL, D. & LEE, J. 2014. Microbe-associated molecular pattern-induced calcium signaling requires the receptor-like cytoplasmic kinases, PBL1 and BIK1. *BMC Plant Biology,* 14**,** 374.

RANF, S., ESCHEN-LIPPOLD, L., PECHER, P., LEE, J. & SCHEEL, D. 2011. Interplay between calcium signalling and early signalling elements during defence responses to microbe- or damage-associated molecular patterns. *Plant J,* 68**,** 100-13.

RANF, S., GISCH, N., SCHAFFER, M., ILLIG, T., WESTPHAL, L., KNIREL, Y. A., SANCHEZ-CARBALLO, P. M., ZAHRINGER, U., HUCKELHOVEN, R., LEE, J. & SCHEEL, D. 2015. A lectin S-domain receptor kinase mediates lipopolysaccharide sensing in *Arabidopsis thaliana*. *Nat Immunol,* 16**,** 426-433.

RAPICAVOLI, J., INGEL, B., BLANCO-ULATE, B., CANTU, D. & ROPER, C. *Xylella fastidiosa*: An examination of a re-emerging plant pathogen. *Molecular Plant Pathology***,** n/a-n/a.

RECORDS, A. R. & GROSS, D. C. 2010. Sensor kinases RetS and LadS regulate *Pseudomonas syringae* type VI secretion and virulence factors. *J Bacteriol,* 192**,** 3584-96.

REMIGI, P., ANISIMOVA, M., GUIDOT, A., GENIN, S. & PEETERS, N. 2011. Functional diversification of the Gala type III effector family contributes to *Ralstonia solanacearum* adaptation on different plant hosts. *New Phytologist,* 192**,** 976-987.

ROBATZEK, S., BITTEL, P., CHINCHILLA, D., KOCHNER, P., FELIX, G., SHIU, S. H. & BOLLER, T. 2007. Molecular identification and characterization of the tomato flagellin receptor

*Le*FLS2, an orthologue of *Arabidopsis* FLS2 exhibiting characteristically different perception specificities. *Plant Mol Biol,* 64**,** 539-47.

ROBATZEK, S., CHINCHILLA, D. & BOLLER, T. 2006. Ligand-induced endocytosis of the pattern recognition receptor fls2 in arabidopsis. *Genes Dev,* 20**,** 537-42.

ROBERTS, A. E. L., KRAGH, K. N., BJARNSHOLT, T. & DIGGLE, S. P. 2015. The Limitations of In Vitro Experimentation in Understanding Biofilms and Chronic Infection. *Journal of Molecular Biology,* 427**,** 3646-3661.

ROBLES-PRICE, A., WONG, T. Y., SLETTA, H., VALLA, S. & SCHILLER, N. L. 2004. AlgX is a periplasmic protein required for alginate biosynthesis in *Pseudomonas aeruginosa*. *Journal of Bacteriology,* 186**,** 7369-7377.

ROBLETO, E. A., LOPEZ-HERNANDEZ, I., SILBY, M. W. & LEVY, S. B. 2003. Genetic analysis of the AdnA regulon in *Pseudomonas fluorescens*: nonessential role of flagella in adhesion to sand and biofilm formation. *J Bacteriol,* 185**,** 453-60.

RODESNEY, C. A., ROMAN, B., DHAMANI, N., COOLEY, B. J., KATIRA, P., TOUHAMI, A. & GORDON, V. D. 2017. Mechanosensing of shear by Pseudomonas aeruginosa leads to increased levels of the cyclic-di-GMP signal initiating biofilm development. *Proceedings of the National Academy of Sciences,* 114**,** 5906-5911.

RODRIGUEZ-MORENO, L., SONG, Y. & THOMMA, B. P. H. J. 2017. Transfer and engineering of immune receptors to improve recognition capacities in crops. *Current Opinion in Plant Biology,* 38**,** 42-49.

RÖMLING, U. & GALPERIN, M. Y. 2015. Bacterial cellulose biosynthesis: diversity of operons, subunits, products, and functions. *Trends in Microbiology,* 23**,** 545-557.

ROMLING, U., GALPERIN, M. Y. & GOMELSKY, M. 2013. Cyclic di-gmp: The first 25 years of a universal bacterial second messenger. *Microbiol Mol Biol Rev,* 77**,** 1-52.

ROSSEZ, Y., WOLFSON, E. B., HOLMES, A., GALLY, D. L. & HOLDEN, N. J. 2015. Bacterial flagella: twist and stick, or dodge across the kingdoms. *PLoS Pathog,* 11**,** e1004483.

ROUND, J. L., LEE, S. M., LI, J., TRAN, G., JABRI, B., CHATILA, T. A. & MAZMANIAN, S. K. 2011. The Toll-Like Receptor 2 Pathway Establishes Colonization by a Commensal of the Human Microbiota. *Science,* 332**,** 974-977.

ROUX, M., SCHWESSINGER, B., ALBRECHT, C., CHINCHILLA, D., JONES, A., HOLTON, N., MALINOVSKY, F. G., TOR, M., DE VRIES, S. & ZIPFEL, C. 2011. The *Arabidopsis* leucine-rich repeat receptor-like kinases BAK1/SERK3 and BKK1/SERK4 are required for innate immunity to hemibiotrophic and biotrophic pathogens. *Plant Cell,* 23**,** 2440-2455.

RUFIAN, J. S., MACHO, A. P., CORRY, D. S., MANSFIELD, J. W., RUIZ-ALBERT, J., ARNOLD, D. L. & BEUZON, C. R. 2017. Confocal microscopy reveals in planta dynamic interactions between pathogenic, avirulent and non-pathogenic *Pseudomonas syringae* strains. *Mol Plant Pathol***,** n/a-n/a.

RUSCONI, R., GARREN, M. & STOCKER, R. 2014. Microfluidics Expanding the Frontiers of Microbial Ecology. *Annual Review of Biophysics,* 43**,** 65-91.

RYAN, R. P. 2013. Cyclic di-gmp signalling and the regulation of bacterial virulence. *Microbiology,* 159**,** 1286-97.

RYAN, R. P., FOUHY, Y., LUCEY, J. F., JIANG, B. L., HE, Y. Q., FENG, J. X., TANG, J. L. & DOW, J. M. 2007. Cyclic di-gmp signalling in the virulence and environmental adaptation of xanthomonas campestris. *Mol Microbiol,* 63**,** 429-42.

RYBTKE, M. T., BORLEE, B. R., MURAKAMI, K., IRIE, Y., HENTZER, M., NIELSEN, T. E., GIVSKOV, M., PARSEK, M. R. & TOLKER-NIELSEN, T. 2012. Fluorescence-Based Reporter for Gauging Cyclic Di-GMP Levels in Pseudomonas aeruginosa. *Applied and Environmental Microbiology,* 78**,** 5060-5069.

RYFFEL, F., HELFRICH, E. J. N., KIEFER, P., PEYRIGA, L., PORTAIS, J.-C., PIEL, J. & VORHOLT, J. A. 2016. Metabolic footprint of epiphytic bacteria on Arabidopsis thaliana leaves. *ISME J,* 10**,** 632-643.

RYU, H., LAFFONT, C., FRUGIER, F. & HWANG, I. 2017. MAP kinase-mediated negative regulation of symbiotic nodule formation in *Medicago truncatula*. *Mol Cells,* 40**,** 17-23.

SALANOUBAT, M., GENIN, S., ARTIGUENAVE, F., GOUZY, J., MANGENOT, S., ARLAT, M., BILLAULT, A., BROTTIER, P., CAMUS, J. C., CATTOLICO, L., CHANDLER, M., CHOISNE, N., CLAUDEL-RENARD, C., CUNNAC, S., DEMANGE, N., GASPIN, C., LAVIE, M., MOISAN, A., ROBERT, C., SAURIN, W., SCHIEX, T., SIGUIER, P., THEBAULT, P., WHALEN, M., WINCKER, P., LEVY, M., WEISSENBACH, J. & BOUCHER, C. A. 2002. Genome sequence of the plant pathogen *Ralstonia solanacearum*. *Nature,* 415**,** 497-502.

SAUR, I. M. L., KADOTA, Y., SKLENAR, J., HOLTON, N. J., SMAKOWSKA, E., BELKHADIR, Y., ZIPFEL, C. & RATHJEN, J. P. 2016. NbCSPR underlies age-dependent immune responses to bacterial cold shock protein in *Nicotiana benthamiana*. *Proceedings of the National Academy of Sciences,* 113**,** 3389-3394.

SCHARF, B., SCHUSTER-WOLFF-BUHRING, H., RACHEL, R. & SCHMITT, R. 2001. Mutational analysis of the rhizobium lupini h13-3 and sinorhizobium meliloti flagellin genes: Importance of flagellin a for flagellar filament structure and transcriptional regulation. *J Bacteriol,* 183**,** 5334-42.

SCHECHTER, L. M., GUENTHER, J., OLCAY, E. A., JANG, S. & KRISHNAN, H. B. 2010. Translocation of nopp by sinorhizobium fredii usda257 into vigna unguiculata root nodules. *Appl Environ Microbiol,* 76**,** 3758-61.

SCHLUTER, J., NADELL, C. D., BASSLER, B. L. & FOSTER, K. R. 2015. Adhesion as a weapon in microbial competition. *ISME J,* 9**,** 139-149.

SCHOONBEEK, H. J., WANG, H. H., STEFANATO, F. L., CRAZE, M., BOWDEN, S., WALLINGTON, E., ZIPFEL, C. & RIDOUT, C. J. 2015. *Arabidopsis* EF-Tu receptor enhances bacterial disease resistance in transgenic wheat. *New Phytol,* 206**,** 606-13.

SCHREIBER, K. J. & DESVEAUX, D. 2011. AlgW regulates multiple Pseudomonas syringae virulence strategies. *Molecular Microbiology,* 80**,** 364-377.

SCHULZE, B., MENTZEL, T., JEHLE, A. K., MUELLER, K., BEELER, S., BOLLER, T., FELIX, G. & CHINCHILLA, D. 2010. Rapid heteromerization and phosphorylation of ligand-activated plant transmembrane receptors and their associated kinase bak1. *J Biol Chem,* 285**,** 9444-51.

SCHURR, M. J. 2013. Which bacterial biofilm exopolysaccharide is preferred, Psl or alginate? *J Bacteriol,* 195**,** 1623-6.

SCHWESSINGER, B., BAHAR, O., THOMAS, N., HOLTON, N., NEKRASOV, V., RUAN, D., CANLAS, P. E., DAUDI, A., PETZOLD, C. J., SINGAN, V. R., KUO, R., CHOVATIA, M., DAUM, C., HEAZLEWOOD, J. L., ZIPFEL, C. & RONALD, P. C. 2015. Transgenic expression of the dicotyledonous pattern recognition receptor EFR in rice leads to ligand-dependent activation of defense responses. *PLoS Pathog,* 11**,** e1004809.

SCHWESSINGER, B., ROUX, M., KADOTA, Y., NTOUKAKIS, V., SKLENAR, J., JONES, A. & ZIPFEL, C. 2011. Phosphorylation-dependent differential regulation of plant growth, cell death, and innate immunity by the regulatory receptor-like kinase BAK1. *PLoS Genet,* 7**,** e1002046.

SCOTT, T. A., HEINE, D., QIN, Z. & WILKINSON, B. 2017. An L-threonine transaldolase is required for L-threo-β-hydroxy-α-amino acid assembly during obafluorin biosynthesis. 8**,** 15935.

SEGONZAC, C., FEIKE, D., GIMENEZ-IBANEZ, S., HANN, D. R., ZIPFEL, C. & RATHJEN, J. P. 2011. Hierarchy and roles of pathogen-associated molecular pattern-induced responses in nicotiana benthamiana. *Plant Physiol,* 156**,** 687-99.

SERRA, D. O. & HENGGE, R. 2014. Stress responses go three dimensional – the spatial order of physiological differentiation in bacterial macrocolony biofilms. *Environmental Microbiology,* 16**,** 1455-1471.

SERRA, D. O., KLAUCK, G. & HENGGE, R. 2015. Vertical stratification of matrix production is essential for physical integrity and architecture of macrocolony biofilms of Escherichia coli. *Environmental Microbiology,* 17**,** 5073-5088.

SERRA, D. O., RICHTER, A. M. & HENGGE, R. 2013. Cellulose as an Architectural Element in Spatially Structured Escherichia coli Biofilms. *Journal of Bacteriology,* 195**,** 5540-5554.

SEYBOLD, H., TREMPEL, F., RANF, S., SCHEEL, D., ROMEIS, T. & LEE, J. 2014. Ca^{2+} signalling in plant immune response: from pattern recognition receptors to Ca^{2+} decoding mechanisms. *New Phytol,* 204**,** 782-90.

SHAN, L., HE, P., LI, J., HEESE, A., PECK, S. C., NURNBERGER, T., MARTIN, G. B. & SHEEN, J. 2008. Bacterial effectors target the common signaling partner bak1 to disrupt multiple mamp receptor-signaling complexes and impede plant immunity. *Cell Host Microbe,* 4**,** 17-27.

SHIU, S. H., KARLOWSKI, W. M., PAN, R., TZENG, Y. H., MAYER, K. F. & LI, W. H. 2004. Comparative analysis of the receptor-like kinase family in arabidopsis and rice. *Plant Cell,* 16**,** 1220-34.

SILIPO, A., ERBS, G., SHINYA, T., DOW, J. M., PARRILLI, M., LANZETTA, R., SHIBUYA, N., NEWMAN, M.-A. & MOLINARO, A. 2010. Glyco-conjugates as elicitors or suppressors of plant innate immunity. *Glycobiology,* 20**,** 406-419.

SILIPO, A., MOLINARO, A., STURIALE, L., DOW, J. M., ERBS, G., LANZETTA, R., NEWMAN, M. A. & PARRILLI, M. 2005. The elicitation of plant innate immunity by lipooligosaccharide of xanthomonas campestris. *J Biol Chem,* 280**,** 33660-8.

SIMON, R., PRIEFER, U. & PUHLER, A. 1983. A broad host range mobilization system for *in vivo* genetic engineering: Transposon mutagenesis in Gram-negative bacteria. *Nat Biotech,* 1**,** 784-791.

SINGH, S., KATZER, K., LAMBERT, J., CERRI, M. & PARNISKE, M. 2014. CYCLOPS, A DNA-Binding Transcriptional Activator, Orchestrates Symbiotic Root Nodule Development. *Cell Host & Microbe,* 15**,** 139-152.

SKORPIL, P., SAAD, M. M., BOUKLI, N. M., KOBAYASHI, H., ARES-ORPEL, F., BROUGHTON, W. J. & DEAKIN, W. J. 2005. NopP, a phosphorylated effector of *Rhizobium* sp. strain NGR234, is a major determinant of nodulation of the tropical legumes *Flemingia congesta* and *Tephrosia vogelii*. *Molecular Microbiology,* 57**,** 1304-1317.

SMITH, D. R., MAESTRE-REYNA, M., LEE, G., GERARD, H., WANG, A. H.-J. & WATNICK, P. I. 2015. In situ proteolysis of the Vibrio cholerae matrix protein RbmA promotes biofilm recruitment. *Proceedings of the National Academy of Sciences,* 112**,** 10491-10496.

SMITH, J. M. & HEESE, A. 2014. Rapid bioassay to measure early reactive oxygen species production in arabidopsis leave tissue in response to living pseudomonas syringae. *Plant Methods,* 10**,** 1-9.

SMITH, K. D., ANDERSEN-NISSEN, E., HAYASHI, F., STROBE, K., BERGMAN, M. A., BARRETT, S. L. R., COOKSON, B. T. & ADEREM, A. 2003. Toll-like receptor 5 recognizes a conserved site on flagellin required for protofilament formation and bacterial motility. *Nature Immunology,* 4**,** 1247-1253.

SONDERMANN, H., SHIKUMA, N. J. & YILDIZ, F. H. 2012. You've come a long way: C-di-gmp signaling. *Curr Opin Microbiol,* 15**,** 140-6.

SOUSA, A. M. & PEREIRA, M. O. 2014. *Pseudomonas aeruginosa* diversification during infection development in cystic fibrosis lungs - A review. *Pathogens,* 3**,** 680-703.

SPANGLER, C., BOHM, A., JENAL, U., SEIFERT, R. & KAEVER, V. 2010. A liquid chromatography-coupled tandem mass spectrometry method for quantitation of cyclic di-guanosine monophosphate. *J Microbiol Methods,* 81**,** 226-31.

SPIERS, A. J., BOHANNON, J., GEHRIG, S. M. & RAINEY, P. B. 2003. Biofilm formation at the air-liquid interface by the *Pseudomonas fluorescens* SBW25 wrinkly spreader requires an acetylated form of cellulose. *Molecular Microbiology,* 50**,** 15-27.

SPIERS, A. J., KAHN, S. G., BOHANNON, J., TRAVISANO, M. & RAINEY, P. B. 2002. Adaptive divergence in experimental populations of pseudomonas fluorescens. I. Genetic and phenotypic bases of wrinkly spreader fitness. *Genetics,* 161**,** 33-46.

SPOEL, S. H. & DONG, X. N. 2012. How do plants achieve immunity? Defence without specialized immune cells. *Nature Reviews Immunology,* 12**,** 89-100.

STACY, A., MCNALLY, L., DARCH, S. E., BROWN, S. P. & WHITELEY, M. 2016. The biogeography of polymicrobial infection. *Nat Rev Micro,* 14**,** 93-105.

STAEHELIN, C. & KRISHNAN, H. B. 2015. Nodulation outer proteins: Double-edged swords of symbiotic rhizobia. *Biochem J,* 470**,** 263-74.

STARKEY, M., HICKMAN, J. H., MA, L., ZHANG, N., DE LONG, S., HINZ, A., PALACIOS, S., MANOIL, C., KIRISITS, M. J., STARNER, T. D., WOZNIAK, D. J., HARWOOD, C. S. & PARSEK, M. R. 2009. Pseudomonas aeruginosa rugose small-colony variants have adaptations that likely promote persistence in the cystic fibrosis lung. *Journal of Bacteriology,* 191**,** 3492-3503.

STARKEY, M. & RAHME, L. G. 2009. Modeling pseudomonas aeruginosa pathogenesis in plant hosts. *Nat Protoc,* 4**,** 117-24.

STEINER, S., LORI, C., BOEHM, A. & JENAL, U. 2013. Allosteric activation of exopolysaccharide synthesis through cyclic di-GMP-stimulated protein-protein interaction. *EMBO J,* 32**,** 354-68.

STOVER, C. K., PHAM, X. Q., ERWIN, A. L., MIZOGUCHI, S. D., WARRENER, P., HICKEY, M. J., BRINKMAN, F. S. L., HUFNAGLE, W. O., KOWALIK, D. J., LAGROU, M., GARBER, R. L., GOLTRY, L., TOLENTINO, E., WESTBROCK-WADMAN, S., YUAN, Y., BRODY, L. L., COULTER, S. N., FOLGER, K. R., KAS, A., LARBIG, K., LIM, R., SMITH, K., SPENCER, D., WONG, G. K. S., WU, Z., PAULSEN, I. T., REIZER, J., SAIER, M. H., HANCOCK, R. E. W.,

LORY, S. & OLSON, M. V. 2000. Complete genome sequence of *Pseudomonas aeruginosa* PAO1, an opportunistic pathogen. *Nature,* 406**,** 959-964.

STRACK, R. L., SONG, W. & JAFFREY, S. R. 2014. Using Spinach-based sensors for fluorescence imaging of intracellular metabolites and proteins in living bacteria. *Nat. Protocols,* 9**,** 146-155.

STRINGLIS, I. A., PROIETTI, S., HICKMAN, R., VAN VERK, M. C., ZAMIOUDIS, C. & PIETERSE, C. M. J. 2018. Root transcriptional dynamics induced by beneficial rhizobacteria and microbial immune elicitors reveal signatures of adaptation to mutualists. *Plant J,* 93**,** 166-180.

SUGAWARA, M., EPSTEIN, B., BADGLEY, B. D., UNNO, T., XU, L., REESE, J., GYANESHWAR, P., DENNY, R., MUDGE, J., BHARTI, A. K., FARMER, A. D., MAY, G. D., WOODWARD, J. E., MÉDIGUE, C., VALLENET, D., LAJUS, A., ROUY, Z., MARTINEZ-VAZ, B., TIFFIN, P., YOUNG, N. D. & SADOWSKY, M. J. 2013. Comparative genomics of the core and accessory genomes of 48 *Sinorhizobium* strains comprising five genospecies. *Genome Biology,* 14**,** R17.

SUGIO, A. & HOGENHOUT, S. A. 2012. The genome biology of phytoplasma: modulators of plants and insects. *Curr Opin Microbiol,* 15**,** 247-54.

SUN, W., DUNNING, F. M., PFUND, C., WEINGARTEN, R. & BENT, A. F. 2006. Within-species flagellin polymorphism in *Xanthomonas campestris* pv *campestris* and its impact on elicitation of *Arabidopsis* FLAGELLIN SENSING2-dependent defenses. *Plant Cell,* 18**,** 764-79.

SUN, Y., LI, L., MACHO, A. P., HAN, Z., HU, Z., ZIPFEL, C., ZHOU, J. M. & CHAI, J. 2013. Structural basis for flg22-induced activation of the *Arabidopsis* FLS2-BAK1 immune complex. *Science,* 342**,** 624-8.

TADEGE, M., WEN, J., HE, J., TU, H., KWAK, Y., ESCHSTRUTH, A., CAYREL, A., ENDRE, G., ZHAO, P. X., CHABAUD, M., RATET, P. & MYSORE, K. S. 2008. Large-scale insertional mutagenesis using the Tnt1 retrotransposon in the model legume Medicago truncatula. *The Plant Journal,* 54**,** 335-347.

TAGUCHI, F., SHIMIZU, R., INAGAKI, Y., TOYODA, K., SHIRAISHI, T. & ICHINOSE, Y. 2003. Post-translational modification of flagellin determines the specificity of hr induction. *Plant Cell Physiol,* 44**,** 342-9.

TAKAI, R., ISOGAI, A., TAKAYAMA, S. & CHE, F. S. 2008. Analysis of flagellin perception mediated by flg22 receptor OsFLS2 in rice. *Mol Plant Microbe Interact,* 21**,** 1635-42.

TAKEUCHI, K., TAGUCHI, F., INAGAKI, Y., TOYODA, K., SHIRAISHI, T. & ICHINOSE, Y. 2003. Flagellin glycosylation island in *Pseudomonas syringae* pv. *glycinea* and its role in host specificity. *J Bacteriol,* 185**,** 6658-65.

TAMAYO, R., PRATT, J. T. & CAMILLI, A. 2007. Roles of cyclic diguanylate in the regulation of bacterial pathogenesis. *Annu Rev Microbiol,* 61**,** 131-48.

TAMPAKAKI, A. P. 2014. Commonalities and differences of T3SSs in rhizobia and plant pathogenic bacteria. *Frontiers in Plant Science,* 5.

TELLSTROEM, V., USADEL, B., THIMM, O., STITT, M., KUESTER, H. & NIEHAUS, K. 2007. The lipopolysaccharide of *Sinorhizobium meliloti* suppresses defense-associated gene expression in cell cultures of the host plant *Medicago truncatula*. *Plant Physiology,* 143**,** 825-837.

THOMMA, B. P. H. J., NUERNBERGER, T. & JOOSTEN, M. H. A. J. 2011. Of PAMPs and effectors: The blurred PTI-ETI dichotomy. *Plant Cell,* 23**,** 4-15.

THOMPSON, P. 2010. *Seeds, sex and civilization: How the hidden life of plants has shaped our world,* London, Thames & Hudson.

TIRICHINE, L., IMAIZUMI-ANRAKU, H., YOSHIDA, S., MURAKAMI, Y., MADSEN, L. H., MIWA, H., NAKAGAWA, T., SANDAL, N., ALBREKTSEN, A. S., KAWAGUCHI, M., DOWNIE, A., SATO, S., TABATA, S., KOUCHI, H., PARNISKE, M., KAWASAKI, S. & STOUGAARD, J. 2006. Deregulation of a Ca^{2+}/calmodulin-dependent kinase leads to spontaneous nodule development. *Nature,* 441**,** 1153-1156.

TORRES, M. A. 2010. ROS in biotic interactions. *Physiologia Plantarum,* 138**,** 414-429.

TRAMPARI, E., STEVENSON, C. E. M., LITTLE, R. H., WILHELM, T., LAWSON, D. M. & MALONE, J. G. 2015. Bacterial Rotary Export ATPases Are Allosterically Regulated by the Nucleotide Second Messenger Cyclic-di-GMP. *Journal of Biological Chemistry,* 290**,** 24470-24483.

TRDÁ, L., BOUTROT, F., CLAVERIE, J., BRULÉ, D., DOREY, S. & POINSSOT, B. 2015. Perception of pathogenic or beneficial bacteria and their evasion of host immunity: pattern recognition receptors in the frontline. *Frontiers in Plant Science,* 6.

TRDA, L., FERNANDEZ, O., BOUTROT, F., HELOIR, M. C., KELLONIEMI, J., DAIRE, X., ADRIAN, M., CLEMENT, C., ZIPFEL, C., DOREY, S. & POINSSOT, B. 2014. The grapevine flagellin receptor vvfls2 differentially recognizes flagellin-derived epitopes from the endophytic growth-promoting bacterium burkholderia phytofirmans and plant pathogenic bacteria. *New Phytol,* 201**,** 1371-84.

TRINICK, M. J., DILWORTH, M. J. & GROUNDS, M. 1976. Factors affecting reduction of acetylene by root-nodules of *Lupinus* species. *New Phytologist,* 77**,** 359-370.

TRIPATHI, J. N., LORENZEN, J., BAHAR, O., RONALD, P. & TRIPATHI, L. 2014. Transgenic expression of the rice *Xa21* pattern-recognition receptor in banana (*Musa* sp.) confers resistance to *Xanthomonas campestris* pv. *musacearum*. *Plant Biotechnol J,* 12**,** 663-73.

TSUDA, K. & KATAGIRI, F. 2010. Comparing signaling mechanisms engaged in pattern-triggered and effector-triggered immunity. *Current Opinion in Plant Biology,* 13**,** 459-465.

UDE, S., ARNOLD, D. L., MOON, C. D., TIMMS-WILSON, T. & SPIERS, A. J. 2006. Biofilm formation and cellulose expression among diverse environmental Pseudomonas isolates. *Environmental Microbiology,* 8**,** 1997-2011.

VAILLEAU, F., SARTOREL, E., JARDINAUD, M. F., CHARDON, F., GENIN, S., HUGUET, T., GENTZBITTEL, L. & PETITPREZ, M. 2007. Characterization of the interaction between the bacterial wilt pathogen *Ralstonia solanacearum* and the model legume plant *Medicago truncatula*. *Mol Plant Microbe Interact,* 20**,** 159-67.

VAKULSKAS, C. A., POTTS, A. H., BABITZKE, P., AHMER, B. M. & ROMEO, T. 2015. Regulation of bacterial virulence by Csr (Rsm) systems. *Microbiol Mol Biol Rev,* 79**,** 193-224.

VALENTINI, M. & FILLOUX, A. 2016. Biofilms and c-di-GMP Signaling: Lessons from Pseudomonas aeruginosa and other Bacteria. *Journal of Biological Chemistry*.

VAN DE VELDE, W., ZEHIROV, G., SZATMARI, A., DEBRECZENY, M., ISHIHARA, H., KEVEI, Z., FARKAS, A., MIKULASS, K., NAGY, A., TIRICZ, H., SATIAT-JEUNEMAITRE, B., ALUNNI, B., BOURGE, M., KUCHO, K., ABE, M., KERESZT, A., MAROTI, G., UCHIUMI, T., KONDOROSI, E. & MERGAERT, P. 2010. Plant peptides govern terminal differentiation of bacteria in symbiosis. *Science,* 327**,** 1122-1126.

VAN LOON, L. C. 2007. Plant responses to plant growth-promoting rhizobacteria. *European Journal of Plant Pathology,* 119**,** 243-254.

VAN LOON, L. C., BAKKER, P. A., VAN DER HEIJDT, W. H., WENDEHENNE, D. & PUGIN, A. 2008. Early responses of tobacco suspension cells to rhizobacterial elicitors of induced systemic resistance. *Mol Plant Microbe Interact,* 21**,** 1609-21.

VAN WEES, S. C., VAN DER ENT, S. & PIETERSE, C. M. 2008. Plant immune responses triggered by beneficial microbes. *Curr Opin Plant Biol,* 11**,** 443-8.

VASSEUR, P., SOSCIA, C., VOULHOUX, R. & FILLOUX, A. 2007. PelC is a *Pseudomonas aeruginosa* outer membrane lipoprotein of the OMA family of proteins involved in exopolysaccharide transport. *Biochimie,* 89**,** 903-15.

VELUCHAMY, S., HIND, S. R., DUNHAM, D. M., MARTIN, G. B. & PANTHEE, D. R. 2014. Natural variation for responsiveness to flg22, flgII-28, and csp22 and *Pseudomonas syringae* pv. *tomato* in heirloom tomatoes. *PLoS One,* 9**,** e106119.

VETTER, M., KARASOV, T. L. & BERGELSON, J. 2016. Differentiation between MAMP triggered defenses in *Arabidopsis thaliana*. *PLOS Genetics,* 12**,** e1006068.

VETTER, M. M., KRONHOLM, I., HE, F., HAWEKER, H., REYMOND, M., BERGELSON, J., ROBATZEK, S. & DE MEAUX, J. 2012. Flagellin perception varies quantitatively in arabidopsis thaliana and its relatives. *Mol Biol Evol,* 29**,** 1655-67.

VIPREY, V., DEL GRECO, A., GOLINOWSKI, W., BROUGHTON, W. J. & PERRET, X. 1998. Symbiotic implications of type III protein secretion machinery in *Rhizobium*. *Mol Microbiol,* 28**,** 1381-9.

VOGEL, C., BODENHAUSEN, N., GRUISSEM, W. & VORHOLT, J. A. 2016. The *Arabidopsis* leaf transcriptome reveals distinct but also overlapping responses to colonization by phyllosphere commensals and pathogen infection with impact on plant health. *New Phytologist,* 212**,** 192-207.

VOISARD, C., BULL, C. T., KEEL, C., LAVILLE, J., MAURHOFER, M., SCHNIDER, U., DÉFAGO, G. & HAAS, D. 2007. Biocontrol of root diseases by *Pseudomonas fluorescens* CHA0: Current concepts and experimental approaches. *Molecular Ecology of Rhizosphere Microorganisms.* Wiley-VCH Verlag GmbH.

VORHOLT, J. A. 2012. Microbial life in the phyllosphere. *Nat Rev Micro,* 10**,** 828-840.

VORHOLT, J. A., VOGEL, C., CARLSTRÖM, C. I. & MÜLLER, D. B. 2017. Establishing causality: Opportunities of synthetic communities for plant microbiome research. *Cell Host & Microbe,* 22**,** 142-155.

WAGNER, M. R., LUNDBERG, D. S., DEL RIO, T. G., TRINGE, S. G., DANGL, J. L. & MITCHELL-OLDS, T. 2016. Host genotype and age shape the leaf and root microbiomes of a wild perennial plant. 7**,** 12151.

WALKER, T. S., BAIS, H. P., DEZIEL, E., SCHWEIZER, H. P., RAHME, L. G., FALL, R. & VIVANCO, J. M. 2004. Pseudomonas aeruginosa-plant root interactions. Pathogenicity, biofilm formation, and root exudation. *Plant Physiol,* 134**,** 320-31.

WANG, C., YU, H., LUO, L., DUAN, L., CAI, L., HE, X., WEN, J., MYSORE, K. S., LI, G., XIAO, A., DUANMU, D., CAO, Y., HONG, Z. & ZHANG, Z. 2016. *NODULES WITH ACTIVATED DEFENSE 1* is required for maintenance of rhizobial endosymbiosis in *Medicago truncatula*. *New Phytologist,* 212**,** 176-191.

WANG, C., ZHOU, M., ZHANG, X., YAO, J., ZHANG, Y. & MOU, Z. 2017. A lectin receptor kinase as a potential sensor for extracellular nicotinamide adenine dinucleotide in *Arabidopsis thaliana*. *eLife,* 6**,** e25474.

WANG, X., PRESTON, J. F., 3RD & ROMEO, T. 2004. The *pgaABCD* locus of *Escherichia coli* promotes the synthesis of a polysaccharide adhesin required for biofilm formation. *J Bacteriol,* 186**,** 2724-34.

WATT, S. A., WILKE, A., PATSCHKOWSKI, T. & NIEHAUS, K. 2005. Comprehensive analysis of the extracellular proteins from *Xanthomonas campestris* pv. *campestris* B100. *PROTEOMICS,* 5**,** 153-167.

WELLER, D. M., MAVRODI, D. V., VAN PELT, J. A., PIETERSE, C. M., VAN LOON, L. C. & BAKKER, P. A. 2012. Induced systemic resistance in *Arabidopsis thaliana* against *Pseudomonas syringae* pv. *tomato* by 2,4-diacetylphloroglucinol-producing *Pseudomonas fluorescens*. *Phytopathology,* 102**,** 403-12.

WENZEL, M., FRIEDRICH, L., GOTTFERT, M. & ZEHNER, S. 2010. The type III-secreted protein NopE1 affects symbiosis and exhibits a calcium-dependent autocleavage activity. *Mol Plant Microbe Interact,* 23**,** 124-9.

WHITNEY, J. C. & HOWELL, P. L. 2013. Synthase-dependent exopolysaccharide secretion in Gram-negative bacteria. *Trends in Microbiology,* 21**,** 63-72.

WHITNEY, J. C., QUENTIN, D., SAWAI, S., LEROUX, M., HARDING, B. N., LEDVINA, H. E., TRAN, B. Q., ROBINSON, H., GOO, Y. A., GOODLETT, D. R., RAUNSER, S. & MOUGOUS, J. D. 2015. An interbacterial NAD(P)(+) glycohydrolase toxin requires elongation factor Tu for delivery to target cells. *Cell,* 163**,** 607-19.

WILLIAMS, A., WILKINSON, A., KREHENBRINK, M., RUSSO, D. M., ZORREGUIETA, A. & DOWNIE, J. A. 2008. Glucomannan-mediated attachment of *Rhizobium leguminosarum* to pea root hairs is required for competitive nodule infection. *J Bacteriol,* 190**,** 4706-15.

WILLMANN, R., LAJUNEN, H. M., ERBS, G., NEWMAN, M. A., KOLB, D., TSUDA, K., KATAGIRI, F., FLIEGMANN, J., BONO, J. J., CULLIMORE, J. V., JEHLE, A. K., GOTZ, F., KULIK, A., MOLINARO, A., LIPKA, V., GUST, A. A. & NURNBERGER, T. 2011. *Arabidopsis* lysin-motif proteins LYM1 LYM3 CERK1 mediate bacterial peptidoglycan sensing and immunity to bacterial infection. *Proc Natl Acad Sci U S A,* 108**,** 19824-9.

WIN, J., CHAPARRO-GARCIA, A., BELHAJ, K., SAUNDERS, D. G., YOSHIDA, K., DONG, S., SCHORNACK, S., ZIPFEL, C., ROBATZEK, S., HOGENHOUT, S. A. & KAMOUN, S. 2012. Effector biology of plant-associated organisms: Concepts and perspectives. *Cold Spring Harb Symp Quant Biol,* 77**,** 235-47.

WINSOR, G. L., GRIFFITHS, E. J., LO, R., DHILLON, B. K., SHAY, J. A. & BRINKMAN, F. S. 2016. Enhanced annotations and features for comparing thousands of *Pseudomonas* genomes in the *Pseudomonas* genome database. *Nucleic Acids Res,* 44**,** D646-53.

WOZNIAK, D. J., WYCKOFF, T. J., STARKEY, M., KEYSER, R., AZADI, P., O'TOOLE, G. A. & PARSEK, M. R. 2003. Alginate is not a significant component of the extracellular polysaccharide matrix of PA14 and PAO1 *Pseudomonas aeruginosa* biofilms. *Proc Natl Acad Sci U S A,* 100**,** 7907-12.

WU, S., ALSEEKH, S., CUADROS-INOSTROZA, Á., FUSARI, C. M., MUTWIL, M., KOOKE, R., KEURENTJES, J. B., FERNIE, A. R., WILLMITZER, L. & BROTMAN, Y. 2016. Combined use of genome-wide association data and correlation networks unravels key regulators of primary metabolism in *Arabidopsis thaliana*. *PLOS Genetics,* 12**,** e1006363.

WURTZEL, O., YODER-HIMES, D. R., HAN, K., DANDEKAR, A. A., EDELHEIT, S., GREENBERG, E. P., SOREK, R. & LORY, S. 2012. The single-nucleotide resolution transcriptome of *Pseudomonas aeruginosa* grown in body temperature. *PLoS Pathog,* 8**,** e1002945.

WYRSCH, I., DOMÍNGUEZ-FERRERAS, A., GELDNER, N. & BOLLER, T. 2015. Tissue-specific *FLAGELLIN-SENSING 2* (*FLS2*) expression in roots restores immune responses in *Arabidopsis fls2* mutants. *New Phytologist,* 206**,** 774-784.

XIANG, T., ZONG, N., ZOU, Y., WU, Y., ZHANG, J., XING, W., LI, Y., TANG, X., ZHU, L., CHAI, J. & ZHOU, J. M. 2008. *Pseudomonas syringae* effector AvrPto blocks innate immunity by targeting receptor kinases. *Curr Biol,* 18**,** 74-80.

XIN, D.-W., LIAO, S., XIE, Z.-P., HANN, D. R., STEINLE, L., BOLLER, T. & STAEHELIN, C. 2012a. Functional analysis of NopM, a novel E3 ubiquitin ligase (NEL) domain effector of *Rhizobium* sp. strain NGR234. *PLOS Pathogens,* 8**,** e1002707.

XIN, D. W., LIAO, S., XIE, Z. P., HANN, D. R., STEINLE, L., BOLLER, T. & STAEHELIN, C. 2012b. Functional analysis of NopM, a novel E3 ubiquitin ligase (NEL) domain effector of *Rhizobium* sp. strain NGR234. *PLoS Pathog,* 8**,** e1002707.

XIN, X. F. & HE, S. Y. 2013. *Pseudomonas syringae* pv. *tomato* DC3000: a model pathogen for probing disease susceptibility and hormone signaling in plants. *Annu Rev Phytopathol,* 51**,** 473-98.

XIN, X. F., NOMURA, K., AUNG, K., VELASQUEZ, A. C., YAO, J., BOUTROT, F., CHANG, J. H., ZIPFEL, C. & HE, S. Y. 2016. Bacteria establish an aqueous living space in plants crucial for virulence. *Nature,* 539**,** 524-529.

YADETA, K. A., ELMORE, J. M., CREER, A. Y., FENG, B., FRANCO, J. Y., RUFIAN, J. S., HE, P., PHINNEY, B. & COAKER, G. 2017. A cysteine-rich protein kinase associates with a membrane immune complex and the cysteine residues are required for cell death. *Plant Physiology,* 173**,** 771-787.

YAMAGUCHI, Y., HUFFAKER, A., BRYAN, A. C., TAX, F. E. & RYAN, C. A. 2010. PEPR2 is a second receptor for the Pep1 and Pep2 peptides and contributes to defense responses in *Arabidopsis*. *Plant Cell,* 22**,** 508-22.

YAMAGUCHI, Y., PEARCE, G. & RYAN, C. A. 2006. The cell surface leucine-rich repeat receptor for AtPep1, an endogenous peptide elicitor in *Arabidopsis*, is functional in transgenic tobacco cells. *Proc Natl Acad Sci U S A,* 103**,** 10104-9.

YI, M. & VALENT, B. 2013. Communication between filamentous pathogens and plants at the biotrophic interface. *Annu Rev Phytopathol,* 51**,** 587-611.

YU, J., PENALOZA-VAZQUEZ, A., CHAKRABARTY, A. M. & BENDER, C. L. 1999. Involvement of the exopolysaccharide alginate in the virulence and epiphytic fitness of *Pseudomonas syringae* pv. *syringae*. *Mol Microbiol,* 33**,** 712-20.

YU, X., FENG, B., HE, P. & SHAN, L. 2017. From chaos to harmony: Responses and signaling upon microbial pattern recognition. *Annu Rev Phytopathol,* 55**,** 109-137.

YU, X., LUND, S. P., SCOTT, R. A., GREENWALD, J. W., RECORDS, A. H., NETTLETON, D., LINDOW, S. E., GROSS, D. C. & BEATTIE, G. A. 2013. Transcriptional responses of *Pseudomonas syringae* to growth in epiphytic versus apoplastic leaf sites. *Proceedings of the National Academy of Sciences,* 110**,** E425-E434.

YUN, M. H., TORRES, P. S., EL OIRDI, M., RIGANO, L. A., GONZALEZ-LAMOTHE, R., MARANO, M. R., CASTAGNARO, A. P., DANKERT, M. A., BOUARAB, K. & VOJNOV, A. A. 2006. Xanthan induces plant susceptibility by suppressing callose deposition. *Plant Physiol,* 141**,** 178-87.

ZAMIOUDIS, C. & PIETERSE, C. M. J. 2012. Modulation of host immunity by beneficial microbes. *Molecular Plant-Microbe Interactions,* 25**,** 139-150.

ZELEZNIAK, A., ANDREJEV, S., PONOMAROVA, O., MENDE, D. R., BORK, P. & PATIL, K. R. 2015. Metabolic dependencies drive species co-occurrence in diverse microbial communities. *Proceedings of the National Academy of Sciences,* 112**,** 6449-6454.

ZENG, W. & HE, S. Y. 2010. A prominent role of the flagellin receptor FLAGELLIN-SENSING2 in mediating stomatal response to *Pseudomonas syringae* pv *tomato* DC3000 in *Arabidopsis*. *Plant Physiol,* 153**,** 1188-98.

ZGADZAJ, R., JAMES, E. K., KELLY, S., KAWAHARADA, Y., DE JONGE, N., JENSEN, D. B., MADSEN, L. H. & RADUTOIU, S. 2015. A legume genetic framework controls infection of nodules by symbiotic and endophytic bacteria. *PLOS Genetics,* 11**,** e1005280.

ZHANG, J., LI, W., XIANG, T., LIU, Z., LALUK, K., DING, X., ZOU, Y., GAO, M., ZHANG, X., CHEN, S., MENGISTE, T., ZHANG, Y. & ZHOU, J. M. 2010. Receptor-like cytoplasmic kinases integrate signaling from multiple plant immune receptors and are targeted by a *Pseudomonas syringae* effector. *Cell Host Microbe,* 7**,** 290-301.

ZHANG, J., SHAO, F., LI, Y., CUI, H., CHEN, L., LI, H., ZOU, Y., LONG, C., LAN, L., CHAI, J., CHEN, S., TANG, X. & ZHOU, J. M. 2007. A *Pseudomonas syringae* effector inactivates MAPKs to suppress PAMP-induced immunity in plants. *Cell Host Microbe,* 1**,** 175-85.

ZIPFEL, C., KUNZE, G., CHINCHILLA, D., CANIARD, A., JONES, J. D., BOLLER, T. & FELIX, G. 2006. Perception of the bacterial PAMP EF-Tu by the receptor EFR restricts *Agrobacterium*-mediated transformation. *Cell,* 125**,** 749-60.

ZIPFEL, C. & OLDROYD, G. E. 2017. Plant signalling in symbiosis and immunity. *Nature,* 543**,** 328-336.

ZIPFEL, C., ROBATZEK, S., NAVARRO, L., OAKELEY, E. J., JONES, J. D. G., FELIX, G. & BOLLER, T. 2004. Bacterial disease resistance in *Arabidopsis* through flagellin perception. *Nature,* 428**,** 764-767.

ZUCCARO, A., LAHRMANN, U., GÜLDENER, U., LANGEN, G., PFIFFI, S., BIEDENKOPF, D., WONG, P., SAMANS, B., GRIMM, C., BASIEWICZ, M., MURAT, C., MARTIN, F. & KOGEL, K.-H. 2011. Endophytic Life Strategies Decoded by Genome and Transcriptome Analyses of the Mutualistic Root Symbiont Piriformospora indica. *PLOS Pathogens,* 7**,** e1002290.

Appendix

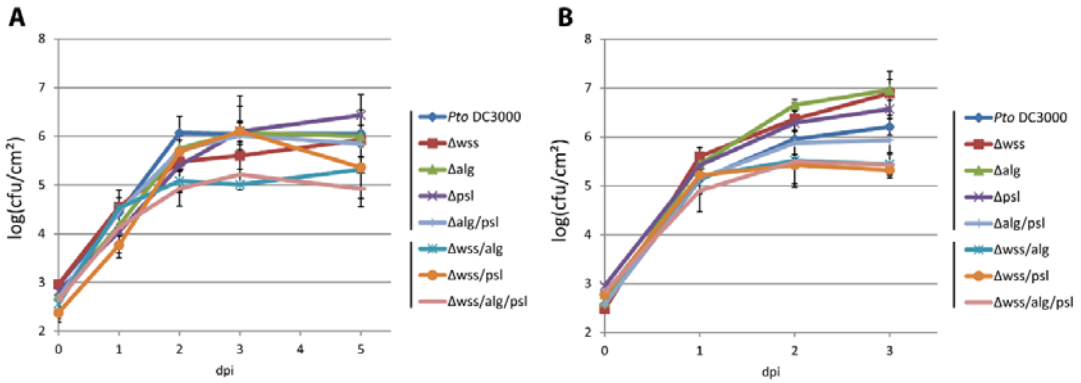

Figure A8.1. Repeats of experiment shown in Figure 4.4. Infection of *A. thaliana* with EPS-deficient *Pto* DC3000 strains. Four-week-old *A. thaliana* plants were infected with *Pto* DC3000 wild-type or indicated EPS mutant strains by infiltration with 10^5 cfu/mL. Bacterial growth *in planta* was monitored over time by leaf sampling, serial dilutions and colony counting in two independent experiments (A and B). Values are means ± standard error (*n* = 4).

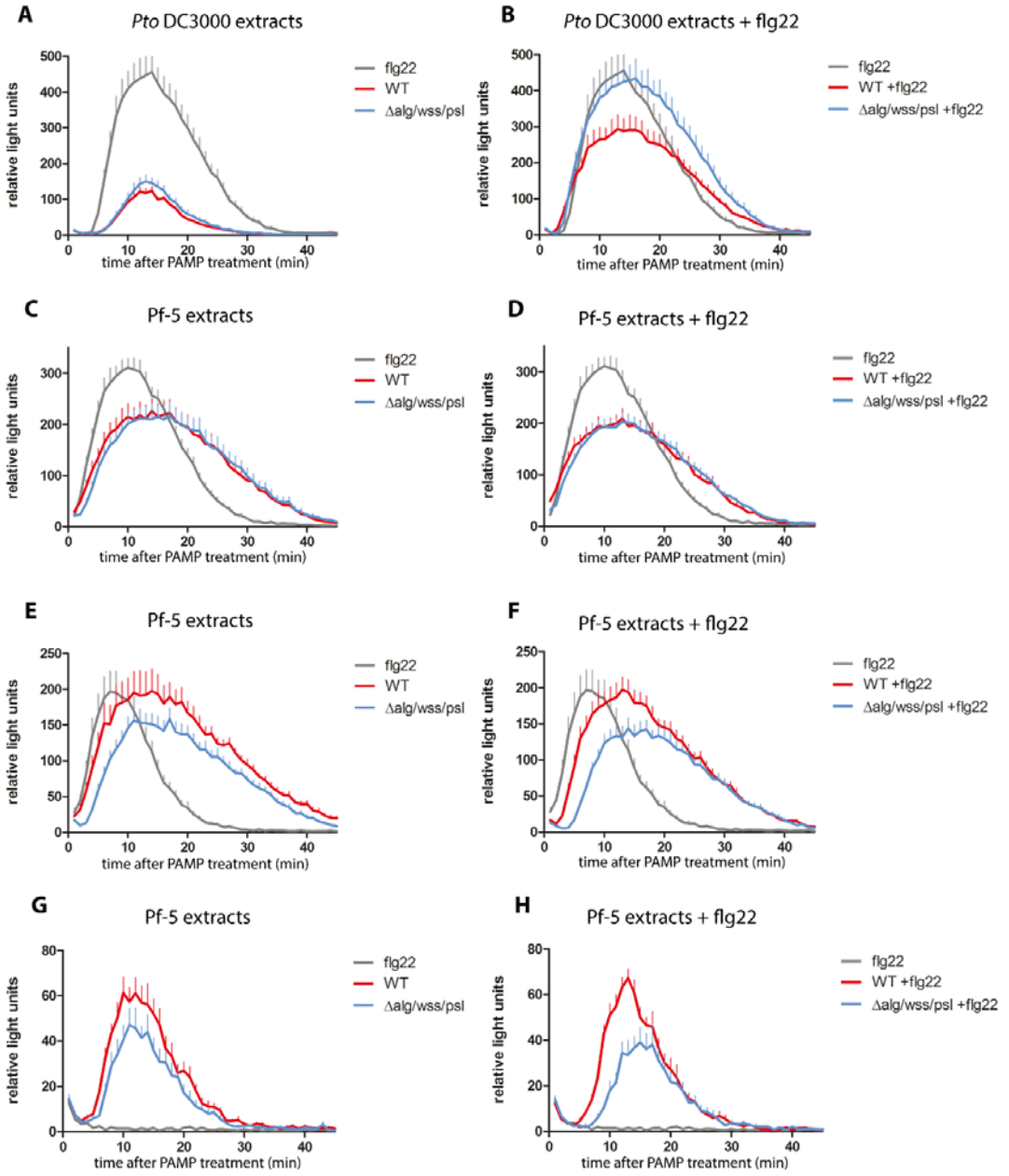

Figure A8.2. Repeats of experiment shown in Figure 4.5. Extracts from *Pseudomonas* wild-type strains and respective EPS-deficient mutants trigger similar ROS burst in *Arabidopsis thaliana*. Leaf discs were treated with extracts from *Pto* DC3000 wild-type and Δ*alg*/*psl*/*wss* (A and B) and *P. protegens* Pf-5 wild-type and Δ*alg*/*psl*/*pel* (C, D, E and F) to assess the ability to induce a ROS burst (A, C, E and G) or to suppress a ROS burst elicited by co-application of flg22 peptide with the respective extracts (B, D, F and H). Flg22 peptide concentration was 100 nM (A to D) or 10 nM (E to H). ROS burst was measured in *A. thaliana* Col-0 (A to F) or *fls2* (G and H). Values are means ± standard error (n = 8). ROS burst is expressed as relative light units.

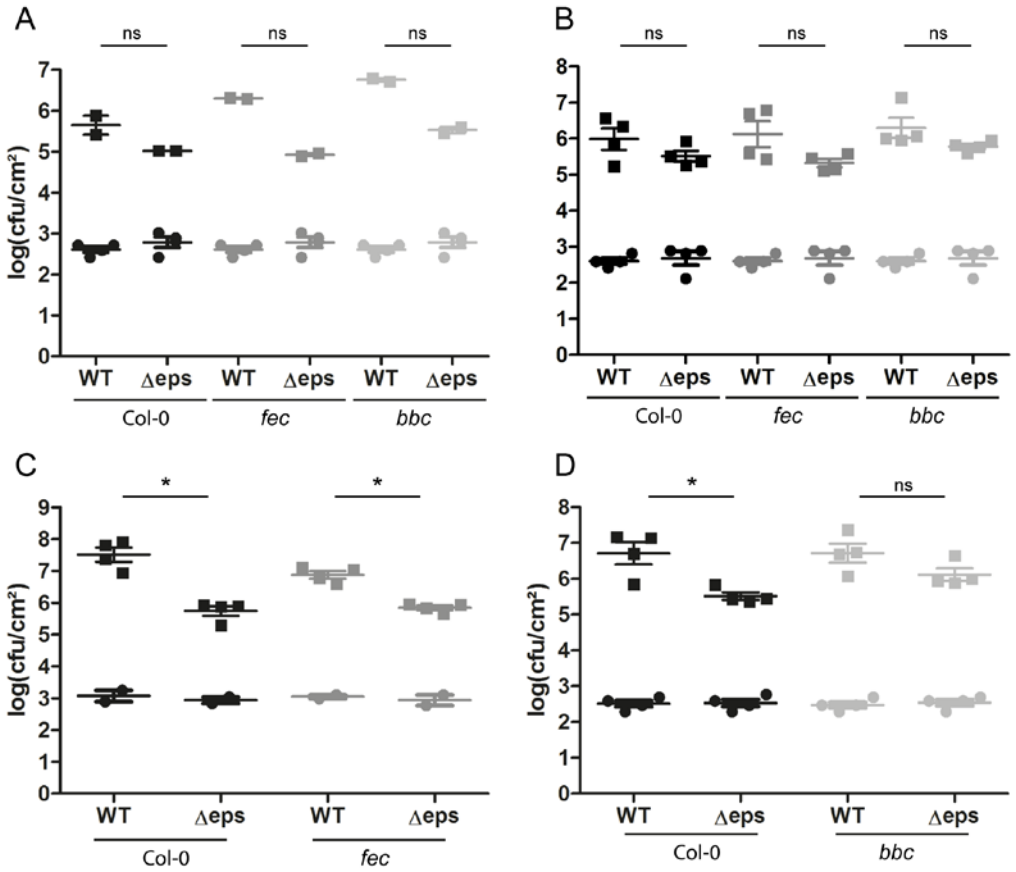

Figure A8.3. Repeats of experiment shown in Figure 4.8. Infection of PTI-compromised *A. thaliana* plants with EPS-deficient *Pto* DC3000. Four-week-old *A. thaliana* Col-0 and mutant genotypes *fec* (*fls2*/*efr*/*cerk1*) and *bbc* (*bak1-5*/*bkk1-1*/*cerk1*) were infiltrated with 10^5 cfu/mL *Pto* DC3000 wild-type or Δeps (*Pto* Δ*alg*/*psl*/*wss*). Bacterial growth *in planta* was assessed at 0 dpi (round symbols) and 3 dpi (square symbol) by leaf sampling, serial dilutions and colony counting in two independent experiments (A and B). Values are means ± standard error (*n* = 2-4). Asterisks indicate statistically significant difference (* $p < 0.05$) between treatment of wild-type and Δeps based on a two-tailed Mann–Whitney test.

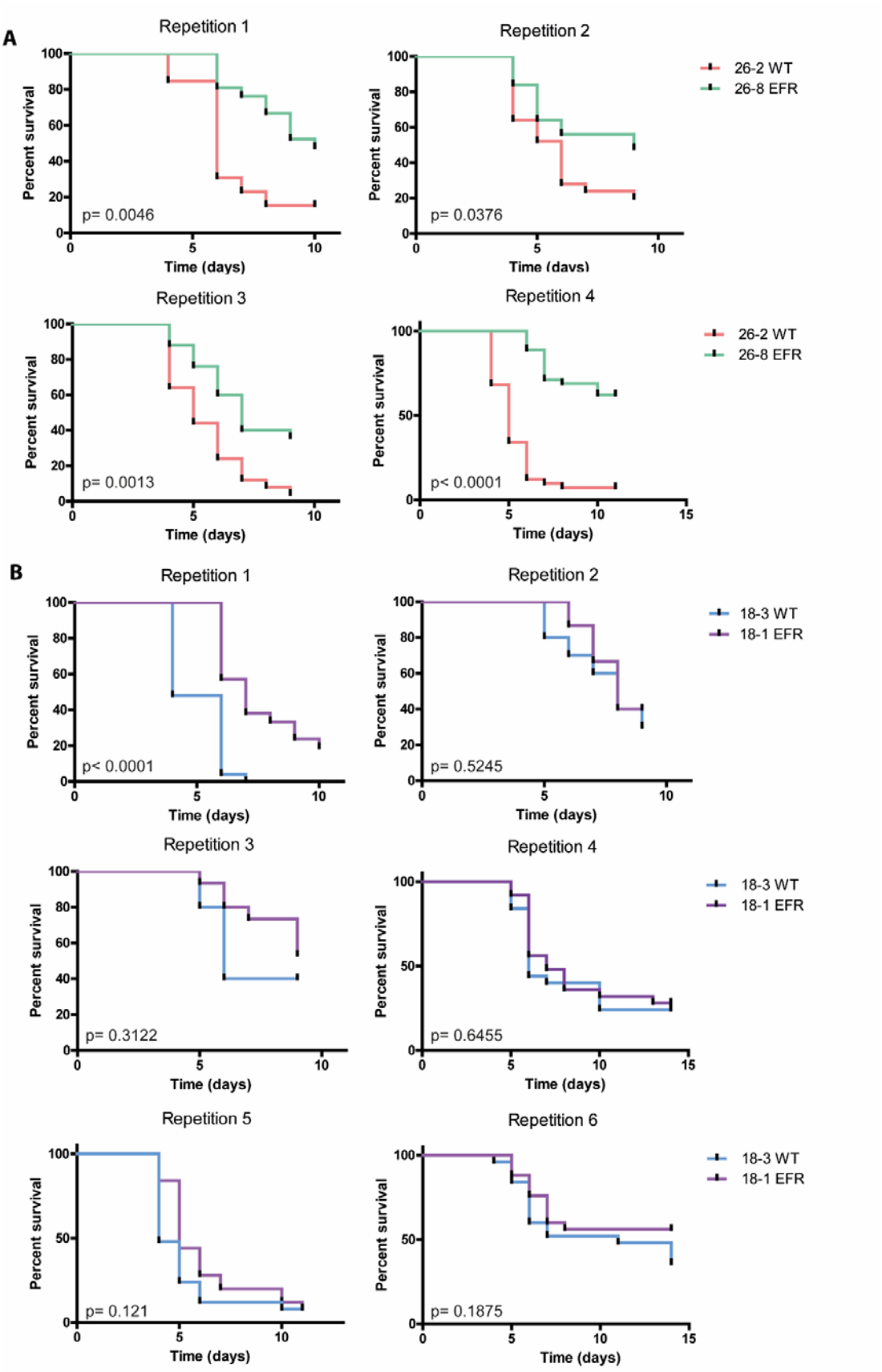

Figure A8.4. Repeats of experiment shown in Figure 5.9. *EFR* expression in *M. truncatula* provides quantitative resistance against the pathogen *R. solanacearum*. (A) *M. truncatula* lines expressing *EFR* 26-8 and control line 26-2 were infected with *R. solanacearum* GMI1000 and disease symptoms assessed daily. Survival rate is displayed over time and statistical analysis performed with

Mantel-Cox test. Each experiment had at least *n*=13 plants. (B) *M. truncatula* lines expressing *EFR* 18-1 and control line 18-3 were infected with *R. solanacearum* GMI1000 and disease symptoms assessed daily. Survival rate is displayed over time and statistical analysis performed with Mantel-Cox test. Each experiment had at least *n*=10 plants.

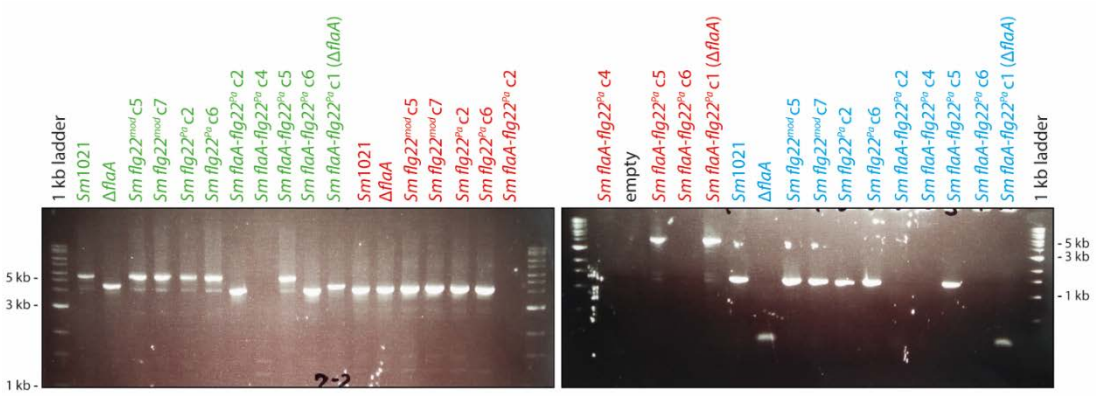

Figure A8.5. PCR amplification of *fla* gene locus in *Sm*1021. *Sm*1021 wild-type, *Sm* Δ*flaA* mutant and mutant strains with flg22 variants were tested for integrity of *fla* gene locus. Three different sets of primers were used #1346 and #1347 (blue), #1348 and #1349 (red), #1346 and #1349 (green). PCR amplification product was loaded on a 1%-agarose gel. Size marker is 1 kb-ladder from NEB.

```
MtFLS2      MPSQNLSLTLVILISILSIIVSHAETSTIKVEIEALKAFKKSITNDPNKALANWI--DTI
AtFLS2      --MKLLSKTFLILTLTFFFFGIALAKQSFEPEIEALKSFKNGISNDPLGVLSDWTIIGSL
               : ** *::**   : ::     ..::: ******:**:.*:***  .*::*    ::

MtFLS2      PHCNWSGIACSNSSKHVISISLFELQLQGEISPFLGNISTLQLIDLTSNSLTGQIPPQIS
AtFLS2      RHCNWTGITCDS-TGHVVSVSLLEKQLEGVLSPAIANLTYLQVLDLTSNSFTGKIPAEIG
             ****:**:*.. : **:*:**:* **:* :** :.*:: **::******:**:** :*.

MtFLS2      LCTQLTTLYLTGNSLSGSIPHELGNLKMLQYLDIGNNYLNGTLPVSIFNITSLLGIAFNF
AtFLS2      KLTELNQLILYLNYFSGSIPSGIWELKNIFYLDLRNNLLSGDVPEEICKTSSLVLIGFDY
              *:*. * *  * :*****  : :** : ***: ** *.* :* .* : :**: *.*::

MtFLS2      NNLTGTIPSNIGNLVNTIQIGGFGNSFVGSIPVSIGQLGSLLSLDFSQNKLSGVIPREIG
AtFLS2      NNLTGKIPECLGDLVHLQMFVAAGNHLTGSIPVSIGTLANLTDLDLSGNQLTGKIPRDFG
            *****.**. :*:**.   : . ** :.******** *..* .**:* *:*:* ***::*

MtFLS2      NLTNLQYLLLLQNSLSGKIPSELALCSNLVNLELYENKFIGSIPHELGNLVQLETLRLFG
AtFLS2      NLLNLQSLVLTENLLEGDIPAEIGNCSSLVQLELYDNQLTGKIPAELGNLVQLQALRIYK
            ** *** *:* :* *.*.**:*:. **.**:****:*:: *.** ********::**::

MtFLS2      NNLNSTIPDSIFKLKSLTHLGLSENNLEGTISSEIGSLSSLKVLTLHLNKFTGTIPSSIT
AtFLS2      NKLTSSIPSSLFRLTQLTHLGLSENHLVGPISEEIGFLESLEVLTLHSNNFTGEFPQSIT
            *:*.*:**.*:*:*..*********.* * **.*** *.**:***** *:*** :*.***

MtFLS2      NLRNLTSLSMSQNLLSGEIPSNIGVLQNLKFLVLNDNFLHGPVPPSITNCTSLVNVSLSI
AtFLS2      NLRNLTVLTVGFNNISGELPADLGLLTNLRNLSAHDNLLTGPIPSSISNCTGLKLLDLSH
            ****** *::. * :***:*:::*:* **: *  .**:* **:* **:***.*  :.**

MtFLS2      NSLTGKIPEGFSRLPNLTFLSLQSNKMSGEIPDDLYICSNLSTLLLADNSFSGSIKSGIK
AtFLS2      NQMTGEIPRGFGRM-NLTFISIGRNHFTGEIPDDIFNCSNLETLSVADNNLTGTLKPLIG
            *.:**:**.**.*: ****:*:  *:::******:: ****.** :***.::*::*  *

MtFLS2      NLFKLMRLKLNKNAFIGPIPPEIGNLNKLIILSLSENRLSGRIPIELSKLSLLQGLSLYD
AtFLS2      KLQKLRILQVSYNSLTGPIPREIGNLKDLNILYLHSNGFTGRIPREMSNLTLLQGLRMYS
            :* **  *::. *:: **** *****:.* ** * .* ::**** *:*:*:***** :*.

MtFLS2      NALEGTIPDKLSELKELTILLLHENKLVGRIPDSISKLEMLSYLDLHGNKLNGSIPKSMG
AtFLS2      NDLEGPIPEEMFDMKLLSVLDLSNNKFSGQIPALFSKLESLTYLSLQGNKFNGSIPASLK
            * *** **::: ::* *::* * :**: *:**  :**** *:**.*:***:***** *:

MtFLS2      KLDHLLLLDLSHNRLSGLIPGYVIAHLKDMQMYLNLSYNHFVGSVPSELGMLEMVQAIDV
AtFLS2      SLSLLNTFDISDNLLTGTIPGELLASLKNMQLYLNFSNNLLTGTIPKELGKLEMVQEIDL
            .*. *  :*:*.* *:* *** ::* **:**:***:* * :.*::*.*** ***** **:

MtFLS2      SNNNLSGFLPKTLAGCRNMFSLDFSVNNISGPIPAEVFSGMDLLQSLNLSRNHLDGEIPE
AtFLS2      SNNLFSGSIPRSLQACKNVFTLDFSQNNLSGHIPDEVFQGMDMIISLNLSRNSFSGEIPQ
```

Figure A8.6. Alignment of *AtFLS2* and its homologue *MtFLS2*. Sequence alignment was done with EMBL-EBI Clustal Omega. *AtFLS2* kinase domain is highlighted in purple. Position of *Tnt1* insertion in *Mtfls2* line NF15434 is marked with yellow highlight.

BamHI-flg22Pa_SMc03037-BamHI-68966

CGGGATCCGCTTCGAGATCGGCTTCCTGATCATGCTGCCCTTCCTCGTGATCGACCTGATCGTCGCG
ACCATCACCATGGCGATGGGCATGATGATGCTTCCCCCGACGGCGATTTCGCTGCCCTTCAAGATCC
TGTTCTTCGTGCTGATCGACGGCTGGAACCTGCTCGTCGGCAGCCTGGTGCGCTCGTTTATCTGAG
GCCCCGCCGCCAGGCACGACGGCCCGGCAAGAATCCGTTAAGCATAGGATTTCACAGTCGATTAAC
CACCTTCTCGCCGCTCCCCGAACACATCTTCTCCGGTTAAACACTTGGCAATGAATGGCTGCGAATT
TCGTCTTCACACGACGGGTTTGGTATCCATCACGAGTTGAGCGGAGCCGAGTGGCATGATGCCGGA
CCGTCGTGACCGGTAGCGATTTTTCAGTCCGGTATGTCCCCCCAATCAGTATTTCGTAGGGACAACG
AATATGACGAGCATTCTCACCAACAACTCCGCAATGGCCGCGCTTTCTACGCTGCGCTCGATCTCCT
CCAGCATGGAAGACACGCAGCAGCGCCTCTCCACCGGCTCGCGCATCAACTCGGCCAAGGACGAC
GCCGCGGGCCTCCAGATCGCGACCACCATGCGCTCCGACAACCAGGCTCTCTCCGCAGTTCAAGAC
GCGCTCGGCCTCGGTGCTGCCAAGGTCGACACCGCCTATTCCGGTATGGAATCGGCCATCGAAGTC
GTCAAGGAGATCAAGGCGAAGCTCGTAGCCGCGACCGAAGACGGCGTCGACAAGGCCAAGATCC
AGGAAGAAATCACCCAACTCAAGGACCAGCTGACGAGCATTGCCGAAGCGGCCTCCTTCTCCGGCG
AGAACTGGCTGCAGGCGGACCTCAGCGGTGGCCCCGTCACCAAGAGCGTCGTCGGGGGATTCGTC
CGTGACTCGAGCGGCGCCGTATCTGTGAAGAAGGTTGACTACAGCCTCAACACCGACACCGTCCTG
TTCGACACGACCGGCAATACCGGCATTCTTGACAAGGTCTACAACGTCTCGCAGGCGAGCGTCACG
CTGCCGGTCAACGTCAACGGCACGACGTCTGAGTACACGGTCGGCGCTTACAACGTCGATGACCTG
ATCGACGCCAGCGCGACCTTCGACGGAGACTATGCCAATGTTGGTGGGATCCGC

Figure A8.7. Synthesised sequence for allele replacement to flg22^{Pa}.

BamHI-flg22mod_SMc03037-BamHI-68965

CGGGATCCGCTTCGAGATCGGCTTCCTGATCATGCTGCCCTTCCTCGTGATCGACCTGATCGTCGCG
ACCATCACCATGGCGATGGGCATGATGATGCTTCCCCCGACGGCGATTTCGCTGCCCTTCAAGATCC
TGTTCTTCGTGCTGATCGACGGCTGGAACCTGCTCGTCGGCAGCCTGGTGCGCTCGTTTATCTGAG
GCCCCGCCGCCAGGCACGACGGCCCGGCAAGAATCCGTTAAGCATAGGATTTCACAGTCGATTAAC
CACCTTCTCGCCGCTCCCCGAACACATCTTCTCCGGTTAAACACTTGGCAATGAATGGCTGCGAATT
TCGTCTTCACACGACGGGTTTGGTATCCATCACGAGTTGAGCGGAGCCGAGTGGCATGATGCCGGA
CCGTCGTGACCGGTAGCGATTTTTCAGTCCGGTATGTCCCCCCAATCAGTATTTCGTAGGGACAACG
AATATGACGAGCATTCTCACCAACAACTCCGCAATGGCCGCGCTTTCTACGCTGCGCTCGATCTCCT
CCAGCATGGAAGACACGCAGAGCCGCCTCTCCTCGGGCCTCCGCATCGGCTCGGCCTCCGACGACG
CCGCGGGCCTCCAGATCGCGACCACCATGCGCTCCGACAACCAGGCTCTCTCCGCAGTTCAAGACG
CGCTCGGCCTCGGTGCTGCCAAGGTCGACACCGCCTATTCCGGTATGGAATCGGCCATCGAAGTCG
TCAAGGAGATCAAGGCGAAGCTCGTAGCCGCGACCGAAGACGGCGTCGACAAGGCCAAGATCCA
GGAAGAAATCACCCAACTCAAGGACCAGCTGACGAGCATTGCCGAAGCGGCCTCCTTCTCCGGCGA
GAACTGGCTGCAGGCGGACCTCAGCGGTGGCCCCGTCACCAAGAGCGTCGTCGGGGGATTCGTCC
GTGACTCGAGCGGCGCCGTATCTGTGAAGAAGGTTGACTACAGCCTCAACACCGACACCGTCCTGT
TCGACACGACCGGCAATACCGGCATTCTTGACAAGGTCTACAACGTCTCGCAGGCGAGCGTCACGC
TGCCGGTCAACGTCAACGGCACGACGTCTGAGTACACGGTCGGCGCTTACAACGTCGATGACCTGA
TCGACGCCAGCGCGACCTTCGACGGAGACTATGCCAATGTTGGTGGGATCCGC

Figure A8.8. Synthesised sequence for allele replacement to flg22^{mod}.

BamHI-flg22Pa_deltaSMc03037-BamHI

CGGGATCCTGCAGCTCTTCATCGACATCGCCCGGGAGAAGGGCCAGACCGTCGTCGTCGACGAGA
AGGTGGACCTGCGCGCCGTCGTGCCGGCCTTCATGATCTCGGAGATCCGCCGCGGCTTCGAGATCG
GCTTCCTGATCATGCTGCCCTTCCTCGTGATCGACCTGATCGTCGCGACCATCACCATGGCGATGGG
CATGATGATGCTTCCCCCGACGGCGATTTCGCTGCCCTTCAAGATCCTGTTCTTCGTGCTGATCGAC
GGCTGGAACCTGCTCGTCGGCAGCCTGGTGCGCTCGTTTATCTGAGGCCCCGCCGCCAGGCACGAC

GGCCCGGCAAGAATCCGTTAAGCATAGGATTTCACAGTCGATTAACCACCTTCTCGCCGCTCCCCGA
ACACATCTTCTCCGGTTAAACACTTGGCAATGAATGGCTGCGAATTTCGTCTTCACACGACGGGTTT
GGTATCCATCACGAGTTGAGCGGAGCCGAGTGGCATGATGCCGGACCGTCGTGACCGGTAGCGAT
TTTTCAGTCCGGTATGTCCCCCCAATCAGTATTTCGTAGGGACAACGAATATGACGAGCATTCTCAC
CAACAACTCCGCAATGGCCGCGCTTTCTACGCTGCGCTCGATCTCCTCCAGCATGGAAGACACGCA
GCAGCGCCTCTCCACCGGCTCGCGCATCAACTCGGCCAAGGACGACGCCGCGGGCCTCCAGATCGC
GACCACCATGCGCTCCGACAACCAGGCTCTCTCCGCAGTTCAAGACGCGCTCGGCCTCGGTGCTGC
CAAGGTCGACACCGCCTATTCCGGTATGGAATCGGCCATCGAAGTCGTCAAGGAGATCAAGGCGA
AGCTCGTAGCCGCGACCGAAGACGGCGTCGACAAGGCCAAGATCCAGGAAGAAATCACCCAACTC
AAGGACCAGCTGACGAGCATTGCCGAAGCGGCCTCCTTCTCCGGCGAGAACTGGCTGCAGGCGGA
CCTCAGCGGTGGCCCCGTCACCAAGAGCGTCGTCGGGGGATTCGTCCGTGACTCGAGCGGCGCCG
TATCTGTGAAGAAGGTTGACTACAGCCTCAACACCGACACCGTCCTGTTCGACACGACCGGCAATA
CCGGCATTCTTGACAAGGTCTACAACGTCTCGCAGGCGAGCGTCACGCTGCCGGTCAACGTCAACG
GCACGACGTCTGAGTACACGGTCGGCGCTTACAACGTCGATGACCTGATCGACGCCAGCGCGACCT
TCGACGGAGACTATGCCAATGTTGGTGCCGGTGCGCTTGCTGGCGATTATGTCAAGGTCCAAGGCA
GCTGGGTGAAGGCGGTCGACGTGGCTGCAACGGGTCAGGAAGTCGTCTATGACGACGGCACGAC
GAAATGGGGGGTTGACACGACCGTTACCGGTGCACCGGCTACCAATGTCGCCGCACCGGCTTCGA
TCGCGACGATCGACATCACCATTGCCGCACAGGCTGGGAACCTTGATGCACTGATCGCAGGCGTCG
ACGAAGCGCTCACCGACATGACCAGCGCCGCTGCTTCGCTTGGTTCGATCTCCTCGCGCATCGACCT
GCAGAGCGATTTCGTGAACAAGCTCTCGGACTCGATCGACTCGGGCGTTGGCCGTCTCGTCGATGC
CGATATGAACGAAGAATCGACCCGCCTGAAGGCTCTGCAGACTCAGCAGCAGCTCGCCATCCAGGC
TCTTTCGATCGCCAACTCGGACTCCCAGAACGTCCTTTCGCTCTTCCGCTAAGAAGACATGCAATGG
CGGACGCAGGCAACCTTGTGCCTGCGTCCGGCTCCTTCGAACCGCGCCCCGGAAACGGGGCGCGG
TTTTTGCTTTCTTCCATGAGCCGTCGGCATTTCACTTTTTCTTAAACATAGTATGGCACGCGCGTGTG
CGCGCAAGGGTTGAAAAATTTATCGTCGTTCTTGCTTCCTTAGTGCTTCTTTAACCAAGACAAGATT
ATCTAAGACCATCGAAAGGACGGGCTAACTCCAGAAATAACAGCTGGTTAGCAAGCATGACGTTG
ACCGTCTTTCGCCGGTGGAACCGGAATGTCCCTTCTTATCAGCCACCAAGGGGCACTAAACCATGA
CGAGCATTCTCACCAACATTGCGGCCATGGCCGCTCTCCAGACCCTGCGTACCATCGGCTCCAACAT
GGAAGAGACGCAGGCGCATGTCTCCTCCGGCCTTCGCGTCGGTCAGGCCGCCGACAACGCCGCGT
ACTGGTCGATCGCGACCACCATGCGCTCCGACAATATGGCCCTTTCCGGATCCGC

Figure A8.9. Synthesised sequence for allele replacement to FlaA-flg22^{Pa}.

Publications

The following publications resulted from the work described in this thesis.

Original research papers:

Pfeilmeier S, George J, Morel A, Roy S, Smoker M, Stransfeld L, Downie A, Peeters N, Malone J, Zipfel C (2017) Heterologous expression of the immune receptor *EFR* in *Medicago truncatula* reduces pathogenic infection, but not rhizobial symbiosis. bioRxiv doi: 10.1101/171868

Pfeilmeier S, Saur IM, Rathjen JP, Zipfel C, Malone JG (2016) High levels of cyclic-di-GMP in plant-associated *Pseudomonas* correlate with evasion of plant immunity. Mol Plant Pathol 17: 521-31

Reviews:

Pfeilmeier S, Caly DL, Malone JG (2016) Bacterial pathogenesis of plants: Future challenges from a microbial perspective: Challenges in bacterial molecular plant pathology. Mol Plant Pathol 17: 1298-1313